Development of zebrafish infection and screening model for *Clostridium difficile*

Von der Der Fakultät für Lebenswissenschaften

der Technischen Universität Carolo-Wilhelmina zu Braunschweig

zur Erlangung des Grades eines

Doktors der Naturwissenschaften

(Dr. rer. nat.)

genehmigte

D i s s e r t a t i o n

von Junkai Li
aus Shandong / China

1. Referent: Prof. Dr. Reinhard Köster
2. Referent: Prof. Dr. Michael Steinert
eingereicht am: 04.07.2018
mündliche Prüfung (Disputation) am: 11.10.2018

Druckjahr 2018

Vorveröffentlichungen der Dissertation

Teilergebnisse aus dieser Arbeit wurden mit Genehmigung der Fakultät für Lebenswissenschaften, vertreten durch den Mentor der Arbeit, in folgenden Beiträgen vorab veröffentlicht:

Tagungsbeiträge

Li, J., Namikawa, K., Köster, R. W.. Analysis of The Innate Immune Response in Zebrafish upon *Clostridium difficile* Infection (Poster). 10th European Zebrafish meeting (2015).

Li, J., Namikawa, K., Köster, R. W.. Zebrafish as infection and inhibitor-screening model for *Clostridium difficile* toxins (Poster). Conference of Epidemiology and systems biology of the pathogen *Clostridium difficile* (CDiff). (2016)

Li, J., Namikawa, K., Ünal, C., Steinert, M., Köster, R. W.. Analysis of neutrophil and macrophage behaviour upon *Clostridium difficile* infection (Poster P-II-054). 11th European Zebrafish meeting (2017).

Abstract

Clostridium difficile (*C. difficile*) infection (CDI) is an antibiotic-associated intestinal disease and is considered to be the main cause of healthcare-associated infections. The typical symptom of CDI manifests as mild to moderate diarrhea and pseudomembranous colitis. The hallmarks of the disease include neutrophil infiltration, and lesions in the colonic epithelium. *C. difficile* produces two major virulence factors, named TcdA and TcdB. Both toxins translocate the N-terminal glucosyltransferase domain (GTD) into the cytosol of target cells and inactivate Rho GTPases by glucosylation. This inactivation causes cell rounding, a redistribution of the actin cytoskeleton, and further an apoptotic cytotoxic effect.

Although metronidazole and vancomycin remain the main drugs to treat CDI in the last three decades, new treatments or non-antibiotics agents are needed due to the emergence of hypervirulent strains. In the first part of this study, a stable transgenic zebrafish that expresses the GTD of TcdA/B under the control of a hatching gland specific enhancer was established. This model would be used for screening and identifying pharmacological substances against Tcd toxicity. Meanwhile, this zebrafish model was co-expressed a fluorescence-based apoptosis biosensor with the GTD of TcdA/B. Thus, the physiological condition of hatching gland cells was monitored by fluorescent signal.

The innate immune system plays a crucial role in CDI onset and progression. In the second part of this study, the response of macrophages and neutrophils against *C. difficile* was analyzed. Using the Gal4/UAS system, a stable transgenic zebrafish line with expression of yellow Citrine fluorescent protein in neutrophils was generated. To combine this line for monitoring macrophages simultaneously, the binary transcriptional LexA/lexAop system was applied to express the fluorescent red tagRFP-T protein in macrophages. Both macrophages and neutrophils were able to phagocytose *C. difficile*. Furthermore, to unravel the function of macrophages in *C. difficile* elimination, Tamoxifen-inducible Caspase was co-expressed in the macrophage transgenic strain to trigger apoptosis (ATTAC^{TM}). The ablation and regeneration kinetics of macrophages were characterized by counting the number of RFP-positive cells. This model represents a tool to analyze the progression of CDI in the presence or absence of macrophages.

Abbreviations

bp	Base pair	PCR	polymerase chain reaction
BSA	Bovine serum albumine	PFA	Paraformaldehyd
DNA	Deoxyribonucleic Acid	PTW	PBS with Tween
DNase	desoxyribonuclease	NBT	nitro-blue tetrazolium chloride
dNTP	Deoxynucleotide triphosphate	n	nano-
dpf	days past fertilization	Tween 20	poly(oxyethylen)n-sorbitan-monolaurate
DMSO	Dimethylsulfoxid	p65	Nuclear factor NF-kappa-B p65 subunit
DPBS	Dulbecco's Phosphate buffered saline	RT-PCR	Reverse polymerase chain reaction
E. coli	*Escherichia coli*	rpm	Rounds per minute
GFP	Green fluorescent protein	PTU	Phenylthiourea
HE	Hatching gland	UAS	Upstream activating sequence
h	hour	Tris	2-Amino-2-hydroxymethyl-1,3-propandiol
hpi	hours post-infection	RNA	Ribonucleic acid
LB	Luria-Bertani medium	4OHT	4-hydroxy-tamoxifen
lexAop	lexA operator	RFP	Red fluorescent protein
kD	kilo dalton	UV	Ultra-Violette
µ	micro-	YFP	Yellow fluorescent protein
MeOH	methanol	V	Volt
NGS	normal goat serum	UTP	Uridine Triphosphate

1 Introduction

1.1 *Clostridium difficile* and *Clostridium difficile* infection (CDI)

C. difficile is a Gram-positive, rod-shaped, and toxin-producing bacillus. In the past 30 years, *C. difficile* has emerged as major enteric pathogen in the world (Longo et al., 2015). In 2012, there were more than 185,000 cases of CDI in Europe, which cost estimated 3 billion Euros (Bouza et al., 2012). This figure is likely to rise in line with an ageing population: more than 134 million Europeans will be aged over 65 years by 2050 (Figure 1) (Bouza et al., 2012). The increased incidences and severity of CDI can be attributed to two reasons; the emergency of hypervirulent strain of *C. difficile* and the abuse of antibiotics (Di Bella et al., 2016; Lessa et al., 2012; Shen, 2015). Novel therapeutic strategies, or non-antibiotics are urgently needed.

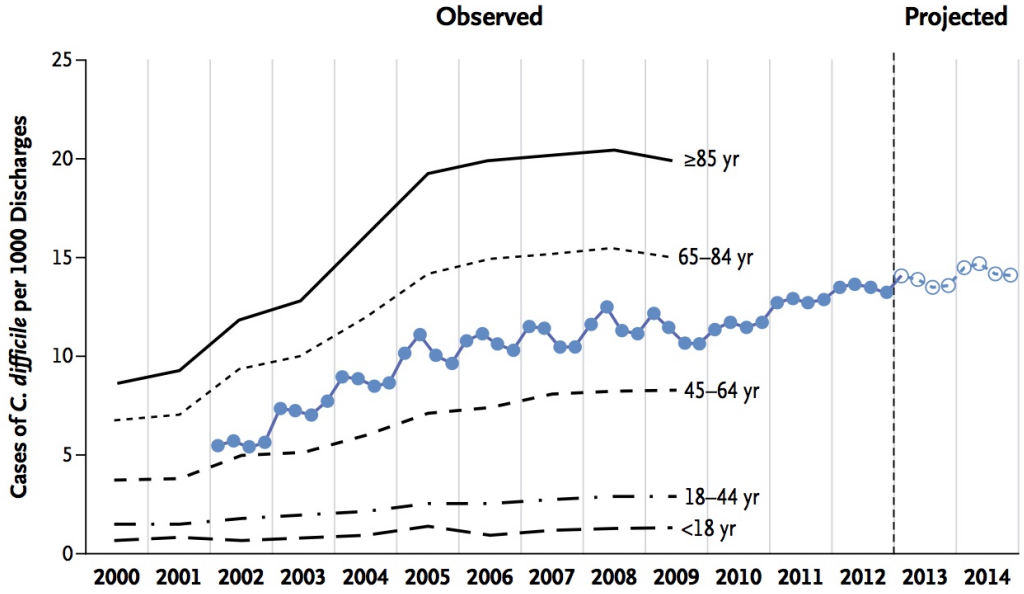

Figure 1 Incidence of nosocomial *C. difficile* Infection

The overall incidence of nosocomial *C. difficile* infection is shown by year (blue), as is the incidence according to patient age (black). Adapted from Longo et al., 2015.

1.1.1 Biology and phylogeny

Clostridium difficile is a member of the family *Peptostreptococcaceae*, and the genus *Clostridium* (Yutin et al., 2013). Colonies of *C. difficile* have ground glass appearance (Delmée, 2001). They are usually around 4mm in diameter on blood agar plate after 24 hour incubation and emit a horse stable odour (George et al., 1979). *C. difficile* vegetative cells are typically 2

to 8µm in length and 0.5µm in width. *C. difficile* are strictly anaerobic and are very sensitive even to low levels of oxygen (Holý et al., 2012). However, some *C. difficile* vegetative cells can survive at least 24 hours in hamster faecal pellets (Edwards et al., 2016). When *C. difficile* is stressed or exposed in aerobic environments, they enter a dormant state by forming resistant spores (Yutin et al., 2013). These resistant spores are considered to be the form to dismiss *C. difficile* via patient-to-patient contact (Yutin et al., 2013). Once reaching the anaerobic environment, i.e. the colon of a host, the ingested *C. difficile* spores germinate to form toxin-producing vegetative cells (Paredes-Sabja et al., 2014).

A variety of genotype-based techniques have been applied to identify the different strain of *C. difficile*, including PCR ribotyping, restriction endonuclease analysis, and pulsed-field gel electrophoresis (Killgore et al., 2008). PCR ribotyping is widely used in Europe, whereas pulsed-field gel electrophoresis is preferred in the US (Maiden, 2006). *C. difficile* strain 630 is a PCR-ribotype 012, virulent, and multidrug-resistant strain. It was isolated from a patient in Zurich, Switzerland in 1982 (Stabler et al., 2010). In 2006, the genome sequencing of *C. difficile* 630 was completed, which revealed a large proportion of mobile genetic elements, and also some adaptations to the gastrointestinal lifestyle (Sebaihia et al., 2006). Since the genome is amenable for genetic manipulation, *C. difficile* 630 has turned into a model strain that is utilized to generate different mutants. For example, *C. difficile* 630Δerm is a spontaneous erythromycin sensitive derivative by serial passaging in antibiotic-free media (Hussain et al., 2005). *C. difficile* 630ΔermΔperR is oxygen-stressed, while *C. difficile* 630ΔermΔfur is affected by iron metabolism (T. D. Ho et al., 2015; van Eijk et al., 2015).

In 2003, outbreaks of severe nosocomial diarrhoea, which were reported in North America and Europe, were caused by a new hypervirulent *C. difficile* strain (Pépin et al., 2005). This new hypervirulent *C. difficile* strain belongs to pulsed-field type 1 (NAP1), PCR-ribotype 027, or group BI by restriction endonuclease analysis, which is referred to as *C. difficile* BI/NAP1/027 (Shen, 2012). *C. difficile* BI/NAP1/027 contributes to prevalence of CDI in many countries (Freeman et al., 2010). Compared to other strains, BI/NAP1/027 produces a much higher level of toxins, which causes a severe morbidity and mortality (Freeman et al., 2010). This strain encodes an additional toxin know as binary toxin, or *C. difficile* transferase (CDT), which has been shown to enhance colonization of *C. difficile* in the gut by increasing its

adherence to the epithelial cells (Cowardin et al., 2016; Gerding et al., 2014). CDI caused by *C. difficile* BI/NAP1/027 is characterized by elevated severity and mortality, intractability by traditional antibiotic treatments, and great risks of relapse (Depestel et al., 2013). More recently, a new hypervirulent strain, PCR-ribotype 078, has been reported to cause a severe CDI in the younger population of the Netherlands (Goorhuis et al., 2008).

1.1.2 Sporulation and germination of *C. difficile*

Due to the strict anaerobic nature, *C. difficile* vegetative cells are unable to survive under aerobic condition. Therefore, it forms infective spores. It is well accepted that hosts acquire the *C. difficile* spores from the environment, and then spores germinate to form vegetative cells in the gut of the hosts (Paredes-Sabja et al., 2014). *C. difficile* spores are resistant to high temperature, and many physical or chemical treatments, such as disinfectants (Edwards et al., 2014). Furthermore, spores are highly infectious, allowing *C. difficile* to transmit and spread in healthcare facilities (Lawley, Croucher, et al., 2009). The mechanism of *C. difficile* sporulation is mainly obtained from research in *Bacillus subtilis,* and *Clostridium perfringens* (Paredes-Sabja et al., 2014). Sporulation of *C. difficile* is initiated by transcription factor stage 0 sporulation protein A (Spo0A), which is phosphorylated and activated by sensor histidine kinases (Edwards et al., 2014). Spo0A is essential for *C. difficile* sporulation. Mutants without Spo0A are unable to form spores. Interestingly, the functional Spo0A gene is required for recurrence of CDI after vancomycin treatment (Deakin et al., 2012).

C. difficile spores are unable to produce toxins, but spores that germinated into vegetative cells in the gastrointestinal tract produce toxins. Toxin production is defined as the onset of CDI. Upon arriving in the duodenum, *C. difficile* spores are stimulated to germinate by a combination of specific bile salts (Francis et al., 2013). Sodium Taurocholate (TCA) is one of the most potent and rapid germinant (described in 1.5.1). However, by analyzing 29 isolated strains, Heeg et al found that *C. difficile* strains respond differently to TCA. Some *C. difficile* are even able to germinate in rich medium without TCA (Heeg et al., 2012). TCA initiates the germination by binding to bile acid receptor, CspC, which transduces the signal to activate CspB. CspB further activates cortex hydrolase, SleC, which degrades the cortex and releases germ cells into the environment (Figure 2) (Edwards et al., 2014). However, genes and

signalling pathways involved in germination of *C. difficile* remain to be investigated (Abt et al., 2016).

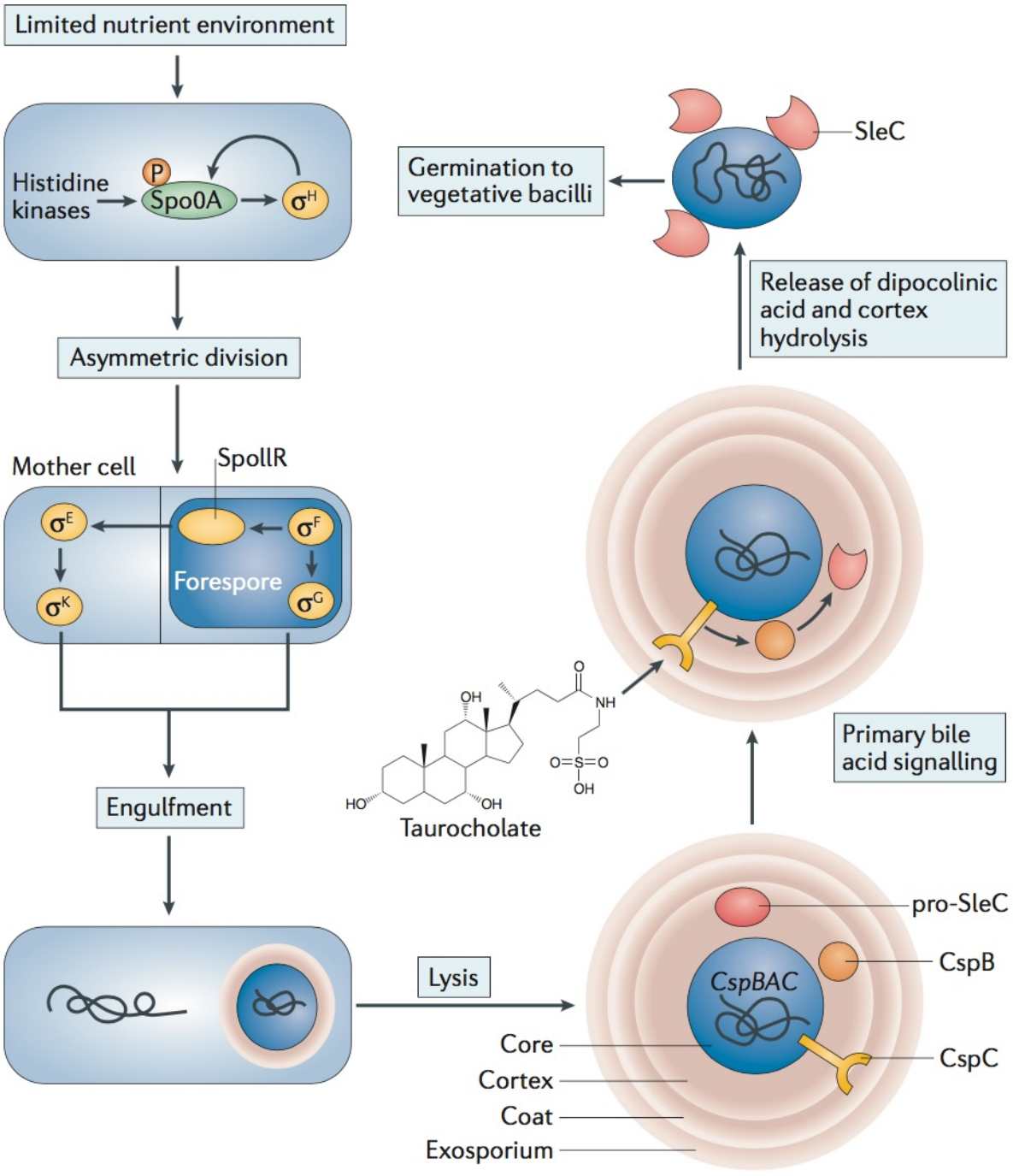

Figure 2 Sporulation and germination of *C. difficile*.

A limited nutrient environment induces sporulation. The transcription factor stage 0 sporulation protein A (Spo0A) is phosphorylated by histidine kinases, activating a cascade of signalling and morphological events that create a forespore within the mother cell of the bacterium. After lysis, the spore is released into the environment. Germination of the spore can be initiated by bile acids, such as taurocholate, which signal through the CspC

receptor. Activation of the SleC enzyme by CspB leads to the degradation of the cortex of the spore and eventually leads to outgrowth of a new vegetative cell. From Abt et al., 2016.

1.1.3 The virulence of *C. difficile*

C. difficile produces three different secreted toxins: TcdA, TcdB, and CDT (Jank et al., 2008). CDT is an actin-specific ADP-ribosyltransferase, which mostly present in hypervariant strains, like *C. difficile* BI/NAP1/027 (Gerding et al., 2014). Cowardin et al reported that CDT enhances the virulence of two *C. difficile* strains in mice by suppressing protective colonic eosinophilia response (Cowardin et al., 2016). However, the role of CDT in pathogenesis needs to be further investigated.

TcdA and TcdB are the major toxins of *C. difficile*. TcdA consists of 2710 amino acid residues, while TcdB consists of 2366 amino acid residues (Jank et al., 2007). The encoding genes *tcdA* and *tcdB* have been sequenced respectively, which are located in a pathogenicity locus together with other additional genes (*tcdC, tcdR*) encoding negative (*tcdC*) and positive (*tcdR*) regulating factors (Jank et al., 2007; Mani et al., 2001). TcdA and TcdB belong to a large *clostridial* cytotoxin family. The homologous toxins from the same family inactivate Rho and Ras family guanosine triphosphatases (GTPase) by glucosylation (Pruitt et al., 2012). The TcdA and TcdB protein have been purified, and the crystal structures of the catalytic fragment have also been analysed by two groups in 2005 (J. G. S. Ho et al., 2005; Reinert et al., 2005).

The structure and function of these toxins has been described as the ABCD model (A: biological activity; B: binding; C: cutting; D: delivery) (Figure 3A) (Pruitt et al., 2012). The N-terminus contains the glucosyltransferase domain (GTD), which is the biologically active domain (Hofmann et al., 1997). Region B, located on the C-terminus, harbours receptor binding domain (RBD) and combined repetitive oligopeptides (CROPs) (Jank et al., 2007). Region C is the protease domain (CPD) that is involved in the auto-catalytic cleavage of toxin processing (Egerer et al., 2007). Region D is the translocation domain (TD) that delivers the glucosyltransferase domain into the cytosol of the targeted cell (Genisyuerek et al., 2011). Once bound to the receptor on a target cell surface, the toxins enter the cell by endocytosis. The translocation requires an acidified endosome (Pruitt et al., 2012). Toxins change their structure between CROP and CPD region in acidified endosomes, which is accompanied by membrane insertion (Barth et al., 2001). In the target cell cytosol, toxins undergo InsP6-

dependent autocatalytic cleavage, and then the GTD is released, which targets Rho proteins (Egerer et al., 2007) (Figure 3B).

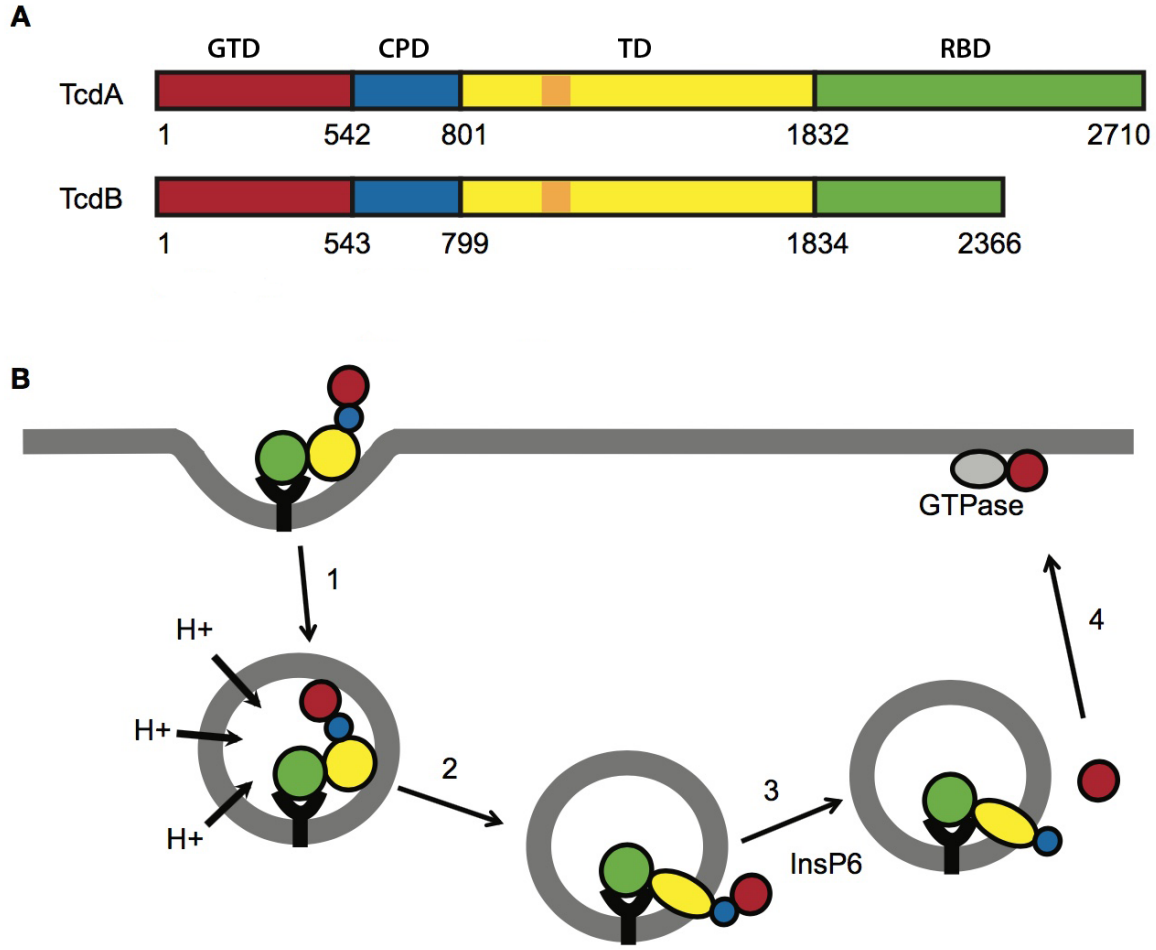

Figure 3 TcdA and TcdB primary structure and mechanism of cellular intoxication.

A) TcdA and TcdB consist of four domains. The N-terminus is the glucosyltransferase domain (GTD) (red). Receptor binding domain (RBD) (green) locates in the C-terminus. Between the RBD and the GTD include delivery domain or pore-forming domain (TD) (yellow), and the protease domain (CPD) (blue). The orange box represents the hydrophobic region of the TD domain that has been proposed to form part of the transmembrane pore. (B) The delivery process is divided into four main steps that are mediated by each of the four domains. (1) The toxin binds to the surface of the cell and is internalized by receptor-mediated endocytosis. (2) Acidification of the endosome triggers the formation of a pore through which the GTD is translocated. (3) The GTD is released into the cytosol by InsP6 dependent autoproteolysis. (4) The GTD glucosylates Rho family GTPases at the cell membrane. Adapted from Pruitt et al., 2012.

In the host cell, the enzymatic domain glycosylates Rho/ Ras family GTPases to irreversibly inactivate them (Di Bella et al., 2016) (Figure 4). Rho GTPases are molecular switches that

control numerous signal transduction pathways, including actin cytoskeleton regulation, cell proliferation, migration, phagocytosis, and immune cell signalling (Etienne-Manneville et al., 2002; Hall, 2012).

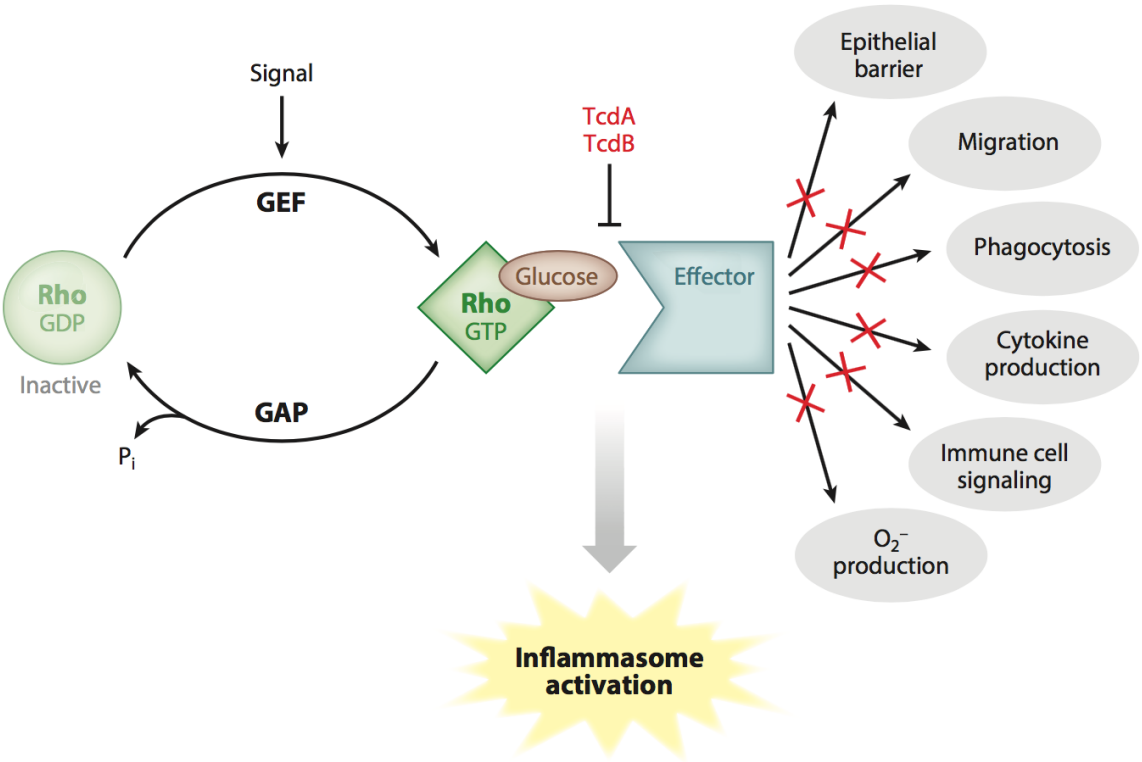

Figure 4 GTPase cycle and inhibition by TcdA and TcdB.

Rho GTPases are inactive in the GDP-bound state and active when GTP bound. Guanine nucleotide exchange factors (GEFs) activate Rho proteins by GDP/GTP exchange. GTPase-activating proteins (GAPs) facilitate GTP hydrolysis and inhibit the active state of Rho proteins. Active Rho proteins interact with multiple effectors to control fundamental cellular functions. Glucosylation of RhoA blocks the interaction with effectors; several signalling pathways and cellular functions are thereby affected that are crucial for host-pathogen interactions. On the other hand, inactivation of RhoA by glucosylation activates the inflammasome. From Aktories et al., 2017.

The inactivation of GTPases causes the disruption of cytoskeletal structure and cell-cell tight junctions (cytopathic effect), leading to cell shrinkage, rounding, and ultimately cell death (Jank et al., 2007). Besides cytopathic effects, the *C. difficile* toxins also induce cytotoxic effects, such as induction of apoptosis, and activation of the inflammasome (Huelsenbeck et al., 2007; Shen, 2012).

Gerhard et al. observed that TcdA-induced apoptosis in human intestinal epithelial cells T84 are through the activation of the caspase-8 and cytochrome C/caspase -9 pathway, which depends on monoglucosylation of Rho protein (Gerhard et al., 2008). They further confirmed that the activation of downstream executioner, caspase 3, 6, 9, and activation of Bid is also detected (Brito et al., 2002). This finding is supported by other study showing that TcdA induces apoptotic monocytes death in a time- and dose-dependent manner (Solomon et al., 2005). Interestingly, this research found that macrophages are more sensitive to toxin A than lymphocytes, but the mechanism is still unclear (Solomon et al., 2005). TcdA is also able to induce the activation of caspase 3, 8, and 9 in HT-29 cells (a colon cell line), which is p53-independent but dependent on glucosylation of Rho GTPases (Nottrott et al., 2007).

TcdB also triggers apoptosis. When exposed to TcdB, IEC-6 cells (rat intestine cells) exhibit nuclear fragmentation and chromatin condensation (Fiorentini et al., 1998). TcdB is not only able to induce caspase-independent apoptosis, but also able to induce caspase-independent cell death through substrate inactivation, for instance, Bcl-2 family members that may be involved such cell death (Qa'Dan et al., 2002). Proteomic analysis of TcdB-treated cells showed fragments of vimentin-type intermediate filaments which are cleaved by caspase-3 (Qa'Dan et al., 2002). Matarrese et al. demonstrated that TcdB induces apoptosis via mitochondrial ATP-dependent potassium channels, which are associated with regulation of calcium concentration and mitochondrial membrane potentials (Matarrese et al., 2007).

1.1.4 Cell surface receptors for TcdA and TcdB

Previous studies have shown that the TcdA and TcdB have different receptors. Glycoprotein 96 (gp96), expressed on human colonocyte apical membranes, has been identified as a TcdA receptor that participates in colonic signal transduction pathways and apoptosis (Na et al., 2008). Other TcdA receptors which have been proposed are rabbit membrane-bound sucrase-isomaltase, and blood antigens I (Charalabos Pothoulakis et al., 1996; Tucker et al., 1991). The sucrase-isomaltase is expressed in rabbit intestinal epithelial cells but not in human. Two TcdB receptors have been reported: chondroitin sulfate proteoglycan 4 (CSPG4) and Poliovirus receptor-like 3 (PVRL3) (LaFrance et al., 2015; Yuan et al., 2015). CSPG4 is initially identified from a human shRNAmir library screen. It is confirmed to be a functional TcdB receptor in HeLa cells and HT-29 cells (Yuan et al., 2015). PVRL3, which is identified

from a gene-trap insertional mutagenesis screen, has been reported to function as a receptor for TcdB-mediated cytotoxicity (LaFrance et al., 2015). However, none of the above receptors is expressed in the colonic epithelium of human. Using unbiased genome-wide CRISPR–Cas9 screenings, Tao et al reported that Wnt receptors of frizzled family (FZDs) are colonic epithelial TcdB receptors involved in TcdB uptake (Tao et al., 2016). In the study, they identified that FZD1, 2, and 7 play critical roles in TcdB-induced cytotoxicity, and FZD1/2/7 triple-knockout cells are highly resistant to TcdB (Tao et al., 2016).

However, more solid data concerning the nature of toxin receptors are urgently required to further understand the virulence of *C. difficile*.

1.1.5 Risk factors associated with CDI

The highest risk factor associated with CDI remains to be the use of antibiotics (Figure 5) (Longo et al., 2015). More than 90% of CDI occur during, or shortly after antibiotic treatment (Barbut et al., 2001). Ampicillin, cephalosporins, amoxicillin, and fluoroquinolones are the most frequently used antibiotics to treat infections, or diseases caused by bacteria, but almost all those antibiotics have been reported to increase the risk of CDI (Longo et al., 2015). Some studies demonstrated that by reducing the use of high-risk antibiotics significantly decreases the healthcare acquired nosocomial *Clostridium difficile* –associated disease (n-CDAD) (Carling et al., 2003; Valiquette et al., 2007). Antibiotic use disrupts the intestinal commensal flora—microbiota and reduces colonisation resistance, resulting in colonization of *C. difficile* and CDI associated disease symptoms (refer to section 1.3.1) (Buffie et al., 2012).

Besides antibiotic use, aging is considered as another risk factor for CDI. *C. difficile* is primarily considered to infect the elderly (> 65 years old), with higher severity and incidence in this population (figure 1) (Simor et al., 2002). This may also be due to the more frequent hospitalization, antibiotic treatment, and immune senescence of elder people. However, as hypervirulent strains emerge, the susceptibility of infection has shifted from the elderly to all age groups (Simor et al., 2002).

Two factors exert major influences on clinical CDI; the virulence of the infection strain, and the host immune response (Longo et al., 2015). Patients who become asymptomatic carriers have significantly increased IgG antibodies against TcdA than those who develop diarrhea within 3 days of *C. difficile* colonization (Kyne et al., 2000). Antibodies against TcdA/TcdB prevent toxins from binding to cell surface receptors, which stops toxins entering targeted cells (Orellana et al., 1992).

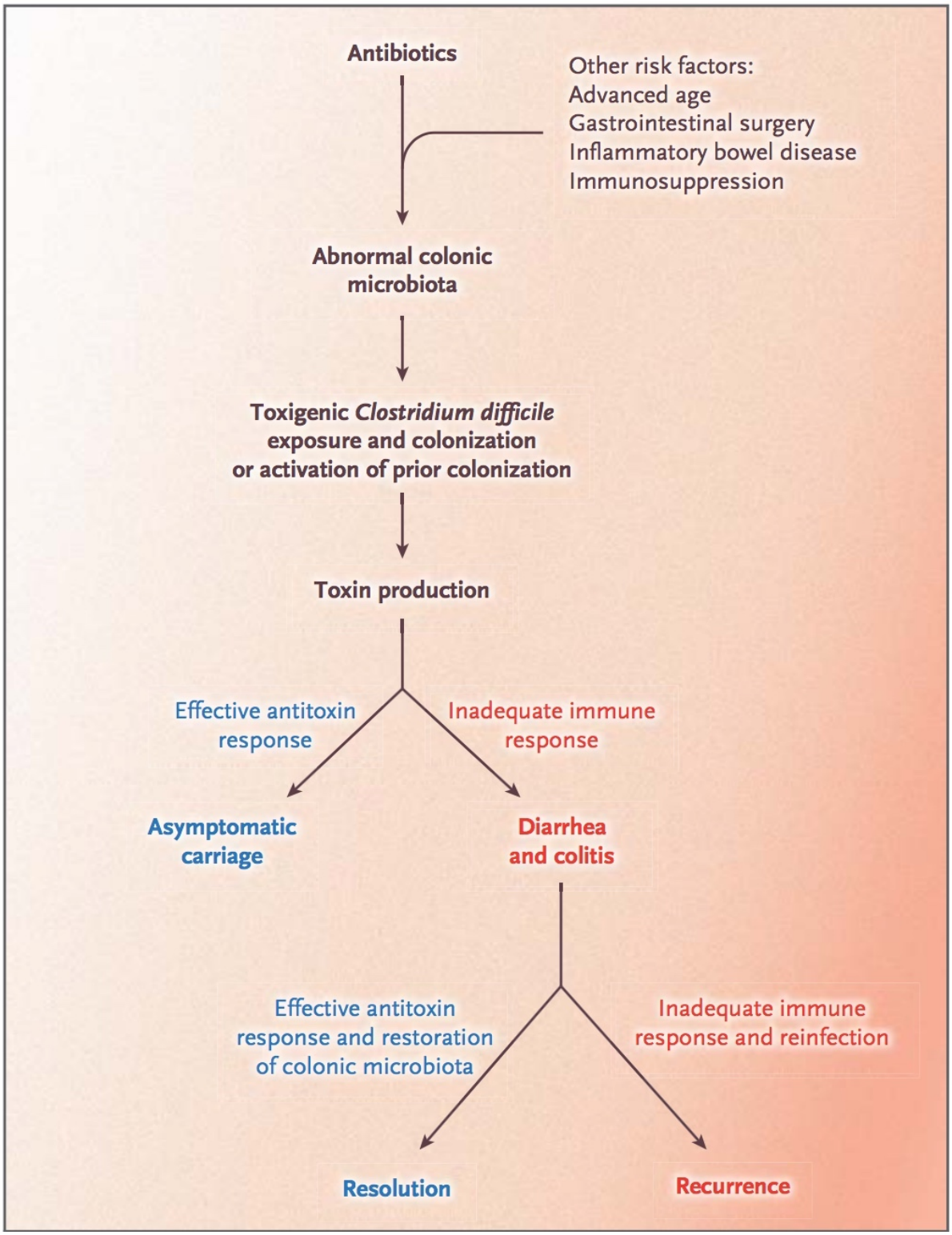

Figure 5 Pathogenesis of CDI

Colonization of the *C. difficile* is prevented by microbiota. Weakening of this barrier by antibiotics is the major risk factor for the disease. If patients fail to mount an anamnestic serum IgG antitoxin to TcdA and TcdB, they develop CDI. If patients mount an effective immune response to *C. difficile* toxins, they become asymptomatic carrier. From Longo et al., 2015.

1.1.6 Treatment for CDI

For more than 30 years, metronidazole and oral vancomycin are used as the main antimicrobial agents to treat CDI. Despite the fact they have been used by millions of patients, resistance to either vancomycin, or metronidazole has not been reported (Longo et al., 2015). However, the rate of clinical failure associated with metronidazole, especially for patients with the BI/NAP1/027 strain, has risen in the past decade (Pépin et al., 2007). Furthermore, treatment for CDI with either metronidazole, or vancomycin is associated with 20%-30% recurrence in an initial episode, and second recurrences are observed in a rate of 40%-60% (Cornely et al., 2012; Leong et al., 2013). There is no alternative therapy to cure the recurrence of CDI. In 2011, the US Food and Drug Administration (FDA) approved fidaxomicin for CDI treatment (Weiss et al., 2014). Fidaxomicin is a novel macrocyclic antibiotic against anaerobic gram-positive bacteria by inhibiting nucleic acid synthesis (Crawford et al., 2012). Although fidaxomicin is superior to vancomycin in clinical trials with narrower spectrum, recurrence rate is still high, and above than 10% (Weiss et al., 2014). Furthermore, widespread application of fidaxomicin is limited by its high cost (Kociolek et al., 2016).

Due to antibiotic-resistant of *C. difficile*, non-antibiotic treatments are pursued to diminish gut microbiota disruption. Probiotics, defined as live microorganisms, are applied additionally to antibiotic treatments (Hickson, 2011; Liao et al., 2015). The benefits of probiotics are: inexpressive, and no drug interaction. The drawbacks of probiotics are: poor standardization, heterogeneous trials, and adverse reaction in patients (McFarland, 2009).

Antibody treatment has been demonstrated to be effective both in research and clinical trials (McFarland, 2009). A study demonstrated that administration of two human monoclonal antibodies against TcdA and TcdB reduces their cytotoxicity and secretory activity in hamsters, which also reduces recurrent CDI in humans (Lowy Israel et al., 2010). In 2016, Bezlotoxumab, a human monoclonal antibody against TcdB, was approved by the FDA to treat recurrent CDI (Wilcox et al., 2017).

With the understanding of the relationship between gut microbiota and CDI, faecal microbiota transplant (FMT) becomes a novel treatment, especially for recurrent CDI (Rohlke

et al., 2012). When the microbiota is disturbed by antibiotics, patients are in a state of microbiota dysbiosis, which means commensal gut flora are unable to protect the host against *C. difficile* invasion (refer to section 1.1.5). FMT restores the damaged gastrointestinal microbial community (Lagier, 2016). FMT involves the administration of gut microbiota from a healthy donor into the patient's colon to re-establish the normal composition of the gut flora (Agito et al., 2013). A study reported that in 317 patients across 27 case series, FMT shows disease resolution in 92% patients (Gough et al., 2011). However, protocols and reported effectiveness of FMT differ widely, and the precise mechanism of why FMT is effective also needs to be appreciated (Dowle, 2016; Gough et al., 2011). These reasons restrict FMT to be a routine therapy for CDI.

1.1.7 Animal model for the study of CDI

CDI has been studied in a number of animal species, including rat, hamster, rabbit, and mouse (Abrams et al., 1980; X. Chen et al., 2008a; Czuprynski et al., 1983; Hirota et al., 2012). Each animal model has its own advantages and disadvantages. The hamster CDI model has been used most extensively (Best et al., 2012). Hamster models share many clinical features of CDI as in human. After pretreatment with clindamycin, and challenge with *C. difficile*, CDI is initiated in the hamster (Abrams et al., 1980). However, hamsters also display many symptoms that do not present in human. For instance, the appearance of the gastrointestinal tract is changed, and the colon is enlarged (Best et al., 2012). In addition, the disease develops very rapidly in hamster, and even kills the host quickly when the host is challenged with toxigenic stains (X. Chen et al., 2008a). Lack of immunological reagents to study hamster immune response also limits the hamster to be utilized to study CDI host response. (Hutton et al., 2014). Moreover, the major drawback is that CDI hamsters do not develop diarrhea, or only exhibit wet tail, while diarrhea is the main pathophysiological feature in CDI (S P Sambol et al., 2001). Despite these disadvantages, the hamster has been used for more than 3 decades to study *C. difficile*.

To overcome the constraint of hamster models, improved infection methods have allowed mouse models to be used to study *C. difficile* pathogenesis (X. Chen et al., 2008b; Hutton et al., 2014). Unlike hamster, neither mouse nor rat is susceptible to *C. difficile* (X. Chen et al., 2008a). This is most likely due to the colonization resistance possessed by mouse or rat

intestinal microbiota (Lawley, Clare, et al., 2009). Although gnotobiotic mice can be colonized by *C. difficile,* and displays symptoms, germ-free animals are more expensive and less amenable than conventional animals (Pawlowski et al., 2010). Therefore, mice are induced to be susceptible to *C. difficile* by disrupting the normal intestinal microflora through antibiotic treatments (X. Chen et al., 2008a). After challenge with *C. difficile*, mice develop key CDI features as in human, including diarrhea and weight loss (Hutton et al., 2014; Lawley, Clare, et al., 2009). Mouse models provide a new insight into CDI pathogenesis. Acute CDI induces weight loss, a relatively minor neutrophils infiltration, and eventually, death of aged gnotobiotic mice (Pawlowski et al., 2010). Even brief exposure to environmental spore contamination results in CDI, which demonstrates that *C. difficile* spores are effective to transmit CDI (Lawley, Clare, et al., 2009).

Zebrafish embryos have also been utilized to study TcdB toxicity *in vivo* (Hamm et al., 2006). Hamm et al found that TcdB localizes at the pericardial region. TcdB-treated embryos exhibit specific cardiovascular damage (Hamm et al., 2006). This finding could explain many observed clincal symptoms of CDI, as patients with severe CDI experience multiorgan failure, including cardiac defects.

1.2 Zebrafish model of drug discovery

1.2.1 The Advantage of the Zebrafish in Drug Discovery

Drug discovery and development is a complex, long and risky process, which involves the design and synthesis of compound libraries, biochemical and cellular assays, preclinical animal testing and ultimately clinical trial in human (Huiting et al., 2015; MacRae et al., 2015; Orry et al., 2006). The time-consuming pipeline faces increasing cost and additional challenges, such as insufficient knowledge of pathogenesis and lack of targets. (Hughes et al., 2011).

In the last decade, zebrafish has become a prominent vertebrate model for drugs identification due to its high fecundity, and morphological /physiological similarity to mammals (Lieschke et al., 2007). It has already contributed to several successful drug discoveries, such as Prohema (MacRae et al., 2015; North et al., 2007; Rennekamp et al., 2015). Proheam is a stable derivative of prostaglandin E2 (PGE2) (North et al., 2007).

Prohema improves kidney marrow recovery after irradiation injury in adult fish and also promotes reconstitution of the haematopoietic system (North et al., 2007). Prohema is in Phase II clinical trials in patients undergoing umbilical cord blood (Hagedorn et al., 2014)..

Zebrafish possess a number of unique advantages making them suitable for rapid drug discovery and development: (i)The maintenance of zebrafish is cheaper than other vertebrate models (Avdesh et al., 2012). (ii) Zebrafish produces a large number of progeny, which offers a high confidence in statistical analysis (Goessling et al., 2007). (iii)The optical transparency of zebrafish permits noninvasive imaging, which facilitates drug toxicity assays on organ development (Mathias et al., 2012). (iv)Zebrafish shows high biological similarity to human. Approximately 70% of human genes have at least one zebrafish orthologue (Howe et al., 2013). (v) Zebrafish embryos can absorb compounds solubilized in water (MacRae et al., 2015).

Screening in zebrafish is considered to be physiologically relevant (Taylor et al., 2010). Cell-based assays only provide restricted information about the absorption, distribution, metabolism, and excretion (ADME) of screening compounds (MacRae et al., 2015). A large number of compounds are excluded at the late stage of animal testing, due to failure to meet standards of ADME *in vivo* (Huiting et al., 2015). Zebrafish screens are carried out in living embryos, offering an advantage to test compounds in the context of a whole organism (Rennekamp et al., 2015). To perform drug screening in zebrafish, compounds must be easily absorbed and eventually reach the targeted organs. In addition, drug screening in zebrafish provides an insight into toxicity of selected compounds during the early process of drug discovery (Zon et al., 2005). These facts allow compounds screened from zebrafish to be rapidly reproduced in mammalian models.

Fluorescent labeling of a specific cell type is frequently used in the zebrafish community, with thousands of fluorescent-labeled-reporter fish lines available. The combination of transparent embryos and florescent labeling strategy makes zebrafish an ideal model to conduct drug screens. Several successful chemical screens have been carried out in zebrafish (Ridges et al., 2012; Saydmohammed et al., 2011; Wang et al., 2015). Wang et al. created a double fluorescent reporter line to search for compounds that induce pancreatic β-cell

growth: a yellow fluorescent protein (PhiYFP) glows when new β-cells form, and red fluorescent protein (tagRFP) glows when pancreatic δ-cells are stimulated. 24 drugs were identified and confirmed from a collection of 3348 compounds, most of those candidates are approved for clinical use in human. Until 2015, more than 65 compound screens have been reported in the literature (MacRae et al., 2015).

1.2.2 Basic process of compound screens in zebrafish

The goal of compound screens is to identify a great number of small molecules which can 'hit' or modulate the endogenous or exogenous zebrafish proteins (W Patrick Walters et al., 2003). Therefore, the success of the compound screens greatly relies on the small-molecule library (Orry et al., 2006). A good library should include as much chemical diversity as possible to maximize hit rates. Better knowledge of target structure or drug-target structure enables drug discovery more easily and efficiently. With the DIVERSet E library designed by Chembridge, Peterson et al identified two structurally related suppressors of aortic coarctation from over 5,000 small molecules (Randall T Peterson et al., 2004).

Drug screens can be divided into two ways: target-based screening and phenotype-based screening (Figure 6). The target-based approach is to discover compounds that modulate defined signaling pathways or specific molecular targets (Sams-Dodd, 2005). Most target-based screens have very clear readouts and relatively high screening throughput. This approach was the mainstay used in both the pharmaceutical industry and academic translational research center (Seay et al., 2015). However, efficiency of target-based screening is questioned in light of declines in pharmaceutical R & D efficiency (Williams et al., 2016). Although target-based screening can be very efficient to search for novel compounds for a validated target or signaling pathway, off-target effects, or side effects are usually not evaluated (Zon et al., 2005). Furthermore, most target-based chemical screens are carried out in cell culture or *in silico*, in which might not hold true *in vivo*.

To overcome the shortcomings of target-based screening, phenotype-based screening is utilized. Phenotype-based screening is approached by evaluating phenotype rescue of a specific disease, which is more physiologically relevant, but not target-related (Competition et al., 2008). Generally, a disease model with a characteristic symptom is set up in zebrafish,

this can then be used for compound screens in an unbiased means. Zebrafish phenotype-based screens are often combined with other analyses. For example, safety evaluation of the drug substance which can discover compounds that produce a desired treatment, while parsing out compounds with undesirable qualities (MacRae et al., 2015). In 2000, R T Peterson et al demonstrated firstly the feasibility of using zebrafish embryos for bioactivity compound screening (R T Peterson et al., 2000). They proposed a concept called 'chemical genetic', where zebrafish embryos or larvae are arrayed into multi-well microtitre plates, and small-molecule libraries are robotically dispensed into the media (Figure 7) (R T Peterson et al., 2000). This approach can target every gene in the genome.

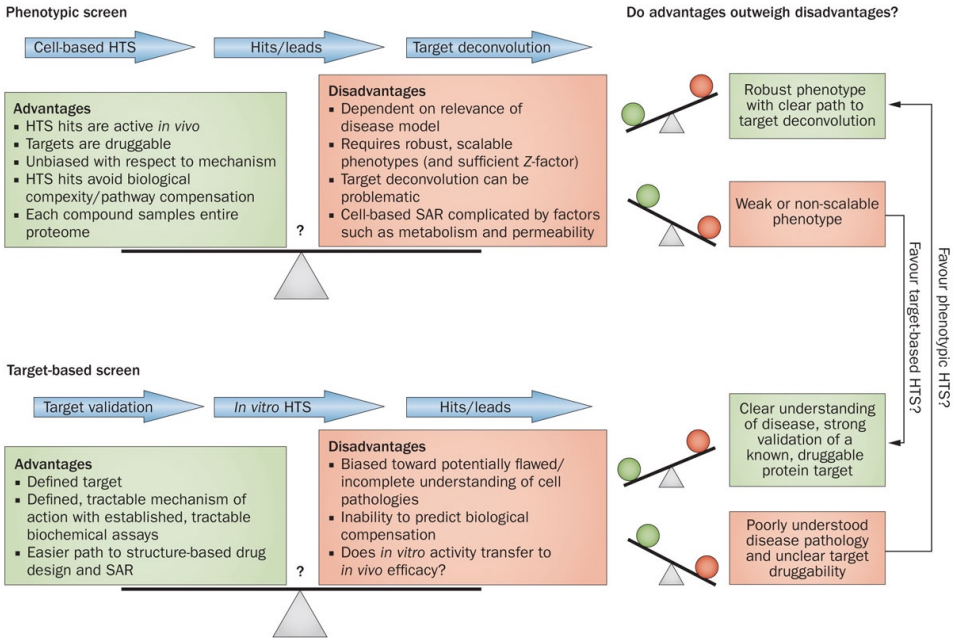

Figure 6 The pros and cons of target-based and phenotypic drug discovery.

Phenotypic screens and *in vitro* target-based screen have advantages and disadvantages. Understanding of the disease, validation of a given target, and robustness of a screening assay all factor into the choice of technique. In either approach, at least one roadblock must be overcome to validate hits and support their further development or early lead compounds. Abbreviation: SAR: structure-activity relationship. From Khurana et al., 2015.

The new techniques developed in biological research, including full genome sequencing and metabolomics analysis, enable researchers to investigate diseases at the molecular level (J. C. Davis et al., 2009). This brings a new insight into molecular mechanisms of phenotype-

based screening (J. C. Davis et al., 2009; Goessling et al., 2007). This notion also enables the discovery of new drugs by target-based approach which are more physiologically relevant.

Over the past two decades, high-throughput screening (HTS) has gained widespread popularity in biological and chemical science, which has also become a common method applied in the pharmaceutical industry (Macarron et al., 2011). HTS employs automation to measure biological/biochemical activity of a large number of drug-like compounds in living cells, or whole-organism rapidly (Hughes et al., 2011). Transparent embryo and fluorescent labeling technique make fluorescence-based screens in zebrafish a perfect system for HTS (Figure 7) (Walker et al., 2012). Fluorescent read-out enables high speed screening by performing the assay in multi-well plates processed by automated confocal laser scanning microscopy (Hughes et al., 2011). Fluorescent-based assays produce not only quantifiable outputs, but also qualifiable phenotype of fluorescent labeling cells. Furthermore, several cell types/ biological processes indicated by different fluorescent proteins/ fluorescence based bio-sensors within the same zebrafish, such as apoptosis/ necrosis, can be analyzed simultaneously (Huiting et al., 2015).

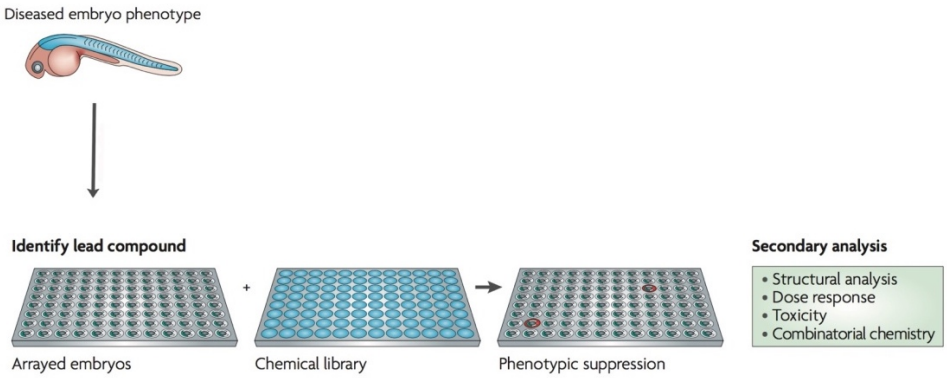

Figure 7 The fluorescence-based drug discovery in zebrafish.

Once a zebrafish disease model is identified, a chemical-suppression screen can be implemented. Characterized phenotypes can be screened against small-molecule libraries. Zebrafish embryos or larvae are arrayed in 96-well plates and different concentration of compounds are robotically added into the raising media in each well. Throughput can be assessed directly by using fluorescent read-outs. Adapted from Lieschke et al., 2007.

1.3 Innate immune response to CDI

The innate immune system is the first defense against the pathogenic microorganisms in the

body, which also plays a critical role in shaping the adaptive immune response (Sickles et al., 2017). The innate defence against *C. difficile* includes gut microbiota, mucus barrier, the intestinal epithelium, and the mucosal immune system (Madan et al., 2012). The *C. difficile* toxins have multiple effects on all innate immune defences, including the damage of intestinal epithelial cells and the recruitment of immune cells into the intestine (Abt et al., 2015). In fact, before *C. difficile* encounter intestinal epithelial cells, they firstly contact with intestinal microbiota. In addition to preventing pathogen colonization in the intestines, gut microbiota also regulate and shape the immune response to pathogenic bacteria (Perez-Lopez et al., 2016). The immune cells include macrophages, neutrophils, eosinophils, basophils, and natural killer cells, among which neutrophil and macrophage are key components in numerous infectious diseases (Sekirov et al., 2010).

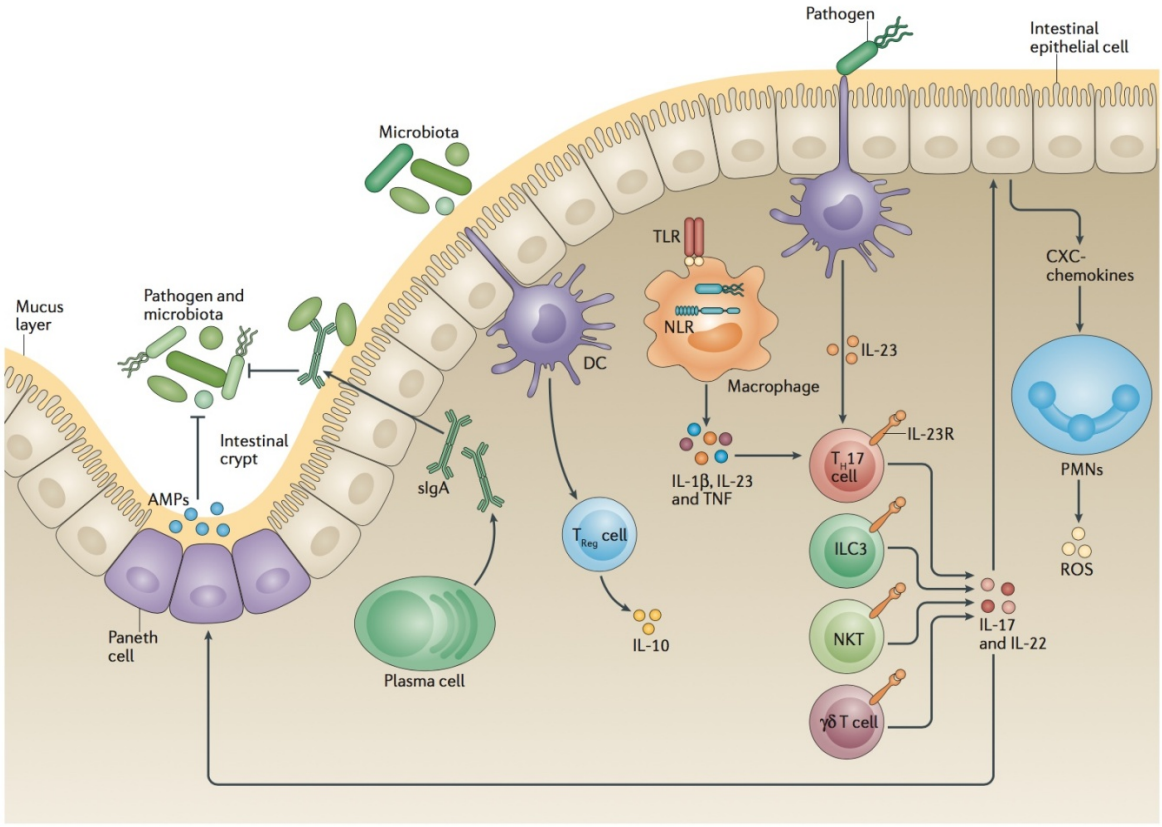

Figure 8 General overview of mucosal immunity to intestinal pathogens and microbiome

Dendritic cells (DCs) sample intestinal microorganisms. Upon sampling the resident microbiota, DCs induce T (TReg) cells to secrete interleukin-10 (IL-10). Resident macrophages and DCs are activated by pathogens and secrete IL-23, which stimulates several subsets of T cells including T helper 17 (T_H17) cells, γδ T cells, natural killer (NK) cells, natural killer T (NKT) cells. These cell subsets promote amplification of the host response by stimulating the intestinal epithelium to secrete CXC-chemokines that attract neutrophils. Plasma cells also

control the microbiota and pathogens via secretory IgA (sIgA).; NLR, NOD-like receptor; PMNs, polymorphonuclear cells; ROS, reactive oxygen species; TLR, Toll-like receptor; TNF, tumour necrosis factor. From Perez-Lopez et al., 2016.

1.3.1 Gut microbiota, bile acids and mucosa

The gut microbiota refers to an enormous population of microorganisms, including bacteria, fungi, archaebacteria, viruses, and protozoans that colonize in the human gastrointestinal tract (GI) (Sekirov et al., 2010). Over the last decade, a combination of innovative metagenomics analysis and conventional approach, have greatly expanded our knowledge of the relationship among the microbiota, the host, and pathogenic bacteria (Thursby et al., 2017). More evidences proved that in addition to providing nutrients, microbiota also play important roles in the immune development, neurological diseases and inflammatory bowel diseases (Hooper et al., 2012; Sartor et al., 2012; Sommer et al., 2013).

Protection of the host intestine from exogenous bacteria by commensal microorganisms, termed colonization resistance, is first described in 1950s (Vollaard et al., 1994). Recent studies indicated that microbiota-mediated colonization resistance prevent the invasion by pathogenic bacteria, particularly pathogens that are broadly resistant to antibiotics, such as *C. difficile* (Buffie et al., 2013). Change of the composition of the gut microbiota might lead to pathological outcomes (Sekirov et al., 2010). For instance, Ferreira et al found that the disruption of the microbiota after antibiotic treatments makes mice more susceptible to *Salmonella enterica* serovar Typhimurium (Ferreira et al., 2011). Another prominent example is CDI, which can be induced when the diversity of microbiota is reduced in the host. CDI occurs when the natural flora is disrupted by antibiotics. Antibiotic abuse is still regarded as the major risk factor for CDI (Figure 9) (Longo et al., 2015; Rupnik et al., 2009). Due to loss of colonization resistance, antibiotic induced CDI has been demonstrated in hamster and mice (X. Chen et al., 2008b; Razaq et al., 2007). Notably, different composition of the intestinal microbiota enables host resistance to different pathogenic species more easily, and it also affects inflammation response (Belkaid et al., 2014; Ferreira et al., 2011). Utilizing the microbiota to combat CDI represents an important therapeutic method, with many promising clinical results obtained from treatment for *C. difficile* colitis (van Nood et al., 2013).

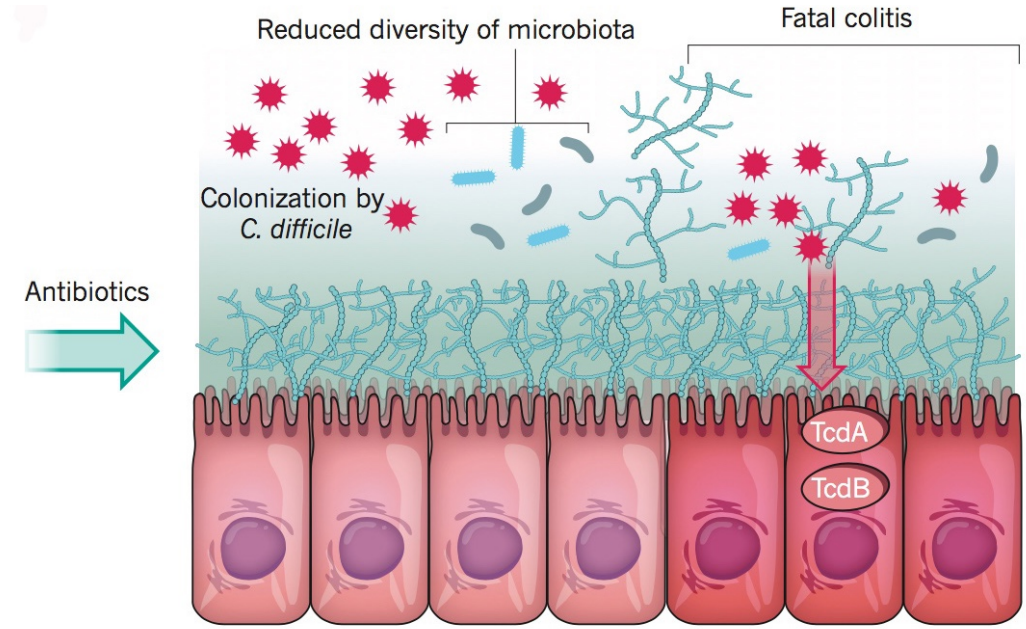

Figure 9 Treatment with antibiotics decreases the diversity of the microbiota and leads to expansion of the *C. difficile* population.

Toxins that are released from *C. difficile* (TcdA and TcdB) enter and damage the cells of the epithelium, which leads to inflammation (colitis) and cell death. From Bäumler et al., 2016.

Some mechanisms have been proposed to explain why antibiotic induced change in the gut microbiota leads to CDI, for instance, the niche exclusion and unbalance of bile acid metabolism (Figure 10) (Britton et al., 2012).

The niche exclusion is proposed based on the fact that hospitalized patients with asymptomatic colonization of *C. difficile* displays a lower risk to develop subsequent *C. difficile* associated disease (CDAD) (Shim et al., 1998). Studies in hamsters proved that pre-colonization with even nontoxigenic *C. difficile* protects hamsters from lethal toxigenic *C. difficile* (Merrigan et al., 2003; Susan P. Sambol et al., 2002). One mechanism of *C. difficile* colonization resistance might be that commensal microflora outcompetes *C. difficile* colonization by limiting carbon sources that favours *C. difficile* growth (Britton et al., 2012). Another study demonstrated that colonization of gnotobiotic mouse gut with a single *Bacteroides* species prevents subsequent colonization of an isogenic strain (S. M. Lee et al., 2013). Whitake et al proved that a successfully colonized RFP-expressing *Bacteroides* strain outcompeted a sequential GFP-expressing strain in intestinal crypts, where *C. difficile* is able

to reproduce (Whitaker et al., 2017). These findings suggest that colonization of symbiotic bacteria in specific intestinal structure is a key step to prevent invading pathogens.

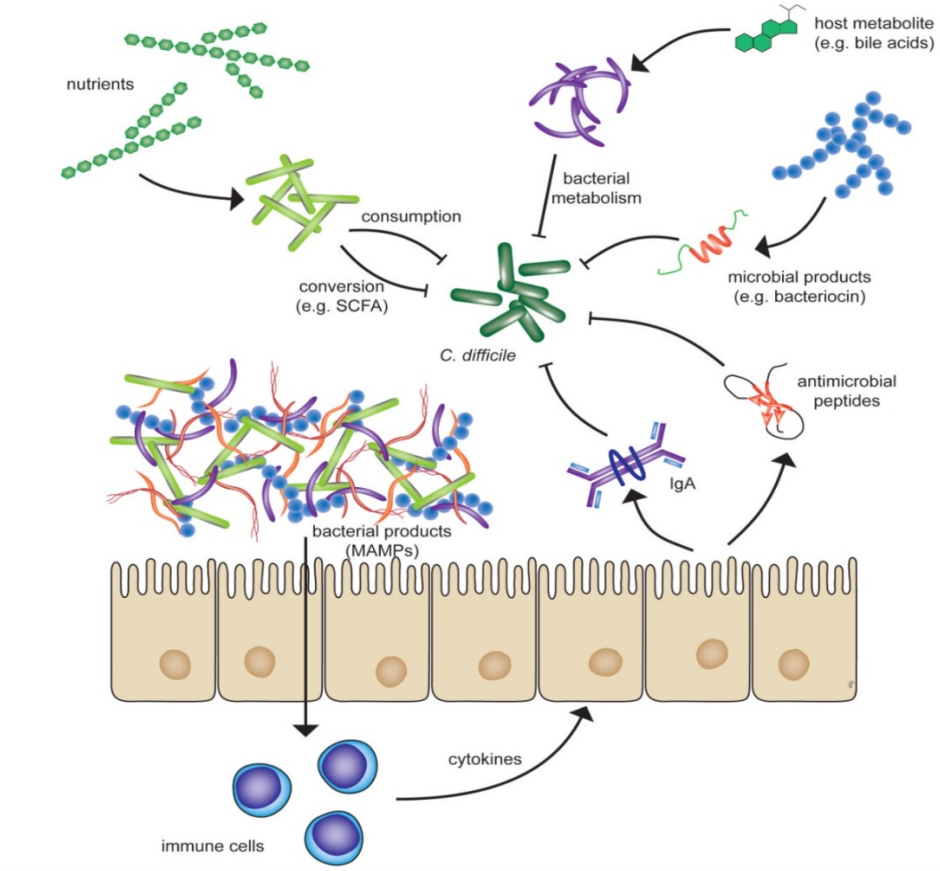

Figure 10 Potential mechanisms by which the indigenous microbiota can mediate colonization resistance against *C. difficile*.

Specific members of the microbiome can either directly, or indirectly interfere with the colonization of *C. difficile* in the gut. Direct inhibition can occur via competition for nutrients or by primary microbial products that inhibit *C. difficile*. Indirect inhibition can occur via interaction between the gut microbiota and the host that results in the host products that can control *C. difficile* colonization and proliferation. MMAP: microbial-associated molecular patterns. SCFA, short-chain fatty acids. From Britton et al., 2012.

Another proposed mechanism is that the transformation of bile acids affects *C. difficile* spore germination, and the vegetative cell growth (Figure 11) (Bäumler et al., 2016; Britton et al., 2012). Bile acids are water-soluble, amphipathic biological detergents that are synthesized exclusively in the liver, and then secreted into the intestinal lumen (Figure 11A). Cholate (CA) and chenodeoxycholate (CDCA) are the two primary bile acids in human and rodent (Ridlon, 2005). The host further metabolizes primary bile acids to form conjugated bile acids, such as

glycocholate (GCA) and taurocholate (TCA). The major function of bile acid is to emulsify and solubilize fat. Besides, they also possess antimicrobial properties. When primary bile acids enter the intestine, they induce the expression of antimicrobial peptides, which aids the host defence system against pathogens (Inagaki et al., 2006). Importantly, some bacterial species that reside in the caecum and colon dehydroxylate the 7α-carbon of CA and CDCA to produce secondary bile acids, deoxycholate (DCA) or lithocholate (LCA), respectively (Ridlon et al., 2005). GCA and TCA can be de-conjugated to produce unconjugated counterparts by bile salt hydrolases (BSH), which are secreted by the commensal bacteria in the gut (Abt et al., 2016). Mammals also rely on the intestinal microbiota to synthesize essential amino acids and vitamins, and to break down undigested food such as plant polysaccharides (Bäckhed et al., 2005).

In 1982, Wilson *et al*. demonstrated that addition of TCA to cycloserine cefoxitin fructose agar (CCFA) media, which is used to culture *C. difficile*, greatly stimulated germination of *C. difficile* spores (Wilson et al., 1982). When antibiotic-induced mice are challenged with *C. difficile*, Theriot et al showed that the level of TCA and other tauro-conjugated bile acids increases, while the level of secondary bile acid deoxycholate decreases (Theriot et al., 2014). Darkoh et al. purified native TcdA and TcdB from culture supernatants, and characterized toxins activities by Cdifftox activity assay in 2011, where they found that TCA inhibits the activities of *C. difficile* toxins *in vitro* (Darkoh et al., 2011). However, it is well accepted that TCA triggers *C. difficile* germination and permits outgrowth of vegetative cells (Theriot et al., 2015). Various efficiency of primary bile acids to stimulate germination *in vitro* are also documented in clinical isolates of *C. difficile* (Carlson et al., 2016; Heeg et al., 2012).

Antibiotic treatment with metronidazole and vancomycin is still considered as an effective method to treat CDI. However, this therapy further disrupts the gastrointestinal microbiota composition, and is associated with more than 20% of case recurrence (Figueroa et al., 2012). Despite that primary bile acids initiate *C. difficile* germination, some secondary bile acids act as inhibitors of spore germination and vegetative growth of *C. difficile* (Sorg et al., 2008, 2010; Wilson, 1983) . Many secondary bile acids are reported to interfere the growth of *C. difficile in vitro*, for instance, hyodeoxycholate (HDCA), ursodeoxycholate (UDCA),

deoxycholate (DCA) and lithocholate (LCA) (Carlson et al., 2016; Heeg et al., 2012; Sorg et al., 2008; Weingarden et al., 2014; Winston et al., 2016). Buffie et al showed that restoration of secondary bile acid by *Clostridium scindens*, a bile acid 7a-dehydroxylating intestinal bacterium, helps to regain colonization resistance against *C. difficile* in mice (Buffie et al., 2014). More recent *in vivo* studies also supported this concept (Theriot et al., 2015; Weingarden et al., 2014). In summary, the previous and current studies suggest that secondary bile acids have a direct impact on the *C. difficile* life cycle *in vitro, ex vivo,* and *in vivo* (Winston et al., 2016). Bile acid might provide a novel approach for the treatment of CDI.

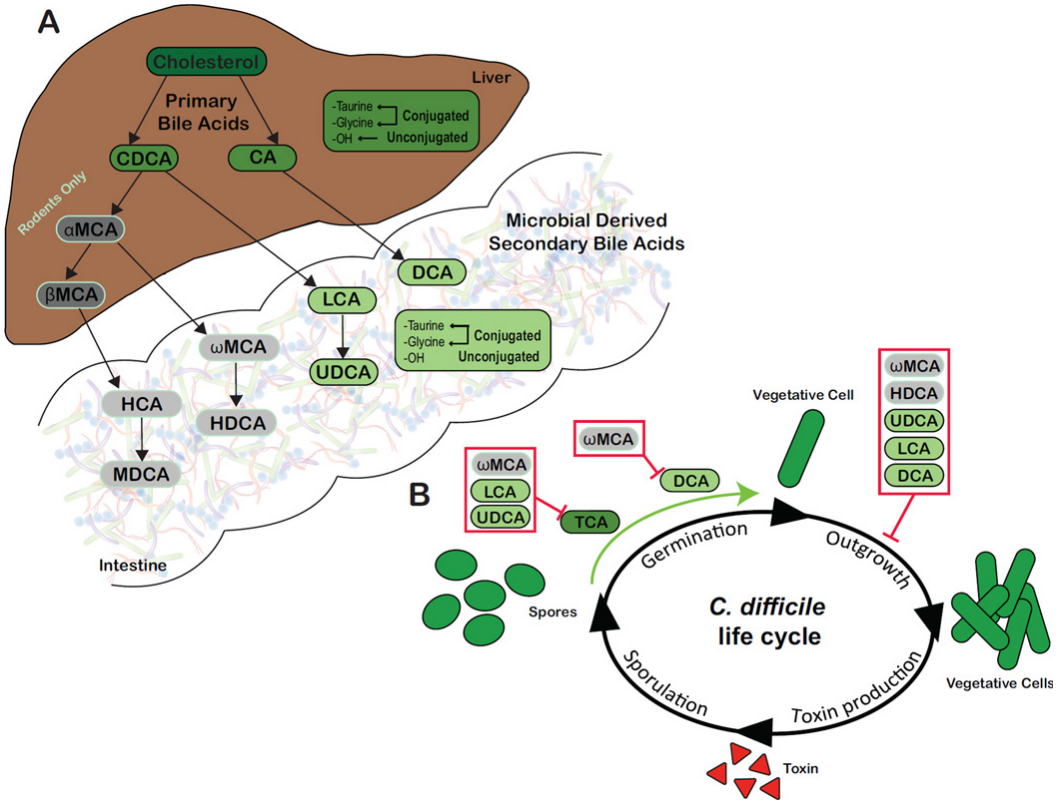

Figure 11 Formation of microbial derived secondary bile acids

A) Production of microbial derived secondary bile acids. Primary bile acids, chenodeoxycholate (CDCA) and cholate (CA) are synthesized from cholesterol by hepatocytes in humans and rodents. Within the GI tract, the gut microbiota can convert host derived primary bile acids (represented in darker shades) into secondary bile acids (represented in lighter shades). Microbial derived secondary bile acids can also be unconjugated or conjugated to taurine or glycine. B) Effects of various secondary bile acids on the life cycle of *C. difficile in vitro*. TCA is essential for germination of *C. difficile* spores (green arrow). TCA-mediated spore germination can be blocked by specific secondary bile acids (red box). DCA can also stimulate germination of *C. difficile* spores, a process that is inhibited by ωMCA in mice. Outgrowth of *C. difficile* vegetative cells is inhibited by multiple

secondary bile acids (red box). Abbreviations: CA, cholate; CDCA, chenodeoxycholate; DCA, deoxycholate; HCA, hyocholate; HDCA, hyodeoxycholate; LCA, lithocholate; MDCA, murideoxycholate; UDCA, ursodeoxycholate; αMCA, α-muricholate; βMCA, β-muricholate; ωMCA, ω-muricholate. From Winston *et al*., 2016.

1.3.2 Innate immune cells: Neutrophil

Neutrophils are the most abundant granulocytes in circulation, which are critical for host innate immune defence (Amulic et al., 2012). Neutrophils were believed to survive from 6 to 8 hours in the bloodstream. However, recent evidence indicated that they are able to survive even longer, 13–19 hours for human neutrophils (Lahoz-Beneytez et al., 2016). Circulating neutrophils are pre-programmed to die by apoptosis, which are further cleared by macrophages in the liver, spleen, and bone marrow (McCracken et al., 2014). This prevents toxic neutrophil contents from inducing harmful inflammatory response (Fox et al., 2010).

Highly abundant neutrophils in circulation are keeping with the fact that these cells are the first responders to be recruited to the sites of inflammation, playing a primary role in the clearance of pathogens (C Nathan, 2002). Typically, neutrophils phagocytose pathogens, and also produce antibacterial proteins and/or cytokines to attract other myeloid cells (Amulic et al., 2012).

An intestinal inflammatory response with neutrophil infiltration and tissue damage is one characteristic of acute CDI (Ciarán P. Kelly et al., 2011). Neutrophils do play an important role in the defence of *C. difficile* (Figure 12). But the exact role of neutrophils in the context of CDI remains unclear.

Neutrophil infiltration is one of the major pathological feature in CDI and is critical for the early defence against *C. difficile* (Madan et al., 2012). Jarchum et al found that depletion of neutrophils results in markedly increased mortality followed infection in mice (Jarchum et al., 2012). Likewise, *C. difficile*-induced NOD1 activation leads to increased chemokine production and neutrophil recruitment. *NOD1*$^{-/-}$ mice displays less neutrophil recruitment, and enhanced lethality, which is accompanied by impaired *C. difficile* clearance (Hasegawa et al., 2011). Multiple signalling pathways and chemokines, are involved in neutrophils recruitment after CDI, for instance, the MyD88-CXCL signalling pathway and chemokine, Interleukin-23 (IL-23) (Jarchum et al., 2012; McDermott et al., 2016). In a study of hematopoietic stem cell

transplants, researchers found that individuals with neutropenia are more likely to have recurrent CDI than non-neutropenic patients (A. M. Huang et al., 2014). Therefore, neutrophil recruitment seems to be a protective mechanism to the host.

However, inhibition of neutrophils infiltration to the intestine by blocking CD18, a neutrophil adhesion molecule, results in a reduction of TcdA-induced tissue disruption in rabbit (Ciaran P. Kelly et al., 1994). Similarly, TcdA-induced neutrophil recruitment is augmented in CX3CR1 $^{-/-}$ (inflammatory chemokine) mice, which increases disease severity (Inui et al., 2011). In patients with *C. difficile* colitis, a higher neutrophil level is associated with more severe disease and increased mortality (Koon et al., 2013).

Collectively, these studies reveal that neutrophils act as double-edged swords in CDI, representing the critical first defense against *C. difficile* while possessing the potential to induce tissue damage.

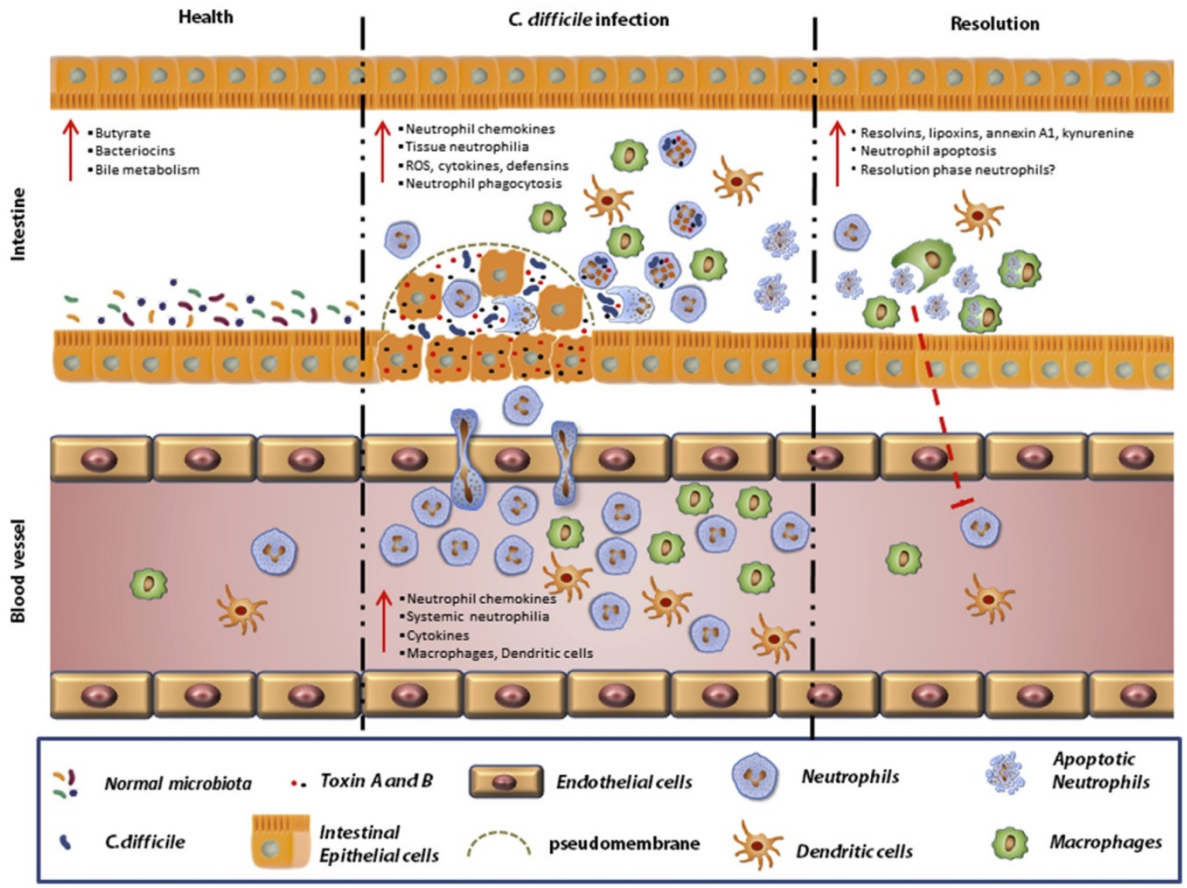

Figure 12 Innate immune-mediate defences against *C. difficile*.

The acute immune response to *C. difficile* is initiated by toxin-mediated damage and disruption of the epithelial integrity. Intoxicated intestinal epithelial cells and resident innate immune cells release pro-inflammatory chemokines and cytokines, which leads to the recruitment of more neutrophils and macrophages. Infiltrated neutrophils generate inflammatory mediators, perform phagocytosis of the pathogen and toxins, and in severe cases lead to pseudomembranous colitis. Apoptotic neutrophils and subsequent phagocytosis by macrophages kicks in the resolution phase. Phagocytosis of apoptotic neutrophils coincides with surge in pro-resolution molecules and reduction in inflammatory cytokines and chemokines leading to tissue and systemic homeostasis.

Although neutrophil-mediated inflammation is critical for the host defence, it is also crucial to clear the neutrophils after they exert their pro-inflammatory effects (Jose et al., 2016). Regulation of neutrophil apoptosis is essential for regulating neutrophil-induced tissue damage or promote wound healing (Carl Nathan, 2006). Defective apoptosis or failure of the clearance of neutrophils leads to secondary deleterious tissue injury (Lucas et al., 2014). As terminally differentiated cells, neutrophils quickly undergo spontaneous apoptosis after their release into the blood stream (B Geering et al., 2011). The initial trigger of apoptosis remains unclear. Unresolved neutrophils inflammation or delayed neutrophils apoptosis is associated with many diseases, like sepsis, and rheumatoid arthritis (Munoz et al., 2010).

Previous researches have shown that neutrophils apoptosis can be driven by cyclin-dependent kinase (CDK) inhibitors, such as roscovitine (Strowig et al., 2012). Hoodless et al reported that CDK9 inhibitor (AT7519, flavopiridol) induces neutrophils apoptosis *in vitro* and promotes resolution of inflammation in rodent models (Hoodless et al., 2016). In zebrafish tailfin injury model, the inhibitor enhances resolution of inflammation by reducing neutrophil number via apoptosis (Hoodless et al., 2016). Lipoxins A_4 (LXA_4) mediator promotes resolution of inflammation through increasing phagocytosis of apoptotic neutrophils by macrophages (Godson et al., 2000). In the clearance of apoptotic neutrophils, there are two routes: systemic recirculation and local death by phagocytosis of recruited macrophages (Serhan et al., 2007). Once phagocytosis is completed, the macrophages exit the inflamed site and acute inflammation is resolved (Serhan et al., 2007). Similar cooperation of macrophage and neutrophil might exist in CDI but have not been investigated.

1.3.3 Innate immune cells: Macrophages

Much attention in inflammation research has focused on the recruitment of leukocytes (Muller, 2003). However, a rapid immune response requires sentinel cells at the site of inflammation. Such cell type is represented by mast cells and macrophages (C Nathan, 2002).

Macrophages are classified as part of the mononuclear phagocytic system, which are generated from bone marrow (Murray et al., 2011). They are characterized by avid phagocytosis that ingests and degrades dead cells and debris, and organizes inflammatory processes (Varol et al., 2015). Monocytes, dendritic cells (DCs), macrophages, along with neutrophils, and mast cells are recognized as professional phagocytic cells (Murray et al., 2011). When mature monocytes migrate from peripheral circulation, and extravasate through endothelium, they differentiate into tissue-resident macrophages, as well as DCs (Gordon et al., 2005).

The GI hosts the largest pool of macrophages in the body, which are essential for maintaining mucosal homeostasis in response to pathogens or inflammation (Mowat et al., 2011). As described above about the phagocytosis of apoptotic neutrophils (Figure 12), macrophage activation is an important step in the pathogenesis of *C. difficile* toxin-induced colitis (Linevsky et al., 1997).

The role of macrophages has mainly been acquired from *in vitro*, or *ex vivo* studies using human or mouse macrophage cell lines. These studies showed that *C. difficile* toxin stimulates the secretion of macrophage-derived chemokines. Both TcdA and TcdB can activate IL-8 production by macrophage-differentiated THP-1 cells (Linevsky et al., 1997). *C. difficile* toxins also trigger interleukin-1β (IL-1β) secretion and caspase-1 activation in both mouse macrophages and human colon biopsy specimens by ASC-containing inflammasome (Ng et al., 2010). Similarly, the murine macrophage cell line RAW 264.7 produces high amount of secreted TNF-α after treatment with either TcdA or TcdB (Sun et al., 2012). In another report, using the RAW 264.7 cell line, researchers found that despite efficient phagocytosis of *C. difficile* spore by RAW 264.7 cells, spores are able to survive and produce cytotoxic effects on RAW 264.7 cells themselves (Paredes-Sabja et al., 2012). However, the exact role of macrophage is shrouded in mystery.

As described, animal models have been used for CDI research, such as hamster, and pig. However, there are not so many *in vivo* reports about the role of macrophage in CDI *in vivo*. Hirota et al developed a novel mouse model that introduced intrarectal instillation of *C. difficile* toxins into the mouse colon (Hirota et al., 2012). They found that TcdA/B trigger the infilatration of macrophage into the colinc tissue in a time-dependent manner, enhance epithelial barrier permeablitly and increase intestinal epithelial cell death, which is a hallmark of human CDI (Hirota et al., 2012).

Therefore, the macrophage response plays critical roles in the host immune response to *C. difficile* and resolution of inflammation, but the precise mechanism of macrophages in CDI is less understood. Furthermore, the behavior and cooperation between neutrophils and macrophages remains largely speculative.

1.4 LexA/lexAop expression system and ATTACTM ablation system

1.4.1 LexA/lexAop system

Spatial and temporal control of transgene expression is essential for the functional study of genes, subcellular structures monitoring, and selective cell ablation. Binary expression systems such as the Gal4-UAS, the LexA/lexAop and the Q-system offer powerful tools to manipulate target tissue in a targeted manner.

The Gal4-UAS system is derived from *Saccharomyces cerevisiae*. Gal4 is a transcription factor that contains a DNA-binding domain and a transcription activation domain. Gal4 binds UAS and activates transcription of its target gene placed downstream of the UAS sites (Duffy, 2002; Traven et al., 2006). Gal4-UAS turns to be the workhouse of *Drosophila* genetics firstly (del Valle Rodríguez et al., 2012), and it has also been successfully adapted to zebrafish (Halpern et al., 2008). Hundreds of Gal4 driver stains or UAS strains have been established and are available, each of which shows distinct expression profile.

Another binary expression system that has been used in zebrafish is LexA/lexAop system. With the same principle of Gal4-UAS, the LexA/lexAop expression system consists of two main components: the transcription activator of LexA is expressed in a cell type specific pattern,

and coupled with transgenes expression under the control of *LexA* operator DNA fragment/s (lexAop) to achieve a precise temporal and spatial control of gene expression (del Valle Rodríguez et al., 2012). The LexA and LexAop, like Gal4-UAS, is also absent in higher eukaryotes. Therefore, it is unlikely to bind to the *cis*-elements of endogenous promoters in zebrafish (Emelyanov et al., 2008).

LexA protein is a bacterial repressor, which regulates SOS response to DNA damage in *Escherichia coli* (John W. Little et al., 1982). When the DNA is damaged, the SOS response is induced. The SOS system is controlled by two regulatory proteins, a repressor LexA and an inducer RecA (Butala et al., 2009). The DNA damage signal reversibly activates the protease activity of RecA. Then RecA mediates a self-cleaving activity in LexA, which inactivates the LexA (Butala et al., 2009; J. W. Little, 1991; John W. Little et al., 1982). In consequence, the SOS regulon is induced and the DNA damage is repaired (J. W. Little, 1991).

The LexA protein is a 202-amino-acid protein consisting of three domains: an N-terminal DNA-binding domain, a dimerization domain, and A latent protease domain (Figure 13) (A. P. P. Zhang et al., 2010). The first two domains are connected by a short flexible linker, with autoproteolytic sites within the C-terminal domain (Butala et al., 2009). In *E. coli* or *in vitro*, LexA protein binds as dimer with various affinities to single or multiple *lexAo*p sites (J. W. Little, 1991; Mohana-Borges et al., 2000). Since LexA binds operators with different affinities, different strain-derived operators were developed. Lai et al have developed *colE1*-binding lexAop with a Drosophila LexA reporter, which turned to possess one of the highest affinities to LexA (Lai et al., 2006). Although the *colE1*-drived motif permits strong expression, the toxicity and leaky expression was found Drosophila (Yagi et al., 2010). Yagi et al tested other LexA-binding sites from *sulA, umuDC,* or a synthetic *lexA* operator. They identified that the *sulA*-derived LexA-binding motif showed strong transgene expression, as well as no expression in the LexA absent situation (Yagi et al., 2010).

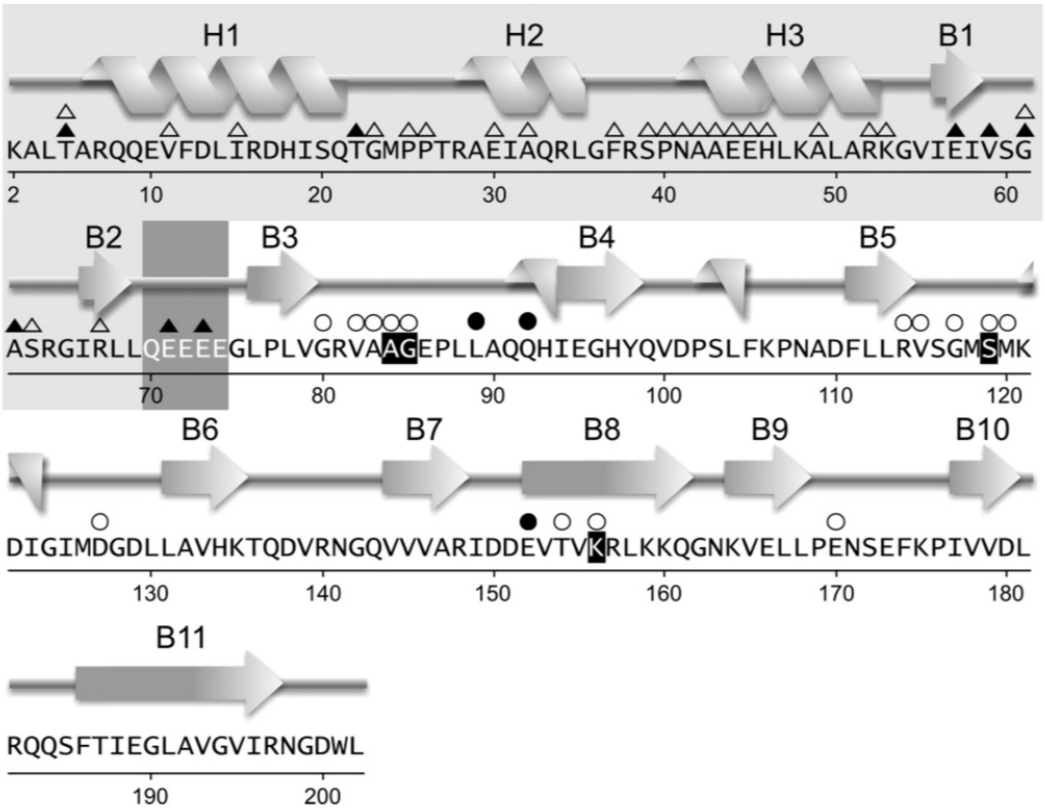

Figure 13 Sequence of LexA protein and its secondary structures.

The DNA binding domain (NTD) is in light grey. The hinge region is shaded dark grey, followed by the carboxy terminal domain (CTD), dimerization domain. Black shading highlights residues Ser119 and Lys156 (the catalytic dyad) and Ala84 and Gly85 (which flank the peptide bond that is cleaved by the catalytic dyad). The triangles above residues indicate positions of substitutions that enhance (solid symbols) or prevent (open symbols) DNA binding. From Butala et al., 2009.

Ever since the LexA/lexAop interaction was elucidated (Butala et al., 2009), the potential of applying this binary system to manipulate gene expression *in vivo* has been well appreciated (Figure 14). It is reported that the LexA linked to the Gal4 activation domain or the transactivation domain VP16 from the herpes simplex virus is able to obtain the expression of transgenes in distinct pattern in *Drosophila* (Lai et al., 2006; Szüts et al., 2000). In Gal4-UAS applied *Drosophila*, LexA/lexAop is primarily used to manipulate additional gene expression simultaneously (del Valle Rodríguez et al., 2012).

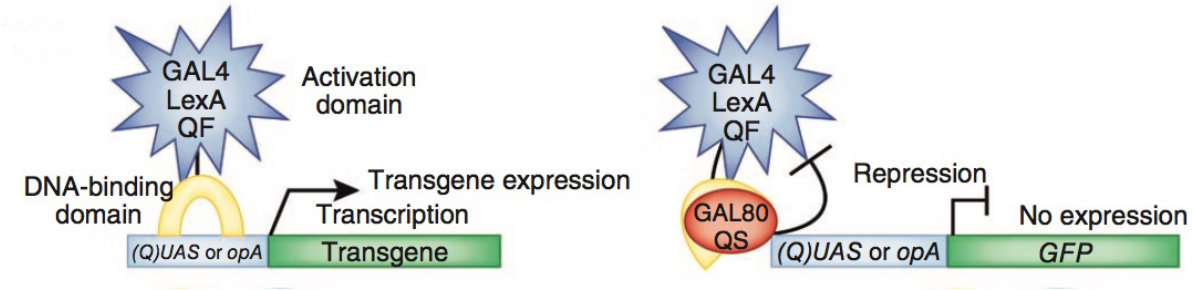

Figure 14 Binary expression systems

Two-component expression systems such as GAL4-*UAS*, LexA/lexAop or QF-*QUAS* consist of a transcriptional activator expressed in a specific pattern and a transgene under the control of a promoter that is largely silent in the absence of the transcriptional activator sometimes. These systems can be repressed by specific molecules such as GAL80 or QS. From del Valle Rodríguez et al., 2012.

In 2008, Emelyanov et al demonstrated that the LexA-based transcriptional system can be used in zebrafish *in vivo* (Emelyanov et al., 2008). In this report, the LexA DNA-binding domain is fused to a truncated ligand-binding domain of the progesterone receptor, and the activation domain of human p65 protein to compose a hybrid transcription factor, LexPR transactivator (Figure 15). Transgene expression is strictly controlled and induced in embryos and adult fish through the administration of mifepristone in media (Emelyanov et al., 2008). Mazaheri et al reported that they modified the LexPR (ΔLexPR) activator, and placed it under the control of a promoter to acquire a constitutive activation in the central nervous system of zebrafish (Mazaheri et al., 2014).

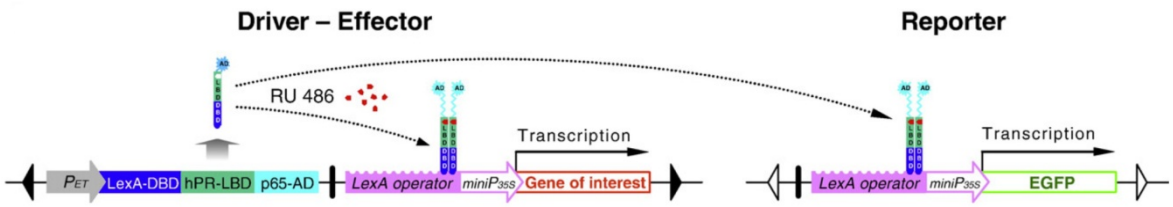

Figure 15 Schematic representation of the mifepristone-inducible LexA-based gene expression system

Schematic representation of the mifepristone-inducible LexA-based gene expression system. The LexPR driver-reporter binary cassette contains two transcription units: the gene encoding a chimeric LexPR transactivator (Lex^{DBD}-$PR^{LBD\Delta}$-$p65^{AD}$) under the control of an enhancer-trap promoter (P_{ET}) and the EGFP reporter gene under the control of a minimal promoter ($miniP_{35S}$) fused to a synthetic LexA operator. The LexPR transactivator binds to the LexA operator sequence to activate the transcription of the downstream genes only in the presence of

mifepristone (RU 486). From Emelyanov et al., 2008.

The availability of Gal4-UAS and LexA/lexAop system in zebrafish allows us to perform multicolour imaging or manipulate two cell types simultaneously in the same organism.

1.4.2 ATTAC^{TM} ablation system

Targeted cell ablation is a useful method to study cell function, interaction, and regeneration in the context of a whole organism. In addition, recovery analysis might uncover new cellular and molecular mechanisms in the regeneration process.

To ablate a specific cell type in a spatially and temporally controlled manner, several inducible genetic ablation methods have been developed. The nitroreductase (NTR)-mediated technique has been widely used in zebrafish in a specific and inducible manner (Pisharath et al., 2007). This technique relies on NTR that can convert prodrug metronidazole into cytotoxic metabolite (Curado et al., 2007). However, as metronidazole is an effective agent for the treatment of CDI, this method cannot be used in this study.

Our group recently developed a novel ablation system based on tamoxifen-inducible Caspase 8 activity, refer to as ATTAC^{TM} ablation system (Weber et al., 2016). In this approach, Caspase 8 is fused to a mutated tamoxifen-interacting estrogen receptor ligand-binding domain (ER^{T2}), Caspase8-ER^{T2}, that renders Caspase 8 active by tamoxifen-induced dimerization (Figure 16) (Chu et al., 2008). The ER^{T2} mutant prevents the binding to natural ligand but retains normal affinity to the synthetic ligand, 4-hydroxy tamoxifen (4-OHT) (Littlewood et al., 1995). After 4-OHT treatment, Caspase8ER^{T2} forms a homotypic dimer and triggers an apoptosis pathway, resulting in cell death. Our group has successfully transferred this ablation system to living zebrafish and specifically ablated Purkinje cells in an apoptotic manner (Weber et al., 2016). Notably, after removal of tamoxifen, the fluorescent reporter facilitates the monitoring of the regeneration processes.

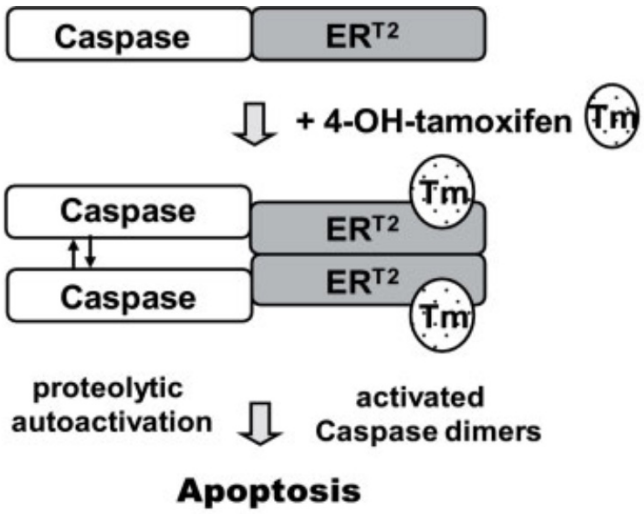

Figure 16 Mechanism of Caspase8ER^{T2} ablation system.

In the presence of 4-OHT, Caspase8ER^{T2} fusion proteins dimerize via the ER^{T2} domain, leading to proteolytic Caspase self-activation that triggers apoptosis. From Chu et al., 2008.

1.5 The aims of the study

1.5.1 Establishment of zebrafish model to screen antagonists of TcdA and TcdB

Based on TcdA and TcdB structure and mechanism of cellular intoxication, the N-terminal glucosyltransferase domain (GTD) was delivered into cytosol of target cell to inactivate host GTPases by glucosylation. The inactivation of GTPases results in disruption of actin cytoskeleton, cell rounding and eventually death of the targeted cell, which cause symptoms of CDI. Therefore, a transgenic zebrafish stain expressing the GTD domain will be established to mimic pathogenesis of CDI. The zebrafish model will be utilized to identify antagonists of TcdA and TcdB. Because of cellular intoxication, the cell type or tissue that target expression of GTD domain would be dead by apoptosis. Therefore, hatching gland will be selected as the target tissue. Hatching gland is required only at the first 48 hours after fertilization. Zebrafish embryos that have malfunctioned hatching gland could be hatched by treatment of pronase. A zebrafish hatching gland specific enhancer has been identified, which makes targeted expression of GTD in hatching gland cell possible.

In order to monitor the morphological change of apoptotic hatching gland cells, a fluorescent protein and an apoptosis sensor will be co-expressed with GTD domain in the hatching gland.

Combine with confocal scanning microscopy, the fluorescence-based screening would enable high-throughput compound analysis.

1.5.1 Analysis of neutrophil and macrophage behaviour upon C. difficile infection

The innate immune cell response plays a crucial role in CDI. Neutrophil and macrophage have been proved to engage in CDI. In the animal models of CDI, the infiltration of neutrophil is one of the major pathological findings. However, the specific function and behavior of both cell types is less understood.

A stable transgenic zebrafish strain with the expression of yellow fluorescent protein in neutrophil will be established. To monitor macrophages simultaneously, the other strain that express a red fluorescent protein in macrophage will also be generated. Confocal time-lapse imaging in embryos of each strain after *C. difficile* infection will reveal the response of macrophage or neutrophil, their time course recruitment, and their phagocytic behaviour. Dual fluorescence time-lapse analysis in double transgenic embryos will uncover the cooperation of these innate immune cells upon *C. difficile* invasion.

Furthermore, the macrophage and neutrophil transgenic train will co-express a Tamoxifen-inducible caspase to trigger apoptosis (ATTAC^{TM}). I will use this technique to eliminate either neutrophil or macrophage, which will reveal their roles at different stage of CDI. Double ablation of both cell types will expose the role of innate immune response to *C. difficile* infection.

2. Materials and methods

2.1 Materials

2.1.1 Bacterial strains and cell lines

2.1.1.1 Bacterial strains

Commercially NEB 5 α and NEB Turbo Competent E. coli were used for transformation and flowing plasmid purification.

XL1-Blue Competent Cells was utilized for bacterial infection of zebrafish.

Table 1

Strain	genotype
NEB 5 α	*fhuA2 Δ(argF-lacZ)U169 phoA glnV44 Φ80 Δ(lacZ)M15 gyrA96 recA1 relA1 endA1 thi-1 hsdR17*
NEB Turbo	F' *proA*$^{+}$*B*$^{+}$ *lacI*^{q} *ΔlacZM15 / fhuA2 Δ(lac-proAB) glnV galK16 galE15 R(zgb-21:Tn10)*Tet^{S} *endA1 thi-1 Δ(hsdS-mcrB)5*

2.1.1.2 *C. difficile* strains

Table 2

Strain	Ribotype	Isolated	Toxinotype
630	012	Switzerland	TcdA^{+}/TcdB^{+}
630Δerm	012	UK	TcdA^{+}/TcdB^{+}
R20291	027	UK	TcdA^{+}/TcdB^{+}/CDT^{+}

2.1.1.3 Cell line

HEK293T cell is a highly transfectable derivative of human embryonic kidney 293 cells.

2.1.2 Chemicals and reagents

2.1.2.1 Chemicals

Table 3

Chemicals	Manufacturer

1kb DNA ladder	New England Biolabs (NEB)
6x Gel loading dye Purple	NEB
m7G(5')G RNA cap structure analogy	NEB
(Z)-4-Hydroxytamoxifen (4-OHT)	Sigma-Aldrich
Dimethyl formamide (DMF)	Sigma-Aldrich
Phenol Red	Sigma-Aldrich
(N)-Phenylthiourea (PTU)	Sigma-Aldrich
Sodium chloride (NaCl)	Sigma-Aldrich
Sodium citrate	Sigma-Aldrich
Torula-RNA (tRNA)	Sigma-Aldrich
Tween 20	Merck
Magnesium chloride ($MgCl_2$)	Roth
Magnesium sulfate ($MgSO_4$)	Roth
Ribolock, RNase-Inhibitor	Thermo Fisher Scientific
Dithiothreitol (DTT) 100 mM	Promega
Ethanol (EtOH)	Sigma-Aldrich
Normal goat serum (NGS)	Vector laboratories
Nitro blue tetrazolium chloride (NBT)	Roth
Paraformaldehyde (PFA)	Roth
Tricaine	Sigma-Aldrich
HPLC water	Roth
Torula-RNA (tRNA)	Sigma-Aldrich
Methanol (MeOH)	VWR
Glycerol	Roth
Heparin	Sigma-Aldrich

2.1.2.2 Enzymes

Table 4

Enzyme	**Manufacturer**
DNase I, RNase-free	Thermo Fisher Scientific
Proteinase K	Promega

T3 RNA-Polymerase	Promega
T7 RNA-Polymerase	Promega
Sp6 RNA-Polymerase	Promega
T4 Ligase	Thermo Fisher Scientific
Klenow	NEB
Phusion DNA Polymerase	Thermo Fisher Scientific

2.1.2.3 Bile acids

Taurocholic acid sodium salt hydrate (TCA), T4009, SIGMA, CAS Number 345909-26-4

Sodium tauroursodeoxycholate (TCDCA) T0266, SIGMA, CAS Number 14605-22-2

Sodium tauroursodeoxycholate (TUDCA) T0266, SIGMA, CAS Number 14605-22-2

2.1.2.4 Staining reagent

BacLight™ Red Bacterial Stain, Thermo Fisher Scientific, Catalog number: B35001

2.1.2.4 Antibody

Table 5

Name	Host Species	Antigen	Dilution	Supplier	Product code
Anti-Caspase-3 antibody	Rabbit	a cleaved form of Caspase 3	1:1000	Abcam	ab13847
Alexa Fluor 488 anti-Rabbit IgG	Donkey	Rabbit IgG	1:500	Thermo Fisher	A-21206
Alexa Fluor 488 Goat anti-mouse	Goat	Goat IgG	1:1000	Invitrogen	
Anti-Digoxigenin-AP Fab	sheep	digoxigenin	1:1000	Roch	1093274910

Fragments					

2.1.3 Media and solutions

2.1.3.1 Fish media

Table 6

30 % Danieau	0.12 mM $MgSO_4$ 0.18 mM Ca $(NO_3)_2$ 0.21 mM KCl 1.5 mM HEPES (pH 7.2) 17.4 mM NaCl The solution was filled up to 1000 ml with ddH2O.
0.3% PTU	1.2 g PTU in 400 ml 30 % Danieau
30 % Danieau/PTU	990 ml 30 % Danieau with 10 ml 0.3 % PTU (f.c. 0.003 %)
Egg water	0.04 g/l Sea salt in ddH_2O
0.4% Tricaine	400 mg tricaine powder 97.9 ml ddH2O Adjust pH to ~7 with 1 M Tris (pH 9)
Phenol Red	0.5 % Phenol Red in 1x PBS
1 mM 4-OHT	5 mg (Z)-4-Hydroxytamoxifen (4-OHT) diluted in 12.9 ml absolute Ethanol
4 % PFA	40 g Paraformaldehyde 1000 ml ddH_2O and the pH was adjusted to 7.2

2.1.3.2 *E. coli* & Cell Culture Media

Table 7

LB-Medium	10g Bacto-tryptone. 5g yeast extract 10g NaCl Adjust pH to 7.4 and add water to 1 L.
LB Agarose	10 g Bacto-Trypton 5 g Yeast Extract 10 g NaCl 15 g Agar In 1 L ddH_2O
Cell Culture Medium	DMEM, high glucose medium 10% Fetal Bovine Serum (v/v) 1% Penicilin/Streptomycin (v/v) 1% Glutamin/Glutamax (v/v)

2.1.3.3 Histology Solution

Table 8

20x SSC	175.3 g Sodium chloride 88.25 g Sodium citrate dehydrate Add ddH2O to 1 l and adjust pH to 7 with citric acid
Citric acid (1 M)	105.07 g Citric acid

	Add ddH_2O to 500 ml.
Sodium chloride (5 M)	46.1 g Sodium chloride Add ddH_2O to 500 ml
Magnesium chloride (1 M)	101.65 g Magnesium chloride Add ddH_2O to 500 ml
Tris (1 M, pH 9.5)	121.14 g Tris Add ddH_2O to 1000 ml and adjust pH to 9.5
20 % Tween20	10 ml Tween20 Add ddH_2O to 50 ml
TE buffer for PK	6.1 g Tris base 0.37g EDTA 5ml Trion X-100 Add ddH_2O to 1000 ml and adjust pH to 8.0.
Proteinase K stock solution (20X)	8mg Proteinase K 10ml TE buffer for PK 10ml Glycerol
Hybridization Buffer	50% Formamide (v/v) 25% 20x SSC (v/v) 150 µg/mL Heparin 5 mg/mL Torula-RNA 0.1 % Tween20 (v/v)

PBST	0.3% Tween20 in PBS (v/v)
Fixation Buffer	4% PFA in PBST (v/v)
NGS Blocking Solution	10% NGS (Normal Goat Serum) in PBST DMSO (v/v)
BCIP stock solution	50 mg/ml BCIP in 100 % DMF
NBT stock solution	50 mg/ml NBT in 70 % DMF/ddH2O (v/v)
Staining solution	3.75 µl BCIP and 5 µl NBT per 1 ml AP buffer

2.1.3.4 Protein Biochemistry

Table 9

1. 10x Running Buffer	30.03 g Tris 144 g Glycine 10 g SDS Add ddH2O to 1L.
2x SDS Sample Buffer	125 mM Tris-HCl 5 %(w/v) Glycerol 4 %(w/v) SDS 0,1 %(w/v) Bromphenol blue 5 %(v/v) β-Mercaptoethanol Filled up with ddH2O

5x SDS Sample Buffer	312.5 mM Tris-HCl 20 %(w/v) Glycerol 4 %(w/v) SDS 0,5 %(w/v) Bromphenol blue 10 %(v/v) β-Mercaptoethanol Filled up with ddH2O
Semi-Dry Transfer Buffer	25 mM Tris 192 mM Glycine 20 % (v/v) Methanol
Separating Gel (10%)	5 ml 30% Acrylamide 3.75 ml 1M Tris-HCl pH 6,8 0.15 ml 10% Ammonium persulfate 0.15 ml 10% SDS 0.006 ml TEMED 5.94 ml ddH2O
2. 10x Transfer Buffer	30.2 g Tris 144 g Glycine Add ddH_2O to 1L

Skim Milk Blocking Buffer	5 %(w/v) Dry Skim Milk powder in TBS-Tween
TBS-Tween	20 mM Tris-HCl (pH 7.6) 150 mM NaCl 0.1 %(v/v) Tween20 Filled up with ddH_2O

2.1.2 Equipment

Table 10

Device	Modell	Manufacturer
Centrifuge	5415C	eppendorf
Confocal Laser-scanning-microscope	TCS SP8 DMI 6000	Leica
Incubator	B 6120	Heraeus
Gel electrophoresis chamber	40-0708	peQlab Biotechnologie GmbH
Horizontal needle puller	P-87	Sutter instrument
Micro injector	FemtoJet express	eppendorf
Pipetboy	ACU2	Integra
Rotator	LD-79	Labinco BV
Stereo fluorescence microscope	M205 FA	Leica
Stereo microscope	S8 APO Stereo zoom 1.0x-8.0x	Leica

Vortex	REAX2000	Heidolph
Thermomixer	Thermomixer 5436	eppendorf
photometer	DS-11	DeNovix

2.1.3 Plasmids

2 pCSII

pCS2+ is a multipurpose expression vector, useful for high-level transient expression in a wide variety of mammalian cells.

#3403 pBS-fyntagRFT:HE-HE:GFP

Hatching gland enhancer driving the expression of RFP and GFP in bidirectional manner, flanked by To2 500 arms.

#3395 pUC57-KozTcdA-HA

N-terminus of TcdA toxin HAtag of *C. difficile,* named as NTcdA, with optimized codon usage for zebrafish.

#3396 pUC57-KozTcdB-HA

N-terminus of TcdB toxin HAtag of *C. difficile*, named as NTcdB, with optimized codon usage for zebrafish,

#3475 pCSII-NTcdA

The N-terminus of TcdA was cloned into pCSII vector with EcoRI/XbaI.

#3476 pCSII-NTcdB

The N-teiminus of TcdB was cloned into pCSII vector with EcoRI/XbaI.

#3483 pBS-NTcdA-2HE-GFP

The NTcdA was cloned into #3403 pBS-fyntagRFO-T2HE-GFP with EcoRV/Asp718.

#3484 pBS-NTcdB-2HE-GFP

The NTcdB was cloned into #3403 pBS-fyntagRFO-T2HE-GFP with EcoRV/Asp718.

#3477 pCDH-CMV-MCS-EF1-Puro (a kind gift from Pro. Dr. Binghui Li)

Venus-based apoptosis biosensor VC3AI was inserted in pCDH.

#3518 pCSII-VC3AI-T2A-tagRFP-T

It drives the expression of VC3AI and tagRFP fluorescence protein, to monitor apoptosis and observe cell morphology via RFP.

#3519 pBS-TcdA: HE-HE: VC3AI-T2A-tagRFP-T

HE enhancers drive the expression of NTcdA, VC3AI and tagRFP in bidirectional manner.

#3520 pBS-TcdB: HE-HE: VC3AI-T2A-tagRFP-T

HE enhancers drive the expression of NTcdB, VC3AI and tagRFP in bidirectional manner.

#3757 pDESTnbtLexAdeltaTALexOPSecA5BFP

It contains the sequence of LexA operator, a kind gift from P Francesca Peri

#4089 pCS-mycCaspase8ERT^{2}GIpA

myc tag was added in front of Caspase8ERT^2. The intron sequence of rabbit β-globin was used in 5' position.

#4090 pBS-LysC-KalTA4GIpA

LysC, neutrophils specific promoter, drives the expression of KalTA4 GIpA.

#4091 pBS-LysC-KalTA4GIpA-spacer

LysC, neutrophils specific promoter, drives the expression of KalTA4 GIpA. A spacer sequence was amplified from #2212 using primer #1940/#1941. PCR product was digest with EagII/NotI and inserted into #4090.

#4092 pCS-FyntdCitrine

tandem Citrin fluorescent protein containing fyn membrane localization signal was inserted into pCSII.

#4099 pC-5UAS:FyntdCitrine

tandem Citrin was isolated from #4092 wtih EcoRI/NotI and then cloned into #3421.

4100 pC-Caspase8ERT2-5UAS-FyntdCitrine

Caspase8ERT2 fragment was isolated from #4089 with EcoRV/Asp718 and cloned into #4099.

#4101 LysC-KalTA4GIpA-UAS: FyntdCitrine/Caspase8ERT2

Gal4 activator was under control of LysC promoter, which drive the expression of fluorescent protein Citrine and Caspase8ERT2. This construct was used for establishment of neutrophil stable transgenic line.

4104 pCS-LexABDp65

LexA DNA-binding domain fused the activation domain of human p65 was inserted into pCSII.

#4105 pB-mpeg1:LexABDp65

mpeg1, macrophage/microglia specific promoter, drive the expression of LexABD-p65.

#4106 pB-mpeg1:LexABDp65-spacer

mpeg1, macrophage/microglia specific promoter, drive the expression of LexABD-p65.
A spacer sequence was amplified from #3757 using primer #1940/#1941. PCR product was digest with EagII/NotI and inserted into #4105.

#4317 pCSII-2lac

The oligo of tandem lac operators was annealed and inserted into empty pCSII vector by BglII/BamHI.

#4318 pCSII-4lac

The oligo of tandem lac operators was annealed and then inserted into #4317 with BglII/BamHI.

#4319 pCSII-rpl9-4lac-mseCFP

The quadruple lac operator was inserted before CFP fluorescence in #3993, where lac operators are flanked by intron of *rpl9*.

#4321 pBS-tagRFP-T: HE-HE:rpl9-4lac-mseCFP

HE enhancers drive the expression of tagRFP-T, rpl9-4lac-mseCFP in bidirectional manner.

#4322 pCSII-AnnexinV-T2A-H2B-tagRFP-T

HE enhancers drive the expression of apoptosis sensor AnnexinV and a nuclear localized tagRFP-T in bidirectional manner.

#4507 pCSII-rpl9-4lac-TcdA

It drives the expression of NTcdA with rpl9-4lac. The rpl9-4lac fragment was PCR amplified from plasmid #4321 using primers #2309/#2310. The PCR produce was inserted into # 3475 with EcoRI/EcoRV.

#4508 pCSII-rpl9-4lac-TcdB

It drives the expression of NTcdA with rpl9-4lac. The rpl9-4lac fragment was PCR amplified from plasmid #4321 using primers #2309/#2310. The PCR produce was inserted into # 3476 with EcoRI/EcoRV.

#4509 pBS-AnnexinV-T2A-H2B-tagRFP-T-2HE-GFP

HE enhancers drive the expression of apoptosis biosensor AnnexinV, tagRFP-T, and GFP fluorescence protein. tagRFP-T indicate the expression of AnnexinV.

#4510 pBS-AnnexinV-T2A-H2B-tagRFP-T-2HE-rpl-4lac-TcdA

HE enhancers drive the expression of apoptosis biosensor AnnexinV, tagRFP-T, and NTcdA within which rpl-4lac was introduced in front of TcdA. #4507 was digested with EcoRI/NotI to isolate rpl-4lac-TcdA fragment and the fragment was inserted into #4509.

#4511 pBS-AnnexinV-T2A-H2B-tagRFP-T-2HE-rpl-4lac-TcdB

HE enhancers drive the expression of apoptosis biosensor AnnexinV, tagRFP-T, and NTcdB within which rpl-4lac was introduced in front of TcdB. #4508 was digested with EcoRI/NotI to isolate rpl-4lac-TcdB fragment and the fragment was inserted into #4509.

#4513 pBS-mpeg1

mpeg1 promoter was isolated from #3257 with XhoI/EcoRI and then inserted into #3822.

#4723 pBS-tagRFP-E1b 2xCar8-4xLexOPE1b-E1b-GFP

4xLexAOP was amplified from plasmid #3757 using primer #2431 #2432. The PCR product was digested with PacI/PstI and was inserted into #4141.

#4724 pBS-tagRFP:E1b-SCP-spacer-4xLexOPE1b:mClover

This construct two reporter genes, tagRFP driving by SCP minimal promoter and mClover driving by E1b minimal promoter. They were linked by a spacer sequence. 4xLexOP E1b fragment was isolated from #4723 with PacI/EcoRI and inserted into #4049.

#4725 pBS-tagRFP:E1b-8xLexOP-E1b:mClover

This construct two reporter genes, tagRFP and mClover. Both were derived by E1b minimal promoter. 4xLexAOP was amplified from plasmid #4724 using primer #2434 #2435. The PCR product was digested with PacI/PstI and was inserted into #4724.

#4726 pBS-fyntdRFP:E1b-8xLexOP-E1b:mClover

Tandem tagRFP-T containing fyn membrane localization signal was inserted into plasmid #4725 to replace tagRFP.

#4727 pBS-fyntdtagRFP:E1b-8xLexOP-E1b:Caspase8ERT2

Myc-Caspase8ERT2GIpA fragment was Isolate from #4089 with EcoRI/NotI and then inserted into #4726.

#4728 pBS-mpeg:LexABDp65-spacer

LexABDp65-spacer was isolated from #4106 with EcoRI/NotI and inserted into #4513.

4731 pBS-mpeg1:LexABDp65-fyntdtagRFP:E1b-8xLexOP-E1b:Casoase8ERT2

LexABDp65 transactivator was under control of control of an enhancer-trap promoter, mpeg1. tagRFP reporter gene and Casoase8ERT2 was under the control of a minimal promoter E1b fused to 8LexA operator. This construct was used for macrophage stable transgenic stain.

#5141 pB-tagRFP:E1b:8xLexOP:E1b:4lac-TcdA

rpl9-4lac-TcdA fragment was isolated from #4507 with EcoRI/NotI and inserted into #4725.

#5142 pB-tagRFP:E1b:8xLexOP-E1b:4lac-TcdB

rpl9-4lac-TcdB fragment was isolated from #4508 with EcoRI/NotI and inserted into #4725.

#5143 pB-AnnexinV-T2A-RFP:8xLexOP-E1b:4lac-TcdA

AnnexinV-T2A-fyntagRFP-T was isolated and inserted into #5141.

#5144 pB-AnnexinV-T2A-RFP:8xLexOP-E1b:4lac-TcdB

AnnexinV-T2A-fyntagRFP-T was isolated and inserted into #5142.

#5145 pHE-cmlc2:BFP2

Heart specific promoter (cmlc2) drive the expression of fluorescent protein mtagBFP2. cmlc2 fragment was amplified on #3759 with primer #3041/#30421 and inserted into #2918 with SalI/AvrII.

#5146 pB-AnnexinV-T2A-RFP:8xLexOP-E1b:4lac-TcdA, cmcl2:BFP2

BFP2 driven by cmlc2 was inserted into #5143.

#5147 pB-AnnexinV-T2A-RFP:8xLexOP-E1b:4lac-TcdB, cmcl2:BFP2

BFP2 driven by cmlc2 was inserted into #5144.

#5148 pB-2HE:LexAp65GI

LexAp65GI fragment was isolated from #4789 with XbaI\NotI and inserted into #3402.

#5148 pB-BFP: 2HE:LexAp65GI

HE enhancer drive the expression of BFP and LexAp65GI. BFP was isolated from #2918 and inserted into #5148.

2.1.4 Oligonucleotides for cloning and sequencing

Table 11

Stock	Name	Sequence
1622	spacer/Bam	CCGGATCCGCAGCACTGGGGCCAGATGG
1623	spacer/SalI	GGGTCGACAAACTTGGTCTGACAGTTACC
1624	HE/Eco-lo	GCGAATTCCCCTAGGGTTGCCTCAGTG
1625	HE/As/EV /Pm-lo	GCGGTACCGGATATCGTTTAAACCCCTAGGGTTGCCTCAGTGTGTAG
1626	HE/Bam-up	GGGGATCCAACCACTCCAGGCATAGCTAG
1701	VC-Apo sensor part1 up	CCCATCGATTCGAATTCCCACCATGATCAAGATCGCCACCAGGAAG
1702	VC-Apo sensor part1 down	TGGGCACCACCCCGGTGAAGCCGTCCACCTCGTCGATCCCGG
1703	VC-Apo sensor part2 up	GTGGTGCCCATCCTGGTCGAGCTGGAC
1704	VC-Apo sensor part1 down	GCTCTAGACTACAGGTCCTCCTCGCTGATC
1719	VC-Apo sensor lower primer	GGACTAGTCAGGTCCTCCTCGCTGATC
1720	JL Cas8 SpeI up primer	GGACTAGTATGAGTGAGTCACGGACTTCAG
1721	JL Cas8 XhoI down primer	CCCTCGAGGGGAGGGAAGAAGAGCTTC
1722	JL tagRFP-TXhoI down primer	CCCTCGAGCTTGTACAGCTCGTCCATGCC
1787	miniCMV MfeI SpeI up	CGCAATTGGACTAGTGGGCTGCAGGAATTAATTCAAG

1788	ERT sequencing down	CTCCATGGAGCGCCAGACGAGAC
1789	linker F primer	CGGTCGACATTTAAATGTTTAAACCTCGAGCCGACCTGTCCGGTGCCCTG
1790	linker R primer	CGGTCGACCTGCCCCGGCACTTCGCCCAATAG
1791	tdRFPT-Bam up	CCGGATCCGGCTCAAGCGGTCGCGTGTCTAAGGGCGAAGAGCTG
1792	tdRFPT-Bam lo	CCGGATCCAGTTGAGCCGGTGCCATGCCCCTTGTACAGCTCGTCCATGCCATTAAG
1929	cmv enhancer up primer	CCCTCGAGGAGTCAATGGGAAAAACCCATTG
1930	cmv enhancer up primer	CCCTCGAGCACCCCTATTGACCTTATGTATG
1931	miniCMV real EcoRI down	CGGAATTCGGCGATCTGACGGTTCACTAAAC
1932	LexA OP KpnI SpeI up	GGGGTACCCTCCACTAGTCGCATTATCATCCCCTCGACGTACTGTACA
1933	LexA OP EcoRI down	CGGAATTCTTCAGCGTGTCCTCTCCAAATGAAATG
1934	LexA BD Kozak EcoRI up	CGGAATTCGCAAACATGGCACCCAAGAAGAAGAGG
1935	LexA BD XhoI down	CCGCTCGAGGTACCGGCGCTCGACGGTTCACCGGC
1936	mpeg1 probe up	CATGAAGTCAAGAGCATTTC
1937	mpeg1 probe down	CACTGTTGAAGCCAATTTGTTC
1938	ERT2+myc up XhoI	CCGCTCGAGCCATCTGCTGGAGACATGAGAGCTGCC
1939	ERT2+myc down stop SpeI	GGACTAGTTCACAGGTCCTCCTCGCTGATCAGCTTCTGCTCAGCTGTGGCAGGGAAACC
1940	lysC Gal4 spacer up EagI	TTCGGCCGAATAAAATATCTTTATTTTCATTACATC

1941	lysC Gal4 spacer down NotI	TTAGCGGCCGCAGAGAAATGTTCTGGCACCTGC
2136	1xLO-BaEv-up	GATCCGATATCGTGGAATTGTGAGCGCTCACAATTCCACAC
2137	1xLO-BaEv-down	AATTGTGTGGAATTGTGAGCGCTCACAATTCCACGATATCG
2138	2xLO-BaEv-up	GATCCGATATCGTGGAATTGTGAGCGCTCACAATTCCACAGTCGAC CCTAGGTTGTGGAATTGTGAGCGCTCACAATTCCAC
2139	2xLO-BaEv-down	AATTGTGGAATTGTGAGCGCTCACAATTCCACAACCTAGGGTCGAC TGTGGAATTGTGAGCGCTCACAATTCCACGATATCG
2140	Intron up1 EcoRI PmeI	CGGAATTCATGTTTAAACGCGTCTCAGCCTCACTTTGAGCTC
2141	Intron up2 EcoRI PmeI	CGGAATTCATGTTTAAACCCCCAAACCTAAGGTGAGTTGATC
2142	Intron down EcoRV	CGGATATCCGGCTGAACTGTAAATGAATGAG
2143	PflFI SwaI SphI up	CAGATTTAAATGAGCATGCCG
2144	PflFI SwaI SphI down	GCGGCATGCTCATTTAAATCT
2145	2Lac up SphI	CGTGGAATTGTGAGCGCTCACAATTCCACAGTCGACCCTAGGTTGT GGAATTGTGAGCGCTCACAATTCCAA
2146	2Lac down AgeI	CCGGTTGGAATTGTGAGCGCTCACAATTCCACAACCTAGGGTCGAC TGTGGAATTGTGAGCGCTCACAATTCCACGCATG
2147	Lex OP Rever XbaI up	TGCTCTAGAGAGGTAAGATTAGATATGGATATGTATATGG
2148	Lex OP Rever KpnI EcoRV	CCGGTACCAAGATATCGGGTTTAAACTTCAGCGTGTCCTCTCCAAA TG
2149	zebrafish fyn Kozak up	CGGAATTCAGCAAACATGGGCTGTGTGCAATGTAAGGATAAAGAA GC
2150	LexOP SCP NheI up	GGGCTAGCCGCATTATCATCCCCTCGACGTACTGTACA

2151	LexOP SCP SbfI down	GGCCTGCAGGTAATCTTACCTCGACTGCTGTATATAAAACC
2299	2Lac up Bam	GATCCGTGGAATTGTGAGCGCTCACAATTCCACAGTCGACCCTAGG TTGTGGAATTGTGAGCGCTCACAATTCCAA
2300	2Lac down Bglii	GATCTTGGAATTGTGAGCGCTCACAATTCCACAACCTAGGGTCGAC TGTGGAATTGTGAGCGCTCACAATTCCACG
2301	CG free EagI linker up	TTCGGCCGCTGCTACCTCTGTGACCTGAAAC
2302	CG free NotI linker down	TTAGCGGCCGCTATTATTTATTGGGTAGTGTGAT
2303	LexA 8OP XbaI up	GCTCTAGATTCAGCTCTCTGTTTCTATAAATATGTACCAGTTTTATTG TTTTTAGTGGTTATCATCCCCTCGACGTACTGTAC
2304	LexA 8OP NheI down	CGGCTAGCACCATATACATATCCATATACATATCCATATCTAATCTT ACCTCGACTGCTGTATAT
2305	Top strand converted up	ATATAGAATGTAGGTATTAGTTAGTGGATTT
2306	Top strand converted down	TCGATCTTCGCCCTTAAACACCATATTTA
2307	Bottom converted up	TCTCAAAAAACAACTATAACCACATAAAATA
2308	Bottom converted down	TCGGTTTTCGTTTTTAGATATTATGTTTG
2309	rpl9 up EcoRI	CGGAATTCAAGACCATTCTCAGTAACCAG
2310	rpl9 down PmeI	TTGTTTAAACACTGTGCGGCCCTTGAGGGAC
2431	8LexOP E1b up PacI	CGTTAATTAACTAATCGCATTATCATCCCCTCGACGTAC
2432	8LexOP E1b down PstI	AGCTGCAGGTCGAGCATATTACATGGCATTACCACC
2434	8LexOP E1b up PpuMI	GGTAGGTCCTAACTAATCGCATTATCATCCCCTCGACG
2435	8LexOP E1b do PmeI SwaI	ATGTTTAAACGATTTAAATGTGTGGAGGAGCTCAAAGTGAG

2436	14UAS-Tau Seq up	GAAGCGCATGAACTCCTTGATGACGTCCTCGGAGG
2437	14UAS-Tau Seq down	TGATCTTCCATCACTTCGAACTCCTGGCGGGGCTC
2438	mpeg frag Xho 1.4	GCCGCTCGAGGTGAACAAAAAAACAAACAAACCTTATTTCCTTTTG
2439	mpeg frag Xho 1.0	ACCGCTCGAGTGGTGTAGTGATTAGTGTGTTGACACAAGGCAC
2440	mpeg frag Xho 0.5	GCCGCTCGAGCACAGCAGTTTTAGGAGATGCTTATAATAAAGAG
2631	TcdA-RT primer up	GAAAGCAGTACGACAGAGGCACTGC
2632	TcdA-RT primer lo	CGCAGAGAATTGGTCCGATAGCTTTC
2633	TcdB-RT primer up	CTGGACGTCGATATGCTGCCAGG
2634	TcdB-RT primer lo	GCCTCCATGTCTCCAAGTGAACTG
2635	RT-PCR Exon TcdA/B up	ACCATTCTCAGTAACCAGACAGTGG
2636	RT-PCR Exon TcdA lo	GCGATGTCAGACACTTCGCCTCC
2637	RT-PCR Exon TcdB lo	CTGTATCGTTGATCTGTCCTCCG
2638	mfap4 Xho up	TGTTCTCGAGGCGTTTCTTGGTACAGCTGG
2639	mfap4 Eco lo	GTGGAATTCCACGATCTAAAGTCATGAAGAAAGA
3041	cmcl2 up AvrII	TGCCTAGGGGTCACTGTCTGCTTTGCTG
3042	cmcl2 lo Not Sal	ATGTCGACATGCGGCCGCAAAGCTTAAATCAGTTGTG

2.1.5 Fish strains

2.1.5.1 Wild type

The wild type Brass line, deficient in melanin synthesis, was used for DNA/mRNA microinjection and for transient transgene assay, to generate stable transgenic lines.

2.1.5.2 Transgenic lines

Tg(5×UAS-E1b:EGFP)

This transgenic effector line was generated to set an EGFP reporter gene.

Tg[mpeg1:KalTA4,Insulator,HE:BFP]

Macrophage specific enhancer (mpeg1) drive the expression f KalTA4, while hatching gland enhancer (HE) drive the expression of blue fluorescent protein (BFP) as screening marker. Insulators are DNA-protein complexes that act as an enhancer blocker or serve as barriers against the spreading of heterochromatin in reporter system. They allow the two different expression units working independently.

Tg(lysC:KalTA4,Insulator,HE:BFP)

Neutrophils specific enhancer (lysC) drive the expression f KalTA4, while hatching gland enhancer (HE) drive the expression of blue fluorescent protein (BFP) as screening marker. Insulator was described as above.

Tg(lysC:KalTA4, fyntdCitrin:E1b-5UAS-E1b:Caspase8ER^{T2})

This transgenic line was generated to obtain fluorescent protein Citrine and fusion Caspase8ER^{T2} expression in neutrophils cells. The membrane localized fyntdCitrine was used to observe the morphology of expressing neutrophils to monitor their behaviour during *C. difficile* infection.

Tg(mpeg1:LexABDp65, fyntdtagRFP-T:E1b-8LexAOP-E1b:Caspase8ER^{T2})

This transgenic line was generated to obtain fluorescent protein RFP and fusion Caspase8ER^{T2} expression in macrophage cells. The membrane localized fyntdtagRFP-T was used to observe the morphology of expressing macrophage to monitor their behaviour during *C. difficile* infection.

Tg(*krox20*:KalTA4)

1.5 kb downstream of the zebrafish egr2b gene known as krox20, which was expressed in rhombomere 3 and 5 during developmental stages of the hindbrain, drive the expression of KalTA4.

Tg(*shhb*:KalTA4)

sonic hedgehog b (*shhb*) gene, drive the expression of KalTA4.

2.2. Experimental Procedures

2.2.1. Nucleotide handling and cloning procedures

2.2.1.1 Mini DNA preparation

The Macherey Nagel Nucleobond Midi Kit was used with a modified protocol to purify plasmid DNA. 1 ml of LB Medium with Ampicillin were inoculated and shake at 180 rpm at 37 °C overnight. The overnight culture was transferred into 1.5 ml tubes, spun down at 14000 rpm for 1 min and the supernatant was discarded. The bacterial pellet was resuspended in 150 µl of Resuspension Buffer and lysed in 150 µl of Lysis Buffer. Then 150 µl of Neutralization Buffer was added and mixed by inverting. The obtained cell debris was spun down at 14000 rpm for 5 min and the supernatant was transferred into a new 1.5 ml reaction tube. This tube was filled up to 1.5 ml with 100% ethanol and was vortexed followed by centrifugation at 1400 rpm for 5 min. The supernatant was removed and the dry DNA pellet resuspended in 30 µl HPLC water. The purified plasmid DNA can be used for test digestion with restriction enzymes.

2.2.1.2 Midi DNA preparation

For large scale purification of plasmid DNA an individual *E. coli* colony was cultured in 100 mL LB medium supplemented with the respective antibiotic in a 500 mL flask on a shaker over night at 37°C. The midi DNA preparation was prepared with the Macherey Nagel Nucleobond Xtra Midi Kit. The bacterial was harvested in a 50 ml tube by centrifugation at 4500 rpm at 4 °C for 30 min. The bacterial pellet was resuspended in 8 ml Resuspension Buffer and vortexed. Cell lysis was achieved by adding 8 ml Lysis Buffer, inverting and incubation for 3-5 min at room temperature. The reaction was stopped by adding 8 ml Neutralization Buffer. To purify the DNA from cell debris the solution was added onto a column activated by 12 ml

Equilibritation Buffer; flow was discarded. The column was washed with 8 ml Equilibration Buffer afterwards. The purified DNA was eluted into a new 50 ml Falcon tube with 5 ml Elution Buffer. The DNA was precipitated with 3.5 ml Isopropanol. The 50 ml Falcon tube was centrifuged at 5000 rpm for 30 min and the supernatant was removed. The DNA pellet was transferred into a new 1.5 ml reaction tube and washed with 1 ml 70% ethanol. The DNA pellet was spun down for 5 min at 14000 rpm. The ethanol was removed. The dry DNA pellet was resuspended in 200 µl HPLC water. The concentration of purified plasmid DNA was measured in a photometer. The DNA was diluted to 1 µg/µl for storage.

2.2.1.3 DNA digestion

For testing enzyme digestion, add components to a clean tube in the order shown:

4 µl DNA (Mini DNA preparation)
1.5 µl 10x buffer
0.3 µl per restriction enzyme
fill up to a total volume of 15µl with HPLC water

The digests were incubated at 37 °C for 30 min and the result was verified on an agarose TAE gel. The digested DNA was mixed with 6x loading dye then was loaded onto a 1% agarose TAE gel. A DNA marker (7 µl) is loaded to the gel to estimate the size of digested DNA fragments. Afterwards the DNA is stained with an Ethidium bromide solution (1:2000) for 10 min.

2.2.1.4 Cloning

Vector:

1 µl DNA (1 µg/µl)
5 µl 10x buffer
1 µl per restriction enzyme

fill up to a total volume of 50 µl with HPLC water. Incubate at 37°C for at least 1 hour.

Insert:

1 µl DNA (1 µg/µl)
5 µl 10x buffer
1 µl per restriction enzyme

fill up to a total volume of 50 µl with HPLC water. Incubate at 37°C for at least 1 hour.

The digested DNA samples were run on a 1% agarose TAE gel and stained with ethidium bromide. The requested bands were cut out from the gel and transferred into a 1.5 ml reaction tube. Gel Extraction Kit was used to purify the DNA out of the gel. All further steps were performed as described by the manual. Afterwards the digested vectors or inserts were ready for ligation.

T4 DNA ligase was used to ligate DNA fragments. The solution of vector and insert DNA were mixed between 1:3 to 1:4 mole ratio depending on their individual concentration. 1.5 µL 10 x ligase buffer and 1 µL T4 ligase were added. The total volume was adjusted to 15 µL with HPLC water. The reactions were incubated at 22°C for 30 min or at 16°C overnight. The ligation mixture was subsequently used to transform competent bacteria as described above. The bacteria were plated onto LB-agar plates and incubated at 37 °C overnight.

2.2.1.5 PCR

PCR reactions were done depending on the polymerase. The following was reaction setup for Phusion® High-Fidelity DNA Polymerase.

10 µl	5X Phusion HF or GC Buffer
1 µl	10 mM dNTPs
2.5 µl	10 µM Forward Primer
2.5 µl	10 µM Reverse Primer
variable	Template DNA
0.5 µl	Phusion DNA Polymerase
Add HPLC water to 50 µl.	

Thermocycling conditions for a routine PCR was in the following example:

Initial Denaturation	98°C	5 minutes
Denaturation	98°C	30 seconds
Annealing	98°C	30 seconds
Elongation	72°C	30 seconds
Final elongation	72°C	5 minutes
Hold	4°C	infinite

2.2.1.6 DNA blunting by Klenow Fragment

Ligation of non-complementary double strand DNA ends can be achieved by blunt end cloning. The 5'-DNA overhangs were filled by using the Klenow fragment. dNTPs (final concentration: 33 µM), 10x restriction buffer H, 1 µL Klenow and purified DNA were mixed (total volume was 30 µL). The reaction mix was incubated at 25°C for 15 minutes. The reaction mixture was purified for further processing using gel extraction or nucleotide purification kit.

2.2.1.7 DNA dephosphorylation

In order to prevent blunt end or single enzyme digested vector re-ligation, the digested vector was dephosphorylated by using calf intestinal phosphatase (CIP) from NEB. CIP is active in all NEB restriction enzyme buffers. Therefore, CIP can be added directly into the digestion reaction after DNA digestion. 0.5-1 µL CIP was added into digestion mixture and incubate extra 1 h at 37°C. Subsequently, the reaction mixture was purified for further processing.

2.2.1.8 Oligo Ligation

For the 2×lac and 4×lac ligation, annealing oligo was used for cloning.

The sense and antisense oligo were phosphorylated as in the following receipt:

Each oligo (50mM)	2 ul
10mM ATP	1 ul
10×T4 Polynucleotide Kinase buffer	1 ul
T4 Polynucleotide Kinase	0.5 ul
MilliQ	5.5 ul

The reaction buffer was incubated at 37°C for 1 h then mix sense and antisense oligo reaction buffer together. Set heat block to 99° and transfer tube containing sense and antisense oligo in it for 2min. Turn off the heat block and cool down to 55° C. Leave the mixture for 5min. Dilute 1 ul annealing oligo in 20 ul HPLC water and take 3 ul for ligation.

2.2.1.9 Tol2 mRNA synthesis

The mRNA for the Tol2 transposase was synthesized and later co-injected with vectors into zebrafish.

The plasmid #3816 was digested with XbaI, purified and 2 µl of the sample was examined for linearization with an agarose gel electrophoresis. 1 µg of this DNA was required for the RNA synthesis. The reaction mixture was set up as following.

10 µl	5X Transcription Buffer
1 µl	linearized DNA
5 µl	NTP/Cap mixture
1.5 µl	Ribolock RNase-Inhibitor (40 U/µl)
1.5 µl	T7 RNA-Polymerase (20 U/µl)
5 µl	DTT (100mM)

Add HPLC water to 50 µl.

The reaction mixture was incubated for 2 h at 37 °C. To degrade the template DNA that was still present in the mixture, 2 µl of DNaseI was added into the reaction tube, mixed and incubated for another 30 min to 1 h at 37 °C. To purify the RNA afterwards, the RNeasy® kit was used.

The quantity and size of the synthesized RNA was analyzed with an agarose gel electrophoresis and measured with the photometer.

2.2.1.10 RNA synthesis for whole-mount *in situ* hybridization (WISH)

RNA probes labeled with digoxigenin-conjugated uridine triphosphates were used in *in situ* hybridization. To generate these RNA probes, plasmid DNA containing T7/T3/Sp6 was linearized by enzyme digestion. The purified linearized DNA were used to create the different RNA probes.

4 µl	5X Transcription Buffer
2 µl	linearized DNA
2 µl	Digoxigenin RNA labelling mix
1 µl	Ribolock RNase-Inhibitor (40 U/µl)
1 µl	respective RNA-Polymerase (20 U/µl)
2 µl	DTT(100mM)

Add HPLC water to 20 µl.

The reaction mixture was incubated for 2 h at 37 °C. To degrade the template DNA that was still present in the mixture, 2 µl of DNaseI was added into the reaction tube, mixed and incubated for another 30 min to 1 h at 37 °C. RNeasy® kit was used to purify the RNA probe afterwards.

2.2.2 Microinjection

Microinjection is one of the most frequently used techniques. Besides introducing substances such as nucleic acids, proteins or drugs into fertilized zebrafish eggs, this technique can be used for infection of zebrafish with *E. coli* or *C. difficile*.

2.2.2.1 Microinjection on one-cell stage cell

In this thesis, the Tol2-system was used to introduce plasmid DNA into fertilized zebrafish eggs. To incorporate the target gene into the genome, a mixture of Tol2 transposase-encoding mRNA and plasmid DNA containing the target gene was injected into the eggs. The target gene in the plasmid was flanked by transposase recognition sites, Tol2 sequence, allowing the random integration into the genome. The introduced gene was retained and passed to the daughter cells during the division. If not, that would be cause mosaic expression of transgene.

In order to position and hold the zebrafish eggs in place during microinjection, agarose plates with inserted grooves were generated. Therefore, 1.5 % agarose was melted in 30 % Danieau (w/v), poured into a petri dish (10 cm) and the mould was positioned on top to create the grooves. After solidification, the mould was removed, the plate was mounted with 30 % Danieau and stored at 4 °C. The microneedles were generated with a horizontal needle puller. Shortly before the microinjection, the injection mixture was mixed together and placed on ice. The injection mixture contained 250 ng plasmid DNA, 250 ng Tol2 mRNA and 1 µl Phenol Red in 10 µl HPLC water. Transfer embryos to the petri dish by using a pipette and sort them into the grooves. The cell on the yolk should be upside. Using a microloading pipette tip load 2 µl of the injection-mix into the injection needle. Fix the injection needle to the micromanipulator and insert its tip into the medium. Adjust the pressure of the injector for getting a slow outflow of solution out of the glass capillary. Using the micromanipulator inject a cell (not yolk) of fertilized eggs. A few nl injection are enough. excess volume of injection mix (especially for

DNA injection) has toxic effect on embryos. When finished with injections, transfer the injected embryos into a new dish and incubate at 28°C.

2.2.2.2 Infection of Zebrafish with *E. coli* or *C. difficile*

I used a protocol modified from a method published by Benard et al.

1. Prepare Injection Needles

Both horizontal puller and vertical puller could be used for making needs. Open the needle tip with tip or tweezer to obtain a tip opening.

2. Prepare *C. difficile* sample

C. difficile is a strict anaerobe and is sensitive to even low concentration of oxygen. Bactera were cultured o/N in 10 mL BHIS liquid medium in an anaerobic hood without shaking. BHIS is BHI (brain-heart-infusion) supplemented with 0,5 % (w/v) yeast extract and 0,1 % (w/v) L-Cysteine. BHI was purchased from Fluka or Carl Roth GmbH.

1 g/L L-Cysteine was dissolved in 10 ml of ddH_2O and added to autoclaved medium after sterile filtration. For agar plates 15 g/L agar was added before autoclaving.

3. Prepare *E. coli* sample

Transfected XL1-Blue Competent Cells with pBS-tdTomato vector. NEB 5α would be stick together to form a mass of cells, while it was easy to get a single and separately XL1-Blue cell. One colony was inoculated in 2ml LB medium for culture overnight. Centrifuge at 4000rpm for 5 min to collect bacteria. Wash three times with PBS then resuspended in 200 µl PBS.

4. Prepare zebrafish larvae for injections

In this step, a hair loop tool was necessary. A piece of human hair was inserted as a loop into the opening of yellow tip and fixed in place with glue. It provided a convenient tool for gently manipulating fragile zebrafish embryos.

Anesthetize the larvae with Tricaine approximately 10 min prior to injections. Please refer to article 'Infection of Zebrafish Embryos with Intracellular Bacterial Pathogens' for further information.

There was alternative route to mount zebrafish embryos. Transfer anesthetized larvae into petri dish and remove most of the water. Embed the larvae in 0.6-0.8% low melting agarose drop. After solidification, the larvae were ready for infection. This route was suitable for older larva.

5. Injection of bacteria into zebrafish larvae

Prepare the injection mixture by adding 1 µl Phenol Red to 9 µl *E. coli* or *C. difficile* solution. Load the injection mixture into injector and check the injection volume.

2.2.3 Microgavage of Zebrafish Larvae

Experiments for studying intestinal biology required the introduction of materials into the lumen of the intestine *in vivo*. Immersion and injection though the abdominal wall are the most common methods. Using immersion method, it is difficult to accurately control the amount or timing of material, or bacteria delivery into the intestine. Although such problems are not encountered for injection though the abdominal wall, it is invasive and causes tissue damage which might affect experimental results. In order to safely and consistently deliver *C. difficile* directly to the lumen of the anterior intestine in larval zebrafish, I used a microgavage protocol modified from previous protocol published by Cocchiaro et al..

1. Preparation of low melting agarose, microgavage mould, and microgavage needle fabrication

I used 1% low melting agarose instead of methylcellulose for mounting larvae. Prepare a 1.5% agarose gel mould in a Petri dish using a plastic cast with same shape with Adaptive Science Tools, TU-1. Add enough zebrafish medium to immerse the plate and store in 4 °C. The agarose plated can be re-used several times. Because the position of heat filament in the horizontal puller was not fixed, the programs I used for needle fabrication were also varied: Pressure 500, Heat 350-400, Pull 75-110, Velocity 50-75, Time 125-150. This setting might be optimized in different puller.

2. Clipping and calibration of the microgavage needles

The needle clipping is a critical step. In order to obtain blunt and smooth needles, clip the needle using fine-tipped forceps. Align the tip of the needle under a stereomicroscopy and clip the needle at 1-2 mm from the tip. The needle should be blunt and smooth. Examine the tip of needle at highest 80x magnification under Stereo Microscope. Sharp or jagged needles should be avoided.

Since our injector could not set the volume of solution to release, it was important to calibrate the microgavage needle. Wrap a plastic Petri dish with parafilm and aliquot 0.2 µl of the calibration testing solution onto the parafilm. The calibration testing solution contained 1x PBS/0.05% phenol red. Press the pedal of injector to release the testing solution onto the parafilm. Then compare the size of droplet with 0.2 µl solution to estimate the droplet volume and adjust the pressure.

3. Anesthetizing and microgavage of Zebrafish

The *C. difficile* or *E. coli* (referred to 2.2.2.2) was diluted at 1:10 dilution rate with phenol red and load the solution was loaded into microgavage needle.

Anesthetize fish by mixing 0.4% of tricaine into petri dish for a final concentration of 0.02-0.04%. When the zebrafish stop moving, transfer them onto of the groove of microgavage mould using Pasteur pipette. Add an amount of low melting agarose to cover the zebrafish. Gently adjust their position with their heads on the 45° or lesser angle of the groove.

Set the pressure of injector and adjust the angle of needle pointed to the mouth of zebrafish. Gently put the needle into the mouth of zebrafish, through the esophagus, and introduce the tip of needle inside the anterior intestinal bulb. Then press the pedal to release the bacteria. The delivered volume should just fill the anterior bulb of the intestine, around 5nl. Do not let it leak out of the esophagus or cloaca. Gently retract the needle. Neutrophil or macrophage reporter line was a good model to examine whether you make esophagus or esophageal sphincter damage. Upon injury, a larger number of neutrophils or macrophages would be recruited. The recruitment of several lymphocytes was acceptable. Rescued the fish from agarose and rinse them in fresh media.

2.2.4 Zebrafish methods

The zebrafish (*Danio rerio*) in this laboratory were maintained according to the protocols published by Westerfield (Westerfield 2007).

The adult zebrafish were housed in an aquarium connected to a tank filtering system to ensure the water quality. The temperature in the tanks was kept between 26-28 °C and a day-night circle of 14 h light and 10 h dark was applied.

Zebrafish are photoperiodic and they produce eggs every morning shortly after the light comes on. One male and one female each were placed into mating tank the night before the collection and separated with a removable plastic disk. The next morning, the disk was removed. Collect eggs in 15 to 20 min later, washed with egg water, and transferred into a petri dish. For microinjection, this time span was crucial to maintain a single cell stage. If only a number of eggs were required, the mating was extended for 2 or even 3 more hours.

For positive transgenic zebrafish larvae, they were transferred into fish room at 6dpf. In order to acquire high survival rate, they also could be transfer into fish room at 4dfp, but flowing water should be applied till 6dpf.

2.2.5 Cell cultures and Western blot

2.2.5.1 Culturing

HEK 293T cells were kept at high Glucose or at low Glucose medium. HEK 293T cells grown much faster in high Glucose than in low Glucose medium. All cells were cultured at 37 °C with 5 % CO^2.

2.2.5.2 Passaging cells

Cells were cultured on 10 cm plates to about 80% confluence. The old medium was removed. Cells were washed with 1 ml 1x PBS or DMEM medium without FCS. Trypsin EDTA (1x) was used to detach cells from the plate, incubated at 37 °C for 1 min. The reaction was stopped by adding 8 ml 1x DMEM. Cells were transferred to a 15 ml tube and collected by spinning for 3 min at 1000 rpm. The supernatant was removed and the pellet was resuspended with 1 ml DMEM. The cells were transferred to a new 10 cm plate.

2.2.5.3 Freezing and thawing cells

The cells were collected. Then the cell pellet was resuspended in 1 ml Serumfree Type Cell Medium. Cyrotubes were filled with 200 µl of cell suspension. The Cyrotubes were transferred into a Cell Freezing Container and stored in - 80°C freezer.

Cells were thawed fast by placing tubes at 37 °C. Afterwards cells were plated on 10 cm plates with DMEM Glucose medium.

2.2.5.4 Transfection of HEK293T

HEK 293T cells were used for western blot experiments. These cells were spread into 6 well plates. About 50 µl of cells were used for each well in 2 ml DMEM high glucose and were cultured overnight. Transfection of cell culture at 50-70% confluence. Transfection was performed as follows:

1-2 µg DNA

100 µl OptiMem

1.5 µl PEI

mixed by pipetting and incubation at room temperature for 15 min.

After 6 h, 2 ml of DMEM containing 10% FCS was added to transfected cells. Medium was changed to DMEM one day later. Depending of cell growth, high or low glucose media was added. Cells were harvested 2 days after transfection.

2.2.5.5 Preparation of cell lysates for western blots

HEK 293T cells were transfected as described. All solutions were kept on ice to reduce protein degradation. Old media was removed and cells were washed with 1 ml PBS twice. Aspirate the PBS, then add 400 µl ice-cold lysis buffer. A scraper was used to detach cells from the plate. Cells were transferred to a new 1.5 ml cooled tube by pipetting and incubated for 15 min with inverting every 5 min to lyse the cells. Cell debris was spun down for 15 min at 4 °C. Aspirate the supernatant to new cooled tube and discard the pellet. discard the pellet. The supernatant was aliquoted and store in - 80°C freezer.

2.2.5.6 Gel preparation and running

Two glass plates with a 1 mm spacer were assembled in a gel caster and were filled up to 2/3 with separating gel solution. To prevent bubbles in the gel, isopropanol is added to cover the separating gel. After polymerization, the isopropanol was removed. Next, pour 5% stacking gel on top of separating gel. Insert comb at an angle (to ensure no bubbles) to create lanes. After polymerization, the gels could be stored at 4 °C.

The samples were boiled at 99 °C for 5 min followed by centrifugation at 12,000 rpm for 5 min. The gels were removed from the gel caster and put into gel chambers that were filled with 1x running buffer. 30 µl was loaded onto the gel for each sample. The samples ran in the stacking gel with 70 V for about 30 min until the samples reached the separating gel. Then run at 95V until dye was all the way at end of gel.

2.2.5.7 Semi dry transfer

Four Whatman papers were cut to match the size of stacking gel (8.5 x 5.5) and all were moistened in 1x semi dry transfer buffer. A PDVF membrane with the same size was cut and moistened in 100 % methanol.

To remove gel from between the glass plates, use a green wedge to gently pry the glass apart and let it slid into semi dry transfer buffer. Gels are very fragile, so be gently.

The blotting stack was set up in the following order: 2 Whatman papers, membrane, gel and 2 Whatman papers. To make sure there was no bubbles between each layer, use the glass rod to roll out any bubbles as you added layers. Close the cassette tightly. Run at about 100V and 100 mA per gel for 1-2 h.

2.2.5.8 Blocking and antibody staining

The membrane was taken out form the transfer system and was washed with TBST. Then the membrane was blocked with 5 % Skim Milk/TBST for 1 h on the shaker. The membrane was washed with TBST and sealed with the primary antibody solution in a plastic bag. The primary antibody incubated on a rotator over night at 4 °C. Next morning, wash 3 times with fresh TBST, 10 min each, with shaking.

Then the secondary antibody was added and sealed in a plastic bag. Incubate 1 h at RT on rotator. Wash 3 times with fresh TBST, 10 min each, with shaking. Then the membrane could be used for detection of proteins bands using SERVALight Eos CL HRP WB Substrate Kit.

2.2.6 Histological Techniques

2.2.6.1 Whole-Mount Immunostaining

5dpf zebrafish embryos were fixed at 4 °C in 4% PFA in PBST (PBS, 0.1-0.3% Triton X-100) on the shaker for 3h. They were washed once with PBST for 10min and incubated in cold-acetone at -20 °C for 15 min. Then they were washed once with PBST and twice with PBS-DT (PBS, 1% BSA, 1% DMSO, 1% Triton X-100) for 10min each, and subsequently incubated in 5% goat serum, PBS-DT at RT for 1 h. For primary Ab reaction, embryos were incubated with the Ab solution (PBS, 1% BSA, 1% DMSO, 0.1-0.3% Triton X-100, 1/1000 dilution rabbit anti-Caspase3 Ab), at 4 °C overnight. In the next day, they were washes four times with PBST for 10 min each and then secondary antibody reaction is as follows: incubate with the Ab solution (PBS, 1% BSA, 1% DMSO, 0.3% Triton X-100), at 4 °C overnight. (1/500dilution, Alexa Fluor 488, anti-Rabbit IgG). Four times washes with PBST for 10 min each. The fish were ready for observation.

2.2.6.2 Whole-mount *in situ* hybridization

Most genes are expressed in a very specific spatio-temporal pattern within the organism. The whole-mount *in situ* hybridization (WISH) is used to detected the expression pattern of developmentally regulated genes with specific nucleic sequences.

The method was executed as following. An antisense probe, which was labelled with digoxigenin covalently bound to UTP, was detected *in situ* with an antibody against the label. This specific antibody had its Fab-fragment fused to an alkaline phosphatase (AP). Upon the formation of a hybrid-nucleotide strand containing the endogenous RNA and the labelled antisense probe, the detection was accomplished by a chromogenic reaction carried out by the AP.

1. Fixation and storage of zebrafish embryos

Zebrafish embryos were fixed overnight in 4% PFA/PBST at 4°C or for 4h at RT on a shaker. They were washed two times in PBST for 5 min each and then dehydrated in 100% methanol.

The fixed larvae were then transferred into 100 % methanol and stored at -20 °C.

2. Rehydration of the zebrafish larvae

Before proceeding to the hybridization, the larvae needed to be rehydrated with a decreasing methanol series. The fixed larvae were incubated on a shaker for 5 min each in 75 %, 50 % and 25 % MeOH/PBST (v/v) and four more times in PBST.

3. Permeabilization of the zebrafish larvae

To permeabilise the tissue for mRNA probes and antibodies, fixed embryos were treated with the proteolytic enzyme Proteinase K. The embryos were incubated in Proteinase K/ PBST (10 µg/mL) for the respective time interval depending on the developmental stage of the embryos. The digest was stopped by washing in PBST and subsequent fixing in 4% PFA for 20min. To remove excessive PFA, embryos were washed 5 times in PBST for 5 min each.

Developmental stage	Duration of Proteinase K treatment
1dpf	5min
2dpf	20min
5dpf	40min
8dpf	100min

4. Hybridisation

During the rehydration of the larvae, the water bath was preheated to 62 °C. PBST was removed and 500 µl hybridization buffer was added. Pre-hybridization lasted for 1-2 hours at 60°C in the incubator. In the meantime, turn on the heating block to 90°C to denature probes. 200 µl hybridization buffer was prepared and 8 µl of each probe was added in RNase free tube. The buffers containing probes was denatured for 5 min at 90 °C. The pre-hybridization solution is quickly removed and replaced by the hybridization buffer containing probe. Hybridization lasts over night at 60°C in the water bath or the air incubator. The following steps were performed in the water bath (60°C) and all solutions have to be preheated, starting with 45 min in 50% FA / 2x SSC / 0.3% Tween for two times, 45 min in 2x SSC / 0.3% Tween for one time, and with 45 min in 0.2x SSC / 0.3% Tween for two times.

5. Antibody detection

The unspecific binding sites for the anti-dioxigenin Fab fragment were blocked with 1ml of 10 %

NGS/PBST for one hour at room temperature on a rotator. The solution was removed and the antibody diluted 1:3000 in 10 % NGS/PTW was added. The incubation was performed overnight at 4 °C on a rotator. To remove excessive unbound antibody, the larvae were washed 5 times in PBST for 15 min each on a shaker the next day.

After the last washing step, the larvae were incubated in the staining solution. Importantly, the staining solution was always prepared fresh. Due to light sensitivity, the staining reaction was carried out in the dark for 1-2 hours until the desired intensity of the blue precipitate. To stop the reaction, larvae were transferred into 4-well plates and washed 3 times in PBST for 10 min each. For long time storage, the larvae were transferred back into 2 ml tubes containing 90% glycerol (v/v) and kept at 4 °C.

2.2.7 *BacLight* Red Staining *C. difficile*

1. Prepare the solution of the *BacLight* bacterial stain

Prepare a 1 mM stock solution of dye by dissolving the vial contents in 69 µL DMSO.

Prepare a 100 µM working solution of the *BacLight*™ bacterial stain by adding 2 µL of the 1 mM stock solution prepared to 18 µL of DMSO in a centrifuge tube and mix well.

2. Prepare *C. difficile* sample

Referred to 2.2.2.1

3. Stain *C. difficile* with *BacLight*

Bacteria in 1 mL of culture were harvested, once washed with 1 x PBS (5000 *g*, 3 min and room temperature), and resuspended in 1 ml of 1 x PBS. 1 µL of the working solution of *BacLight*™ was added to 1 mL of bacteria suspension. The sample was incubated for 15 minutes at room temperature in the dark. Stained C. *difficile* were washed once with 1 x PBS in order to remove residual dye and resuspended in PBS to OD_{600} of 1.0.

2.2.8 Imaging

1. Embedding

Zebrafish were anaesthetized for 5-10 min with 0.004 % Tricaine. A hole was made on the

bottom of 35mm dish and a glass slide was attached, referred as imaging chamber. Embryos were transferred into the imaging dish. The 30 % Danieau was removed and 200-300 µl of 1 % low-melting agarose were added. The interested part was placed to touch the glass slide as close as possible. To solidify the low melting agarose, the dish was put on ice for 30-60 s. The agarose was covered with Tricaine in 30 % Danieau to suppress muscle spasms during imaging.

2. Confocal microscopy

The Leica Microsystems TCS SP8 inverted CLSM was utilized to make 3D and 2D images, and time-lapse imaging. Three objective lenses were used. One was a 20x oil immersion objective lens, which was used for the counting of the number of macrophage and neutrophil in zebrafish. The second was a 40x water immersion objective, which was used for the infection assay and the behavior assay of macrophage and neutrophil. The last one was 63x water immersion objective for the subcellular resolution images. The corrected laser and laser power should be selected as the following table (Table 12). For time-lapsing imaging, low power but high gain was used to protect zebrafish. To obtained detailed imaging of cell migration by increasing the image format, reducing the scan speed. But these settings would increase the acquisition time. Due to high migration speed of macrophages and neutrophils, it was necessary to set up the interval time shorter between 60 seconds to 120 seconds. For cell tracking, the interval time should be shorter than 90 seconds.

Table 12

Fluorescent Proteins	Excitation (nm)	Emission (nm)	Laser
CFP	405	477	405
EGFP	488	508	Argon
YFP	514	527	Argon
Monomeric Citrine	514	529	Argon
tagRFP-T	561	588	561

2.2.9 Generating gnotobiotic zebrafish

The protocol modified from previous method published by Pham et al., 2008.

1. Reagents setup

Antibiotics: Amphotericin B stock (1 mg/ml), Kanamycin stock (50 mg/ml), Ampicillin stock (20 mg/ml). Those antibiotics could be stored freezer for several years.

10% (wt/vol) polyvinyl pyrrolidone-iodine complex (PVP-I) stocking solution was prepare and stored in dark at 4 ℃. Diluted as 1:100 to 0.1% PVP-I for working concentration.

3% bleach stock solution and 0.003% bleach solution.

0.22μm filter was used to sterilized at least four liter of zebrafish system water (for two breeding tanks).

Autoclaved 30 % Danieau.

The day before experiment, prepare AKA-Danieau: Add 50ul of Amphotericin B stock solution, 20ul of Kanamycin stock solution, 50ul of Ampicillin stock solution into 50ml autoclaved 30 % Danieau. Store at 4 ℃.

2. Procedure

Transfer breeding pairs to a clean breeding tank with filter-sterilized system water. The sterilized system water should be warm-up in zebrafish room more than 5h.

Transfer breeding pairs to an extra clean breeding tank with filter-sterilized system water and remove plastic disk.

Collect embryos with a sterile pipette (collect eggs for no longer than 2 h) and transfer into a 15-ml tube. Remove excess system water, replace with AKA-Danieau.

Wash 3 times with AKA-Danieau in a culture hood and place the 15-ml tube into incubator for 3-8h.

At least 3h later, remove AKA-Danieau and gently immerse embryos with 0.1% PVP-I solution

for 1 min. Ensure that PVP-I incubation is no longer than 1.5 min and longer incubation cause increased fish mortality rates.

Wash embryos 3 times in autoclaved 30 % Danieau.

Immerse embryos with 0.003% bleach solution and incubate for 20 min at room temperature.

Wash embryos 3 times in autoclaved 30 % Danieau and transfer embryos to a sterile petri dish.

Change the media daily.

3 Results

3.1 Establishment of zebrafish genetic model to screen antagonists of *Clostridium difficile* toxins

3.1.1 Both TcdA and TcdB induced cardiac edema, cell death, and mortality in zebrafish embryos

Hamm et al. identified that TcdB functions as a potent cardiotoxin in a zebrafish model of intoxication (Hamm et al., 2006). To find out whether TcdA shares similar function with TcdB, TcdA, TcdB, TcdA mutant, and TcdB mutant (recombinant proteins received from Prof. Dr. Gerhard) were used. TcdA D285/287N and TcdB D286/288N are mutants that are deficient in glucosyltransferase activity (Chumbler et al., 2016; Teichert et al., 2006). Zebrafish embryos were collected at 72hpf and exposed to medium containing different toxins. Both TcdA and TcdB mutants did not show toxicity in zebrafish (data not shown). However, both TcdA and TcdB lead to different mortality rates within 72h of exposure (Figure 17 A, B). 10 nM TcdB did not lead to zebrafish death, but 20 nM TcdB was associated with an increase in mortality, with a 14% mortality rate after 1 day of exposure and a 80% mortality rate after 3 days of exposure (Figure 17 B). For a long time TcdB has been believed to be more potent than TcdA in damaging some cell types, but TcdA was found to be more toxic than TcdB to zebrafish at the same concentration (Figure 17 A, B) (Aktories, 1997; Chaves-Olarte et al., 1997). 10 nM TcdA caused 100% mortality after 24h of exposure and was therefore not evaluated further (Figure 17 A). 5 nM TcdA led to a mortality rate of 87% after 24h of exposure, and 100% mortality after 48h of exposure. This finding demonstrated that both TcdA and TcdB were toxic (depending on concentration and time) to zebrafish, which relied on the functional glucosyltransferase activity.

Also, some TcdA-treated fish also exhibited pericardial edema (Figure 17 C). But acridine orange staining showed an increased cell death throughout the entire embryo (Figure 17 D). Interestingly, fluorescence signal was found predominately at pericardial region, indicating that TcdA might also lead to cardiovascular damage. This finding suggested that TcdA also possessed cardiotoxicity as TcdB did.

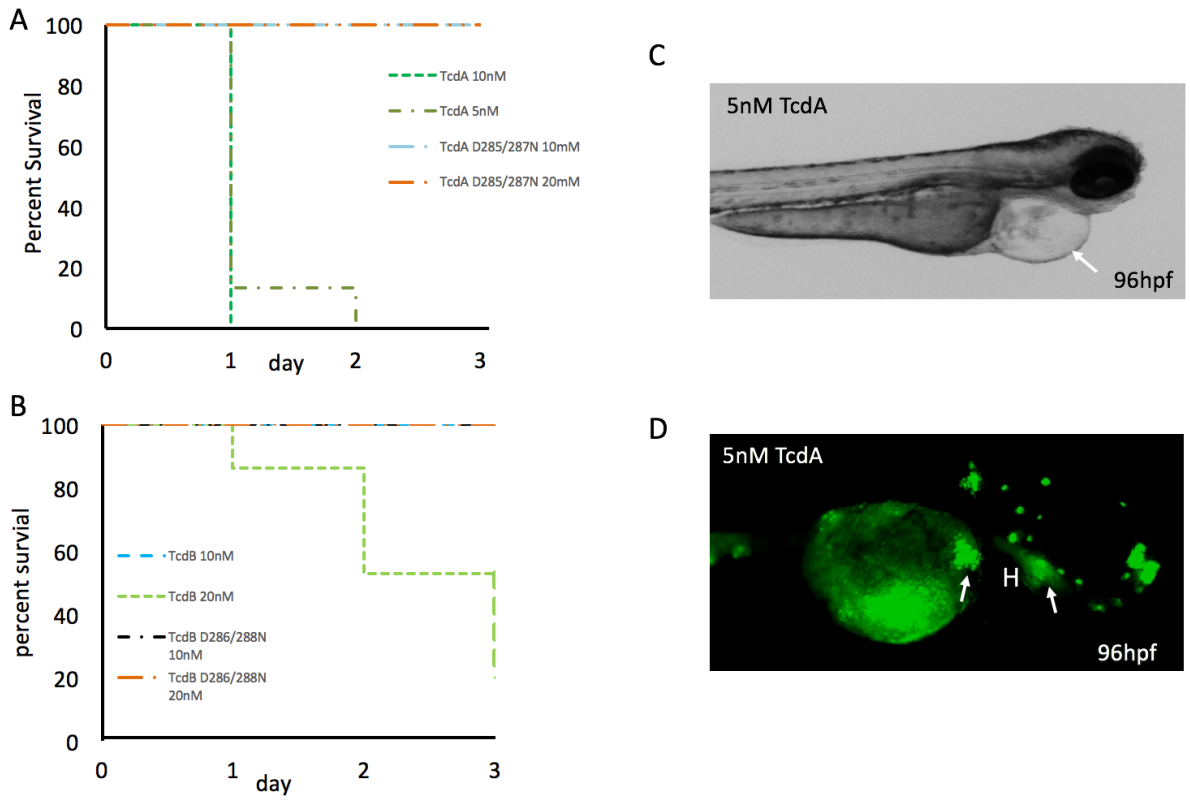

Figure 17 Survival rates and morphological changes of zebrafish after recombinant TcdA and TcdB treatment

A) Percentage of surviving embryos at 72hpf upon treatment with TcdA or TcdA D285/287N at denoted concentrations for 3days. n=20 fish/treatment. B) Percentage of surviving embryos upon treatment with TcdB or TcdB D286/288N at denoted concentrations for 3days. n=20 fish/treatment. C) Brightfield image of zebrafish treated with 5nM TcdA for 24h. D) 72hpf embryo was treated with 5nM TcdA for 24h and cell death was detected by acridine orange staining. H: heart.

3.1.2 Target selection for compound screening

Drug discovery often begins with identifying a novel promising target. However, even though extensive work has been performed to validate useful targets that play critical roles in human diseases, or infections, the number of good targets remains low. Therefore, it is a considerable challenge to identify a right target.

The two main toxins, TcdA and TcdB, have been studied intensively. They are identified as major *C.difficile* virulence factors. As mentioned, once C-terminal GROPS bind to the receptors of epithelial cells, the N-terminal GTD is delivered into the cytosol, inactivating host GTPases by glucosylation. The inactivation of GTPases results in the epithelial cell death and intestinal membrane damage, which induce inflammatory response, and furthermore leads to intestinal

hemorrhage and diarrhea. Based on this molecular pathogenesis, an inhibitor targeting GTD could further solve this disease. Therefore, we selected GTD as the target to screen antagonists of *C. difficile* toxins.

Highly expressed prokaryotic genes have a biased codon usage compared to zebrafish. In order to obtain adequate toxin expression, we synthesized the N-terminal fragments of TcdA and TcdB cDNA with codon usage optimized expressions in zebrafish. I named them as NTcdA and NTcdB.

The *C. difficile* 630 strain is used as the virulent and common strain for characterization of *C. difficile*. The DNA sequence of NTcdA and NTcdB are 72% and 75% identical to their corresponding toxins in *C. difficile* 630 strain respectively (Figure 18). The amino acid sequence of GTD in both NTcdA and NTcdB is 100% identical to their corresponding toxins sequence in the *C. difficile* 630 strain. At the C-terminal of NTcdA and NTcdB, an HA tag was fused, facilitating the detection of the toxins in zebrafish.

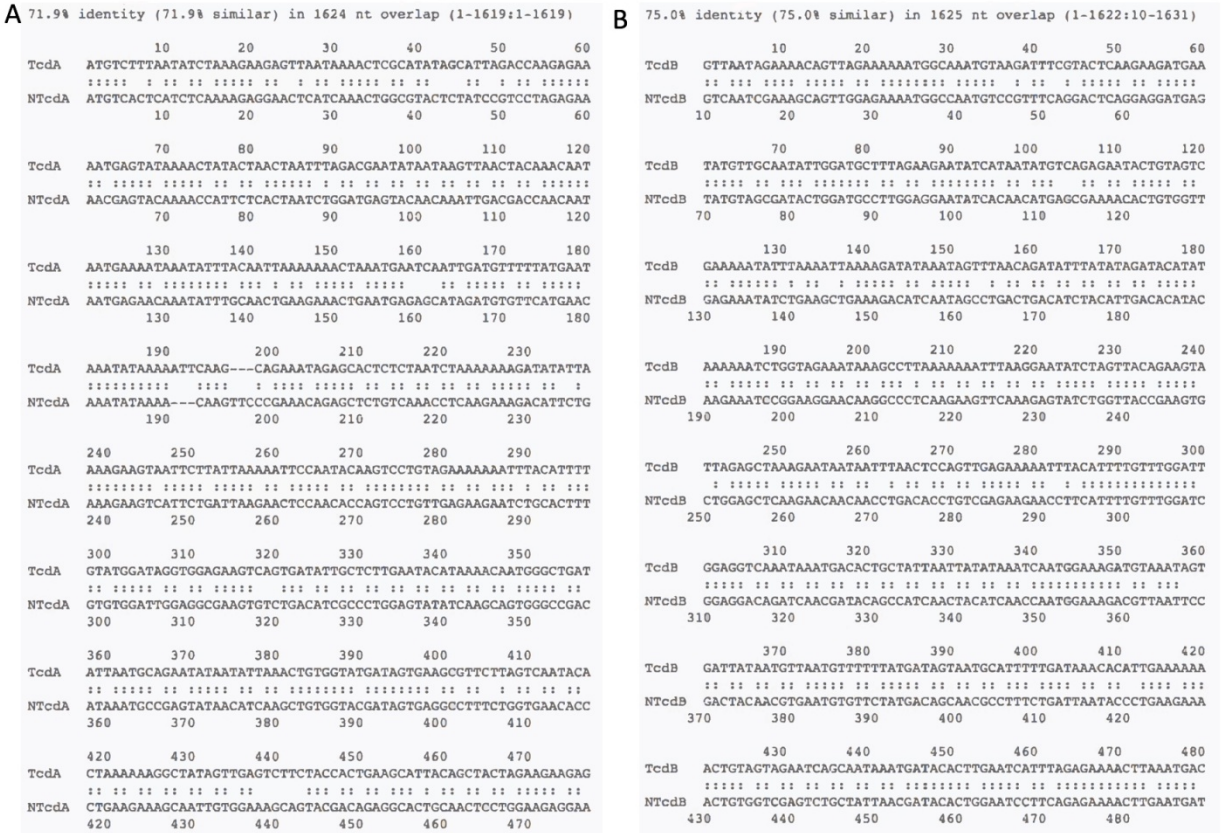

Figure 18 The sequence comparison between NTcdA and NTcdB and *C. difficile* 630 TcdA and TcdB sequences.

A) 480bp upstream sequence of NTcdA compared with TcdA from *C.difficile* 630 strain. TcdA sequence that was used can be found in GeneBank under accession no. HG002394.1. B) 480bp upstream sequence of NTcdB compared with TcdB in GnenBank. TcdB sequence that was used can be found in GeneBank under accession no. CP022524.1.

3.1.3 Bi-directional hatching gland specific promoter expression system

To establish a transgenic zebrafish model to identify and validate antagonists of Tcds, the targeting cells are required to fulfill an important function during early embryogenesis to simplify antagonist evaluation. In addition, this cell population should be easily accessible for rescue approaches. Such an ideal cell type is represented by the zebrafish hatching gland.

The hatching gland is a set of transversely oriented cells on the pericardial membrane, ventral to the head, where the hatching enzymes are produced and stored (Kimmel et al., 1995). The hatching enzymes are required to break down the chorion in the first 48 hours after fertilization, after which hatching gland is not further required. A malfunctioned hatching gland impairs embryo hatching, which can be overcome easily by pronase mediated enzymatic hatching. Particularly, a zebrafish hatching gland specific promoter (HE, kind gift from Dr. Jeff S Mumm) has been identified, which is exclusively expressed in hatching gland.

GTD inactivates host GTPases and induces apoptosis in infected cells. To monitor the physiology of hatching gland cells simultaneously, an apoptotic reporter was co-expressed with N-terminal fragment of toxins in a bidirectional manner. For this purpose, the feasibility of a bidirectional expression unit was tested under the control of HE enhancer. The bidirectional cassette contains two HE enhancers that are flanked on either side by E1b minimal promoters driving fyntagRFP-T/ GFP fluorescent protein as shown in Figure 19 A. The vector named bi-HE, was used for injection at the one-cell stage. High levels of reporter gene co-expression were observed in hatching gland cells of injected embryos after 24h of injection (Figure 19 B). This indicated that HE enhancer drove adequate expression of both genes in those hatching gland cells.

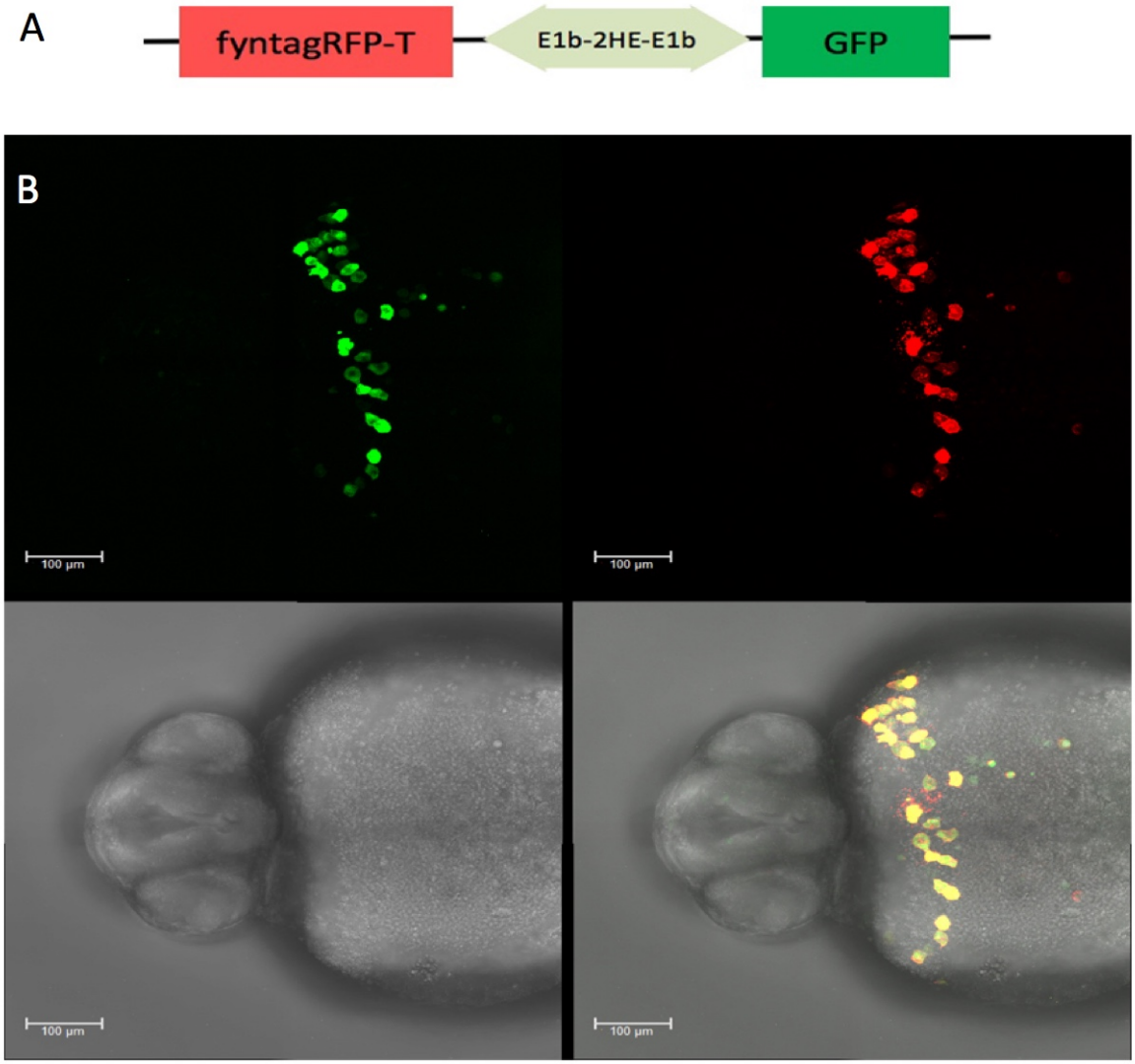

Figure 19 bi-HE construct for simultaneous expression of multiple fluorescent proteins.

A) Schematic representation of the bi-directional HE vector. B) In transient injection, RFP and GFP were co-expressed simultaneously in hatching gland cells of injected embryos.

To assess if the bidirectional HE cassette constitutively expressed two reporter genes, co-expression activity was determined by the ratio of double-positive cells (red and green) to the total number of single- and double-positive cells (Figure 20 A). In 20 embryos, there were 605 double-positive cells and 8 single-positive cells. This analysis demonstrated that the bi-HE construct reliably co-expressed two transgenes *in vivo* (co-expression rate 99%) (Figure 20 B).

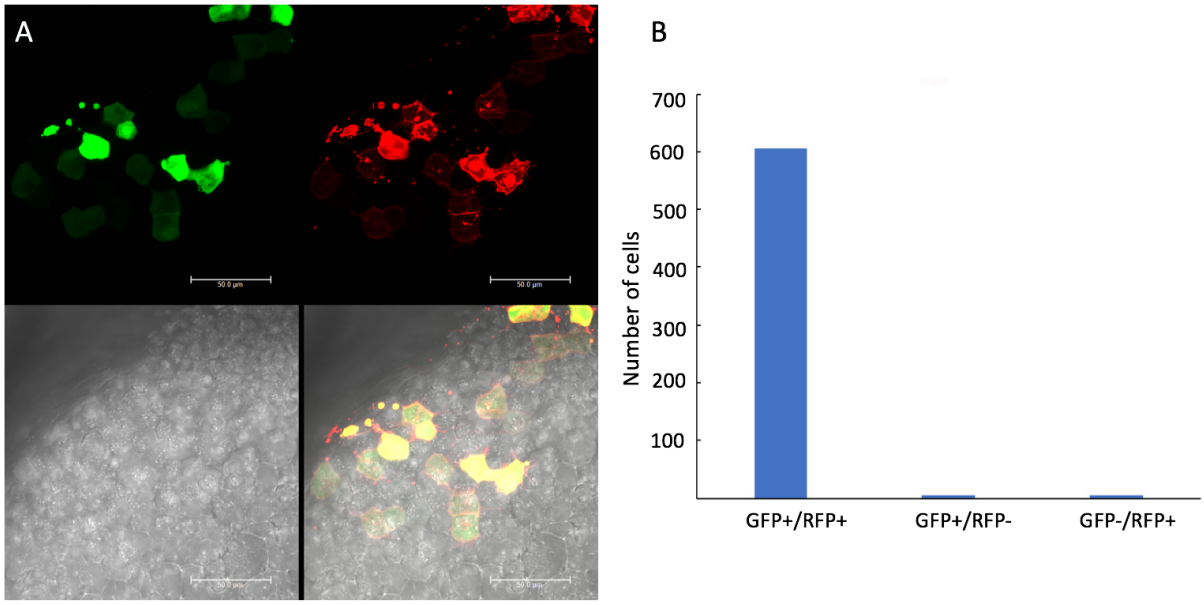

Figure 20 Co-expression ration of two fluorescent proteins in bi-HE construct

A) The image captured by confocal for counting. B) Bar chart illustrated the number of double positive (GFP+/RFP+) or single positive cell (GFP+/RFP- or GFP-/RFP+) in 20 injected embryos.

In transient assays, several non-hatching gland cells of injected embryos expressed fluorescent protein. To examine the specificity of HE enhancer, whole mount *in situ* hybridization (WMISH) using antisense RNA probes against RFP or GFP mRNA was performed in bi-HE injected embryos (24 hpf). Intense signals were detected in hatching gland cells of in a half-moon shape on top of the yolk exclusively by using either probe (RFP/GFP) (Figure 21 B, D). This result indicated that the HE enhancer has a specific expression in hatching gland cells.

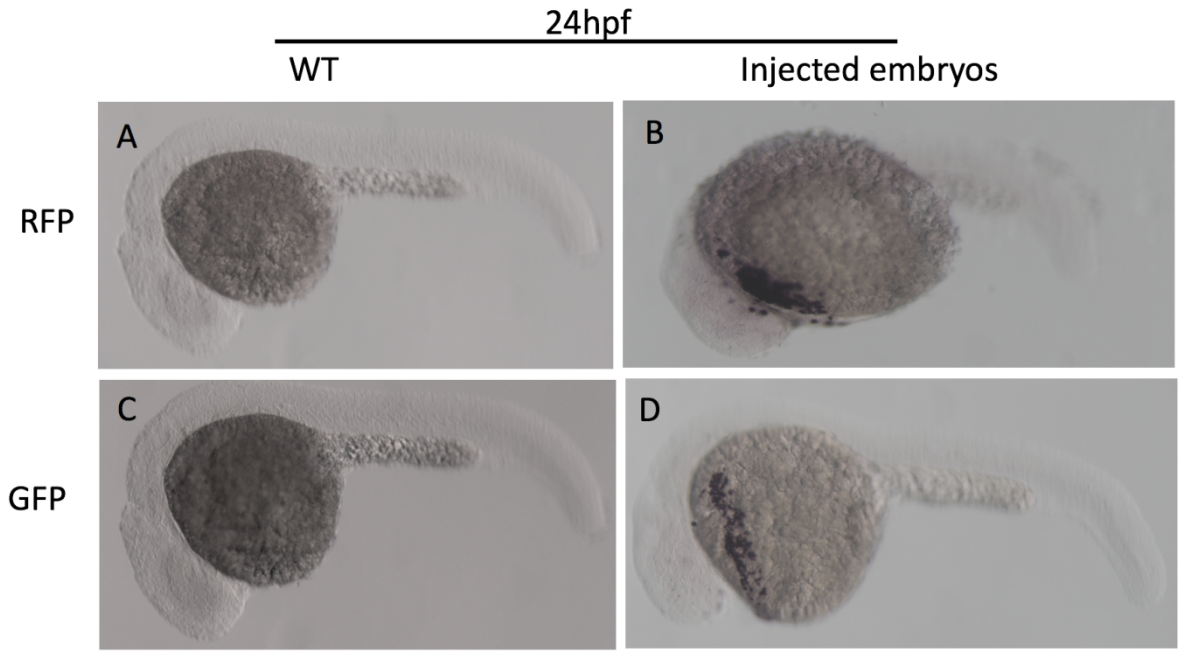

Figure 21 Expression of GFP and RFP was detected by whole mount *in situ* hybridization.

(A-B) *In situ* hybridization for RFP at 24 hpf. (C-D) *In situ* hybridization for GFP at 24 hpf

Taken together, the HE enhancer has a restricted expression pattern in cells of hatching gland and could induce high level expressions of two transgenes specifically in a bidirectional manner. This should be applied to transgenic fish, in which the GTD of TcdA and TcdB would specific be expressed in hatching gland to trigger apoptosis, while the apoptosis would not diffuse to other organs to affect zebrafish embryogenesis.

3.1.4 Establishment of transgenic fish lines for compound screening

3.1.4.1 The leaky expression of toxins in NEB 5α competent cells

In order to establish transgenic zebrafish lines, NTcdA or NTcdB was inserted into bi-HE vector, referred to as bi-HE-TcdA or bi-HE-TcdB, and subsequently these vectors were used for microinjection into one-cell stage of zebrafish embryos. It turned out that all the embryos died around within 7 hours after microinjection.

Since the bi-HE vector alone was not lethal, we hypothesized that there might be leaky expression of toxins in bacteria used for plasmid preparation, which led to the death of embryo. To confirm this hypothesis, toxin expression was evaluated by western blotting using an anti-HA tag antibody. pCS-NTcdA or pCS-NTcdB were transfected into HEK293T cells, and

cells were harvested and lysed 48h later as positive control. NEB 5α cells were transformed with the bi-HE vector expressing GFP and RFP as negative control.

Western blot analysis detected 2 prominent bands with molecular masses of approximately 63kD in the lysates of HEK293T cells transfected with NTcdA and NTcdB. Also, slight but clear bands at the same size can be detected in the lysate of NEB 5α bacterial, indicating NTcdA and NTcdB were expressed in *E. coli* (Figure 22 A). I supposed the eukaryotic post-translation modification resulted in the different molecular weights of toxins purified from *E. coli* and HEK293T (Figure 22 A).

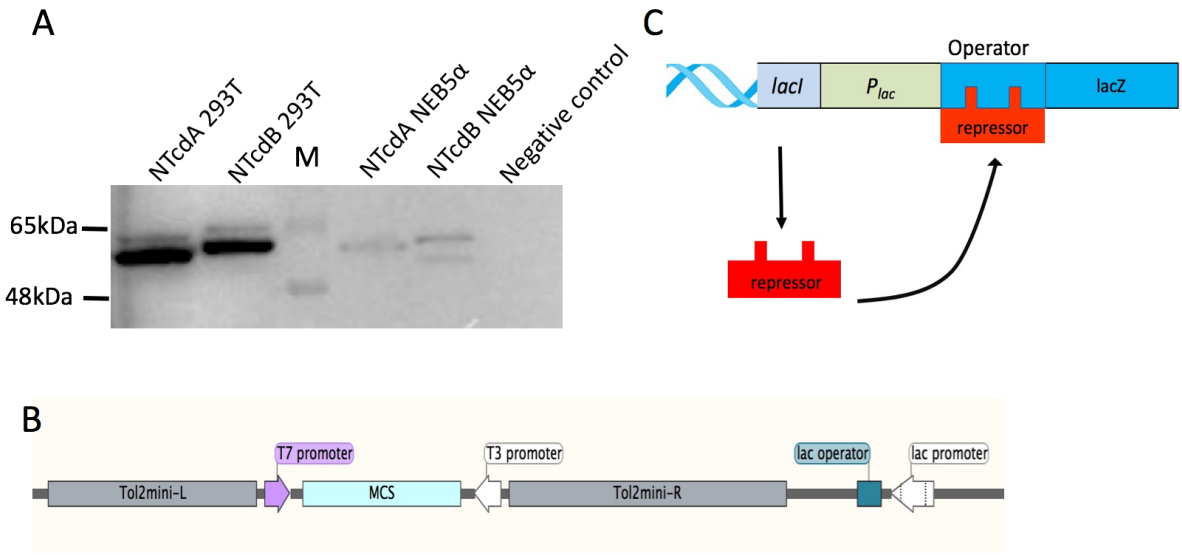

Figure 22 Leaky protein expression of NTcdA and NTcdB in bacteria.

A) Westernblot analysis with anti-HA antibody of lysates from HEK293T cells and NEB5α. Both pCS-NTcdA or pCS-NTcdB were expressed in 293T cells. M, marker. B) A schematic diagram of Tol2 vector. The multiple cloning region was flanked by three promoters: T7, T3 and lac promoter. C) *lac* operon. The lacI (*lacI*) gene, located near promoter (P_{lac}), regulates operon by producing the lac repressor protein. In the absence of lactose, the repressor binds tightly to operator and prevents access of RNA polymerase to the promoter. Thus, translation is blocked and the operon is repressed.

Some promoters or enhancers are not tightly regulated, which causes baseline gene expression before addition of inducers. To solve the leaky expression, constructs were analyzed by sequence to find out which enhancer or promoter might cause such leaky expression. The analysis identified 3 promoters in the bi-HE construct: a T3 promoter, a T7

promoter, and a *lac* promoter (Figure 22 B). T7 and lac promoters are used widely for protein expression, while the T3 promoter is not generally adopted. There is also no report about T3 regulation problem.

The T7 promoter has been commonly used in protein expression vector, for instance, reputably pET series vectors (Rosano et al., 2014). In this system, T7 promoter is recognized and activated by phage T7 RNA polymerase which is provided by either other vectors, or the host cell (like, BL21 DE) with T7 polymerase integrated into the genome (Rosano et al., 2014). Since NEB 5α neither contains other T7 polymerase vectors nor has any T7 polymerase integrated into genome, T7 promoter was excluded from leading to the leaky expression. All evidences indicated that the leaking toxins transcription was induced by *lac* promoter.

The lac promoter is a component of the *lac* operon. The lac operon consists of a set of genes that are involved in the metabolism of lactose. Inducer-repressor control of the *lac* operon is a classic example of gene regulation. The regulatory components of *lac* system include (Figure 22 C):

1) The lac promoter. Which is the site where RNA polymerase binds to initiate transcription.

2) The lac operator (lacO), which is a short sequence to which repressor proteins bind. It is located between the promoter and inserted genes near the transcription start site.

3)The lacI or lacIq repressor encode by *lacI* and *lacI*^{q} gene, which recognizes and binds to the lac operator and then turns off gene expression.

However, only one lac operator, which was also far from transcription start site of NTcdA or NTcdB, was identified in the construct. The single operator could not provide tight regulation of the *lac* promoter. Furthermore, the NEB5α competent cells do not contain either the *lacI* or *lacI*^{q} gene, which causes inefficient regulation of the *lac* promoter. Overall, inefficient regulation of either the lacI/lacI^{q} repressor or the lac operator might cause low-level constitute toxins expression in NEB 5α bacterial cells.

3.1.4.2 Application of NEB turbo and *lac* operator

To test the hypothesis about the *lac* promoter, a different competent cell line, NEB turbo, was used to amplify the toxin constructs. NEB turbo features the ideal traits for cloning toxic genes

(Figure 23 A). NEB turbo cells show high expression of $lacI^q$ to supress leaky expression of transgene, which allows potentially toxic genes to be amplified.

Bi-HE-TcdA or bi-HE-TcdB vector were transformed into NEB 5α or NEB turbo. After plasmid purification, 5ng/µl of either NTcdA or NTcdB DNA was injected into one-cell stage embryos. The survival rate was recorded 24h after injection (Figure 23 B). 51% or 10% embryos survived with plasmid purified from NEB turbo, while all embryos were dead from NEB 5α-derived DNA injection. NTcdA injected embryos showed higher survival rate, supporting previous studies that TcdB was more toxic than TcdA (Carter et al., 2010; Voth et al., 2005). This result suggested that NEB turbo was suitable for the amplification of toxic constructs. However, the survival rate of embryos was still low.

A

	Genotype
NEB turbo	*F' proA⁺B⁺ lacI^q ΔlacZM15 / fhuA2 Δ(lac proAB) glnV galK16 galE15 R(zgb-210::Tn10)Tet^S endA1 thi-1 Δ(hsdS-mcrB)5*
NEB 5α	*fhuA2 Δ(argF-lacZ)U169 phoA glnV44 Φ80 Δ(lacZ)M15 gyrA96 recA1 relA1 endA1 thi-1 hsdR17*

B

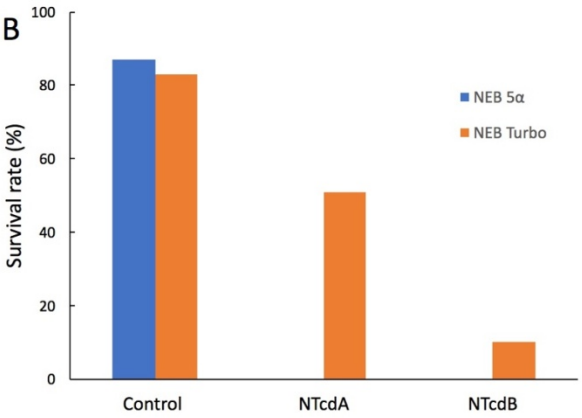

Figure 23 Application of NEB turbo competent cells for constructs purification

A) Genotype comparison between NEB turbo and NEB 5α. NEB turbo is characterized by high expression of the lac repressor protein. B) Survival rate of zebrafish embryos with plasmid purified from NEB turbo or NEB 5α. Control indicates un-injected embryos.

Based on our sequence about the lac promoter, the second possible solution to supress the leaky toxins expression was to insert extra *lac* operators (lacO) near the transcription start site of the toxin transgenes. To confirm the feasibility of this hypothesis to acquire higher survival rate, lacO were inserted into the toxin-containing constructs to further suppress the activation of the lac promoter. lacO sequence is usually located between the promoter and the downstream gene, close to the transcription start site. 4 copies of the lac operator sequence (4xlacO) were placed in front of NTcdA or NTcdB transgenes. Indeed, survival rate of zebrafish

embryos after plasmid injection further improved than amplifying plasmid in NEB turbo cells without adding 4xlacO sequence (data not shown). However, we wondered if such repression effect would transfer from bacteria to zebrafish, which down-regulate the expression of toxins.

To address this question, a new construct was created in which 4xlacO sequence were placed in front of tagRFP-T in the bi-HE vector (Figure 24 B). Zebrafish embryos were injected with this bi-HE-4xlacO construct or the bi-HE vector to evaluate the expression level of fluorescent protein (Figure 24). The fluorescent images were obtained 24h after plasmid injection, which revealed a visible difference in the RFP fluorescence level (Figure 24). Using the same expose time as for bi-HE injected-embryos, RFP fluorescence was barely visible in 4xlacO construct injected embryos. I was concerned about whether the decreased toxin expression level would cause non-cytotoxic effects in hatching gland cells.

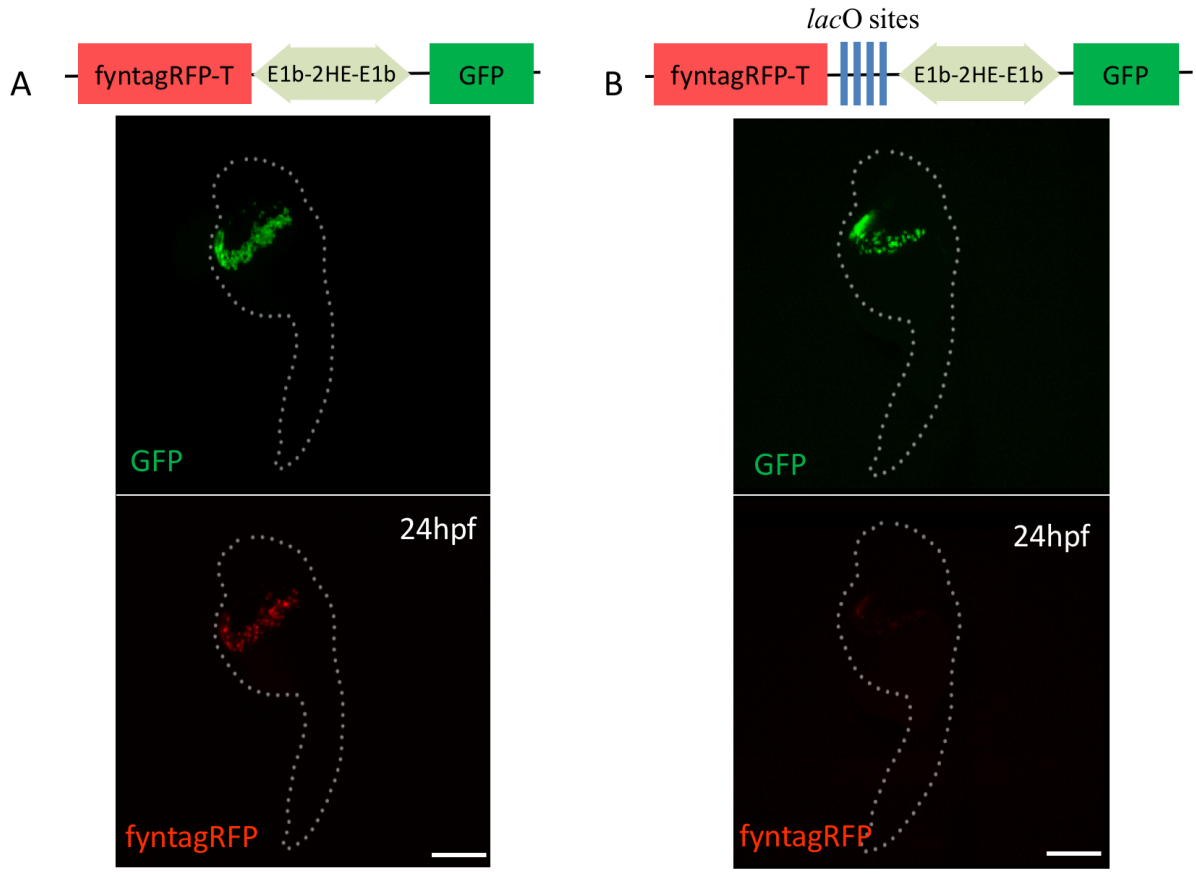

Figure 24 Comparison of fluorescent protein expression level in transient assay.

A) Schematic representation of the bi-HE construct and an embryo injected with the bi-HE construct. B) Schematic representation of 4xlac construct and an embryo injected with bi-HE-4xlacO construct. Scale bar, 200 µm.

In case the repression effect would transfer from bacteria to zebrafish, we used an Exon-Intron system to splice out 4xlacO in zebrafish (Figure 25 A). We therefore order the synthesis of DNA-fragment containing exon 2, intron 2, and exon 3 of zebrafish housekeeping gene *rpl9*. 4xlacO sequence were inserted into the intron 2, where the 4xlacO sequence would be spliced out together with intron 2 in zebrafish after transcription. Notably, the size of exon2 or exon3 was less than 50bp, which means 4x*lacO* was still close enough to the transcription start site to repress toxin production in bacteria.

In order to confirm if the expression level of fluorescent protein could be restored, the construct was injected into one-cell stage zebrafish embryos. The images were taken 24h after injection. The mean fluorescent intensity was measured and calculated using ImageJ (Figure 24 B). The fluorescent intensity of Exon-4xlacO injected group was set to 100 percent. the relative fluorescent intensity of the control group injected with bi-HE was 131%, which as still statistically insignificant (Figure 25 C). This result indicated that a slight fluorescent restoration after splicing out 4xlacO in zebrafish.

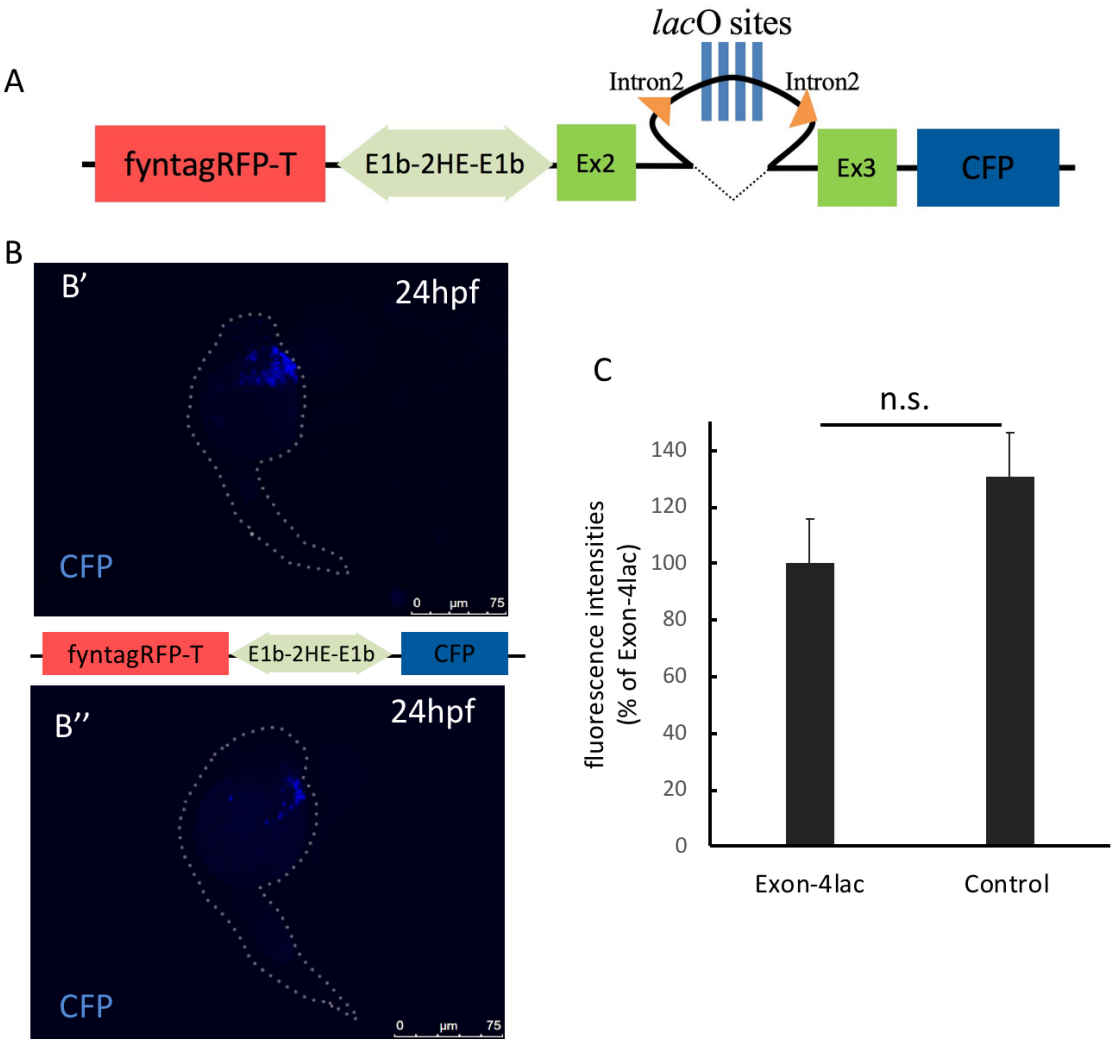

Figure 25 Schematic diagram of bi-HE vector containing 4xlacO and application of Exon-Intron system

A) Schematic representation of the bi-HE construct containing the exon-intron-exon sequence and 4xlacO. B) Schematic representation of Exon-4x*lacO* and control construct injected embryo 24 hour later. C) The fluorescent intensities of the exon-4xlacO and control group injected with bi-HE was calculated by ImageJ. n.s.: no significant difference. mean +SEM. $p< 0.05$, statistically significant.

3.1.4.3 Application of bile acid in the established transgenic lines

As shown in Figure 23 B, the survival rate of NTcdB-injected embryos was lower compared to NTcdA injected embryos, which indicated that NTcdB was more lethal than NTcdA for zebrafish embryos (Chaves-Olarte et al., 1997). As mentioned in introduction 1.3.1, some bile acids prevent the onset of CDI. By testing three bile acids, Taurocholic acid sodium (TCA), tauroursodeoxycholate (TCDCA) and tauroursodeoxycholate (TUDCA), it was found that TUDCA was able to inhibit TcdB activity and rescue TcdB-induced cytotoxicity in cells (Genth's unpublished data).

Before applying bile acids in zebrafish, whether NTcdB was expressed after microinjection was investigated by RT-PCR. Since intron2 of *rpl9* was inserted into the construct, primers were designed to span the intron region. If the intron2 containing 4×lacO sequence were spliced out, RT-PCR would show a shortened DNA band without the intron sequence. Total RNA was isolated from bi-HE-TcdB injected embryos 5h after microinjection. Interestingly, RT-PCR detected a shortened band, indicating NTcdB was already expressed 5 hours after microinjection (Figure 26 A and A'). Sequencing of these RT-PCR products showed that intron2 containing 4×lacO sequence indeed were spiced out. NTcdA was also detectable (data not shown). Besides, western blot already demonstrated that low level of the toxins was expressed in *E. coli* (Figure 22 A), this result indicated that toxins were also expressed in embryos. However, it was difficult to distinguish which was the main reason that leads to embryo mortality.

Thus, to obtain higher survival rates and to get more healthy embryos after plasmid injection, three bile acids were tested in zebrafish (Figure 26). To assess the toxicity of the bile acids for embryos, one-cell stage embryos were injected with bile acids ranging from 0.2 mM to 22 mM. Mortality and malformations were recorded 24 h after injection. 4mM TUDCA, 0.8 mM TCDCA and 1 mM TCA was adopted respectively for co-injection with 5 ng/µl of bi-HE-TcdB construct. The survival rate was recorded 24 h later (Figure 26 B, C, and D). As Figure 26 B' showed TCA did not rescue the NTcdB-induced embryos death (Figure 26 B'). The bi-HE-TcdB injected embryos treated with TCDCA showed an even little lower survival rate than control injected embryos (Figure 26 D'). In contrast, after treatment with TUDCA, the survival rate increased from around 20% to 40%, which was statistically significant (Figure 26 C'). These results indicated that TUDCA could confer protection against NTcdB-induced embryonic death, and also increase the ratio of visibly healthy embryos. This finding fit to previous studies in which TUDCA rescued TcdB-induced cytotoxicity in cultured cells. Therefore, 4mM TUDCA was applied to the injection mixture in further studies.

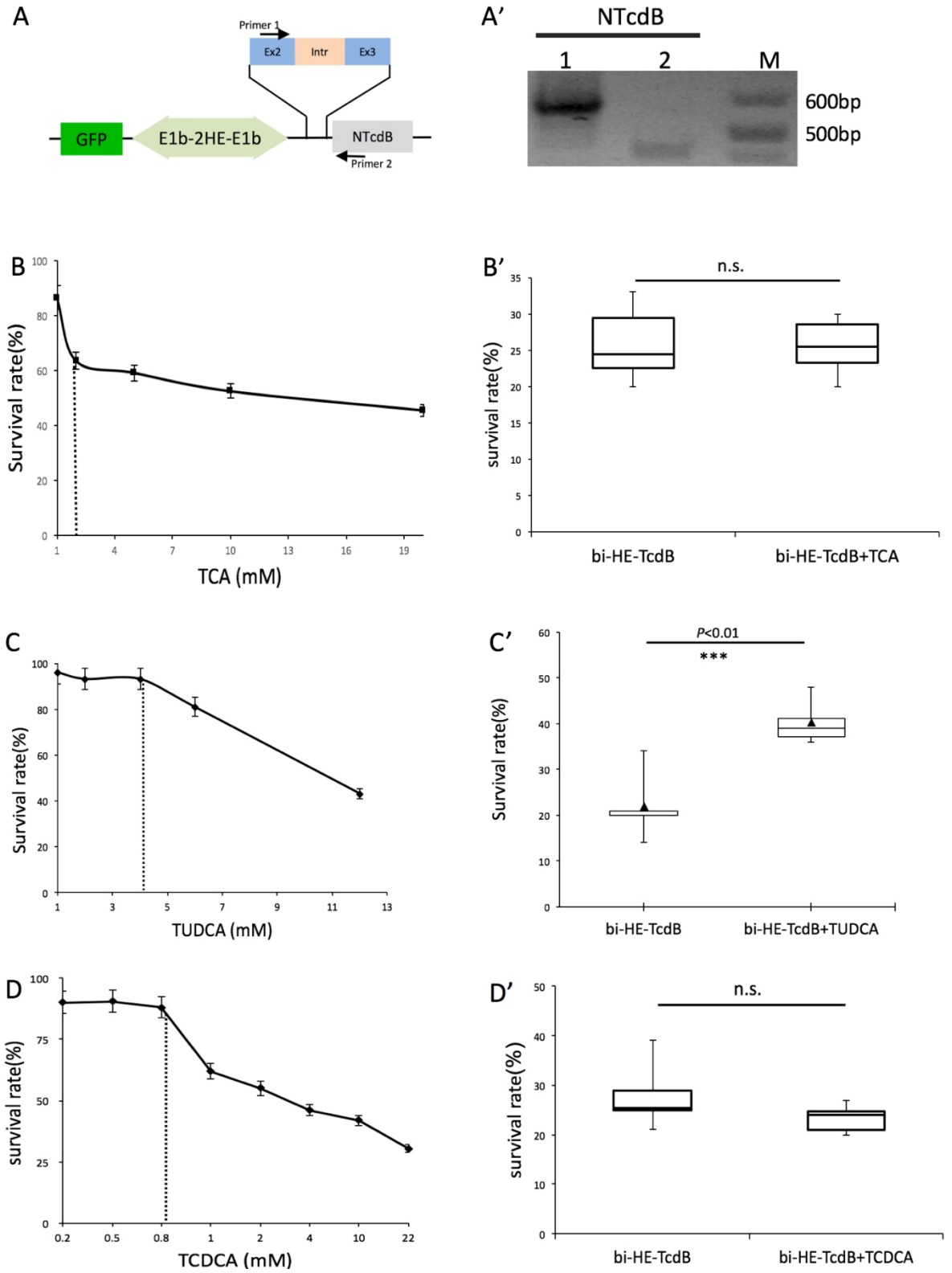

Figure 26 Application of bile acid in NTcdB injection.

A) Schematic representation of construct bi-HE-TcdB. Primers were designed to span the intron region. The size of the PCR product indicates whether NTcdB was expressed by the zygote. A') NTcdB expression was measured by RT-PCR in injected embryos (n=3) Lane 1. Positive control using pcs-NTcd vector as template. Lane 2. TcdB

injected embryos. Note the reduced size of the RT-PCR product by about 100bp of Intron size. M: size marker. B) Survival rate after TCA injection. Serial dilutions of TCA from 1mM to 2mM were injected into one-cell stage embryos and the survival rate was recorded 24h later (n=3, 362 embryos). Dashed line indicated the highest non-toxic concentration (1mM) which was applied in further studies. B') Survival rate after co-injection of 5µg/µl TcdB vector and 1mM TCA (n=3 injections, 423 embryos). p=0.142696. C) Survival rate after TUDCA injection. Serial dilutions of TUDCA from 1mM to 12mM were injected into one-cell stage embryos and the survival rate was recorded 24h later (n=3, 558 embryos). Dashed line indicated the highest non-toxic concentration (4mM) which was applied in further studies. C') Survival rate after co-injection of bi-HE-TcdB and TUDCA (n=6 injections, 929 embryos). D) Survival rate after TCDCA injection. Serial dilutions of TCDCA from 0.2mM to 22mM were injected into one-cell stage embryos and the survival rate was recorded 24h later (n=3, 481 embryos). Dashed line indicated the highest non-toxic concentration (0.8mM) which was applied in further studies. D') Survival rate after co-injection of 5ng/µl bi-HE-TcdB and 0.8mM TCDCA (n=6 injections, 392 embryos). p=0.1523.

3.1.4.4 The apoptosis biosensor secA5-YFP

After toxins are delivered into cells, GTD domains are released into the cytosol. GTD inactivate Rho GTPases in targeted cells. Inactivation of Rho proteins disrupts the organization of the cytoskeleton and induces apoptosis, eventually leading to cell death. Therefore, released GTD domain in hatching gland cells might lead to apoptotic cell death.

In order to monitor apoptosis in hatching gland cells, a fluorescence-based apoptosis reporter was co-expressed with toxins in hatchling gland cells. Currently, several noninvasive apoptosis biosensors that monitor caspase activation, have been developed, such as, Apoliner and VC3AI (Bardet et al., 2008; J. Zhang et al., 2013). However, Apoliner and VC3AI either showed constant but weak signal, or no fluorescent signal at all in zebrafish (data not shown). Another apoptosis sensor, secA5-YFP, was tested, which had been demonstrate to work in zebrafish embryos (Figure 27 A) (van Ham et al., 2010). During apoptosis, phospholipid phosphatidylserine (PS) translocated from inner leaflet to outer leaflet of the plasma membrane. The calcium-dependent Annexin V (A5) binds PS with high affinity, which is utilized to detect apoptosis. secA5-YFP is a fusion of secreted Annexin V (secA5) and the yellow fluorescent protein (YFP), which specifically condenses and thereby labels apoptotic cells in living zebrafish (van Ham et al., 2010).

SecA5-YFP mRNA was microinjected into one-cell-stage embryos. At 24hpf, the injected embryos were exposed to 5µM thapsigargin for 4 hours. Thapsigargin is a specific ER calcium-ATPase inhibitor, which induces apoptosis in zebrafish embryos (Pyati et al., 2011). After

treatment with thapsigargin, green fluorescence intensity was enhanced markedly, and fluorescence-positive cells were also increased (Figure 27 B and C). This result confirmed that secA5-YFP labeled apoptotic cells in zebrafish embryos.

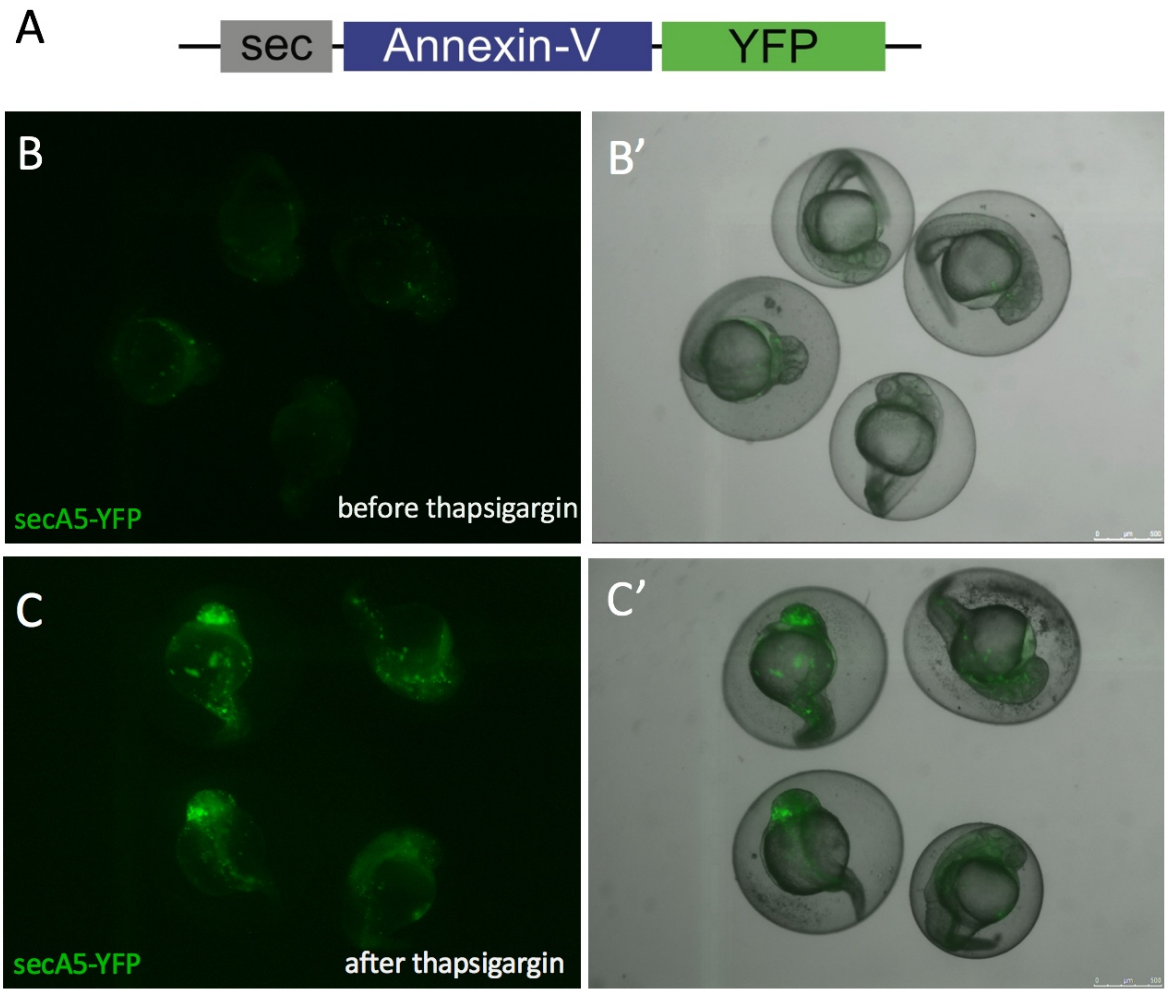

Figure 27 secA5-YFP labelled apoptotic cells in live zebrafish embryos.

A) Schematic representation of secreted secA5-YFP fusion construct. (From van Ham et al., 2010). B and B, C and C') Fluorescence images (B and C) and bright field overlay images showing apoptotic cells after 4 hours of 5µM thapsigargin treatment. B and C were obtained with same microscopy setup.

3.1.4.5 Establishment of toxins transgenic fish lines

Using LexA/lexAop system (refer to section 3.2.4.1), establishment of NTcdA and NTcdB stable transgenic zebrafish lines are in progress.

3.2 *C. difficile* infection model for imaging innate immune response

3.2.1 Neutrophils and macrophages responded to *C. difficile in vivo*

Neutrophils and macrophages play critical roles in fighting against *C. difficile* infection, but their behavior in this defense needs to be better understood. Using Gal4/UAS system, a macrophage reporter strain and a neutrophil reporter strain were generated. *lyz* (lysC), a neutrophil specific promoter, was used to drive the expression of KalTA4 in neutrophil. *mpeg1,* a macrophage specific promoter, was used to drive the expression of KalTA4 in macrophages (Figure 28).

The first step was to generate a macrophage specific KalTA4 activator strain and a neutrophil specific KalTA4 activator strain. An insulator and HE enhancer were used in these two constructs used for generating KalTA4 activator strains (Figure 28). Because of the invisibility of KalTA4 expression, every transgenic zebrafish is necessary to be confirmed as positive by crossing with UAS fish line. To get the positive KalTA4 activator zebrafish directly, these two constructs were introduced an insulator and HE enhancer driving BFP expression. BFP fluorescent signal would be the screening marker for the positive KAlTA4 activator zebrafish. HE enhancer would be silenced after 3 dpf, which means no BFP fluorescent signal would be detected after that. The insulator is DNA-protein complexes that act as an enhancer blocker or serve as barriers against the spreading of heterochromatin in reporter system. It allows the two different expression units working independently.

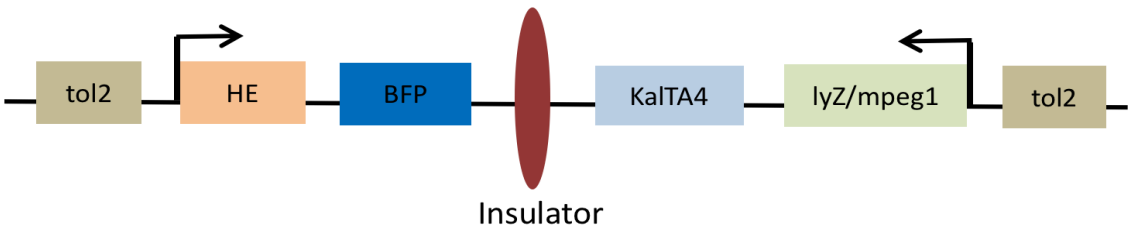

Figure 28 Schematic structure of the plasmid used for generating macrophage and neutrophil KalTA4 activator strains.

KalTA4 is under control of either *lyZ* or *mpeg1* promoter and BFP fluorescent proteins is under control of HE enhancer. An insulator sequences isolates the two expression cassettes. The construct is flanked by Tol2 recognition sites (Tol2) for transposase mediated integration.

These two vectors were co-injected into one-cell stage of zebrafish embryos with mRNA encoding Tol2 transposase. BFP fluorescent embryos were raised to adult stages after 3 months later. Then they crossed with *Tg*(*UAS-E1b:EGFP*) to get macrophage reporter zebrafish strain *Tg*(*mpeg1: Kalta4*, *UAS-E1b:EGFP*) and neutrophil reporter strain *Tg*(*lyZ: Kalta4*, *UAS-E1b:EGFP*).

In order to detect and track *C. difficile*, the bacteria was labeled. Given that most fluorescent proteins require oxygen to mature their chromophore, made it difficult to use such fluorescent proteins in strict anaerobic *C. difficile* (Craggs, 2009). Ransom et al. developed a codon-optimized *mCherryOpt* to label *C. difficile* successfully, but cells had to be fixed before *C. difficile* exhibited fluorescence (Ransom et al., 2015). Therefore, I used a fluorescent labeling reagent, *Bac*Light, to detect and monitor living *C. difficile*. After staining with *Bac*Light, *C. difficile* exhibited bright red fluorescence (Figure 29 A).

The stained *C. difficile* were injected into the zebrafish intestinal tract of 5dfp macrophage or neutrophil transgenic larvae, and then zebrafish were imaged near the infection site after 1 hour incubation (Figure 29 B) (Benard et al., 2012). Time-lapse imaging showed that neutrophils and macrophages were recruited to the inoculation site, and the number of these two innate cells increased over time till the *C. difficile* were cleared. When macrophages and neutrophils reached the infection site, they started to phagocytose and digest labeled *C. difficile* (Figure 29 C and D). This result demonstrated that zebrafish innate immune cell could recognize and phagocytose *C. difficile* cell *in vivo*.

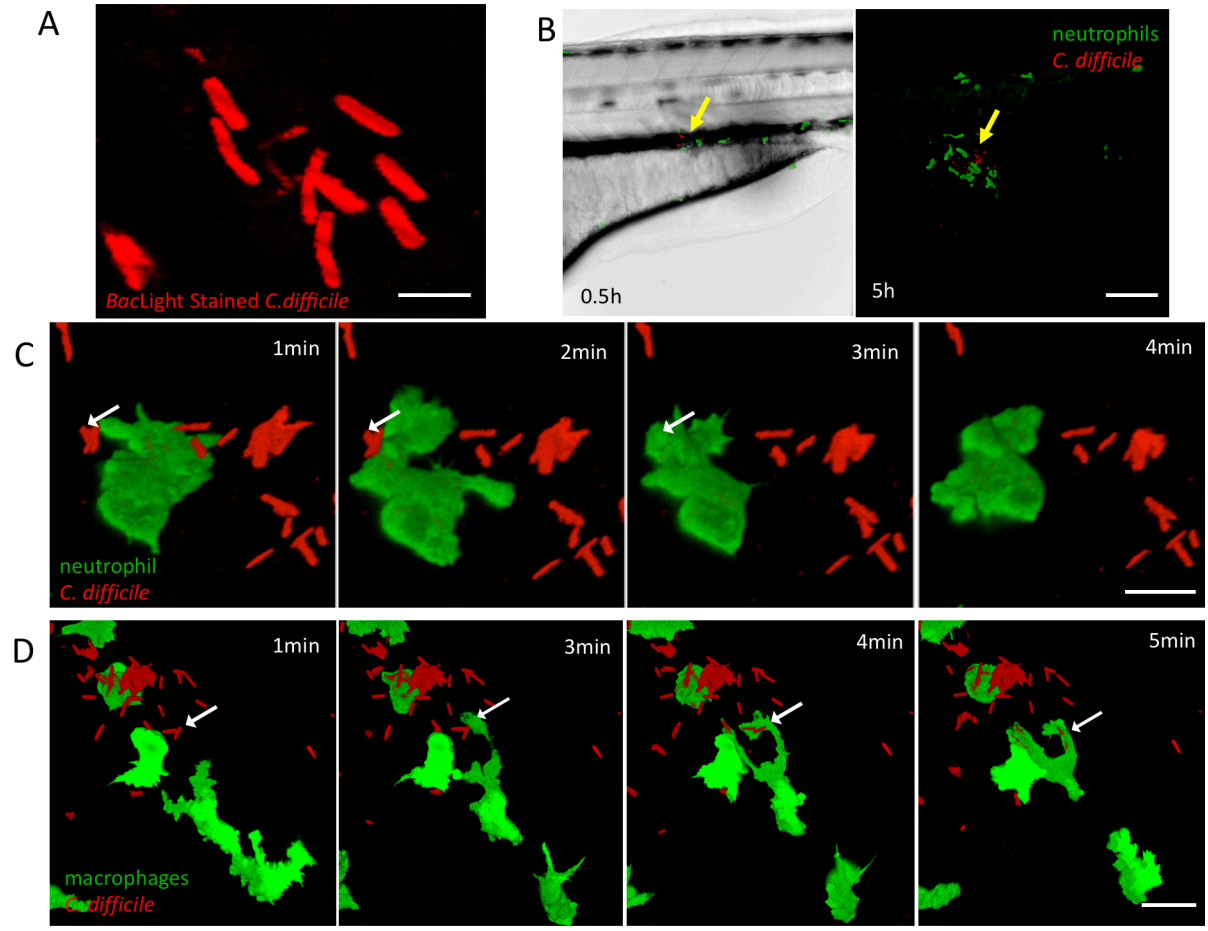

Figure 29 Neutrophils and macrophages phagocytose of *C. difficile in vivo*

A) Fluorescent *Bac*Light labeled *C. difficile* cells. Scale bar, 5 µm. B) Confocal 3-D image showed that neutrophils accumulated in the *C. difficile* infection site (yellow arrow) Scale bar, 50 µm. C) Time-lapse image of GFP-labeled neutrophil ingesting red fluorescent *C. difficile*. Scale bar, 20 µm. D) Time-lapse image of GFP-labeled macrophage ingesting red fluorescent *C. difficile*. Scale bar, 20 µm

Before phagocytosis of *C. difficile*, macrophages showed a characteristic macrophage morphology and behavior as indicated by long and branching pseudopodia and high motility. However, after phagocytosis of *C. difficile*, macrophages displayed markedly different cell behavior and a round morphology (Figure 30 A2, yellow arrow head). Simultaneously, they also turned to be immobile. In confocal microscopy image, the fragmentation of labeled *C. difficile* corpses was visible inside a macrophage, which indicated that *C. difficile* had been digested (Figure 30 A1, yellow arrow head). However, even after taking up several *C. difficile* cells, the macrophage still displayed normal morphology (Figure 30 A2, white arrow head). But *C. difficile* did not lose their rod shape, which indicated that they were just engulfed by the macrophage and phagocytic degradation had not started yet. This result demonstrated

that macrophage was able to digest *C. difficile*, but the degradation of *C. difficile* might be cytotoxic to macrophages, which was indicated by the morphology and mobility changes.

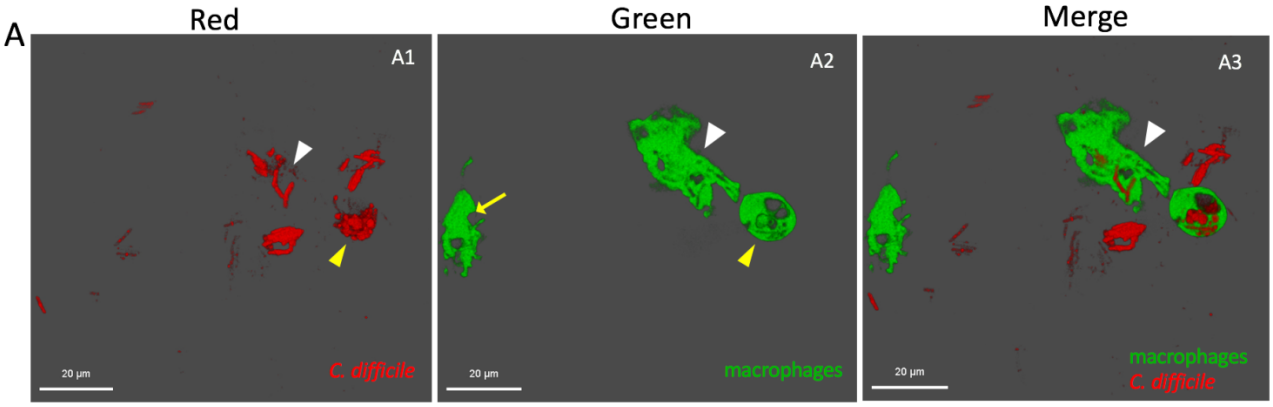

Figure 30 Morphology of macrophage after phagocytosis of *C. difficile*

A1) Red labeled *C. difficile* cells were engulfed by macrophage. A2) Macrophages showed different morphologies. A3) Merge of red and green channel. n = 4 larvae.

3.2.2 Cooperation of neutrophils in the clearance *C. difficile in vivo*

It is well accepted that neutrophils cooperate with macrophages to defend the invasion of the pathogen. It was not clear yet whether neutrophils interacted with each other to against infection. Our neutrophil infection model demonstrated that neutrophil interacted with other neutrophils when they were recruited to clean *C. difficile* (Figure 31). Three neutrophils migrated to the infection site as shown in Figure 31 a1, then two of them made contact to form a cell as shown in Figure 31 a2. The two joint neutrophils encountered another neutrophil to form a three-neutrophil-union (Figure 31 a4). This the union dissociated after 4 minutes (Figure 31 a6). This finding suggested that the dynamic association and dissociation of several neutrophils might be a regular process in phagocytosis of pathogens.

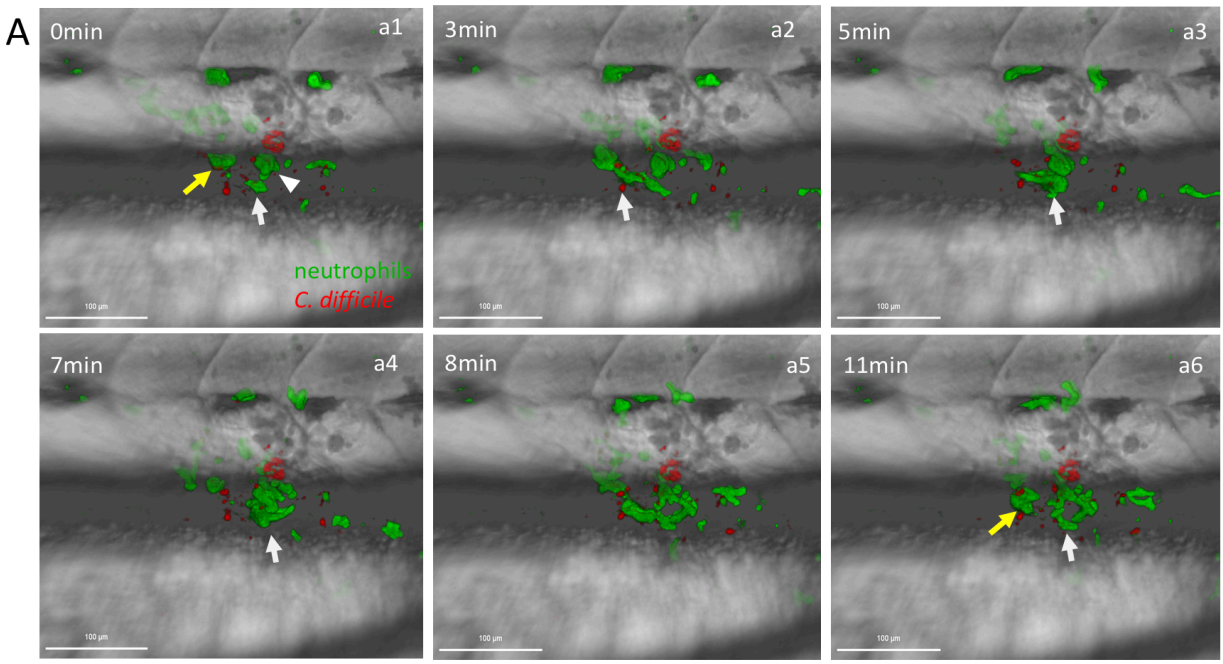

Figure 31 Cooperation of neutrophils in the clearance of *C. difficile*

A) Confocal time-lapse image of 5dfp zebrafish larvae injected with *C. difficile.* Image was recorded 2h after infection.

3.2.3 Establishment of neutrophils ablation transgenic zebrafish

To reveal the importance of neutrophils against *C. difficile*, a transgenic fish line that co-expressed yellow fluorescent protein Citrine and the Tamoxifen-induced Caspase8ER^{T2} *Tg(lyZ:Kal4TA4, 5UAS-E1b:mCitrin, Casp8ER^{T2})* , named Neu-ATTAC^{TM} strain, was established. The construct as shown in Figure 32 was co-injected into one-cell stage of zebrafish embryos with mRNA encoding Tol2 transposase. Fluorescent embryos were raised to adult stage, about 10 adult zebrafish, and then crossed with wild type zebrafish to F1 generation. The larvae of F2 and F3 generation were used for this study (Figure 33 A).

Figure 32 Construct design for the generation of a stable transgenic neutrophil ablation strains.

KalTA4 is under control of *lyZ* promoter. 5×UAS drives the expression of fyndtdmCitrine and Caspase8ER^{T2} in bidirectional manner. fyndtdmCitrine, a membrane localization signal fused to tandem mCitrine fluorescent protein. The construct is flanked by Tol2 recognition sites (Tol2) for transposase mediated integration.

ATTAC^{TM} is a new genetic ablation technique, in which cells are driven into apoptotic cell death by tamoxifen-inducible Caspase 8 (Weber et al., 2016). Weber et al demonstrated that 5 µM 4-hydroxy-tamoxifen (4OHT) induces near-complete loss of Purkinje cells in PC-ATTAC^{TM} larvae after 16h treatment (Weber et al., 2016). With this protocol, I found that the number of fluorescent neutrophils did not decrease after 4OHT treatment compared to a control group. 4OHT concentrations ranging from 5 µM to 10µM, followed by extended treatment time (16-24 hours) were tested, but neutrophils were not ablated (data not shown).

Since a Myc-tag was inseted after ER^{T2} domain, I wondered whether Caspase8ER^{T2} was inactivated due to the Myc-tag. To rule out this possibility, the carriers of Neu-ATTAC^{TM} was crossed with the carrier of rhombomere reporter line Tg(*krox20: KalTA4)* or skeletal muscle reporter line Tg(*shhb:KalTA4)*, which allowed embryos to express Caspase8ER^{T2} either in rhombomere 3 and 5, or in skeletal muscle cells specifically (Figure 33 B, C). After 6 h of 4OHT treatment, distinct cell death was detected in both rhombomere and skeletal muscle cells (Figure 33 B, C). All rhombomere cells elongated and lost their original shape, while apoptotic bodies appeared (Figure 33 B). Before treatment, muscle cells were thin and long with large spaces between them. Although some muscle cells still maintain their original morphology after 6h treatment, some muscle cells had formed apoptotic bodies (Figure 33 C). This finding demonstrated that Caspase8ER^{T2} triggered apoptosis in rhombomere and skeletal muscle cells and hence Caspase8ER^{T2} was functional. This result also suggested that rhombomere cells were more susceptible to 4OHT-induced apoptotic cell death than skeletal muscle cells and neutrophils.

Furthermore, we wondered if 4OHT treatment could also trigger apoptosis in neutrophils. Given that caspase 8 directly activates downstream procaspase 3, activated Caspase 3 is considered to be the most direct executioner during apoptosis (Elmore, 2007).
Immunostaining against activated Caspase 3 was performed. However, no apoptotic neutrophil were detected (data not show).

To further determine whether 4OHT-treated neutrophils respond to inflammatory stimuli, we examined neutrophil recruitment in response to tailfin transection. At 3dpf, tailfin transection was performed using larvae of Neu-ATTAC^{TM} strain after Tamoxifen treatment (Figure 33 D).

After the initial transection, neutrophils were increased in wounded tailfin in control fish, peaking after around 4h. However, neutrophils also showed strong recruitment in 4OHT-treated fish, which exhibited strong directionality and similar velocity as in control fish. This result indicated that 4OHT treatment did not impair chemotaxis of neutrophil to tail wound.

Therefore, even though ATTAC^{TM} worked very well in rhombomeres and skeletal muscle cells, Caspase8ER^{T2} was incapable to induce apoptotic neutrophils death in the neutrophil reporter fish line. This could be due to the low activity of the *lyz* neutrophil promoter.

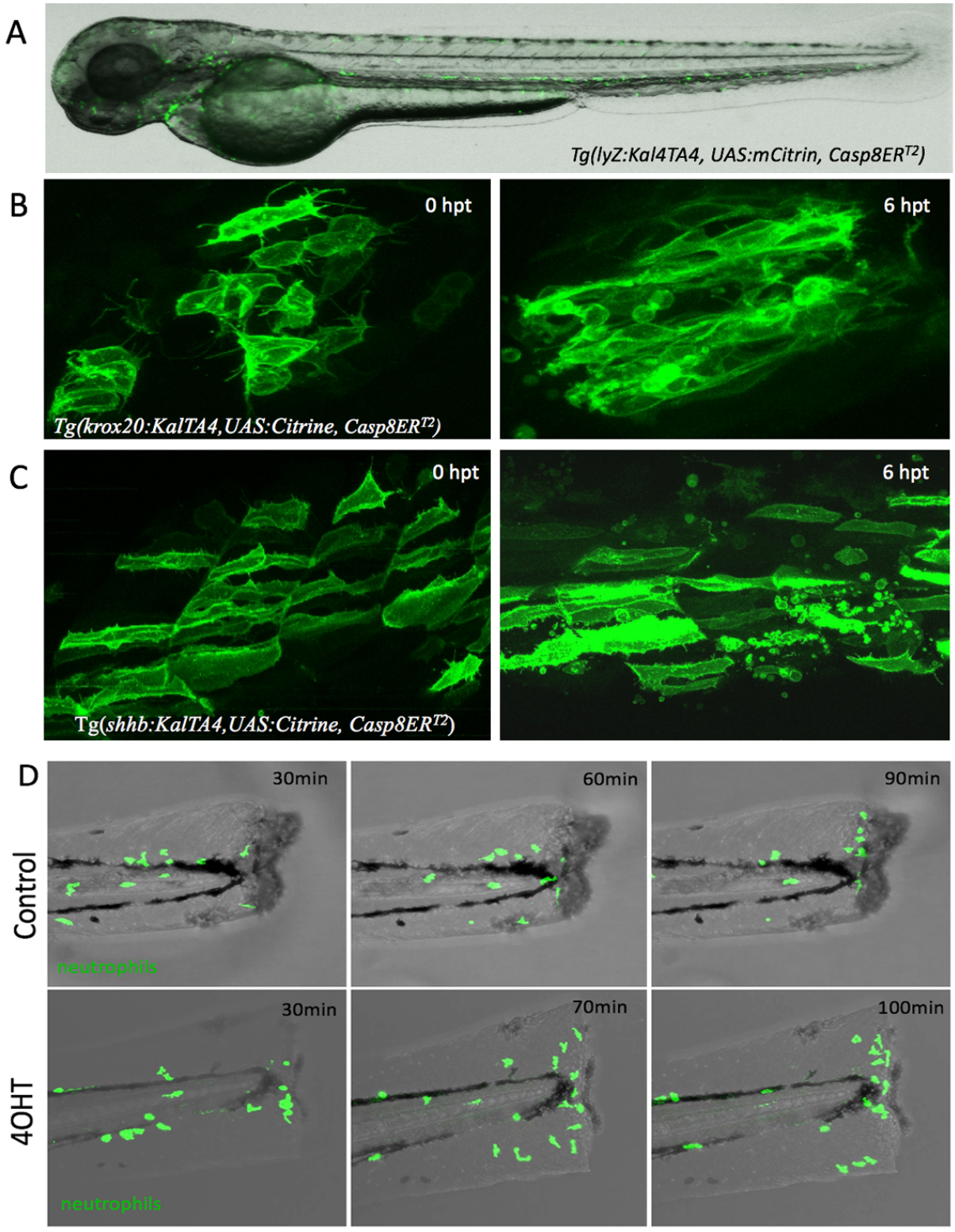

Figure 33 Application of ATTAC^{TM} in neutrophils

A) Fluorescence and bright field overlay of 3dpf *Tg(lyZ:Kal4TA4, 5UAS:mCitrin, Casp8ER^{T2})* fish. Green fluorescence: neutrophils. B) Fluorescent cells in rhombomeres 3 and 5 before and after 4OHT treatment. C) Fluorescent muscle cells before and after 4OHT treatment. n=5. D) Confocal time-lapse analysis of neutrophils (green) in tail transection of zebrafish treated with or without 4OHT. hpt, hours post-treatment. n=3.

3.2.4 Generation of macrophage-ATTAC^{TM} transgenic zebrafish

Neutrophils are engaged in phagocytosing of *C. difficile* after intestinal tract infection. However, the function of macrophages in CDI progression was less understood. Moreover, not much is known about the behaviour and cooperation of macrophages and neutrophils in clearance of *C. difficile*. To answer these questions, a new macrophage transgenic line was needed.

3.2.4.1 Application of LexA/lexAop system in macrophage transgenic strain

Gal4-*UAS* was already adopted for neutrophils strain, Neu-ATTAC^{TM}. In order to image and manipulate neutrophils and macrophages simultaneously in the same zebrafish, another binary expression system was required. Besides Gal4-*UAS*, there are two other binary transcriptional systems used in zebrafish: The QF transcriptional regulatory system and the LexA/lexAop system (Subedi et al., 2014; Emelyanov et al., 2008). Since high expression of QF might be toxic to early zebrafish development, the LexA/lexAop was chosen to establish a macrophage zebrafish strain (Subedi et al., 2014). Although the existence of a mifepristone-inducible LexA system has been reported, this approach has not yet been widely used in zebrafish. It might due to the requirement of ligands to induce gene expression, or low level activation of LexA reported in *Drosophila* (Potter et al., 2011).

In order to overcome these problems, a constitutive activated LexA/lexAop system was designed. This system contained a constitutively activated LexA transcription factor (residues 1–87) and *colE1*-derived binding motif (*colE1*-lexAop*)* with high affinity to LexA (Figure 34D).

The aim was to co-express a fluorescent protein and Caspase8ER^{T2} simultaneously. Therefore, whether 4×lexAop worked in a bi-directional manner was tested (Figure 34A). Emelyanov et al demonstrated that the transcriptional domain of the human p65 (residues 283–551) p65 AD and the minimal 35S promoter (35S) worked for a mifepristone-inducible LexA system. p65AD and 35S were examined in bi-directional lexAop constructs. LexA-p65AD and lexAop constructs were either co-transfected into HEK293T cells or co-injected into one-cell stage zebrafish embryos. When 35S was placed downstream of 4×lexAop, GFP was detected in cells and embryos (lexAop-35S: GFP) (Figure 34 A). When another 35S was inserted upstream of 4×lexAop, no transcription for both genes could be obtained (RFP:35S-4×lexAop-35S:GFP)

(Figure 34A). However, when another inverted 4×lexAop-35S fragment was inserted, formed back-to-back configuration, transcription of RFP and GFP was restored (RFP:35S-8×lexAop-35S:GFP) (Figure 34A). These results suggested that transcription initiation of lexAop was controlled in an orientation-dependent fashion. Nevertheless, 8×lexAop in a back-to-back configuration worked in a bi-directional manner in both cells and zebrafish embryos.

Besides 35S, there are other small basal promoters that have been used successfully in zebrafish and could be applied for the LexA/lexAop system, for instance, the super core promoter 2 (SCP2) and the minimal E1b promoter (Juven-Gershon et al., 2006; Zuo et al., 2000). Co-transfected with pCS-LexA-p65AD, lexAop-E1b and lexAop-SCP2 were strongly activated in HEK293T cells (Figure 34B). In order to further test E1b and SCP2 in zebrafish, LexA-p65AD was put under the control of the *mpeg1* macrophage-specific promoter. However, when co-injected with *mpeg1*-LexA-p65AD into embryos, lexAop-SCP2 were expressed in highly ectopically manner (data not shown). Therefore, compared with 35S and SCP2, the E1b exhibited strong and specific activity with lexAop motif and was chosen for further use.

The transcription activating domain TA3 exhibits high transcription activation in the Gal4 system. In order to obtain a strong transcriptional activator, LexA-p65AD and LexA-TA3 were constructed and their activity was compared in cell culture (Figure 34C). The LexA-p65AD-transfected cells exhibited a much stronger GFP and RFP expression than LexA-TA3-transfected cells, indicating that the p65AD had a higher activity than TA3 in the LexA system. Consistent with cell culture result, the same results were obtained in zebrafish (data not shown).

This series of experiments conclusively demonstrated the feasibility of using a constitutively activated LexA binary expression system to generate a macrophage specific fish trains (Figure 34D).

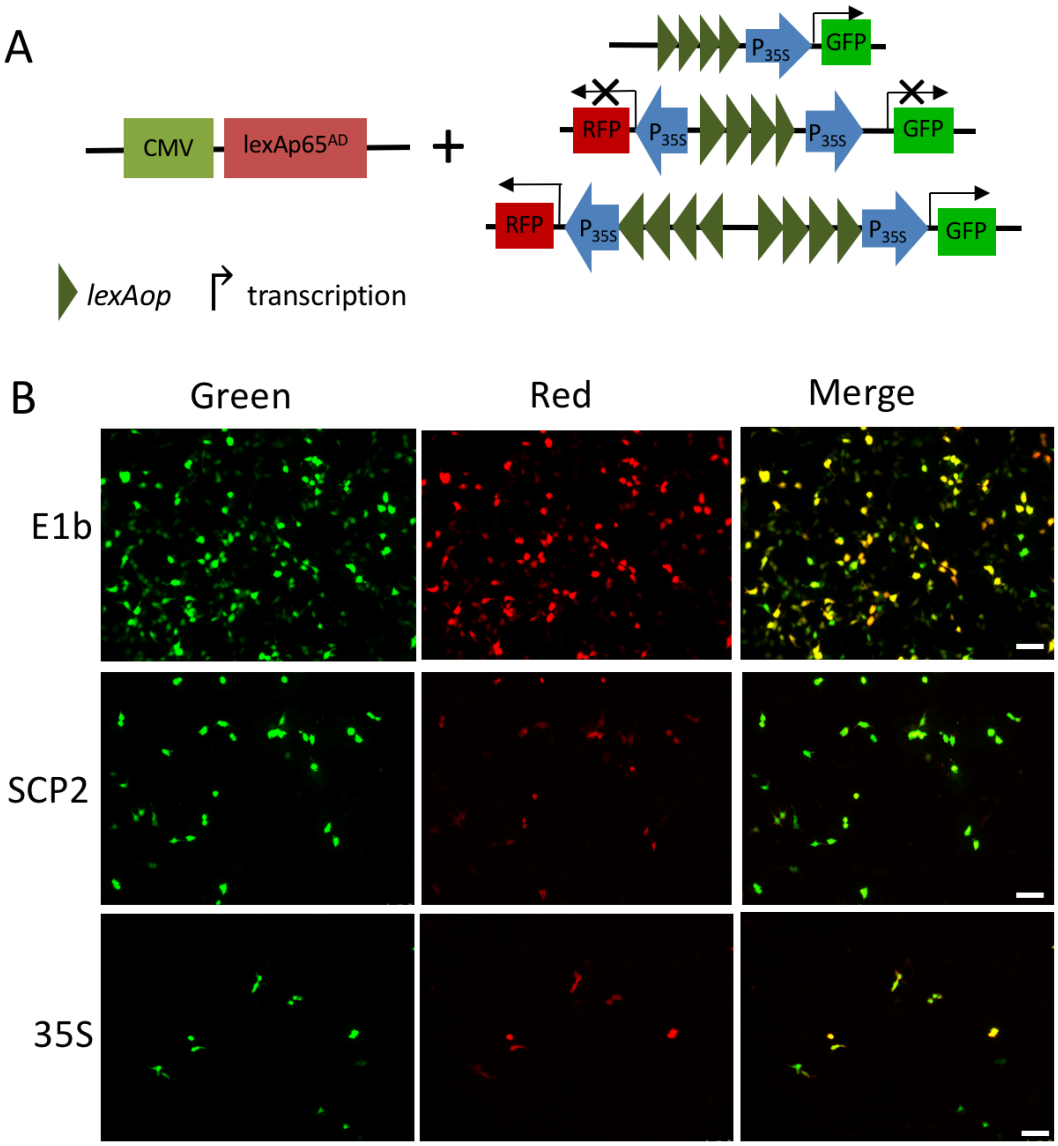
A
CMV
lexAp65AD
+
P35S
GFP
RFP
P35S
P35S
GFP
RFP
P35S
P35S
GFP
lexAop
transcription
B
Green
Red
Merge
E1b
SCP2
35S

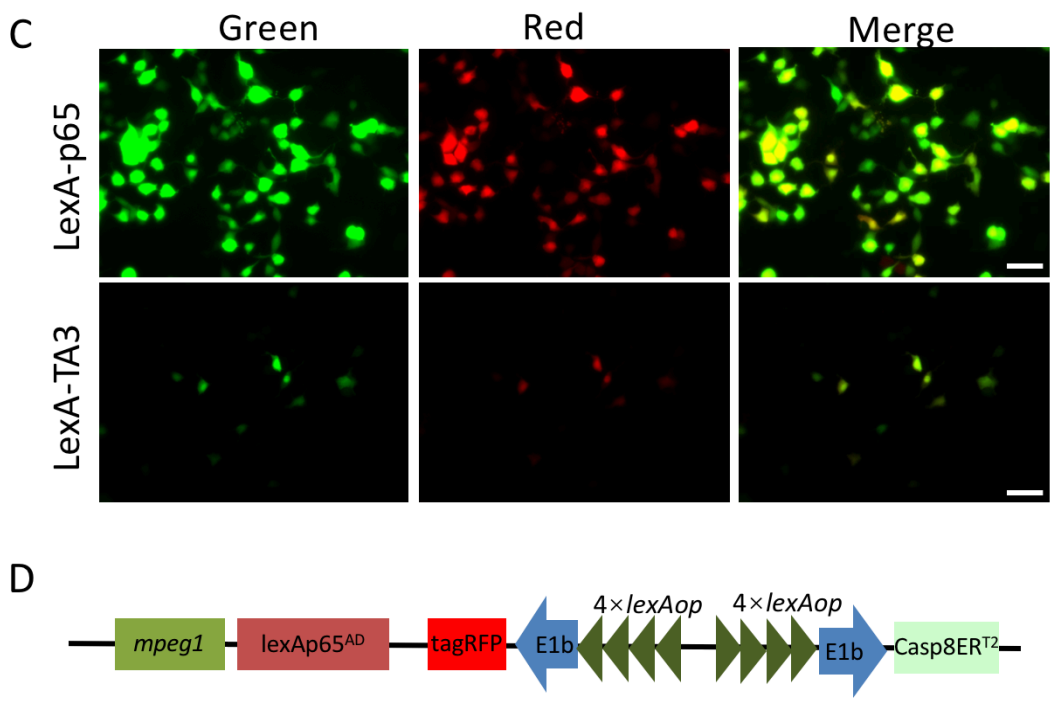

Figure 34 Establishment of a constitutive LexA-based binary expression system

A) LexA-p65^{AD} was placed under either CMV promoter or *mpeg1* promoter. Different lexAop constructs containing 4 or 8 copies of lexAop flanked by the 35S minimal promoter. Driver construct and reporter construct were co-transfected into 293T cells or co-injected into one-cell stage zebrafish embryos. B) 8×lexAop fused to the E1b, 35S or the SCP2 minimal promoter, which was co-transfected with LexA-p65^{AD} into 293T cells. Scale bar, 75 µm. C) LexA-p65^{AD} or LexA-TA3 were co-transfected with E1b:8×lexAop*:* E1b into 293T cells. D) Schematic structure of the plasmid used for the generation of stable transgenic macrophage ablation strains. Scale bar, 50 µm.

3.2.4.2 Generation of a stable transgenic macrophage-ATTAC^{TM} zebrafish strain

To address whether the ATTAC^{TM} transgene worked for macrophages, I established a zebrafish strain that co-expressed fyntagRFP-T together with Caspase8ER^{T2} under the control of *mpeg1* promoter, referred to as Mac-ATTAC^{TM}. The construct as shown is Figure 34D was co-injected into one-cell stage of zebrafish embryos. Fluorescent embryos were raised to adult stage than then crossed with wild type zebrafish. The larvae of F1 and F2 generation were used for further study.

The larvae of F1 generation were treated with 5µM 4OHT for 16h. Cell ablation was determined by fluorescent signal disappearing over the time course of treatment (Figure 35). Larvae incubated with 0.5% EtOH showed no signs of cell debris or decreased macrophage

number, indicating no leaky Caspase8ER^{T2} toxicity under the control of the *mpeg1* promoter. The same result was obtained in 2dpf, 4dpf, and 5dpf larvae (data not shown). This result demonstrated that macrophage could be ablated by caspase8-mediated apoptotic cell death, and caspase 8 activity was strictly contained to macrophage.

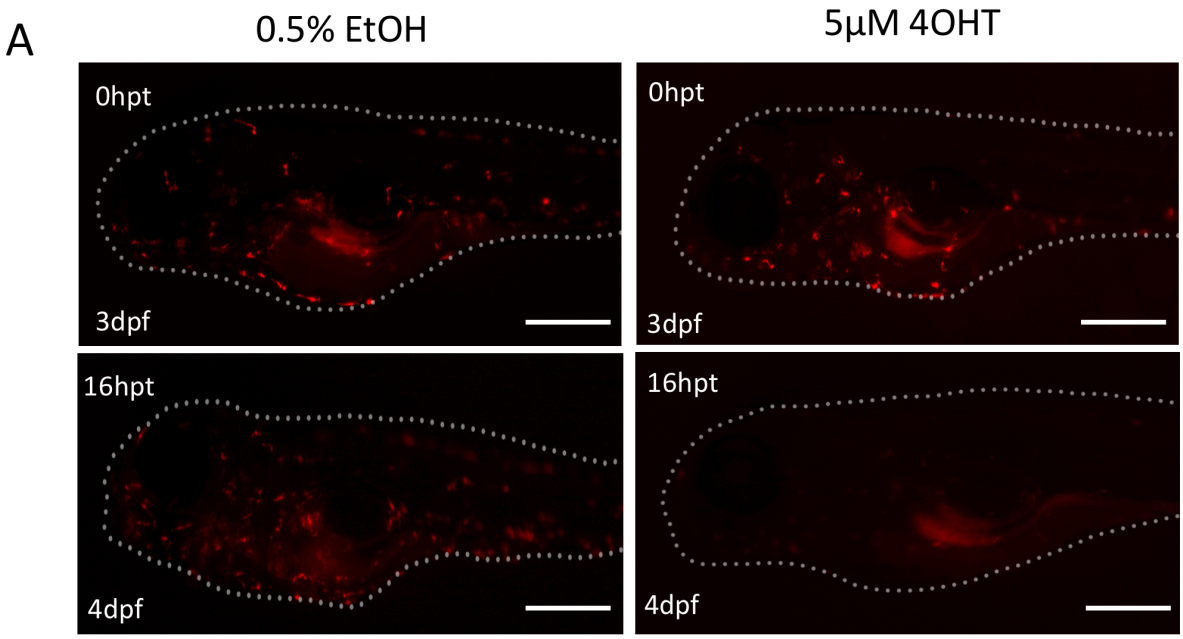

Figure 35 Tamoxifen-induced macrophage death in Mac-ATTAC^{TM} larvae

A) Incubation of 3dpf Mac-ATTAC^{TM} embryos with 5µM 4OHT or 0.5% EtOH for 16h. scale bar, 250µm. hpt, hours post-treatment. Scale bar, 250 µm

A characteristic feature of apoptotic cells was the present of membrane blebbing, cell shrinkage and apoptotic body formation. After pre-treat 3dpf larvae with 4OHT for 3h, macrophage apoptosis was monitored by confocal time-lapse imaging (Figure 36 A). The apoptotic macrophages showed cell shrinkage and apoptotic body formation. First, the macrophage retracted lamellipodia (Figure 36 a1, white arrow), indicating it was in an early-stage of apoptosis after 3h of 4OHT treatment. Lamellipodia retraction resulted in cell shrinkage and rounding (Figure 36 a2). Then macrophage entered a process of disassembly: formation of apoptotic membrane protrusion (Figure 36 a3-a4), and eventually apoptotic bodies broke down the cell (Figure 36 a5-a6). Probably, apoptotic macrophages released chemotactic signals that stimulated a nearby macrophage to migrate to the apoptotic macrophage (Figure 36 a6, yellow arrow). The apoptotic macrophage died and disappeared

quickly within around 45 minutes. The difficulty to determine the apoptosis starting time made it impossible to measure the duration of the whole process.

AnnexinV-Cy5 is used as an apoptotic cell indicator. In order to illustrate that macrophages were eliminated via apoptosis, heterozygous Mac-ATTAC^{TM} larvae were treated at 4dpf with 4OHT for 4h, and then incubated with AnnexinV-Cy5 for 2 h. Three red fluorescent macrophages were labelled by AnnexinV-Cy5, which demonstrated that apoptosis occurred in macrophages (Figure 36 B). Since Annexin V is an early apoptotic marker, those three macrophages were in an an-stage of apoptosis (G. H. Zhang et al., 1997). No AnnexinV-labelled macrophages were found in control larvae (data not shown). This result demonstrated that apoptosis indeed occurred as a result of 4OHT activation of the ATTAC^{TM} gene to eliminate macrophages.

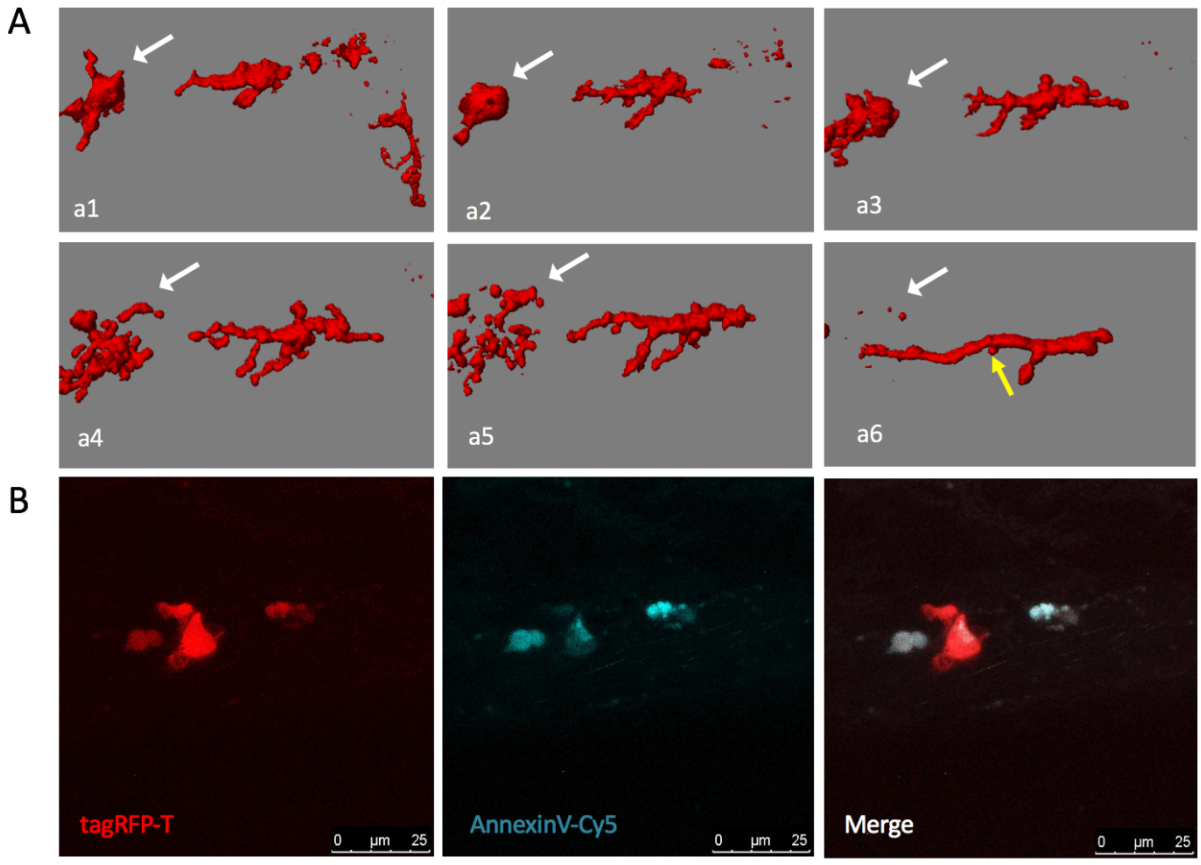

Figure 36 Analysis of macrophage apoptosis.

A) 3D confocal time-lapse imaging showed an apoptotic macrophage. White arrow: apoptotic macrophage; Yellow arrow: healthy macrophage. B) AnnexinV-Cy5 labelled apoptotic macrophages. fyntagRFP-T was expressed by macrophages and Cy5 fluorescence was presented a color in cyan. The larvae were treated with

5µm 4OHT for 4h and then incubated with 1/500 AnnexinV-Cy5 stock solution for 2h in dark box. Then extensively washed before mounting and confocal imaging.

To quantify macrophage ablation, I analyzed one region of the caudal hematopoietic tissue (CHT) in the ventral mesenchyme of the tail, where the definitive waves of hematopoiesis take place during late stage of zebrafish development (Figure 37 A). Mac-ATTAC^{TM} heterozygous larvae were treated with 5µM 4OHT for 4,7,10 or 14h at 5dpf. RFP-labelled macrophages were counted from confocal *z*-stack images (Figure 37 A).

Macrophages significantly decreased after 7h of 4OHT treatment, compared to the control specimens ($p \leq 0.05$) (Figure 37 B). After 10h of 4OHT treatment, macrophages were almost undetectable in Mac-ATTAC^{TM} larvae (Figure 31 A and B). This data suggested that most macrophages were triggered into apoptosis after 7h of 4OHT treatment and were further induced to cell death after around 10h treatment. After 14hof 4OHT treatment, the number of macrophage dropped to very low level below than 1% (Figure 37 A and B). This number might underestimate the efficiency of ablation, as macrophage progenitors which produce macrophages even when 31pdf, might counteract the loss of macrophages (Shiau et al., 2015).

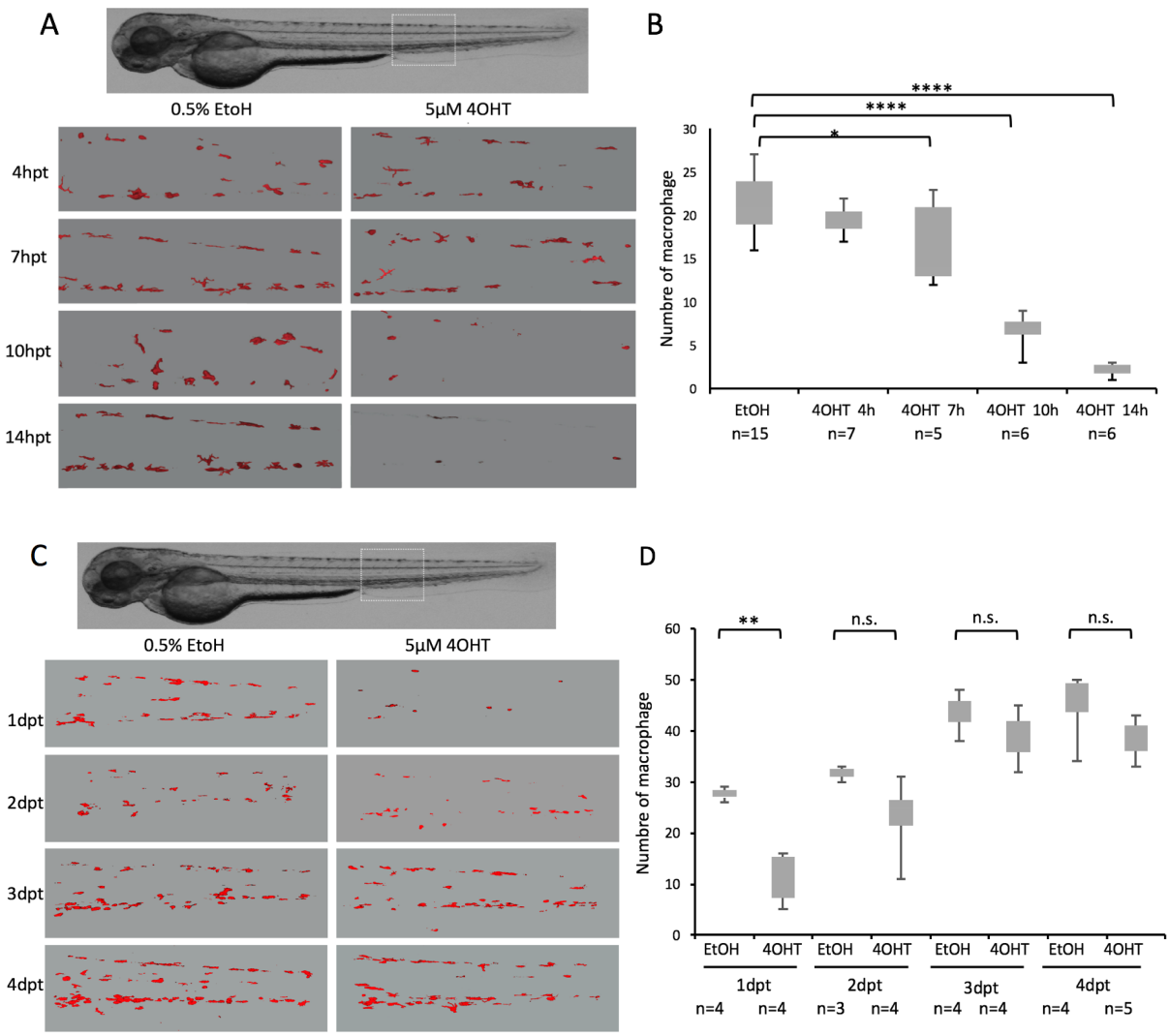

Figure 37 The time course of macrophage ablation and macrophage regeneration in Mac-ATTAC^{TM} larvae

A) Illustration of caudal hematopoietic tissue (CHT) in the ventral mesenchyme of the tail (white box), which was taken with the same magnification and field size of view at all stages. The size of the image was *x,* 775µm. *y,* 775µm. *z,* 117.36-220 µm. B) Box plot of macrophages after 4, 7, 10, or 14h 0.5% ethanol (control), or 5µM 4OHT treatment. C) Illustration of caudal hematopoietic tissue (CHT) in the ventral mesenchyme of the tail after 1, 2, 3, or 4 days after withdrawal of 0.5% ethanol (control), or 5µM 4OHT treatment (white box), which was recorded with the same magnification and field size of view at all stages. The size of image was *x,* 775µm. *y,* 775µm. *z,* 130-230 µm. dpt, days post-treatment. D) Box plot of recovery of macrophages over time after removal of 4OHT. n.s, not significant. * $p \leq 0.05$, ** $p \leq 0.01$, **** $p \leq 0.0001$.

To figure out how long it took for macrophages to recover. 4OHT was removed from the culture medium, and the re-appearance fluorescent macrophages were counted in the CHT region at 1, 2, 3, and 4 dpt (days post-treatment) (Figure 37 C). Macrophage number increased, indicating that the regeneration of macrophages occurred soon after removal of 4OHT (Figure

37 D). RFP positive macrophages increased considerably at 2dpt in the 4OHT treated group compared to control group, which is, however, statistically insignificant (Figure 37 D). At 3dpt, macrophages in the4OHT treated group increased to a comparable level to the control group, which is statistically insignificant (Figure 37 C, D). This finding suggested that the regeneration of macrophages occurred rapidly and efficiently, which might be due to many different types of progenitors that macrophages have, such as , myeloid progenitors (CMPs), common DC progenitors (CDPs), and common monocyte progenitors (cMoPs) (Geissmann et al., 2010; Onai et al., 2014). Mac-ATTAC^{TM} shown as a suitable model to investigate ablation and regeneration of macrophages *in vivo*.

3.2.4.3 The interaction of neutrophils and apoptotic macrophages

Macrophages, neutrophils, dendritic cells (DCs), and monocytes mast cells are the professional phagocytic cells in the body (Murray et al., 2011). Following a common origin, macrophages and neutrophils share some overlapping and complementary features in the host defense against microbial infection. Several lines of evidence indicated that macrophages and neutrophils work in a cooperative manner against pathogen invasion (M. T. Silva, 2010). Macrophages are able to phagocyte apoptotic neutrophils in infection-associated inflammation and tissue regeneration (Ellett et al., 2011; Manuel T. Silva et al., 2012; Tan et al., 2006). Since macrophages and neutrophils are considered the main cells type at the phagocytic system, we wondered how neutrophils respond to apoptotic macrophages, and whether neutrophils are involved in clearance of apoptotic macrophages.

To address these questions, Mac-ATTAC^{TM} carriers were crossed with neutrophils-reporter line *Tg(lyZ:KalTA4, UAS-E1b:EGFP*) . These double transgenic larvae were treated with 4OHT for 3h to trigger macrophage apoptosis (Figure 38 A). Confocal time-lapse imaging was performed (Figure 38 B). A neutrophil phagocytosing an apoptotic macrophage was observed (Figure 38 b4-b5). The neutrophil recognized and engulfed the apoptotic macrophage within 6 minutes (Figure 38 b4-b5). Interestingly, before the macrophage was engulfed by the neutrophil, this macrophage split into two cells parts (Figure 38 b1-b3, white arrow and arrow head). Only one of them was engulfed by the neutrophil (Figure 38 b4, white arrow head and yellow arrow), whereas the other seemed healthy and was highly mobile (Figure 38 b4-5, white arrow). This finding suggested that neutrophils were indeed in clearance of apoptotic

macrophages.

However, I was puzzled by the splitter of macrophage 'division' during the apoptosis (Figure 38 B). I speculated that this split might be the dissociation of an apoptotic body from healthy macrophage. If this is the case, this should be observed regularly in the clearance of dying macrophages. To address this question, 5dpf larvae were treated with 4OHT for 1, 4, and 6h. After 6h pre-treatment, I only observed neutrophils phagocytosing apoptotic macrophages, but no other interactions between macrophages and neutrophils. However, macrophage-neutrophil coordination was indeed recorded by time-lapse imaging in larvae treated with 4OHT for only one hour (Figure 38 C). Two adjacent neutrophils contacted each other (Figure 38 c1, yellow arrow and yellow arrow head) and then seemingly formed a complex neutrophil (Figure c2, yellow arrow). When the joint neutrophils approached a rounding macrophage (Figure 38 c2, white arrow head), another macrophage (Figure 38 c3, white arrow) migrated toward this macrophage, and subsequently formed macrophages-neutrophils complex (Figure 38 c4, white arrow). However, following the neutrophil dissociation, the macrophages also dissociated (Figure 38 c5, yellow arrow and c6, white arrow head), where one neutrophil was still enwrapping the rounding macrophage (Figure 38 c6). More neutrophil-macrophage interactions were found in other larvae (data not shown). This result hinted at a cooperative behavior between neutrophils and healthy macrophages to clean apoptotic macrophages. However, as most macrophage went into apoptosis after around 4h 4OHT treatment, such cooperation only happened shortly after the onset of 4OHT treatment.

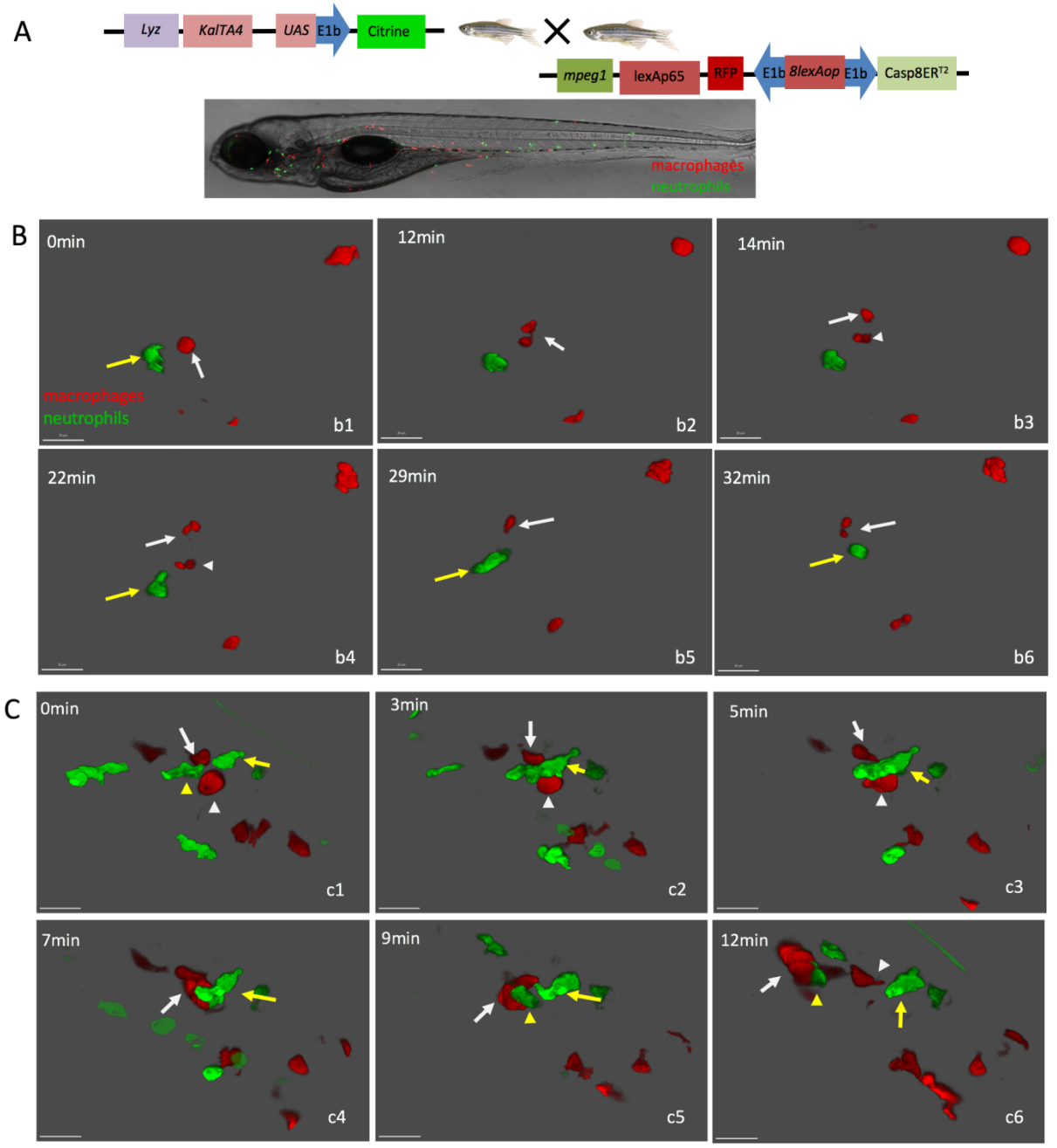

Figure 38 Interaction of macrophages and neutrophils to clear apoptotic macrophages

A) LexA/lexAop Mac-ATTAC^{TM} strain was crossed with neutrophils line expressing KalTA4. B) Image sequence of a neutrophil phagocytosing an apoptotic macrophage. Confocal microscopy time-lapse imaging of 5dpf double transgenic larva treated with 4OHT for 3h to induce macrophage apoptosis. C) The cooperation of neutrophils and macrophages during macrophage phagocytosis. Confocal microscopy imaging of 5dpf double transgenic larva treated with 4OHT for 1h to induce macrophage apoptosis.

3.2.5 Establishment of a noninvasive *C. difficile* infection protocol by microgavage

Injection is wildly used to induce infection in zebrafish disease models. However, injection is invasive and leads to tissue damage that trigger a wound healing response. Therefore, a non-invasive microgavage infection protocol was established to deliver *C. difficile* into the intestine of zebrafish larvae (Cocchiaro et al., 2013) (Figure 39 A). *C. difficile* was cultured for 48h and then was collected for *BacLight* staining. Set injector to deliver around 5nl BacLight-labelled C. difficile into the lumen of the intestine (Figure 39 B). For details, refer to section 2.2.3.

Microgavage prevented tissue damage. Furthermore, it has been proven that *C. difficile* colonize in the host intestine and cause bowel infection (Nitzan et al., 2013). Microgavage nicely mimic the natural route of infection in humans, which allowed us to analyze if *C. difficile* can colonize on the zebrafish intestinal lumen and disrupt epithelial integrity.

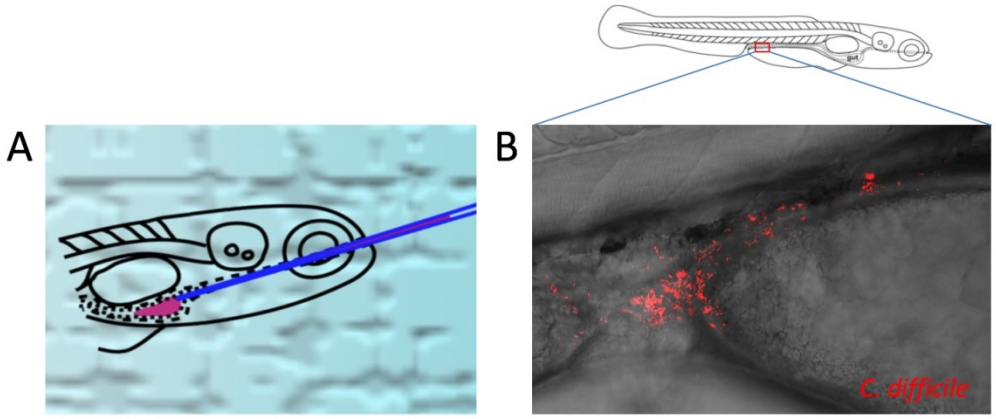

Figure 39 Microgavage of zebrafish larvae with *BacLight* labeled *C. difficile*

A) Microgavage in zebrafish larvae. Bacteria or chemicals were administered into the intestinal lumen of zebrafish. (Adapted from Cocchiaro et al., 2013). B) Location of *C. difficile* after microgavage. *C. difficile* was delivered into the anterior intestine. Confocal image shown BacLight stained *C. difficile* in the posterior intestine 3 hours after microgavage.

3.2.4 Infection of zebrafish with *C. difficile* by microgavage

In order to study the course of CDI and leukocyte recuitment in zebrafish, *BacLight* labeled *C. difficile* were delivered into the intestine of F2 generation macrophage or neutrophil reporter lines at 5dpf. However, neutrophils or macrophges did not show apparent migration to the gastrointestinal tract during 0-12h after microgavage (Figure 40). A potential explanation was that 12h incubation to activate an innate immune response is not sufficient in the intestine of

zebrafish.

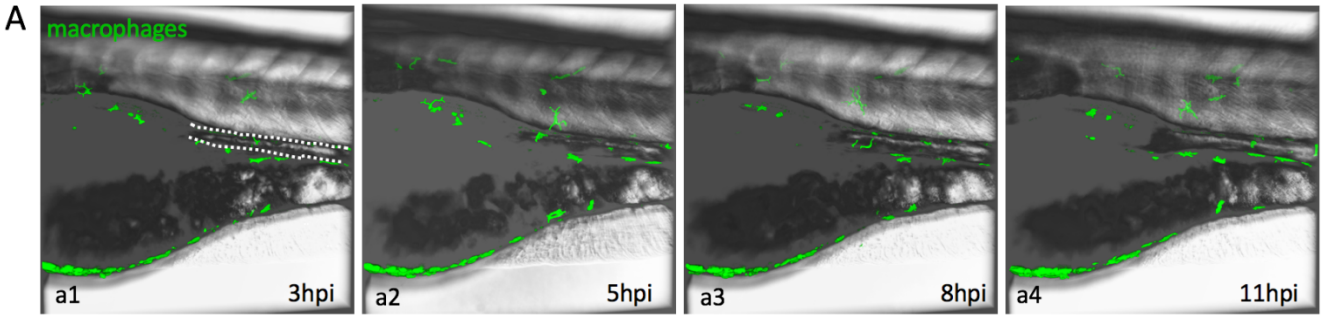

Figure 40 Time-lapse imaging of macrophages motility

A) Zebrafish larvae *Tg(mpeg1: Kalta4, UAS-E1b:EGFP)* at 5dfp was microgavaged with *BacLight* labeled *C. difficile*. Confocal time-lapse imaging of macrophage behavior was performed. hpi: hours post-infection.

Due to unknown reason, the fluorescence labeled *C. difficile* was bleached in the intestine around 5h after microgavage probably due to enzymatic destruction or pH in the intestine. Therefore, another approach was needed to confirm if CDI could be achieved in zebrafish.

After challenging mice with *C. difficile* spores, CDI is achieved after 2 days of incubation (Jarchum et al., 2012; Semenyuk et al., 2015). Therefore, I hypothesized that if *C. difficile* was detectable in the zebrafish intestine more than 2 days after challenging, CDI might be achieved in zebrafish gastrointestinal tract. To confirm this , the wile type zebrafish larvae were challenged with *C. difficile* strains R20291 cells, hypervirulent ribotype 027 (TcdA+/TcdB+/CDT+), by microgavage (Jafari et al., 2013). Zebrafish intestines were isolated at 24, 48, and 72h post-infection. The intestines were homogenized with pestles and then the homogenates were incubated in the *C. difficile* medium containing D-Cycloserine, Cefoxitin, and with or without TCA. However, *C. difficile* were detected at 24h, but not at 48h and at 72h post-infection (data not show).

I speculated that the endogenous microbial community in the zebrafish larvae possessed colonization resistance, which prevented *C. difficile* invasion. Therefore, gnotobiotic zebrafish larvae were used. To determine whether germ-free larvae were susceptible to *C. difficile*, 5dpf gnotobiotic zebrafish larvae were challenged with *C. difficile* by microgavage. There was no death of larvae observed even when zebrafish larvae treated with 10^8 CFU of *C. difficile* for each (n=3). To test if *C. difficile* was able to reside in zebrafish, zebrafish intestines were

isolated 24, 48, and 72h after microgavage. No bacterial growth in un-challenged control zebrafish larvae, which indicated that our gnotobiotic larvae were highly sterile (Figure 41 A). 24h incubated-sample grew in the media containing TCA or without TCA (data not show). However, 48 and 72h incubated-bacteria only grew in the media containing TCA (Figure 41 B). The grown bacterial were identified as *C. difficile* by 16S rDNA PCR, which yielded PCR amplicons at expected size, around 800bp (Figure 41 C). The bacterial cultures were plated on BHIS-plate. Then single colonies that showed typical *C. difficile* morphology was stroke on chromID plate which supported specific *C. difficile* growth. *C. difficile* grew into black colonies (Figure 41 D).

As described above, TCA promotes germination of *C. difficile* spores *in vitro*. This finding suggested that strict anaerobic *C. difficile* formed spores in the zebrafish intestine 48h and 72h after microgavage. This result also indicated that, compared to conventional larvae, gnotobiotic zebrafish were more likely to be an alternative animal model to study *C. difficile* infection process.

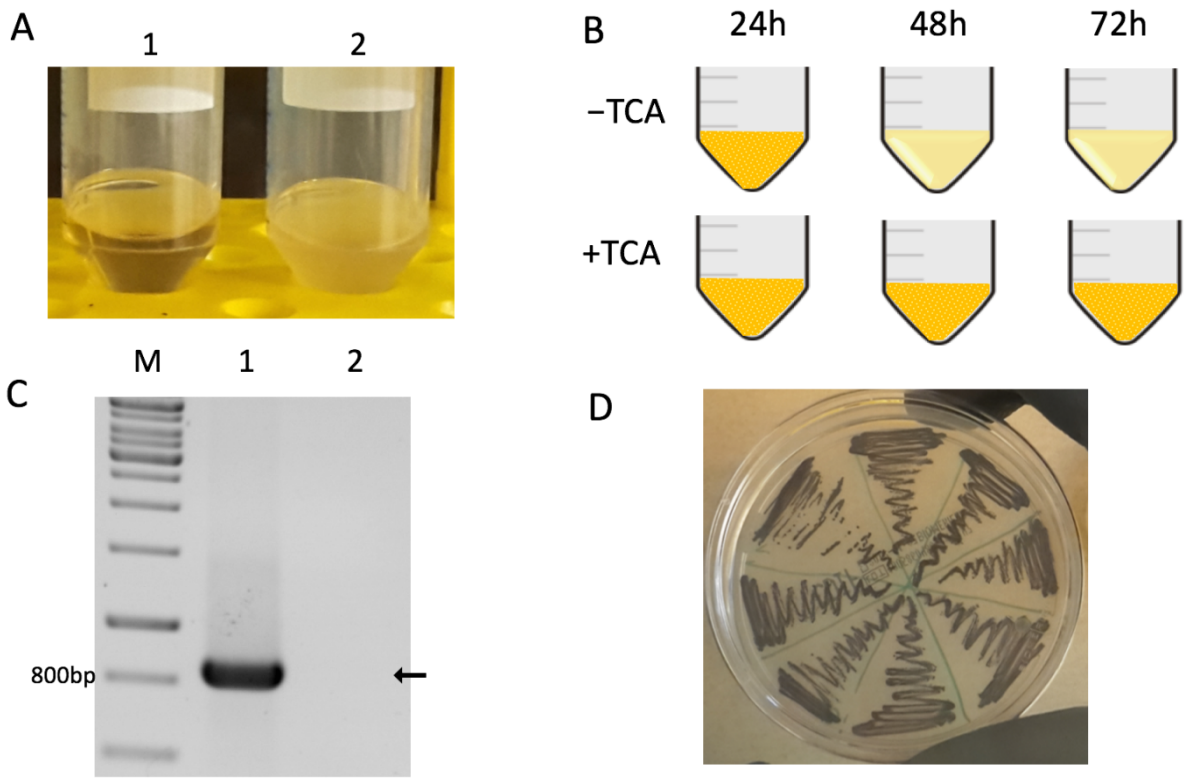

Figure 41 Detection of *C. difficile* in zebrafish intestine after challenging

A) Bacterial growth in the media containing TCA 72h after infection of gnotobiotic 5dpf zebrafish larvae with *C. difficile* by microgavage. 1, non-infected zebrafish control. 2, R20291-infected zebrafish. n=3. B) Schematic

illustration of overall experiment results after 24, 48, and 72h microgavaging with *C. difficile*. n=3. C) Bacterial samples were tested by 16S rDNA PCR after 72h after microgavage. n=3. D) The growth of *C. difficile* on chromID plate, note the indicative black color of C. difficile. n=3.

3.2.6 Frizzled receptor in the gastrointestinal tract of zebrafish

Wnt receptors, FZD1, 2, and 7 are involved in the binding and the uptake of TcdB in cells of the colonic epithelium in mouse. In order to investigate whether Frizzled receptors are expressed in the zebrafish gut, *in situ* hybridization was performed at 5dpf and 8dpf wild-type larvae with antisense RNA probe against the mRNA of FZD1, FZD2, FZD7a, and FZD7b. Intestinal fatty acid binding protein (*ifabp* gene*)* was used as positive control for *in situ* hybridization (Hong et al., 2008). Robust signal in the gut was detected in 5dpf and 8dpf embryos respectively (Figure 42 E, F, black arrow). However, *in situ* hybridization with FZD1, FZD2, FZD7a, and FZD7b probes did not reveal strong signal in the gastrointestinal tract of zebrafish (FZD2 and FZD7A not shown) (Figure 42 A-B), which suggested that FZD1, FZD2, FZD7a, and FZD7b were either not expressed or weakly expressed in zebrafish intestine at 5dpf and 8dpf.

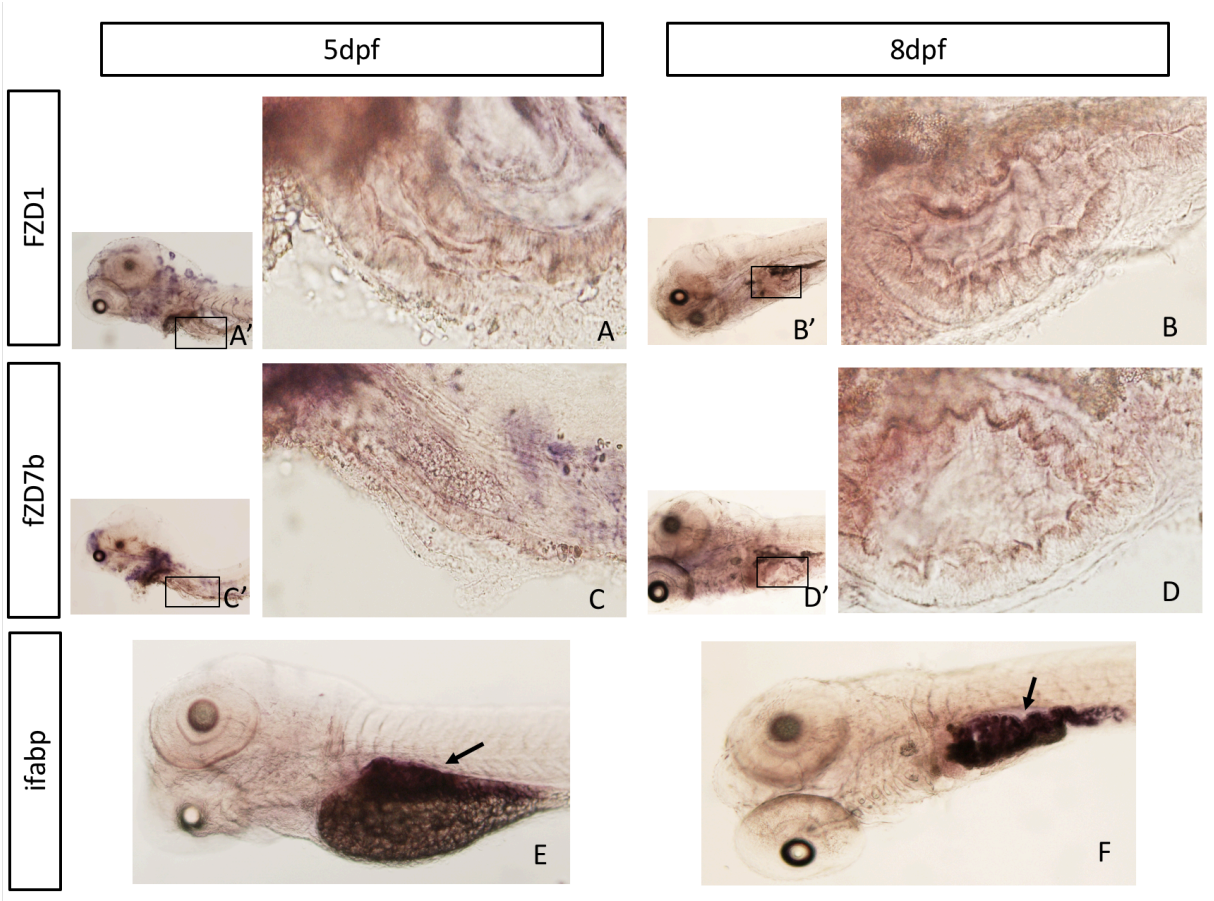

Figure 42 Whole-mount *in situ* hybridization of frizzled receptors in zebrafish

Whole-mount *in situ* hybridization against *FZD1*(A, A', B, and B'), *FZD7b* (C, C', D, and D'), and *ifabp* (E and F) in 5dpf and 8dpf wild-type embryos.

4 Discussion

4.1 Hatching gland-based zebrafish small molecule screen

Whole-organism chemical screening can circumvent shortcomings of cell-based screening. Zebrafish has been proven to be an outstanding model for whole-organism small-molecule screening (Zon et al., 2005). Over the last ten years, phenotypic screening was revived in drug research and development (R&D) with the hope that this method increases the success rate of drug approvals (Swinney et al., 2011). The phenotypic approach identifies drugs that are relevant to physiological or disease processes, whereas a target-driven approach finds compounds that bind to specific targets but are not relevant to the pathogenesis of diseases (MacRae et al., 2015; Rennekamp et al., 2015; Williams et al., 2016). Zebrafish as a model has several advantages for phenotypic small-molecule screening over other approaches. Firstly, the completion of zebrafish genome sequence reveals that 82% of disease-associated human genes (2,601) have at least one zebrafish orthologue, implying that zebrafish proteins or disease related targets are similar to their human counterparts (Howe et al., 2013). Zebrafish possess a similar organ system as humans, which performs the same physiological function. Further, a broad range of biological processes can be assayed during screening, such as pain, which are not appreciable with cell-based assays (MacRae et al., 2015). In this study, I aimed to establish a transgenic zebrafish model to identify and validate compounds against TcdA or TcdB, the major toxins of *C. difficile*.

4.1.1 The N-terminal glucosyltransferase domain of Tcd toxin is selected as the target for screening

The phenotypic screens in zebrafish were carried out either in wild type or transgenic fish with diverse phenotypic readout ranging from morphological changes to alterations in behavior (Hao et al., 2013; S. Jin et al., 2013; Kokel et al., 2010; Sandoval et al., 2013). From 2000 to 2015, 51% of chemical screens reported in the literature were performed in wild type zebrafish, while 35% in transgenic, and 14% in mutant animals (Rennekamp et al., 2015). However, application of mutant or transgenic lines with disease-relevant phenotypes has advantages over wild type fish. Rescue of mutant phenotypes or disease symptoms by specific compounds gives a hint to reveal relevant molecular pathways or biochemical events related to the mutations or diseases.

The key step of this study is to select a target that can recapitulate phenotypes of CDI in zebrafish. Some successful cases have been reported in the literature (MacRae et al., 2015). To identify the inhibitor of hepatocellular carcinoma (HCC), Evason et al created a transgenic zebrafish expressing activated β-catenin under a hepatocyte-specific promoter (*fabp10a*), where 33% zebrafish develop HCC two months post fertilization (Evason et al., 2015). They successfully identified two N-terminal kinase (JNK) inhibitors and two antidepressants which suppressed HCC development (Evason et al., 2015).

The major virulence factors of *C. difficile* are TcdA and TcdB. In animal models, TcdA or TcdB alone cause all the symptoms of CDI, including intestinal epithelial cell death, neutrophil infiltration, and fluid release (Shen, 2012). Both toxins have a classical ABCD domain structure (Jank et al., 2007). When the toxins are internalized by a receptor-mediated, the N-terminal GTD modifies and inactivates Rho GTPase, which leads to epithelial permeability and luminal fluid accumulation (Pruitt et al., 2012). Our primary experiment demonstrated that the GDT domain alone was able to induce dramatic HEK293T cell death. One day after transfection, HEK293T transfected with plasmid expressing the GDT domain of TcdA or TcdB respectively showed cell rounding and plate adhesion loss. When embryos were injected with the plasmid GDT in which was under the control of HE enhancer developed with a disrupted structure of the hatching gland.

Based on these findings, I selected GTD domain of TcdA and TcdB as the target to screen the antagonists of the toxins. HE enhancer would drive the expression of GTD only in hatching gland cells. Since there was no C-terminal binding domain, modified toxins were not able to intoxicate other cell types and further affect embryogenesis.

Although the GTD domain represents an ideal target, I cannot exclude that the C-terminus of TcdA and TcdB, such as combined repetitive oligopeptides (CROPs), is an alternative target for screening. Two human monoclonal antibodies, Actoxumab and Bezlotoxumabhave have been demonstrated to reduce the rate of CDI recurrence in clinical trials (Z. Yang et al., 2015). These two antibodies are designed to target the CROP domain of their respective toxins, actoxumab for TcdA and bezlotoxumab for TcdB (Hernandez et al., 2017; Orth et al., 2014). However, TcdB CROP domain might be a good target for cell-based screening *in vitro* but is not suitable

for zebrafish whole-organism screening. Because the C-terminus did not contain any catalytic domain. If the C-terminus is selected as target for screening, it would be hard to choose a phenotype as readout. Furthermore, only several cell-surface receptors for these toxins have been proposed. Glycoprotein 96 (gp96) have been proposed as the receptor for TcdA, while three identified receptors CSPG4, FZD, and PVRL3 have been reported as TcdB receptors (Orrell et al., 2017). Therefore, using C-terminus as target might cause unexpected toxin-receptor bindings and affect the embryogenesis.

4.1.2 4xlacO suppress the leaky expression of toxins in NEB turbo competent bacteria

To avoid the interference of early development, it is common to treat zebrafish with compounds after 1dpf (Evason et al., 2015; Hu et al., 2014; Setola et al., 2013). If the phenotypic readout is embryogenesis, compounds could be administrated within several hours after fertilization (Hao et al., 2013; Sandoval et al., 2013).

Lethal gene expression could be controlled in a conditional manner that allows for the generation of a transgenic zebrafish strain (Evason et al., 2015; Gutierrez et al., 2014). Those lethal genes induce disease or symptoms either in the present of an inducer or at late developmental stages of zebrafish. Gutierrez et al developed a conditionally MYC-induced T-ALL (acute lymphoblastic leukaemia) zebrafish model, in which 4-hydroxytamoxifen (4HT) treatment induces tumour, and withdrawal of 4HT results in tumour regression (Gutierrez et al., 2011, 2014). A zebrafish model of ACM (arrhythmogenic cardiomyopathy) expressing a mutant human γ-catenin was established, in which transgenic fish developed the ACM pathophysiology within 4 to 6 weeks (Asimaki et al., 2015).

In my study, glucosyltransferase, encoded by the GTD domain of TcdA or TcdB toxin, was proved to be toxic. When NTcdA or NTcdB construct was injected into one-cell stage embryos, it caused 100% mortality of embryo within 7 hours after microinjection. I firstly hypothesized that the DNA was not pure, which led to the 100% mortality of the embryos. Injection of purified the NTcdA or NTcdB construct by using other purification methods and endotoxin-free plasmid kit, the mortality rate remained high.

Then I assumed that there might be leaky expressed of GTD domain of TcdA or TcdB in bacteria used for plasmid preparation. This hypothesis was proved by western blot analysis.

Some promoters that have baseline expression in the absence of inducers have been reported. The *lac* promoter was identified by sequence analysis, which might cause the leaky expression of toxins. The regulatory components of the *lac* system include the *lac* repressor and its DNA-binding sequence, the *lac* operator. The combination of NEB turbo competent *E. coli* and 4xlacO supressed the leaky toxins expression successfully in bacteria. The NEB turbo strain contains the *lacI*^{q} gene encoding for the lacIq repressor, which achieved a tight expression control of genes downstream of lacO sites. 4xlacO were placed in front of NTcdA or NTcdB to further repress the leaky expression of toxins in *E. coli*. The application of these two approaches improved the overall survival and allowed us to get more healthy fish after microinjection. However, I wondered if 4xlacO downregulate the expression of downstream genes also in zebrafish. Therefore, a fluorescent gene was inserted behind 4xlacO sites hereby replacing the toxin encoding sequence. The fluorescent intensity was measured 24h after injection, which showed that the expression level of fluorescent protein was decreased compared the control without 4xlacO sites. To overcome this problem, the 4xlacO sites were inserted into an Exon-Intron sequence, which restored the expression strength of downstream genes of 4xlacO sites in zebrafish. This system could be a useful tool to study toxic genes in zebrafish.

However, two questions remained to be answered. The first one is how many copies of lacO are appropriate to repress the leaky transcription in *E. coli* or zebrafish. The plasmids which are commonly used contain only one copy of lacO, such as the pET series or the pBluescript series, but the *lacIq* mutation is used to increase the expression of the *lac* repressor in these strains. The lac repressor binds to the lacO leading to a tightening regulation of the lac promoter in *E. coli*. Besides *E*. *coli*, the *lac* operator-repressor system has also been used for gene regulation in mammalian cell culture, mice, and axolotl (Chang et al., 1996; Deans et al., 2007; Edamatsu et al., 1997; Morton et al., 2014; Whited et al., 2012). Deans et al demonstrated that 3xlacO provided a greater repression in mouse and human cells (Deans et al., 2007). In transgenic mice, 3 copies of the lacO fully inhibited transgene expression (Morton et al., 2014). However, complete repression also requires a higher expression level of the LacI repressor in cells or transgenic mice (Cronin et al., 2001; Deans et al., 2007; Morton et al., 2014). These findings suggested that 3xlacO could render the *lac* promoter tightly only under

high repressor expression conditions. Therefore, a tight regulation could be achieved by the application of 3xlacO sties together with the *lacIq* mutation.

The second question is where to locate lacO(s) in the construct. The lac operon of *E. coli* actually contains three operator genes, but they bind to repressors with different affinities (Reznikoff et al., 1974). The primary operator is near the transcription start site, and the two auxiliary operators are located 401bp downstream and 93bp upstream of the primary operator (Glickman et al., 2002). An optimum distance between operator genes is reported to be 92.5bp (Müller et al., 1996). Morton et al reported that 3 copies of the *lacO* sequence, which were inserted at specific distant sites (positions -117, -25 and +67), achieved a full repression of a transgene without higher levels of the LacI repressor expression (Cronin et al., 2001; Morton et al., 2014). Based on these findings, I assumed that a tight regulation could be achieved with fewer lacO sites by placing these lacO sites in a specific distance. This assumption could be tested by designing a series of vectors which contain different copy number of lacO at different distance between each other.

4.1.3 Expression of lacO downstream genes was restored by Exon-Intron system

In order to suppress the leaky expression of NTcdA and NTcdB in bacteria, lacO sites were placed upstream of the toxin genes. However, lacO sites not only suppressed the leaky transcription of NTcdA or NTcdB in bacteria, but they also down-regulated the expression of downstream genes in zebrafish. I was wondering which mechanisms caused the downregulation of downstream genes in these eukaryotic cells.

The *lac* operon is well known to regulate gene transcription in prokaryote. One of the regulatory mechanisms involves the formation of a DNA loop (Cournac et al., 2013; Priest et al., 2014). The formation of this DNA loop is essential for lac operon function to regulate gene transcription. The DNA loop either represses or activates gene transcription, depending on the distance between protein binding sites and the transcriptional start site (Cournac et al., 2013). The mechanisms of transcriptional repression has been interpreted (Müller et al., 1996; Priest et al., 2014). In the repression model, bivalent transcription factors bind to two binding sites, e.g. at the lac operators, and create a loop (Cournac et al., 2013). RNA polymerases are either trapped in the loop or are not able to recruit general transcription factors to start

transcription. It has been reported that tightly constrained DNA loop prevent RNA polymerases to access to promoters *in vivo* (Becker et al., 2014).

DNA loops have also been found to either activate or repress transcription in eukaryotes. The components of the transcription factors, such as Polymerase II, track along the chromatin and form a loop, which brings enhancer and promoter close to one another to start transcription (Zhao et al., 2005). There are two types of repression models: global repression and gene-specific repression. In the global repression model, repressors bind to DNA sequences and block transcription factors to access to the DNA, resulting in the down-regulation of all genes (Gaston et al., 2003; Hanna-Rose et al., 1996). Gene-specific repression occurs when a particular gene or a set of genes are down-regulated by gene-specific repressors. Gene specific repressors may restrict transcription activators by looping (Gaston et al., 2003). Based on this, I postulated that the gene-specific repression might have contributed the downregulation of transgene downstream of lacO sites in zebrafish expression vectors when they were injected into the embryos of the zebrafish. Some repressors which bind to lacO sequence specifically form DNA loop to inhibit transcription in zebrafish.

In order to restore gene expression, lacOs was inserted into the intron2 sequence of *rpl9* gene flanked by exon2 and exon3 sequence of *rpl9,* where lacOs would be spliced out during translation. Due to the repression occurred in transcription, the restoration relying on translation was not satisfying. However, the Exon-Intron system restored a certain amount of downregulation of gene expression. In eukaryotes, translation initiation requires the recruitment of the small (40S) ribosomal subunit, which binds to mRNA at the 5' end and scans the 5' untranslated region (5'UTR) to identify the start codon (Araujo et al., 2012; Sonenberg et al., 2009). If the structure or sequence of the mRNA impedes the ribosomes when they are scanning the 5'UTR, the efficiency of translation initiation would be decreased. Since lacO sites were placed in front of the start codon in open reading frames, lacO sites could hamper the 5'UTR scanning by the ribosomal subunit. Therefore, one explanation could be that removal of lacO sites boosted the ribosomal subunit binding 5'UTR, which increased the efficiency of translation initiation.

4.1.4 The apoptosis sensor secA5-YFP in zebrafish intoxication model

Both *C. difficile* toxins TcdA and TcdB induce apoptosis (Brito et al., 2002; Gerhard et al., 2008; Mahida et al., 1998; Matarrese et al., 2007; Na et al., 2008; Qa'Dan et al., 2002). In order to monitor the morphological changes of apoptotic cells, an apoptosis sensor, secA5-YFP, was co-expressed with the toxins under the control of the HE enhancer which drives expression specifically in cells of zebrafish hatching gland (van Ham et al., 2010). It provides an insight into apoptotic signaling pathways that are induced by toxins within this reporter zebrafish strain.

However, some studies also proposed that *C. difficile* toxins induce necrosis (Chumbler et al., 2016; LaFrance et al., 2015; Olson et al., 2013; C Pothoulakis, 2000; Warny et al., 2000). CDI is characterized by intestinal epithelial cell death, colonic inflammation, and neutrophil and macrophage infiltration. Concerning this pathogenesis, necrosis should occur. Cytoplasmic contents, which induce local inflammation, is released by necrosis but not by apoptosis (C Pothoulakis, 2000).

It has been reported that the intestinal epithelial cell death is induced by both apoptosis and necrosis after intrarectal instillation of toxins into the mouse colon (Hirota et al., 2012). Although some studies proved that TcdA and TcdB only induce apoptosis in HT-29 cells, Olson et al demosntrated that TcdA also induces necrosis in this cell line. (Olson et al., 2013). In THP-1 monocytic cells, TcdA induces cell necrosis by activating of p38 MAP kinase (Warny et al., 2000). TcdB also induces necrosis. Farrow et al showed that TcdB induces necrosis in both human colonic cell lines and porcine colonic explants (Farrow et al., 2013). At higher concentrations, TcdB is able to induce glucosyltransferase-independent necrotic death in mouse colonic epithelial cells (Chumbler et al., 2016).

Collectively, *C. difficile* toxins induce both apoptosis and necrosis in some tissue culture models. However, the necrosis induced by TcdA or TcdB depends on the cell type, and even the concentration of toxins.

In the zebraifsh model, TcdB was found to be toxic to cardiovascular cells(Hamm et al., 2006). This organ-specific damage was reduced by Caspase-3 inhibitors, which indicates that TcdB induces apoptosis in the cardiovascular system of zebrafish (Hamm et al., 2006). In addition,

inactivation of Rho proteins, the main targets of TcdA and TcdB, is known to induces apoptosis (Hippenstiel et al., 2002). Moreover, other data from clinical cases and mouse models also indicated that apoptosis occurs during CDI (Aktories et al., 2017). Unlike in cell or tissue culture models, only apoptosis is observed and reported in living model organisms. Therefore, hatching gland cells likely undergo apoptosis upon toxins expression, but currently we cannot exclude that these toxins might induce necrosis.

4.1.5 Both TcdA and TcdB caused cardiovascular damage

Zebrafish have been a promising model to assess an organ specific toxicity of compounds, such as cardiotoxicity and neurotoxicity (MacRae et al., 2015). Using 24hpf zebrafish, Hamm et al found that recombinant TcdB has cardiotoxicity (Hamm et al., 2006). Zebrafish treated with 37nM TcdB exhibited cardiovascular damage and extensive pericardial edema (Hamm et al., 2006). I replicated their findings by treating 72hpf zebrafish with lower TcdB concentrations (20nM), which is might due to 72hpf zebrafish are more sensitivity to TcdB. Interestingly, TcdA also induced similar phenotypes as TcdB, such as, cardiovascular defects and pericardial edema. A decrease in heart rate was also observed in TcdA-treated fish. This indicated that TcdA also impaired cardiovascular function via its cardiotoxic properties.

Both TcdA D285/287N and TcdB D286/288N, which were deficient in glucosyltransferase activity, did not cause detectable damage to zebrafish larvae. This result indicated that the cytopathic and cytotoxic effects of TcdA and TcdB rely on the functional glucosyltransferase activity.

Moreover, TcdB possesses 100-fold higher glucosyltransferase activity than TcdA in some cell lines (Aktories, 1997; Chaves-Olarte et al., 1997). However, I found that by using the same concentration, TcdA leads to a much higher mortality than TcdB to zebrafish. Notably, TcdB has 1,000-fold more cytotoxic potency than TcdA on Don cells, but TcdA turns out to have 10-fold more cytotoxic effects than TcdB on T84 cells (Chaves-Olarte et al., 1997). TcdA is more cytotoxic to T84 cells due to the following reasons: Firstly, TcdA possesses higher affinity to T84 cells than TcdB. Secondly, TcdA targets more enzymatic substrates than TcdB does, such as, Rap1A and Rap2A. (Chaves-Olarte et al., 1997). The crystal structure coupled with biochemical data showed TcdA and TcdB shares the similar core structure of the GTD domain.

But the GTPase binding surfaces are highly diverse, which is likely responsible for differential substrate recognition (Di Bella et al., 2016). Based on these studies, I presented two hypotheses that might explain why TcdA showed higher cytotoxic activity than TcdB in 72hpf zebrafish larvae: The first one is that TcdA recognizes more membrane receptors than TcdB does in zebrafish larvae, which promotes more cellular intoxication. TcdA inactivates more Ras family members than TcdB does in zebrafish as well. The second one is that TcdA and TcdB might perform differently at 28 ℃ and 37℃. The structure of TcdA might possess high cytotoxic activity at 28 ℃.

4.1.6 TUDCA mediates inhibition of TcdB

Antibiotic treatment with metronidazole and vancomycin is still the common therapy for CDI. However, antibiotic treatment presents very high recurrence rate (Cornely et al., 2012; Leong et al., 2013). Antibiotic treatment further disrupts the gut microbiota composition, resulting in the loss of colonization resistance (Theriot et al., 2014). Although the exact mechanism of colonization resistance against *C. difficile* is still unknown, it was proposed that antibiotic-treatment alter the metabolome of the gut, particularly the composition of secondary bile acids, which sensitizes mice to *C. difficile* (Antunes et al., 2011; Theriot et al., 2014). Some studies showed that the restoration of secondary bile acids restored the colonization resistance against *C. difficile* (Buffie et al., 2014; Weingarden et al., 2014). Deoxycholate (DCA), a metabolite of cholate produced by the gut microbiota, impairs the growth of vegetative *C. difficile* (Sorg et al., 2008). Taurocholate was reported to inhibit the enzymatic activity of TcdA and TcdB *in vitro* (Darkoh et al., 2011). These findings indicate that secondary bile acids have therapeutic potential to treat CDI.

TUDCA, a secondary bile acid, inhibits TcdB-induced cytotoxicity in cell culture (Brandes et al., 2012). TUDCA inhibits TcdB-catalysed glucosylation and cytopathic effects in human hepatocarcinoma (HepG2) cells by increasing pS71-Rac1/Cdc42 phosphorylation levels (Brandes et al., 2012). I found that the application of TUDCA decreased the mortality rate of embryos injected with NTcdB expression construct. Additionally, survived embryos showed less malformed appearing after TUDCA treatment. In contrast, TCA and TCDCA did not show similar protective effects in zebrafish embryos. The therapy of CDI has been hampered by increased resistance of *C. difficile* to multiple antibiotics and by lack of medicine to restore

intestinal microbiota. To develop a non-antibiotic treatment is therefore a new approach. My study suggested that TUDCA could be a non-antibiotic agent for the treatment of CDI.

4.1.7 TcdB binds to the Wnt receptor Frizzled family (FZDs)

FZD proteins are TcdB receptors, which play important roles in the cellular uptake of TcdB. FZD receptors are critical for Wnt signal transduction (MacDonald et al., 2009). Wnt/Frizzled signaling pathways involve the activation of Rho and Rac proteins (Habas et al., 2003). TcdB binds to the conserved Wnt-binding site of FZD1, 2, and 7 (Tao et al., 2016). Interestingly, Wnt/Frizzled signaling is also important for the maintenance of colonic stem cells, which are essential for self-renewal and repair of the colonic epithelial cells (Tao et al., 2016; van der Flier et al., 2009). In CDI, the colonic epithelial cells are the first target of *C. difficile* toxins. This finding indicated that the Wnt signaling pathway could be involved in TcdB pathogenesis (Tao et al., 2016).

However, there was not much information available on the expression of *fzd* genes in the gut of zebrafish, especially in fish older than 5dpf. Sisson et al showed that *fzd7b* is expressed in the mesenchymal tissue surrounding the gut, while *fzd8a* expression is detected in the gut at 55hpf (Sisson et al., 2009). To determine the gene expression level of several *fzd* homologs in the gastrointestinal tract of zebrafish, whole-mount *in situ* hybridization was performed with probes detecting *fzd1, fzd2, fzd7a,* and *fzd7b* in 5dpf and 8dpf larval zebrafish. However, no clear signal of expression was detected in the intestine of zebrafish in compared to the strong signal for intestinal marker gene, *ifabp* gene.

Hybridization efficiency is mainly determined by probe accessibility and permeable cell membrane and the affinity to the complementary mRNA sequence. The accessibility is regarded as the ability of probes to access the mRNA target sites (Yilmaz et al., 2004). Since all embryos were treated with the same permeabilization procedure, permeability was supposed to be constant. As positive control, RNA probe of *ifabp* revealed a strong signal in the gastrointestinal tract of zebrafish, which suggested that cell permeability did not affect the accessibility of *fzd* RNA probes. Affinity is defined as RNA-RNA interaction that take place *in situ* (Yilmaz et al., 2004). The RNA probes with high binding-affinity enhance the specificity and sensitivity. *fzd* RNA probes were compared with their corresponding probes that have

already been published. The sequences of our four probes were almost the same with published corresponding probes (H.-C. Huang et al., 2004; Nikaido et al., 2013). Therefore, the only explanation is that *fzd* genes are expressed at low level in the intestine of zebrafish or ate not expressed at all the intestinal cells. To overcome this problem, the intestines of zebrafish could be isolated for either *in situ* hybridization or RT-PCR.

There are 10 Fzd genes in mouse and 14 *fzd* genes in zebrafish (Dong et al., 2015). To investigate phylogenetic relationships of Fzd genes in teleost and higher organisms, Dong et al collected 116 Fzd genes to construct two phylogenetic trees based on either alignments of the amino acid sequences or topology (Dong et al., 2015). In these two phylogenetic trees, mouse Frizzled genes are not closely related to zebrafish orthologous genes (Dong et al., 2015). For instance, one Fzd8 is discovered in mouse, but two *fzd8* gene are presented in zebrafish: *fzd8a* and *fzd8b* (Dong et al., 2015). It would be intriguing to examine the expression of other Frizzled receptors or other receptor of Wnt signaling in the intestine of zebrafish.

Notably, the Wnt signal pathway is activate in the development of the zebrafish intestine, which is essential for the organogenesis and homeostasis of the intestinal epithelium (Cheesman et al., 2011; Faro et al., 2009). Like in mouse, Wnt signalling maintaines the intestinal stem cells and controls proliferation of the intestinal epithelium in zebrafish (Crosnier et al., 2006). Intestinal stem cells are found in the intervillus pockets of zebrafish, know as crypts in mammalian (Brugman, 2016; Schall et al., 2015). Current technique allow us to directly visualize the intestinal stem cells by fluorescent protein labelling in zebrafish (Aghaallaei et al., 2016). Moreover, Whitaker et al developed a tunable expression strategy that enables strain-level distinction of gut bacterial cell by unique fluorescent-protein-expression in mouse (Whitaker et al., 2017). They found that colonization of indigenous bacterial in crypts prevents pathogens from invading (Whitaker et al., 2017). Combining of these techniques, zebrafish would be a great model to study the relationship among Wnt signaling pathway, intestinal stem cells, and the crypts in CDI.

Interestingly, TcdB was found to specifically localize at the pericardial region of zebrafish after 24 h of TcdB treatment (Hamm et al., 2006). This finding suggested that either FZD receptors

have a high expression in the heart of zebrafish, or some proteins expressed in the heart of zebrafish are TcdB receptor.

4.2 Analysis of innate immune cell behaviour upon *C. difficile* infection

Given that the function of the intestine and immune systems are highly conserved between zebrafish and mammals, zebrafish is a suitable model to investigate intestinal inflammation (Y. Yang, 2014). In a mouse model for CDI, the infiltration of neutrophils, macrophages, and the release of cytokines and chemokines are observed (Ciaran P. Kelly et al., 1994; Sadighi Akha et al., 2013). The transparency of larvae make zebrafish an exceptionally useful model to study innate immune response for infection diseases (Van Der Sar et al., 2004). Several stable transgenic lymphocyte reporter lines are available (Ellett et al., 2011). In the second part of my PhD project, I aimed to study the behaviour of macrophages and neutrophils during *C. difficile* infection in the intestine of zebrafish.

As mammals, zebrafish have two waves of hematopoiesis: the primitive wave and the definitive wave, which give rise to different immune cells (Jagannathan-Bogdan et al., 2013). In addition, the development of different transgenic reporter zebrafish strains for different innate immune cells enables live imaging of the interaction between the innate cells and pathogens. Furthermore, innate immune cells are present the intestine of zebrafish. Macrophages and neutrophils are observed in the lamina propria beneath the intestinal epithelium (Hanyang et al., 2017).

The neutrophil stable transgenic strain Neu-ATTAC^{TM} and the macrophage transgenic strain Mac-ATTAC^{TM} were established. *lyz,* encoding zebrafish lysozyme C (lysC), is a reliable and specific marker for neutrophils from 48hpf on, and *mpeg1* is a specific marker gene for macrophages (Ellett et al., 2011; C. T. Yang et al., 2012). The *lyz* promoter was used to drive the expression of mCitrine in neutrophils, while *mpeg1* was used to drive macrophage specific expression of FyntagRFP-T. In order to visualize and manipulate those cells, our initial idea was to use a 2A self-cleaving multi-gene expression system to co-express a fluorescent protein and Caspase8ER^{T2} in neutrophil or macrophage (J. H. Kim et al., 2011). Unfortunately, fluorescence was not detectable in neutrophils or macrophages in transient assays. Therefore, we chosen

two binary expression systems the Gal4/UAS and the LexA/lexAop system: the Gal4/UAS for the Neu-ATTAC^{TM} line and the LexA/lexAop for the Mac-ATTAC^{TM} line.

To investigate the role of neutrophils or macrophages in the defence of *C. difficile*, we ablated one of them to reveal their function. NTR-MTZ ablation technology has been used in zebrafish to successfully ablated specific cell types with the help of metronidazole-induced apoptosis (Curado et al., 2007; Petrie et al., 2014). However, NTR-MTZ cannot be used in this study due to metronidazole is an effective antibiotic for CDI (Petrie et al., 2014; Pisharath et al., 2007). More recently, our group developed the ATTAC^{TM} technique, a 4OHT-induced genetic ablation technology (Weber et al., 2016). ATTAC^{TM} technique was used in this study.

4.2.1 The morphological changes of macrophages after phagocytosis of *C. difficile*

C. difficile is strictly anaerobic. Therefore, fluorescent proteins are unable to fluoresce in anaerobic environment due to chromophore maturation of protein requiring oxygen. To overcome this problem, I used a fluorescent labeling reagent, *Bac*Light, to stain living *C. difficile*.

Fluorescent *C. difficile* were injected into the zebrafish intestine to mimic intestinal infection. Both macrophages and neutrophils rapidly accumulated at the site of infection and started to phagocytose *C. difficile*. Consistent with previous studies in mammalian models that both macrophages and neutrophils were recruited upon *C. difficile* infection, zebrafish innate immune cells recognized this pathogen as well.

Although macrophages were able to ingest *C. difficile*, they exhibited a change in morphology and behavior when *C. difficile* were digested. They used to be large cells with extensive pseudopodia. However, macrophages with degradation of internalized pathogens, turned to be round and immobile. This finding suggested that the phagocytic degradation of *C. difficile* is cytotoxic to macrophages.

Mycobacterium tuberculosis (Mtb) has been well-studied as an intercellular pathogen inducing macrophages death. Mtb is internalized through phagocytosis by macrophages, which leads to aggregation of Mtb in macrophages. Macrophage, displayed Mtb aggregation,

are likely dead (Pieters, 2008). Mtb-mediated macrophage death occurs by apoptotic and non-apoptotic mechanisms (Mahamed et al., 2017). More importantly, Mtb cells use macrophages for their replication, where Mtb remains viable in dead macrophages (Pieters, 2008).

Previous studies have shown that human monocytes/macrophages are more sensitive to TcdA-induced apoptosis than lymphocytes *in vitro* (Solomon et al., 2005; Mahida et al., 1998). After intrarectal instillation of TcdA and TcdB, both toxins penetrate the epithelial barrier and kill immune cells, and notably most of them are macrophages (Hirota et al., 2012). However, the reason remains to be determined.

Neutrophil infiltration of the intestinal epithelium is one of the most important pathologic feature in CDI (Madan et al., 2012). Then influx neutrophils lead tissue damage and the phagocytosis of infecting *C. difficile* in the intestine as well. Our finding might explain that macrophages are not suitable immune cells to clean *C. difficile* because of their sensitivity to this pathogen.

4.2.2 The application of bi-directional LexA/lexAop for Mac-ATTAC^{TM}

Because the Gal4/UAS system has been used for the neutrophil transgenic strain, another binary expression system was needed for generating Mac-ATTAC^{TM} strain. The LexA/lexAop system was chosen to generate the Mac-ATTAC^{TM} strain.

There are two advantages of the LexA/lexAop system: Firstly, the LexA/lexAop system can be used independently or in combination with the Gal4/UAS system; secondly, *lexAop* sequence do not contain CpG dinucleotide sites, the target of DNA methyltransferases. Because of CpG dinucleotides in UAS, many researchers have observed progressive transcriptional silencing in Gal4/UAS transgenic zebrafish due to cytosine methylation in CpG dinucleotides (Akitake et al., 2011; Goll et al., 2009). Lack of CpG dinucleotides should not be transcriptional silencing by DNA methylation when using the LexA/lexAop system.

A bi-directional LexA/lexAop system was established. The system contained two parts: a chimeric transcription factor and lexAop cis-regulatory sites. The transcription factor was a fusion of the DNA binding domain of LexA protein but lacking dimerization domain (residue 1-

87) and the transcriptional activation domain of the human p65 protein (p65 AD, residues 283–551). The operator-promoter sequence was constructed by fusing eight copies of *ColE1*-lexAop sequences to E1b minimal promoters in a bi-directional manner on both sides of the four copies of lexAop sequence. Although our LexA/lexAop system was applied in the Mac-ATTAC^{TM} stain successfully, still few questions need to be clarified.

The first question was how LexA proteins start the transcription without a dimerization domain. The LexA protein, used in this study, did not contain a dimerization motif, but LexA protein naturally binds as dimer to the operators of SOS genes to inhibit the expression of SOS genes in *E. coli*. Previous studies suggested that free LexA proteins form a dimer predominantly rather than a monomer, which represses transcription more efficiently (Dmitrova et al., 1998; Mohana-Borges et al., 2000). The LexA dimers dissociate into monomers only when LexA loses its ability to bind specific DNA sequences (Mohana-Borges et al., 2000). Thliveris et al proposed two possible mechanisms for LexA-DNA binding, in which LexA monomers first form a dimer and then bind to *recA* (a gene in SOS system) operators, or LexA monomers bind to *recA* operators sequentially and then dimerize on DNA (Thliveris et al., 1991). The LexA protein in our LexA/lexAop system, referred to LexA-DBD, only contained the DNA binding domain. Nevertheless, a high expression level of either fluorescent protein or Caspase8ER^{T2} was found in Mac-ATTAC^{TM} zebrafish, indicating that LexA-DBD alone bind to lexAop and start transcription.

One possible explanation is that the binding between a LexA monomer and lexAop sequence could provide sufficient affinity to activate transcription. LexA-DNA binding has been investigated in *E. coli*, in which two LexA monomers bind operators sequentially and cooperatively (B. Kim et al., 1992). The first LexA monomer binds to a half-*recA* operator site with low affinity, but the second monomer binds to the operator with 100-fold more affinity than the first one (B. Kim et al., 1992). The first bound monomer increases the affinity between the second monomer and *recA* operator. This finding suggested that the LexA monomer could bind lexAop with low affinity but subsequent binding of other monomers is strong enough to start the transcription of genes (Dahlman-Wright et al., 1991). In addition, eight copies of lexAop sequences were used in our LexA/lexAop system, which might provide additional binding sites for LexA monomers.

The second possible explanation is that the p65 AD (residues 283–551) itself could induce the dimerization of the LexA-p65 proteins and then initiate transcriptional activation. p65, encoded by the *RELA* gene, is one component of the NK-κb transcription factor family. The p65 protein contains 551 amino acids, which is composed of an N-terminal DNA binding region, referred as *REL* homology region (RHR), and C-terminal transcriptional activation domain (TAD) (Y. Q. Chen et al., 2000). The TAD is divided into two different domains, TA1 (residues 521–551) and TA2 (residues 428–521), both of which are necessary for the transcriptional activation initiated by p65 (O 'shea et al., 2008). It has been shown that the NF-κB transcription factor binds to DNA as a p50/p65 heterodimer (Schmitz et al., 1991). But the p50 and p65 can also form homodimers as p50/p50 or p65/p65 (Y. Q. Chen et al., 2000; Phelps et al., 2000).

Protein dimerization is frequently mediated by leucine zipper, helix-loop-helix (HLH) motif and ankyrin motifs. Schmitz et al fused the DNA binding domain of Gal4 to different truncations of the transcription activation domain of p65, and found a stronger transcriptional activity of Gal4 –$p65^{468-550}$ (which include TA1 domain and a part of TA2 domain)or Gal4 –$p65^{520-550}$ (which include TA1 domain) compared to full length of Gal4-$p65^{1-550}$ in COS cells and mouse fibroblasts (Schmitz et al., 1991). They further identified that a clustering of serine residues in the amphipathic helix of TA1 could form a leucine zipper structure, which might serve to mediate a protein-protein interaction (Schmitz et al., 1991; William et al., 1988).

The p65 AD, used in this study, include TA1 domain and TA2 domain (O 'shea et al., 2008). This might be the same reason that p65 AD induced the dimerization of the LexA-p65 protein. This dimer increased the transcription activity of LexA-65. This can also explain why KalTA4-p65 AD induced a much stronger transcription of transgenes than KalTA4-TA4 and KalTA4-TA3 in my results. However, more evidence needs to be obtained to support that the p65 AD domain indeed mediate protein-protein interaction.

The second question that needed to be discussed is why lexAop sequences have a strong directional preference in actual transcription.

The promoter-operator sequence used here consists of eight copies of lexAop fused to E1b

minimal promoters in a back-to-back configuration. I found that lexAop showed an orientation-dependent activation. It has been investigated that this feature involves the recognition between the lexA DNA binding amino-terminal domain (NTD) and the lexAop sequences (Butala et al., 2009; Dumoulin et al., 1993). For a stable and specific operator binding, the recognition helix of the LexA protein should reorient NTD into the major groove of operator DNA (Chattopadhyaya et al., 2004; Dumoulin et al., 1993). The LexA recognition helix exhibits a specific direction within the major groove. It is the same reason why the first bound LexA monomer binds to DNA with low affinity but promotes the formation of a major groove of the operator DNA, which enhances the affinity between the second LexA monomer and the operator. These findings suggest that the lexAop is an orientation-dependent transcriptional activator. Because of this, only back-to-back configuration of lexAop sequences could start the transcription of both transgenes locating the operators in opposite direction.

It is known that the LexA protein has different affinities to lexAop motifs derived from different species (Pfeiffer et al., 2010). Although the LexA protein has the highest affinity to the *ColE1*-derived lexAop motif (the same motif used in this study), this *ColE1*-derived lexAop showed a leaky expression in the absence of LexA protein in *Drosophila* (Ebina et al., 1983; Pfeiffer et al., 2010). Even this result might not be consistent between species, it is important to address a possible leaky expression from the *ColE1*-lexAop in zebrafish. Also, it would be interesting to test other LexA-binding motifs, such as *sluA*-lexAop, in zebrafish. *sluA*-lexAop is found to give strong transgene expression with minimal leaky expression. This operator might be more suitable for transgenic expression in zebrafish.

4.2.3 4OHT cannot induce neutrophil apoptotic death in Neu-ATTAC^{TM} larvae

The neutrophil specific zebrafish, Neu-ATTAC^{TM} strain, expressing Citrine and Caspase8ER^{T2} was established. However, fluorescent signal did not decrease or disappear after 4OHT treatment. Immunostaining analysis against activated Caspase3 did not show any signal, suggesting that 4OHT treatment did not trigger apoptosis in neutrophils. To validate whether Caspase8ER^{T2} still functioned, the carrier of Neu-ATTAC^{TM} are crossed with carrier of the Tg(*krox20: KalTA4)* or Tg(*krox20: KalTA4)* transgenic line expressing KalTA4 in rhombomere 3 and 5 or the skeletal muscle cells respectively. Then double transgenic larvae were incubated

with 4OHT. After 6 hours of treatment, I observed cell apoptosis in rhombomere and muscle tissue, indicating that Caspase8ER^{T2} was still functional.

Neutrophils die via apoptosis under healthy conditions. The most leukocytes in the peripheral blood—circulating neutrophils undergo apoptotic cell death, which maintains a homeostatic cell number (B Geering et al., 2011). It is agreed upon that tissue-resident macrophages, including Kupffer cells, and bone marrow stromal macrophages, clean the apoptotic neutrophils (Furze et al., 2008; Summers et al., 2010).

Neutrophil apoptosis is also the central part of inflammation resolution (Fox et al., 2010). Phagocytosis of pathogens accelerates neutrophil apoptosis at the inflammation sites, which ultimately promotes the resolution of infection (Savill et al., 1989). Apoptotic neutrophils are recognized and removed by macrophages (Carl Nathan et al., 2010). Neutrophil apoptosis guaranties the safe disposal of engulfed bacterial, which is beneficial for the host (Deleo, 2004). Defective apoptosis and failure of removal of apoptotic neutrophils is associated with many inflammatory diseases, such as acute respiratory distress syndrome and inflammatory bowel disease (Summers et al., 2010).

Neutrophils undergo either intrinsic or extrinsic apoptosis (B Geering et al., 2011; Leitch et al., 2008). The extrinsic pathway is activated by the interaction between death receptors and ligands, such as, TNF-α, Fas ligand, or TRAIL (Renshaw et al., 2003). The intrinsic pathway occurs when neutrophils experience genotoxic stress or ultraviolet irradiation (Leitch et al., 2008). This pathway is triggered by cytochrome C and proapoptotic factors, which are released by disruption of the outer mitochondrial membrane (McCracken et al., 2014). The intrinsic apoptosis is believed to be responsible for the lifespan of neutrophil (Fox et al., 2010).

Both apoptotic pathways are dependent on the activation of caspase proteins (McCracken et al., 2014). The binding between death receptors and ligands leads to the formation of death-inducing signaling complex (DISC) (Leitch et al., 2008). DISC activates the upstream initiator caspases and cleave the downstream effector Caspase-3, which eventually starts the final steps of apoptosis (Leitch et al., 2008). Caspase-8 and Caspase-9 are the caspases for the extrinsic and intrinsic apoptosis pathways respectively (McCracken et al., 2014).

Neutrophils have few mitochondria which hardly participate in ATP synthesis, but mitochondrial cytochrome C and other mitochondrial proteins, such as Smac/DIABLO and HtrA2/Omi, are essential for the activation of caspases (McCracken et al., 2014; Murphy et al., 2003). Although it is clear that the intrinsic and extrinsic pathways are trigger by distinct but different death factors, these two pathways are joined by the BH3-interacting domain death agonist (Bid) (McCracken et al., 2014). Bid is truncated by Caspase-8 and then translocate to mitochondria, where it assists oligomerization of Bax and Bak (B Geering et al., 2011; Korsmeyer et al., 2000). Bax and Bak disrupt the outer mitochondrial membrane and then induce cytochrome c efflux, which triggers the intrinsic apoptosis pathway (Korsmeyer et al., 2000).

In addition, Daigle et al reported that Caspase 8 is critical in the regulation of neutrophil apoptosis *in vitro* (Daigle et al., 2001). For example, inactivation of Caspase-8 delays neutrophil apoptosis (Daigle et al., 2001). Caspase-9 activation was also detected. Caspae-9 inhibitors decrease neutrophil apoptosis (Daigle et al., 2001). Collectively, caspase proteins, especially Caspase 8, represent ideal candidate to trigger apoptosis in neutrophils. However, my study suggested that an unknown mechanism could inactivate the Caspase 8 pathway to protect neutrophils.

Some pro-inflammatory factors prolong neutrophil lifespan by suppressing apoptosis, such as granulocyte/macrophage colony-stimulating factor (GM-CSF) (Maianski et al., 2004; McCracken et al., 2014). GM-CSF is secreted by a variety of cell types, including monocytes/macrophages, T and B cells, and neutrophils (Hamilton, 2002; Shiomi et al., 2015). GM-CSF is a major hematopoietic growth factor to regulate proliferation and differentiation of granulocyte and macrophages from their precursor cells (Shiomi et al., 2015).

An early work suggest that GM-CSF induces tyrosine phosphorylation of several intracellular proteins in neutrophils (Yousefi et al., 1994). In a subsequent study, the lck/yes-related novel (Lyn) protein is identified as one of the important tyrosine kinases that provides a survival signal and prevents apoptosis (Wei et al., 1996). Activation of tyrosine kinase upon GM-CSF simulation results in Jak2 phosphorylation and activation of several STAT proteins, which

increases Mcl-1 and XIAP protein stability to enhance neutrophil survival (Al-shami et al., 1998; Brizzi et al., 1996; Derouet et al., 2004). Interestingly, Mcl-1 is essential for neutrophil viability and survival, but not for macrophage (Dzhagalov et al., 2012; Milot et al., 2011).

Besides of the STAT pathway, the mitogen-activated protein kinase (MAPK) pathway is also implicated in prohibiting neutrophil from apoptosis (Alvarado-Kristensson et al., 2001). GM-CSF induces the activity of p38 MAPK (Alvarado-Kristensson et al., 2001). Then p38 MAPK phosphorylates and subsequently inhibits the activity of Caspase-8 and Caspase-3, which protects neutrophil from apoptosis (Alvarado-Kristensson et al., 2001, 2004). However, phosphorylation of p38 was also detected in TNF-α-induced apoptosis, which generates reactive oxygen species (ROS) and subsequently activates Caspase-3 (Barbara Geering et al., 2012). TNF-α also shows anti-apoptotic potential and prolong neutrophils lifespan (Keel et al., 1997). Therefore, the role of p38 MAPK and TNF-α are unclear in the regulation of neutrophil.

A possible interpretation of neutrophil survival upon 4OHT treatment is that GM-CSF prevents neutrophil death. Since macrophages secret GM-CSF, I would like to confirm whether the elimination of macrophages affects the survival of neutrophils. To this end, the Mac-ATTAC^{TM} line was crossed with Neu-ATTAC^{TM} line and the double transgenic larvae, expressing Caspase8ER^{T2} in macrophages and neutrophils, were selected for 4OHT treatment. However, neutrophils survived even when macrophages were eliminated. Therefore, macrophages were excluded as possible GM-CSF producer. Since there are various GM-CSF cellular sources, it is hard to determine which cell type is the main source. Besides GM-CSF, several other survival factors, such as fMLP, hrC5a, and ATP, have been shown inhibit neutrophil apoptosis *in vitro* (Gasmi et al., 1996; a Lee et al., 1993).

Another possible explanation is that zebrafish neonatal neutrophils are resistant to apoptosis. Human neonatal neutrophils, which are isolated from newborn infants, showed a lower expression level of Caspase-3 protein than adult neutrophil (Song et al., 2011). Several studied showed that the level of Fas-induced chemotaxis and FasR, which engage with death receptors, are low in neonatal neutrophils (Allgaier et al., 1998; Hanna et al., 2005). Neutrophils originate from the primitive and definitive waves of hematopoiesis in zebrafish (Bennett et al., 2001). In the primitive wave, myeloid precursors arise from mesoderm and differentiate in the yolk

sac at around 22hpf, which are called 'primitive macrophages' (Bennett et al., 2001). A subset of the primitive macrophages differentiate into neutrophils by 48hpf (Bennett et al., 2001). The definitive hematopoiesis starts at 24hpf in the CHT with the multipotent hematopoietic stem and progenitor cells (HSPC) (Bertrand et al., 2007). A group of hematopoietic progenitors colonize in the CHT by 48hpf, where they give rise to neutrophils (H. Jin et al., 2009; Murayama et al., 2006). Neutrophils reporter larvae that were used in this study are between 2dfp to 6dfp of stage, where neutrophils are still neonatal. It is possible that zebrafish neonatal neutrophils share the same feature with human neonatal neutrophils, which are resistant to apoptosis.

One unique feature of neutrophils is their short lifespan. The reason and mechanism for the short lifespan is unclear, but as Amulic hypothesized, it may ensure the integrity of neutrophils (Amulic et al., 2012). The short life might also guarantee that neutrophils are either robustly alive or die by apoptosis.

4.2.4 The interaction between macrophages and neutrophils

Neutrophils and healthy macrophages cooperate to clear apoptotic macrophages. As neutrophils and macrophages are the main partners in the phagocytic system, I would like to find out whether and how neutrophils participate in the phagocytosis of dying macrophages. The confocal microscopy analysis revealed that a direct contact between neutrophils and macrophages took place at the early stage of macrophage apoptosis. I was wondering what the function of this contact is.

There are *in vitro* evidences in support of the interaction between neutrophils and macrophage. Magnarin et al reported that human neutrophils specifically adhere to human macrophages *in vitro* (Magnarin et al., 2000). Their interaction increases the release of inflammation factors by the both cell types (Magnarin et al., 2000). It was showed that the interaction between neutrophils and macrophages covert the mechanism of muscle cell killing by both cell types (Nguyen et al., 2003).

There are reporters about neutrophils and macrophages directly interact *in vivo* (Ellett et al., 2011; Tobin et al., 2010; Vincent et al., 2017). Ellett et al reported that macrophages directly

and dynamically contact with neutrophils after wounding (Ellett et al., 2011). Interestingly, a direct cytoplasmic transfer from a donor neutrophil to a macrophage is observed during their interaction (Ellett et al., 2011). When the ventral tailfin is wounded, neutrophils frequently contact macrophages and induce resolution of inflammation (Tauzin et al., 2014). The molecular mechanism and biological function about neutrophil-macrophage interactions remain unclear, but their behaviors implied that communication occurred through their contact.

The communication between immune cells is crucial for immune cell survival, migration, and coordination of inflammatory responses (McCoy-Simandle et al., 2016). Cell-cell communication could be classified into cytokine-based communication and contact-based communication. Cytokines, such as cytokines and chemokines, are secreted by immune or non-immune cells, and then spread and bind to target cells. Cytokine-based approach contribute to the global communication between immune cells (Rivera et al., 2016).

Cell-cell communication takes place via direct cells contact as well. Tunneling nanotubes (TNTs), a contact-depend communication, have been investigated (Gerdes et al., 2013). TNTs are a thin membranous tubes that typically range between 50-200nm in diameter and are up to several cell diameters long (Önfelt et al., 2006). Multiple cells could be connected by TNTs, which facilitates the intercellular exchange of cellular components, such as mitochondria and intracellular vesicles (McCoy-Simandle et al., 2016). TNTs are seen in variant cell types, such as NK cells, macrophages, and B cells (Onfelt et al., 2004).

The cytokine-based communication and TNTs are usually found for long-range interaction, but the contact between macrophage and neutrophil is a short-range interaction.
Immunological synapse (IS) is a well-studied example for short-range interaction. The IS is cell-cell junction between an antigen presenting cell (APC) and a T cell, which initiates the antigen-specific immune response (Dustin et al., 2015). The IS is characterized by close apposition of the immune cell membrane, adhesion, stability and directed secretion between the immune cells (Dustin et al., 2017). As T cells are activated, T cell receptors (TCR) form a central supramolecular activation cluster (cSMAC). These cSMAC are surrounded by talin-formed peripheral SMAC (pSMAC) and F-actin enriched distal SMAC (dSMAC), which stabilize the T

cell-APC contact (Dustin et al., 2016). Some researchers proposed that a similar structure might be applied by other immune cell types, such as mast cells, NK cells, neutrophils, macrophages, and dendritic cells (Dustin et al., 2017). Supramolecular organization of proteins, like cSMAC, has been observed in natural killer (NK) cells, B cells, and dendritic cells (D. M. Davis et al., 2004). Notably, a specific organization of proteins is involved in the formation of IS in different cell types. The IS has several functions. The directing secretion between immune cells is considered as the major function, in which T cells polarize the secretion of lytic granules and the Golgi complex toward the target cells (Stinchcombe et al., 2001). The cytoskeletal polarization in the assembly of an IS serves as checkpoints for lymphocyte activation (Wulfing et al., 2003).

There is a possibility that a similar structure of IS is also applied by neutrophils and macrophages for exchanging information or activating cells during phagocytosis of apoptotic cells or *C. difficile*. Tauzin et al showed that, after contacting with macrophages, neutrophils exhibit a much higher meandering index and increased velocity at wound site (Tauzin et al., 2014). It is possible that neutrophil and macrophage contacts, like the IS, could enhance or terminate some signaling pathways to facilitate their function of these innate immune cells. However, there is one difference between IS and the macrophage-neutrophil contact. The formation of an IS structure is a dynamic process, which takes around 30 minutes for $CD4^+$T cell and B cell to form it *in vitro* (Ueda et al., 2011). The contact between neutrophils and macrophages is dynamic as well but the time of their conjugation was shorter than the one for IS formation and range around than 5 minutes. Probably, different cell types might take variable time to form IS like structures.

As the dominant effector cells of the innate immune system, neutrophils also engage in interaction with other immune cells, including dendritic cells (DCs), and NKs (Scapini et al., 2000). Activated neutrophils cluster with immature DCs to induce DC maturation by binding C-type lectin DC-SIGN to β-integrin Mac-1, which triggers a strong T cell proliferation (van Gisbergen et al., 2005). Neutrophils also cross-talk with NK cells and modulate the activation state of NK cells in response to pathogens (Costantini et al., 2011).

4.2.5 The inflammasome of macrophages and neutrophils in CDI

Both TcdA and TcdB activate inflammasome formation, a protein complex assembled in response to pathogens or dangerous signals, but the role of inflammasome in CDI is still controversial. Using murine and human *ex vivo* infection models, Jafari et al found that recombinant TcdA or TcdB trigger BMDC (bone-marrow-derived dendritic cell) IL-1β secretion by activating the NLRP3 inflammasome (Jafari et al., 2013). They further confirmed that ASC (apoptosis-associated speck-like protein containing a caspase recruitment domain) is a critical component for *C. difficile*-mediated BMDC inflammasome activation (Jafari et al., 2013). Ng et al verified that both toxins induce NLRP3 inflammasome activation in an ASC-dependent manner, which triggers the release of IL-1β in mouse (Ng et al., 2010).

The inflammasome-dependent IL-1β secretion contributes to the pathogenesis of CDI. Inhibition of inflammasome signaling, through administration of IL-1 receptor antagonist or genetic deletion of ASC, protects toxin-induced inflammation and intestinal damage in mice (Ng et al., 2010). IL-1β plays an essential role in the induction of the CXCL1 signaling pathway and rapid infiltration of neutrophils in CDI (Cowardin et al., 2015; Hasegawa et al., 2017; Jarchum et al., 2012). Blocking of IL-1β signaling inhibits TcdA/B-induced neutrophil recruitment (Hasegawa et al., 2017). It is important to mention that this IL-1β-induced inflammasome was studied in either mammalian cell culture or an ileal loop mouse model with purified toxins.

In mammals, the core components of the inflammasome have been identified as two protein families, the NOD-like receptor (NLR) family, and the PYHIN protein family, including NLRP3, NLRC4, AIM2, and Pyrin (Strowig et al., 2012). ASC has been identified as an inflammasome adaptor and it is required for inflammasome activation (Sagoo et al., 2015). As to the hallmark of inflammasome activation, ASC is utilized to test inflammasome activation (Sagoo et al., 2015; Sheedy et al., 2013; Tzeng et al., 2016). Recently, an ASC-citrine reporter mouse was generated to study inflammasome activation in real time *in vivo* (Tzeng et al., 2016).

The orthologues of ASC (zAsc) and two pyrin-containing caspases, Caspy and Caspy2 have been characterized in zebrafish (Masumoto et al., 2003). Using genome database mining of various non-mammalian vertebrates, three distinct NLR subfamilies in teleost fish were

identified: the first subfamily (NLR-A) resembles the mammalian NLR family; the second one (NLR-B) resembles the mammalian NALPs; the third one is unique to teleost fish (Laing et al., 2008).

Those studies make it possible to use zebrafish to study inflammasome activation. The inflammasome is the key signaling platform that controls Caspase-1-dependent maturation of pro-inflammatory cytokines (Tzeng et al., 2016). We could take advantage of these discoveries and the ASC-reporter technique to establish an inflammasome zebrafish model. Although the mouse model provides information on the mechanisms of inflammasome activation in the context of purified toxin injections, zebrafish has the advantage for deciphering the inflammasome activation against live *C. difficile in vivo*. This model could uncover the process of inflammatory cytokines release upon *C. difficile* infection. Previous studies implied that the inflammasome play a role in clearance of pathogens, which could be confirmed in the zebrafish inflammasome model (Jafari et al., 2013). The transparency of zebrafish larvae also allows for visualization of inflammasome assembly in macrophages and neutrophils in real time in response to *C. difficile* infection.

In addition, the zebrafish inflammasome model could be used to study the role of CDT toxin (the binary ADP-ribosyltransferase toxin). The CDT induces microtubule-based protrusion to form a dense meshwork at the surface of intestinal epithelial cells, which increases the adherence of bacteria (Schwan et al., 2009). Notably, pyrin inflammasome activation relies on the dynamics of microtubules (Gao et al., 2016). The *C. difficile* strain R20291 produces TcdA, TcdB, and CDT, whereas the *C. difficile* 630 WT strain only produces TcdA and TcdB (Jafari et al., 2013). Therefore, the zebrafish inflammasome model could be applied to survey the contribution of CDT in TcdA/B-induced inflammasome with different *C. difficile* strain infections (Aktories et al., 2017).

Interestingly, Ng et al reported that inflammasome activation is independent of the GTD domain of TcdB, but it is dependent on the recognition of intact toxin (Ng et al., 2010). In contrary, Xu et al found that the glucosyltransferase-deficient TcdB does not induce inflammasome activation in BMDMs cells (Xu et al., 2014). They identified that a Pyrin, the pattern recognition receptor (PRR), is a mediator in the TcdB induced caspase inflammasome

activation (Xu et al., 2014). In fact, inactivation of Rho activates Pyrin inflammasome by glucosylation (Aktories et al., 2017; Park et al., 2014). Targeting the inflammasome or its substrate might provide a new therapeutic method for CDI. We could combine zebrafish intoxication model with the inflammasome model to investigate the relationship between Rho GTPase signaling and inflammasome activation *in vivo*.

4.2.6 Zebrafish as an alternative model for studying *C. difficile*

Several animal models have been used for *C. difficile* research. The most commonly used *C. difficile* model is hamster during the last decade. Mouse, rat, and pig models have been developed to reveal different aspects of *C. difficile* pathology. Yet each animal model has its own advantages and disadvantages. However, none of those animal models are appropriate to analyze innate immune cells *in vivo* upon *C. difficile* infection due to technical limitations. The zebrafish model offers an optically transparent organism to study host-pathogen interactions. At early larval stages, zebrafish survive with only innate immunity, because adaptive immune response is functionally matured only 4-6 weeks after fertilization (Page et al., 2014). Given that lymphocytes appear as early as 2 days of embryogenesis, zebrafish larvae might be a unique tool to study the response and function of innate immune cells in response to *C. difficile* infection.

When considering whether the zebrafish could be used as a *C. difficile* infection model, some factors should be taken into account, such as: Does the temperature of replication and infection of *C. difficile* match with the maintenance temperature of zebrafish, at 28°C? Is infection achieved by micro-injection, or static immersion? Is mimicking the natural route of infection critical for the zebrafish model?

To determine the occurrence of *C. difficile* contamination in seafood and fish, Metcalf et al found that 4.8 % of the samples were contaminated in Canadian grocery stores (Metcalf et al., 2011). This result suggests that *C. difficile* could grow at lower temperature than 37°C. Despite this, the maintenance temperature of the zebrafish still could be adjusted higher than 28°C to adapt the growth temperature of *C. difficile*.

Several infection techniques have been established for zebrafish larvae (Milligan-Myhre et al., 2011; van Soest et al., 2011). Micro-injection is the most common method to intravenously or locally infect zebrafish embryos with pathogens (Benard et al., 2012). After injecting zebrafish embryos with *C. difficile*, macrophages and neutrophils accumulated quickly at infection site. However, unlike *Mycobacterium marinum* which induces the formation of necrotic granulomas (a key feature of human tuberculosis) in zebrafish, no marker for *C. difficile* infection is currently available in zebrafish. Therefore, it was difficult to discriminate whether the recruitment of lymphocytes was induced either by *C. difficile* itself or tissue damage (Behr et al., 2014). To avoid this issue, I used non-invasive microgavage to deliver *C. difficile* into the proximal intestine of zebrafish. This method mimics the natural path of infection. However, in wild type zebrafish, *C. difficile* was detected only 24h after infection. One explanation for this could be that commensal bacteria protect the intestines from exogenous *C. difficile*—a phenomenon termed as colonization resistance.

In addition, gnotobiotic zebrafish larvae were used for *C. difficile* infection. *C. difficile* were now detected at 24, 48, and 72h post-infection. Interestingly, samples from 48h and 72h post-infection intestinal tissue only grew in media containing TCA, suggesting that *C. difficile* already formed spores. Intriguingly, germ-free zebrafish still did not show any symptoms of CDI, such as neutrophil influx into the intestine of zebrafish, or even mortality of zebrafish.

There was one possibility that could explain why zebrafish did not develop disease symptoms in 3 days. The intestinal mucus layer could provide protection against exogenous pathogens.

In addition to the intestinal microbiome, the gastrointestinal tract is also covered by a mucus layer, referred as intestinal barrier. In fact, the mucosal layer is the home to the gut microbiota. The mucosal layer has been recognized as the first line of defence against microbial invaders and toxins. Mucosal surface is the crucial site for innate and adaptive immune regulation (Turner, 2009). Most gastrointestinal infections, for instance, infected by *Shigella spp.* or *C. difficile*, start from the mucosal surface (Holmgren et al., 2005). The *C. difficile* associated diarrhoea is characterized by the loss of function of the mucosal barrier and secretory diarrhea. *C. difficile* toxins act quickly on the dissociation of junctions between epithelial cells in order to disrupt the protective mucosal barrier (Solomon, 2013). Once the mucosal and epithelial

barriers are broken down, *C. difficile* toxins and other proteins contact with submucosal macrophages and monocytes, leading to inflammatory cascade that release pro-inflammatory chemokines. Leber *et al* combined a computational modelling with *in vivo* experiments to reveal the importance of the mucosal immune response in the course of CDI (Leber et al., 2015). Secretory IgA, which is an immunoglobulin produced by plasma cells, has been shown to protect barriers against pathogens in mucosal immunity (Johal et al., 2004). Interestingly, inflammasome is found to regulates mucus secretion to promote resistance to pathogens (Perez-Lopez et al., 2016).

The mucosal layer of gnotobiotic zebrafish might protect the host from *C. difficile*. Dextran sodium sulfate (DSS), a detergent, has been reported to decrease the thickness of the mouse mucus layer, which makes it permeable for bacteria (Johansson et al., 2010). DSS administration to zebrafish larvae induces enterocolitis symptoms, with recruitment of leukocytes and raised pro-inflammatory gene expression (Marjoram et al., 2015). The DSS-induced enterocolitis zebrafish model has been shown to also recruit the intestinal neutrophils, a key feature of CDI in human, which prevents application of DSS in this study.

The infection of intestinal cells might be achieved by *C. difficile* spores instead of vegetative cells. *C. difficile* produces highly infective spores, which persist for prolonged periods of time in the environment. Following ingestion by susceptible patients, spores can germinate and produce new vegetative cells (Abt et al., 2016). Because of this, spores are used in most animal models of CDI (X. Chen et al., 2008a; Hutton et al., 2014; Semenyuk et al., 2015). Mice treated with antibiotics were challenged with spores and develop the disease (X. Chen et al., 2008a). Our initial idea was to induce the acute stage of infection with vegetative cells in zebrafish. However, only *C. difficile* spores were detectable in my results, which it is likely that vegetative cells first formed spores in the intestine of zebrafish. Therefore, the use of spores might shorten the time between infection and onset of symptom.

Due to the lower temperature to maintain the zebrafish, or the structural differences between zebrafish and mammalian intestine, the onset of disease symptom in zebrafish might be delayed, not as fast as that in mammalian models. Nevertheless, the gastrointestinal tract of gnotobiotic zebrafish larvae was inhabited by *C. difficile* up to 3 days. This zebrafish model

could be further used for an oral immersion experiment. The immersion of zebrafish carrier with commensal bacteria from human or zebrafish could investigate which bacteria could protect zebrafish against *C. difficile* invasion or outcompete *C. difficile* in the intestine of zebrafish.

5. Appendix

5.1 Sequence of NTcd-A and NTcd-B

NTcdA:

GAATTCGATATCCACCATGTCACTCATCTCAAAAGAGGAACTCATCAAACTGGCGTACTCTATCCGTC
CTAGAGAAAACGAGTACAAAACCATTCTCACTAATCTGGATGAGTACAACAAATTGACGACCAACAA
TAATGAGAACAAATATTTGCAACTGAAGAAACTGAATGAGAGCATAGATGTGTTCATGAACAAATAT
AAAACAAGTTCCCGAAACAGAGCTCTGTCAAACCTCAAGAAAGACATTCTGAAAGAAGTCATTCTGA
TTAAGAACTCCAACACCAGTCCTGTTGAGAAGAATCTGCACTTTGTGTGGATTGGAGGCGAAGTGTC
TGACATCGCCCTGGAGTATATCAAGCAGTGGGCCGACATAAATGCCGAGTATAACATCAAGCTGTGG
TACGATAGTGAGGCCTTTCTGGTGAACACCCTGAAGAAAGCAATTGTGGAAAGCAGTACGACAGAG
GCACTGCAACTCCTGGAAGAGGAAATCCAGAATCCGCAGTTCGACAACATGAAGTTTTACAAGAAGC
GAATGGAATTTATCTATGATAGACAGAAGAGGTTCATCAACTACTACAAATCACAGATAAACAAACC
CACTGTACCCACGATTGATGACATAATCAAGTCCCATCTGGTCAGCGAATACAACCGGGATGAGACT
GTCCTCGAAAGCTATCGGACCAATTCTCTGCGCAAAATTAACAGCAACCACGGCATTGACATCAGAG
CCAACAGCCTCTTCACTGAACAGGAGCTGCTTAATATCTACTCCCAGGAGCTTCTCAATCGTGGAAAT
CTGGCAGCAGCTTCCGATATTGTCAGGCTTTTGGCGCTTAAGAACTTTGGAGGCGTTTATCTGGACGT
TGATATGCTGCCAGGAATCCATTCTGACCTGTTTAAGACCATTAGTAGACCTAGCTCTATCGGGCTTG
ATCGCTGGGAAATGATCAAACTGGAGGCCATAATGAAATACAAGAAGTACATCAACAATTACACCAG
CGAAAACTTCGACAAGCTGGATCAGCAACTGAAAGACAACTTTAAACTGATCATTGAGTCAAAGTCT
GAGAAGAGCGAGATTTTCTCAAAACTCGAAAATCTTAATGTTAGCGACCTGGAGATTAAGATAGCGT
TCGCACTGGGTTCTGTGATCAACCAGGCACTCATCAGCAAACAGGGCTCCTATTTGACAAACCTGGT
GATCGAGCAAGTGAAGAACCGCTATCAGTTTCTTAACCAGCATCTGAATCCAGCCATAGAATCCGAC
AACAACTTCACTGACACAACGAAGATTTTCCACGATTCCTTGTTCAATAGTGCTACAGCTGAGAATAG
CATGTTCCTGACAAAGATCGCTCCCTATCTCCAAGTAGGGTTTATGCCTGAAGCTAGGTCAACTATTA
GTCTTTCTGGGCCAGGTGCTTATGCATCTGCTTATTACGATTTCATCAATCTGCAGGAGAATACAATC
GAGAAAACATTGAAGGCCAGCGACCTGATTGAGTTCAAGTTTCCGGAGAATAACTTGAGTCAGTTGA
CCGAGCAGGAGATAAACTCACTGTGGTCCTTTGACCAAGCCTCTGCGAAATACCAGTTTGAGAAATA
CGTGAGGGATTACACCGGAGGTAGCCTGGGCTCGAGATACCCATACGATGTGCCTGACTACGCTTG
AGTCTAGAG

NTcdB:

GAATTCGATATCCACCATGTCACTCGTCAATCGAAAGCAGTTGGAGAAAATGGCCAATGTCCGTTTC
AGGACTCAGGAGGATGAGTATGTAGCGATACTGGATGCCTTGGAGGAATATCACAACATGAGCGAA
AACACTGTGGTTGAGAAATATCTGAAGCTGAAAGACATCAATAGCCTGACTGACATCTACATTGACA
CATACAAGAAATCCGGAAGGAACAAGGCCCTCAAGAAGTTCAAAGAGTATCTGGTTACCGAAGTGC
TGGAGCTCAAGAACAACAACCTGACACCTGTCGAGAAGAACCTTCATTTTGTTTGGATCGGAGGACA
GATCAACGATACAGCCATCAACTACATCAACCAATGGAAAGACGTTAATTCCGACTACAACGTGAAT
GTGTTCTATGACAGCAACGCCTTTCTGATTAATACCCTGAAGAAAACTGTGGTCGAGTCTGCTATTAA
CGATACACTGGAATCCTTCAGAGAAAACTTGAATGATCCCAGGTTTGATTACAACAAATTCTTCCGCA
AGAGGATGGAGATCATCTACGACAAGCAGAAGAATTTTATCAATTACTACAAAGCCCAGAGAGAGG
AAAATCCCGAACTCATCATAGATGACATCGTTAAGACCTATCTTAGCAACGAGTACTCAAAGGAGAT
TGATGAGCTGAATACCTATATTGAGGAGTCTCTGAACAAAATCACACAGAACTCTGGGAATGATGTG
AGAAACTTTGAAGAGTTTAAGAACGGTGAAAGTTTCAACCTGTACGAGCAGGAGCTCGTAGAACGC
TGGAATCTGGCAGCTGCATCTGACATACTGCGGATTTCTGCACTGAAAGAGATTGGAGGCATGTATC
TGGACGTCGATATGCTGCCAGGCATACAGCCAGACCTGTTTGAATCCATAGAGAAACCCTCAAGCGT
AACAGTGGACTTCTGGGAGATGACCAAACTCGAAGCTATCATGAAATACAAAGAATATATCCCGGAA
TACACGAGCGAACATTTCGATATGCTCGATGAAGAGGTGCAATCATCTTTCGAGTCTGTTCTTGCGTC
TAAGAGCGATAAAAGCGAGATCTTCAGTTCACTTGGAGACATGGAGGCATCTCCTCTGGAGGTGAA
AATAGCGTTTAACTCAAAGGGCATTATCAACCAAGGCCTCATTAGTGTGAAGGATTCCTATTGTAGTA
ATCTCATTGTGAAGCAGATCGAAAACCGCTATAAAATTCTGAATAATAGTCTGAATCCTGCTATCAGC
GAGGACAATGACTTCAACACAACGACGAACACTTTTATCGACTCCATAATGGCCGAAGCTAATGCCG
ATAACGGGCGATTCATGATGGAGTTGGGTAAATACCTTAGAGTCGGGTTCTTTCCGGACGTGAAAAC
CACCATCAATCTGAGCGGTCCAGAGGCATATGCAGCCGCTTACCAGGATCTGTTGATGTTCAAAGAG
GGAAGCATGAACATTCACCTGATTGAAGCTGACTTGCGTAACTTTGAGATTTCCAAGACTAACATCA
GTCAGAGTACAGAGCAAGAGATGGCGTCACTGTGGTCCTTTGATGACGCAAGAGCAAAGGCTCAGT
TTGAGGAATACAAGCGGAATTACTTTGAGGGTTCCCTGGGCTCGAGATACCCATACGATGTGCCTGA
CTACGCTTGAGTCTAGAG

References

Abrams, G. D., Allo, M., Rifkin, G. D., Fekety, R., & Silva Jr., J. (1980). Mucosal damage mediated by clostridial toxin in experimental clindamycin-associated colitis. *Gut*, *21*(6), 493–499.

Abt, M. C., Lewis, B. B., Caballero, S., Xiong, H., Carter, R. A., Susac, B., … Pamer, E. G. (2015). Innate immune defenses mediated by two ilc subsets are critical for protection against acute clostridium difficile infection. *Cell Host and Microbe*, *18*(1), 27–37.

Abt, M. C., McKenney, P. T., & Pamer, E. G. (2016). Clostridium difficile colitis: pathogenesis and host defence. *Nature Reviews Microbiology*, *14*(10), 609–620.

Aghaallaei, N., Gruhl, F., Schaefer, C. Q., Wernet, T., Weinhardt, V., Centanin, L., … Wittbrodt, J. (2016). Identification, visualization and clonal analysis of intestinal stem cells in fish. *Development*, *143*(19), 3470–3480.

Agito, M. D., Atreja, A., & Rizk, M. K. (2013). Fecal microbiota transplantation for recurrent C difficile infection: Ready for prime time? *Cleveland Clinic Journal of Medicine*, *80*(2), 101–108.

Akitake, C. M., Macurak, M., Halpern, M. E., & Goll, M. G. (2011). Transgenerational analysis of transcriptional silencing in zebrafish. *Developmental Biology*, *352*(2), 191–201.

Aktories, K. (1997). Rho proteins: Targets for bacterial toxins. *Trends in Microbiology*, *5*(7), 282–288.

Aktories, K., Schwan, C., & Jank, T. (2017). Toxin Biology, (June), 281–307.

Al-shami, A., Mahanna, W., & Naccache, P. H. (1998). Signaling Pathways in Human Neutrophils : Signaling Pathways in Human Neutrophils. *The Journal of Biological Chemistry*, *273*(2), 1058–1063.

Allgaier, B., Shi, M., Luo, D. F., & Koenig, J. (1998). *Spontaneous and Fas-mediated apoptosis are diminished in umbilical cord blood neutrophils compared with adult neutrophils*. *Journal of leukocyte biology* (Vol. 64).

Alvarado-Kristensson, M., Melander, F., Leandersson, K., Rönnstrand, L., Wernstedt, C., & Andersson, T. (2004). p38-MAPK Signals Survival by Phosphorylation of Caspase-8 and Caspase-3 in Human Neutrophils. *The Journal of Experimental Medicine*, *199*(4), 449–458.

Alvarado-Kristensson, M., Pörn-Ares, M. I., Grethe, S., Smith, D., Zheng, L., & Andersson, T. (2001). p38 Mitogen-activated protein kinase and phosphatidylinositol 3-kinase activities have opposite effects on human neutrophil apoptosis. *The FASEB Journal*, *16*(1), 129–131.

Amulic, B., Cazalet, C., Hayes, G. L., Metzler, K. D., & Zychlinsky, A. (2012). Neutrophil Function: From Mechanisms to Disease. *Annual Review of Immunology*, *30*(1), 459–489.

Antunes, L. C. M., Han, J., Ferreira, R. B. R., Lolić, P., Borchers, C. H., & Finlay, B. B. (2011). Effect of antibiotic treatment on the intestinal metabolome. *Antimicrobial Agents and Chemotherapy*, *55*(4), 1494–1503.

Araujo, P. R., Yoon, K., Ko, D., Smith, A. D., Qiao, M., Suresh, U., … Penalva, L. O. F. (2012). Before it gets started: Regulating translation at the 5???; UTR. *Comparative and Functional Genomics*, *2012*.

Asimaki, A., Kapoor, S., Plovie, E., Arndt, A. K., Adams, E., Liu, Z., … Saffitz, J. E. (2015). HHS Public Access, *6*(240), 1–32.

Avdesh, A., Chen, M., Martin-Iverson, M. T., Mondal, A., Ong, D., Rainey-Smith, S., … Martins, R. N. (2012). Regular care and maintenance of a zebrafish (Danio rerio) laboratory: an introduction. *Journal of Visualized Experiments : JoVE*, (69), e4196.

Bäckhed, F., Ley, R. E., Sonnenburg, J. L., Peterson, D. A., & Gordon, J. I. (2005). Host-Bacterial Mutualism in the Human Intestine. *Science*, *307*(5717), 1915 LP-1920. Retrieved from http://science.sciencemag.org/content/307/5717/1915.abstract

Barbut, F., & Petit, J.-C. (2001). Epidemiology of Clostridium difficile-associated infections. *Clinical Microbiology and Infection*, *7*(8), 405–410.

Bardet, P. L., Kolahgar, G., Mynett, A., Miguel-Aliaga, I., Briscoe, J., Meier, P., & Vincent, J. P. (2008). A fluorescent reporter of caspase activity for live imaging. *Proc Natl Acad Sci U S A*, *105*(37), 13901–13905.

Barth, H., Pfeifer, G., Hofmann, F., Maier, E., Benz, R., & Aktories, K. (2001). Low ph-induced Formation of Ion Channels by Clostridium difficile Toxin B in Target Cells. *Journal of Biological Chemistry*, *276*(14), 10670–10676.

Bäumler, A. J., & Sperandio, V. (2016). Interactions between the microbiota and pathogenic bacteria in the gut. *Nature*, *535*(7610), 85–93.

Becker, N. A., Greiner, A. M., Peters, J. P., & Maher, L. J. (2014). Bacterial promoter repression by DNA looping without protein-protein binding competition. *Nucleic Acids Research*, *42*(9), 5495–5504.

Behr, M. a, Glaziou, P., Sismanidis, C., Floyd, K., Achkar, J. M., Chan, J., & Cooper, A. M. (2014). Animal Models of Tuberculosis : Zebrafish Animal Models of Tuberculosis : Zebrafish. *Cold Spring Harbor Laboratory Press*, 1–14.

Belkaid, Y., & Hand, T. W. (2014). Role of the microbiota in immunity and inflammation. *Cell*, *157*(1), 121–141.

Benard, E. L., van der Sar, A. M., Ellett, F., Lieschke, G. J., Spaink, H. P., & Meijer, A. H. (2012). Infection of Zebrafish Embryos with Intracellular Bacterial Pathogens. *Journal of Visualized Experiments*, (61), 1–8.

Bennett, C. M., Kanki, J. P., Rhodes, J., Liu, T. X., Paw, B. H., Kieran, M. W., … Look, a T. (2001). Myelopoiesis in the zebrafish, Danio rerio. *Blood*, *98*(3), 643–651.

Bertrand, J. Y., Kim, A. D., Violette, E. P., Stachura, D. L., Cisson, J. L., & Traver, D. (2007). Definitive hematopoiesis initiates through a committed erythromyeloid progenitor in the zebrafish embryo. *Development*, *134*(23), 4147–4156.

Best, E. L., Freeman, J., & Wilcox, M. H. (2012). Models for the study of Clostridium difficile infection. *Gut Microbes*, *3*(2), 145–167.

Bouza, E. (2012). Consequences of Clostridium difficile infection: Understanding the healthcare burden. *Clinical Microbiology and Infection*, *18*(SUPPL.6), 5–12.

Brandes, V., Schelle, I., Brinkmann, S., Schulz, F., Schwarz, J., Gerhard, R., & Genth, H. (2012). Protection from Clostridium difficile toxin B-catalysed Rac1/Cdc42 glucosylation by tauroursodeoxycholic acid-induced Rac1/Cdc42 phosphorylation. *Biological Chemistry*, *393*(1–2), 77–84.

Brito, G. A., Fujji, J., Carneiro-Filho, B. A., Lima, A. A. M., Obrig, T., & Guerrant, R. L. (2002). Mechanism of Clostridium difficile toxin A-induced apoptosis in T84 cells. *The Journal of Infectious Diseases*, *186*(10), 1438–1447.

Britton, R. A., & Young, V. B. (2012). Interaction between the intestinal microbiota and host in Clostridium difficile colonization resistance. *Trends in Microbiology*, *20*(7), 313–319.

Brizzi, M. F., Aronica, M. G., Rosso, A., Bagnara, G. P., Yarden, Y., & Pegoraro, L. (1996). Granulocyte-macrophage colony-stimulating factor stimulates JAK2 signaling pathway and rapidly activates p93fes, STAT1 p91, and STAT3 p92 in polymorphonuclear leukocytes. *Journal of Biological Chemistry*, *271*(7), 3562–3567.

Brugman, S. (2016). The zebrafish as a model to study intestinal inflammation. *Developmental and Comparative Immunology*, *64*, 82–92.

Buffie, C. G., Bucci, V., Stein, R. R., McKenney, P. T., Ling, L., Gobourne, A., … Pamer, E. G. (2014). Precision microbiome reconstitution restores bile acid mediated resistance to Clostridium difficile. *Nature*, *517*(7533), 205–208.

Buffie, C. G., Jarchum, I., Equinda, M., Lipuma, L., Gobourne, A., Viale, A., … Pamer, E. G. (2012). Profound alterations of intestinal microbiota following a single dose of clindamycin results in sustained susceptibility to Clostridium difficile-induced colitis. *Infection and Immunity*, *80*(1), 62–73.

Buffie, C. G., & Pamer, E. G. (2013). Microbiota-mediated colonization resistance against intestinal pathogens. *Nature Reviews Immunology*, *13*(11), 790–801.

Butala, M., Žgur-Bertok, D., & Busby, S. J. W. (2009). The bacterial LexA transcriptional repressor. *Cellular and Molecular Life Sciences*, *66*(1), 82–93.

Carling, P., Fung, T., Killion, A., Terrin, N., & Barza, M. (2003). Favorable Impact of a Multidisciplinary Antibiotic Management Program Conducted During 7 Years. *Infection Control & Hospital Epidemiology*, *24*(9), 699–706.

Carlson, P. E., Kaiser, A. M., Mccolm, S. A., Bauer, J. M., Vincent, B., Aronoff, D. M., & Hanna, P. C. (2016). Variation in germination of Clostridium difficile clinical isolates correlates to disease severity, 64–70.

Carter, G. P., Rood, J. I., & Lyras, D. (2010). The role of toxin A and toxin B in Clostridium difficile-associated disease. Past and present perspectives. *Nature*, *1*(1), 58–64.

Chang, B. D., & Roninson, I. B. (1996). Inducible retroviral vectors regulated by lac repressor in mammalian cells. *Gene*, *183*(1–2), 137–142.

Chattopadhyaya, R., & Pal, A. (2004). Improved Model of a LexA Repressor Dimer Bound to recA Operator. *Journal of Biomolecular Structure and Dynamics*, *21*(5), 681–689.

Chaves-Olarte, E., Weidmann, M., Von Eichel-Streiber, C., & Thelestam, M. (1997). Toxins A and B from Clostridium difficile differ with respect to enzymatic potencies, cellular substrate specificities, and surface binding to cultured cells. *Journal of Clinical Investigation*, *100*(7), 1734–1741.

Cheesman, S. E., Neal, J. T., Mittge, E., Seredick, B. M., & Guillemin, K. (2011). Epithelial cell proliferation in the developing zebrafish intestine is regulated by the Wnt pathway and microbial signaling via Myd88. *Proceedings of the National Academy of Sciences*, *108*(Supplement_1), 4570–4577.

Chen, X., Katchar, K., Goldsmith, J. D., Nanthakumar, N., Cheknis, A., Gerding, D. N., & Kelly, C. P. (2008a). A Mouse Model of Clostridium difficile-Associated Disease. *Gastroenterology*, *135*(6), 1984–1992.

Chen, X., Katchar, K., Goldsmith, J. D., Nanthakumar, N., Cheknis, A., Gerding, D. N., & Kelly, C.

P. (2008b). A Mouse Model of Clostridium difficile?Associated Disease. *Gastroenterology*, *135*(6), 1984–1992.

Chen, Y. Q., Sengchanthalangsy, L. L., Hackett, A., & Ghosh, G. (2000). NF-??B p65 (RelA) homodimer uses distinct mechanisms to recognize DNA targets. *Structure*, *8*(4), 419–428.

Chu, Y., Senghaas, N., Köster, R. W., Wurst, W., & Kühn, R. (2008). Novel Caspase-suicide proteins for tamoxifen-inducible apoptosis. *Genesis*, *46*(10), 530–536.

Chumbler, N. M., Farrow, M. A., Lapierre, L. A., Franklin, J. L., & Lacy, D. B. (2016). Clostridium difficile toxins TcdA and TcdB cause colonic tissue damage by distinct mechanisms. *Infection and Immunity*, *84*(10), 2871–2877.

Cocchiaro, J. L., & Rawls, J. F. (2013). Microgavage of Zebrafish Larvae. *Journal of Visualized Experiments*, (72), e4434.

Competition, L., Affects, D., & In, I. (2008). The Application of Phenotypic High-Throughput Screening Techniques to Cardiovascular Research, *86*(12), 3279–3288.

Cornely, O. A., Miller, M. A., Louie, T. J., Crook, D. W., & Gorbach, S. L. (2012). Treatment of first recurrence of clostridium difficile infection: Fidaxomicin versus vancomycin. *Clinical Infectious Diseases*, *55*(SUPPL.2), 154–161.

Costantini, C., & Cassatella, M. A. (2011). The defensive alliance between neutrophils and NK cells as a novel arm of innate immunity. *Journal of Leukocyte Biology*, *89*(2), 221–233.

Cournac, A., & Plumbridge, J. (2013). DNA Looping in Prokaryotes: Experimental and theoretical approaches. *Journal of Bacteriology*, *195*(6), 1109–1119.

Cowardin, C. A., Buonomo, E. L., Saleh, M. M., Wilson, M. G., Burgess, S. L., Kuehne, S. A., … Petri, W. A. (2016). The binary toxin CDT enhances Clostridium difficile virulence by suppressing protective colonic eosinophilia. *Nature Microbiology*, *1*(8), 16108.

Cowardin, C. A., Kuehne, S. A., Buonomo, E. L., Marie, C. S., Minton, N. P., & Petri, W. A. (2015). Inflammasome Activation Contributes to Interleukin-23 Production in Response to Clostridium difficile, *6*(1), 1–9.

Craggs, T. D. (2009). Green fluorescent protein: structure, folding and chromophore maturation. *Chemical Society Reviews*, *38*(10), 2865–2875.

Crawford, T., Huesgen, E., & Danziger, L. (2012). Fidaxomicin: A novel macrocyclic antibiotic for the treatment of Clostridium difficile infection. *American Journal of Health-System Pharmacy*, *69*(11), 933–943.

Cronin, C. A., Gluba, W., & Scrable, H. (2001). The lac operator-repressor system is functional

in the mouse. *Genes and Development*, *15*(12), 1506–1517.

Crosnier, C., Stamataki, D., & Lewis, J. (2006). Organizing cell renewal in the intestine: stem cells, signals and combinatorial control. *Nature Reviews Genetics*, *7*(5), 349–359.

Curado, S., Anderson, R. M., Jungblut, B., Mumm, J., Schroeter, E., & Stainier, D. Y. R. (2007). Conditional targeted cell ablation in zebrafish: A new tool for regeneration studies. *Developmental Dynamics*, *236*(4), 1025–1035.

Czuprynski, C. J., Johnson, W. J., Balish, E., & Wilkins, T. (1983). Pseudomembranous colitis in Clostridium difficile-monoassociated rats. *Infection and Immunity*, *39*(3), 1368–1376.

Dahlman-Wright, K., Wright, A., Gustafsson, J. Å., & Carlstedt-Duke, J. (1991). Interaction of the glucocorticoid receptor DNA-binding domain with DNA as a dimer is mediated by a short segment of five amino acids. *Journal of Biological Chemistry*, *266*(5), 3107–3112.

Daigle, I., & Simon, H. U. (2001). Critical role for caspases 3 and 8 in neutrophil but not eosinophil apoptosis. *International Archives of Allergy and Immunology*, *126*(2), 147–156.

Darkoh, C., Kaplan, H. B., & DuPont, H. L. (2011). Harnessing the glucosyltransferase activities of Clostridium difficile for functional studies of toxins A and B. *Journal of Clinical Microbiology*, *49*(8), 2933–2941.

Davis, D. M., & Dustin, M. L. (2004). What is the importance of the immunological synapse? *Trends in Immunology*, *25*(6), 323–327.

Davis, J. C., Furstenthal, L., Desai, A. A., Norris, T., Sutaria, S., Fleming, E., & Ma, P. (2009). The microeconomics of personalized medicine: today's challenge and tomorrow's promise. *Nature Reviews Drug Discovery*, *8*(4), 279–286.

Deakin, L. J., Clare, S., Fagan, R. P., Dawson, L. F., Pickard, D. J., West, M. R., … Lawley, T. D. (2012). The Clostridium difficile spo0A gene is a persistence and transmission factor. *Infection and Immunity*, *80*(8), 2704–2711.

Deans, T. L., Cantor, C. R., & Collins, J. J. (2007). A Tunable Genetic Switch Based on RNAi and Repressor Proteins for Regulating Gene Expression in Mammalian Cells. *Cell*, *130*(2), 363–372.

del Valle Rodríguez, A., Didiano, D., & Desplan, C. (2012). Power tools for gene expression and clonal analysis in Drosophila. *Nature Methods*, *9*(1), 47–55.

Deleo, F. R. (2004). Modulation of phagocyte apoptosis by bacterial pathogens, *9*(4), 399–413.

Delmée, M. (2001). Laboratory diagnosis of Clostridium difficile disease. *Clinical Microbiology and Infection*, *7*(8), 411–416.

Depestel, D. D., & Aronoff, D. M. (2013). Epidemiology of Clostridium difficile infection. *Journal of Pharmacy Practice*, *26*(5), 464–75.

Derouet, M., Thomas, L., Cross, A., Moots, R. J., & Edwards, S. W. (2004). Granulocyte macrophage colony-stimulating factor signaling and proteasome inhibition delay neutrophil apoptosis by increasing the stability of Mcl-1. *Journal of Biological Chemistry*, *279*(26), 26915–26921.

Di Bella, S., Ascenzi, P., Siarakas, S., Petrosillo, N., & di Masi, A. (2016). Clostridium difficile toxins A and B: Insights into pathogenic properties and extraintestinal effects. *Toxins*, *8*(5), 1–25.

Dmitrova, M., Younès-Cauet, G., Oertel-Buchheit, P., Porte, D., Schnarr, M., & Granger-Schnarr, M. (1998). A new LexA-based genetic system for monitoring and analyzing protein heterodimerization in Escherichia coli. *Molecular and General Genetics*, *257*(2), 205–212.

Dong, C., Jiang, L., Peng, W., Xu, J., Mahboob, S., Al-Ghanim, K. A., … Xu, P. (2015). Phylogenetic and evolutionary analyses of the frizzled gene family in common carp (Cyprinus carpio) provide insights into gene expansion from whole-genome duplications. *PLoS ONE*, *10*(12), 1–16.

Dowle, C. (2016). Review article Faecal microbiota transplantation : a review of FMT as an alternative treatment for Clostridium dif fi cile infection, *9*, 14.

Duffy, J. B. (2002). GAL4 system indrosophila: A fly geneticist's swiss army knife. *Genesis*, *34*(1–2), 1–15.

Dumoulin, P., Oertel-Buchheit, P., Granger-Schnarr, M., & Schnarr, M. (1993). Orientation of the LexA DNA-binding motif on operator DNA as inferred from cysteine-mediated phenyl azide crosslinking. *Proceedings of the National Academy of Sciences of the United States of America*, *90*(March), 2030–2034.

Dustin, M. L., & Baldari, C. T. (2017). The Immune Synapse: Past, Present, and Future. In C. T. Baldari & M. L. Dustin (Eds.), *The Immune Synapse: Methods and Protocols* (pp. 1–5). New York, NY: Springer New York.

Dustin, M. L., & Choudhuri, K. (2016). Signaling and Polarized Communication Across the T Cell Immunological Synapse. *Annual Review of Cell and Developmental Biology*, *32*(1), 303–325.

Dustin, M. L., & Sciences, M. (2015). The immunological synapse, *2*(11), 1023–1033.

Dzhagalov, I., John, A. S., He, Y., & Dc, W. (2012). The antiapoptotic protein Mcl-1 is essential

for the survival of neutrophils but not macrophages The antiapoptotic protein Mcl-1 is essential for the survival of neutrophils but not macrophages, *109*(4), 1620–1626.

Ebina, Y., Takahara, Y., Kishi, F., Nakazawa, A., Brent, R., & Brent, R. (1983). LexA protein is a repressor of the colicin LexA Protein Is a Repressor of the Colicin E l Gene *. *The Journal of Biological Chemistry*, *258*(21), 0–4.

Edamatsu, H., Kaziro, Y., & Itoh, H. (1997). Inducible high-level expression vector for mammalian cells, pEF-LAC carrying human elongation factor 1?? promoter and lac operator. *Gene*, *187*(2), 289–294.

Edwards, A. N., & Mcbride, S. M. (2014). Initiation of sporulation in Clostridium difficile: A twist on the classic model. *FEMS Microbiology Letters*, *358*(2), 110–118.

Edwards, A. N., Tamayo, R., & McBride, S. M. (2016). A novel regulator controls Clostridium difficile sporulation, motility and toxin production. *Molecular Microbiology*, *100*(6), 954–971.

Egerer, M., Giesemann, T., Jank, T., Fullner Satchell, K. J., & Aktories, K. (2007). Auto-catalytic cleavage of Clostridium difficile toxins A and B depends on cysteine protease activity. *Journal of Biological Chemistry*, *282*(35), 25314–25321.

Ellett, F., Pase, L., Hayman, J. W., Andrianopoulos, A., & Lieschke, G. J. (2011). Mpeg1 Promoter Transgenes Direct Macrophage-Lineage Expression in Zebrafish. *Blood*, *117*(4), e49-56.

Elmore, S. (2007). Apoptosis: A Review of Programmed Cell Death. *Toxicologic Pathology*, *35*(4), 495–516.

Emelyanov, A., & Parinov, S. (2008). Mifepristone-inducible LexPR system to drive and control gene expression in transgenic zebrafish. *Developmental Biology*, *320*(1), 113–121.

Etienne-Manneville, S., & Hall, A. (2002). Rho GTPases in cell biology. *Nature*, *420*(6916), 629–635.

Evason, K. J., Francisco, M. T., Juric, V., Balakrishnan, S., Lopez Pazmino, M. del P., Gordan, J. D., … Stainier, D. Y. R. (2015). Identification of Chemical Inhibitors of β-Catenin-Driven Liver Tumorigenesis in Zebrafish. *PLoS Genetics*, *11*(7), 1–32.

Faro, A., Boj, S. F. S. F., Ambrósio, R., van Den Broek, O., Korving, J., & Clevers, H. (2009). T-Cell Factor 4 (tcf7l2) Is the Main Effector of Wnt Signaling During Zebrafish Intestine Organogenesis. *Zebrafish*, *6*(1), 59–68.

Farrow, M. A., Chumbler, N. M., Lapierre, L. A., Franklin, J. L., Rutherford, S. A., Goldenring, J. R., & Lacy, D. B. (2013). Clostridium difficile toxin B-induced necrosis is mediated by the

host epithelial cell NADPH oxidase complex. *Proceedings of the National Academy of Sciences of the United States of America*, *110*(46), 18674–9.

Ferreira, R. B. R., Gill, N., Willing, B. P., Antunes, L. C. M., Russell, S. L., Croxen, M. A., & Finlay, B. B. (2011). The intestinal microbiota plays a role in salmonella-induced colitis independent of pathogen colonization. *PLoS ONE*, *6*(5).

Figueroa, I., Johnson, S., Sambol, S. P., Goldstein, E. J. C., Citron, D. M., & Gerding, D. N. (2012). Relapse versus reinfection: Recurrent clostridium difficile infection following treatment with fidaxomicin or vancomycin. *Clinical Infectious Diseases*, *55*(SUPPL.2), 104–109.

Fiorentini, C., Fabbri, a, Falzano, L., Fattorossi, a, Matarrese, P., Rivabene, R., & Donelli, G. (1998). Clostridium difficile toxin B induces apoptosis in intestinal cultured cells. *Infection and Immunity*, *66*(6), 2660–2665.

Fox, S., Leitch, A. E., Duffin, R., Haslett, C., & Rossi, A. G. (2010). Neutrophil apoptosis: Relevance to the innate immune response and inflammatory disease. *Journal of Innate Immunity*, *2*(3), 216–227.

Francis, M. B., Allen, C. A., Shrestha, R., & Sorg, J. A. (2013). Bile Acid Recognition by the Clostridium difficile Germinant Receptor, CspC, Is Important for Establishing Infection. *PLoS Pathogens*, *9*(5).

Freeman, J., Bauer, M. P., Baines, S. D., Corver, J., Fawley, W. N., Goorhuis, B., … Wilcox, M. H. (2010). The changing epidemiology of Clostridium difficile infections. *Clinical Microbiology Reviews*, *23*(3), 529–549.

Furze, R. C., & Rankin, S. M. (2008). The role of the bone marrow in neutrophil clearance under homeostatic conditions in the mouse. *The FASEB Journal*, *22*(9), 3111–3119.

Gao, W., Yang, J., Liu, W., Wang, Y., & Shao, F. (2016). Site-specific phosphorylation and microtubule dynamics control Pyrin inflammasome activation. *Proceedings of the National Academy of Sciences*, *113*(33), E4857–E4866.

Gasmi, L., McLennan, a G., & Edwards, S. W. (1996). The diadenosine polyphosphates Ap3A and Ap4A and adenosine triphosphate interact with granulocyte-macrophage colony-stimulating factor to delay neutrophil apoptosis: implications for neutrophil: platelet interactions during inflammation. *Blood*, *87*(8), 3442–9. Retrieved from http://www.bloodjournal.org/content/87/8/3442.abstract

Gaston, K., & Jayaraman, P. S. (2003). Transcriptional repression in eukaryotes: Repressors and repression mechanisms. *Cellular and Molecular Life Sciences*, *60*(4), 721–741.

Geering, B., Gurzeler, U., Federzoni, E., Kaufmann, T., Simon, H., Dc, W., … Simon, H. (2012). A novel TNFR1-triggered apoptosis pathway mediated by class IA PI3Ks in neutrophils A novel TNFR1-triggered apoptosis pathway mediated by class IA PI3Ks in neutrophils, *117*(D), 5953–5962.

Geering, B., & Simon, H.-U. (2011). Peculiarities of cell death mechanisms in neutrophils. *Cell Death and Differentiation*, *18*(9), 1457–1469.

Geissmann, F., Manz, M. G., Jung, S., Sieweke, M. H., & Ley, K. (2010). Development of monocytes, macrophages and dendritic cells. *Science*, *327*(5966), 656–661.

Genisyuerek, S., Papatheodorou, P., Guttenberg, G., Schubert, R., Benz, R., & Aktories, K. (2011). Structural determinants for membrane insertion, pore formation and translocation of Clostridium difficile toxin B. *Molecular Microbiology*, *79*(6), 1643–1654.

George, W. L., Sutter, V. L., & Citron, D. (1979). Selective and differential medium for isolation of Selective and Differential Medium for Isolation of Clostridium difficile. *Journal of Clinical Microbiology*, *9*(2), 214–219.

Gerdes, H. H., Rustom, A., & Wang, X. (2013). Tunneling nanotubes, an emerging intercellular communication route in development. *Mechanisms of Development*, *130*(6–8), 381–387.

Gerding, D. N., Johnson, S., Rupnik, M., & Aktories, K. (2014). Clostridium difficile binary toxin CDT: mechanism, epidemiology, and potential clinical importance. *Gut Microbes*, *5*(1), 15–27.

Gerhard, R., Nottrott, S., Schoentaube, J., Tatge, H., Oiling, A., & Just, I. (2008). Glucosylation of Rho GTPases by Clostridium difficile toxin A triggers apoptosis in intestinal epithelial cells. *Journal of Medical Microbiology*, *57*(6), 765–770.

Glickman, N. S., & Yelon, D. (2002). Cardiac development in zebrafish: coordination of form and function. *Seminars in Cell & Developmental Biology*, *13*(6), 507–513.

Godson, C., Mitchell, S., Harvey, K., Petasis, N. A., Hogg, N., & Brady, H. R. (2000). Lipoxins rapidly stimulate nonphlogistic phagocytosis of apoptotic neutrophils by monocyte-derived macrophages. *Journal of Immunology (Baltimore, Md. : 1950)*, *164*(4), 1663–1667.

Goessling, W., North, T. E., & Zon, L. I. (2007). New waves of discovery: Modeling cancer in zebrafish. *Journal of Clinical Oncology*, *25*(17), 2473–2479.

Goll, M. G., Anderson, R., Stainier, D. Y. R., Spradling, A. C., & Halpern, M. E. (2009). Transcriptional silencing and reactivation in transgenic zebrafish. *Genetics*, *182*(3), 747–

755.

Goorhuis, A., Bakker, D., Corver, J., Debast, S. B., Harmanus, C., Notermans, D. W., … Kuijper, E. J. (2008). Emergence of *Clostridium difficile* Infection Due to a New Hypervirulent Strain, Polymerase Chain Reaction Ribotype 078. *Clinical Infectious Diseases*, *47*(9), 1162–1170.

Gordon, S., & Taylor, P. R. (2005). Monocyte and macrophage heterogeneity. *Nature Reviews. Immunology*, *5*(12), 953–64.

Gough, E., Shaikh, H., & Manges, A. R. (2011). Systematic review of intestinal microbiota transplantation (fecal bacteriotherapy) for recurrent clostridium difficile infection. *Clinical Infectious Diseases*, *53*(10), 994–1002.

Gutierrez, A., Grebliunaite, R., Feng, H., Kozakewich, E., Zhu, S., Guo, F., … Look, A. T. (2011). Pten mediates Myc oncogene dependence in a conditional zebrafish model of T cell acute lymphoblastic leukemia. *The Journal of Experimental Medicine*, *208*(8), 1595–1603.

Gutierrez, A., Pan, L., Groen, R. W. J., Baleydier, F., Kentsis, A., Marineau, J., … Aster, J. C. (2014). Phenothiazines induce PP2A-mediated apoptosis in T cell acute lymphoblastic leukemia. *Journal of Clinical Investigations*, *124*(2).

Habas, R., Dawid, I. B., & He, X. (2003). Coactivation of Rac and Rho by Wnt/Frizzled signaling is required for vertebrate gastrulation. *Genes and Development*, *17*(2), 295–309.

Hagedorn, E. J., Durand, E. M., Fast, E. M., & Zon, L. I. (2014). Getting more for your marrow: Boosting hematopoietic stem cell numbers with PGE2. *Experimental Cell Research*, *329*(2), 220–226.

Hall, A. (2012). Rho family GTPases. *Biochemical Society Transactions*, *40*(6), 1378–82.

Halpern, M. E., Rhee, J., Goll, M. G., Akitake, C. M., Parsons, M., & Leach, S. D. (2008). Gal4/UAS transgenic tools and their application to zebrafish. *Zebrafish*, *5*(2), 97–110.

Hamilton, J. A. (2002). GM-CSF in inflammation and autoimmunity. *Trends in Immunology*, *23*(8), 403–408.

Hamm, E. E., Voth, D. E., & Ballard, J. D. (2006). Identification of Clostridium difficile toxin B cardiotoxicity using a zebrafish embryo model of intoxication. *Proceedings of the National Academy of Sciences of the United States of America*, *103*(38), 14176–81.

Hanna-Rose, W., & Hansen, U. (1996). Active repression mechanisms of eukaryotic transcription repressors. *Trends in Genetics*, *12*(6), 229–234.

Hanna, N., Vasquez, P., Pham, P., Heck, D. E., Laskin, J. D., Laskin, D. L., & Weinberger, B. (2005). Mechanisms underlying reduced apoptosis in neonatal neutrophils. *Pediatric Research*,

57(1), 56–62.

Hanyang, L., Xuanzhe, L., Xuyang, C., Yujia, Q., Jiarong, F., Jun, S., & Zhihua, R. (2017). Application of zebrafish models in inflammatory bowel disease. *Frontiers in Immunology*, *8*(MAY).

Hao, J., Ao, A., Zhou, L., Murphy, C. K., Frist, A. Y., Keel, J. J., … Hong, C. C. (2013). Selective small molecule targeting β-catenin function discovered by in vivo chemical genetic screen. *Cell Reports*, *4*(5), 898–904.

Hasegawa, M., Kamada, N., & Jiao, Y. (2017). Protective Role of Commensals against Clostridium difficile Infection via an IL-1 β − Mediated Positive-Feedback Loop.

Hasegawa, M., Yamazaki, T., Kamada, N., Tawaratsumida, K., Kim, Y.-G., Núñez, G., & Inohara, N. (2011). Nucleotide-binding oligomerization domain 1 mediates recognition of Clostridium difficile and induces neutrophil recruitment and protection against the pathogen. *Journal of Immunology (Baltimore, Md. : 1950)*, *186*(8), 4872–80.

Heeg, D., Burns, D. A., Cartman, S. T., & Minton, N. P. (2012). Spores of clostridium difficile clinical isolates display a diverse germination response to bile salts. *PLoS ONE*, *7*(2).

Hernandez, L. D., Kroh, H. K., Hsieh, E., Yang, X., Beaumont, M., Sheth, P. R., … Therien, A. G. (2017). Epitopes and Mechanism of Action of the Clostridium difficile Toxin A-Neutralizing Antibody Actoxumab. *Journal of Molecular Biology*, *429*(7), 1030–1044.

Hickson, M. (2011). Probiotics in the prevention of antibiotic-associated diarrhoea and Clostridium difficile infection. *Therapeutic Advances in Gastroenterology*, *4*(3), 185–97.

Hippenstiel, S., Schmeck, B., N'Guessan, P. D., Seybold, J., Krüll, M., Preissner, K., … Suttorp, N. (2002). Rho protein inactivation induced apoptosis of cultured human endothelial cells. *American Journal of Physiology - Lung Cellular and Molecular Physiology*, *283*(4), L830–L838.

Hirota, S. A., Iablokov, V., Tulk, S. E., Schenck, L. P., Becker, H., Nguyen, J., … Beck, P. L. (2012). Intrarectal instillation of clostridium difficile toxin a triggers colonic inflammation and tissue damage: Development of a novel and efficient mouse model of clostridium difficile toxin exposure. *Infection and Immunity*, *80*(12), 4474–4484.

Ho, J. G. S., Greco, A., Rupnik, M., & Ng, K. K.-S. (2005). Crystal structure of receptor-binding C-terminal repeats from < i >Clostridium difficile< /i > toxin A. *Proceedings of the National Academy of Sciences of the United States of America*, *102*(51), 18373–8.

Ho, T. D., & Ellermeier, C. D. (2015). Ferric uptake regulator fur control of putative iron

acquisition systems in Clostridium difficile. *Journal of Bacteriology*, *197*(18), 2930–2940.

Hofmann, F., Busch, C., Just, I., Aktories, K., & Prepens, U. (1997). Cell Biology and Metabolism : Localization of the Glucosyltransferase Activity of Clostridium difficile Toxin B to the N-terminal Part of the Holotoxin Localization of the Glucosyltransferase Activity of Clostridium difficile Toxin B to the N-terminal Par. *Journal of Biological Chemistry*, *272*(17), 11074–11078.

Holmgren, J., & Czerkinsky, C. (2005). Mucosal immunity and vaccines. *Nature Medicine*, *11*(4 Suppl), S45-53.

Holý, O., & Chmelař, D. (2012). Oxygen tolerance in anaerobic pathogenic bacteria. *Folia Microbiologica*, *57*(5), 443–446.

Hong, S. K., & Dawid, I. B. (2008). Alpha2 macroglobulin-like is essential for liver development in zebrafish. *PLoS ONE*, *3*(11).

Hoodless, L. J., Lucas, C. D., Duffin, R., Denvir, M. A., Haslett, C., Tucker, C. S., & Rossi, A. G. (2016). Genetic and pharmacological inhibition of CDK9 drives neutrophil apoptosis to resolve inflammation in zebrafish in vivo. *Scientific Reports*, *5*(1), 36980.

Hooper, L. V, Littman, D. R., & Macpherson, A. J. (2012). Interactions Between the Microbiota and the Immune System. *Science*, *336*(6086), 1268 LP-1273. Retrieved from http://science.sciencemag.org/content/336/6086/1268.abstract

Howe, K., Clark, M. D., Torroja, C. F., Torrance, J., Berthelot, C., Muffato, M., … Stemple, D. L. (2013). The zebrafish reference genome sequence and its relationship to the human genome. *Nature*, *496*(7446), 498–503.

Hu, Y., Dietrich, D., Xu, W., Patel, A., Thuss, J. A. J., Wang, J., … Tang, Y. (2014). Visnagin protects against doxorubicin-induced cardiomyopathy through modulation of mitochondrial malate dehydrogenase. *Nat Chem Biol.*, *10*(7), 552–554.

Huang, A. M., Marini, B. L., Frame, D., Aronoff, D. M., & Nagel, J. L. (2014). Risk factors for recurrent Clostridium difficile infection in hematopoietic stem cell transplant recipients. *Transplant Infectious Disease*, *16*(5), 744–750.

Huang, H.-C., & Klein, P. S. (2004). The Frizzled family: receptors for multiple signal transduction pathways. *Genome Biology*, *5*(7), 234.

Huelsenbeck, J., Dreger, S., Gerhard, R., Barth, H., Just, I., & Genth, H. (2007). Difference in the cytotoxic effects of toxin B from Clostridium difficile strain VPI 10463 and toxin B from variant Clostridium difficile strain 1470. *Infection and Immunity*, *75*(2), 801–809.

Hughes, J. P., Rees, S. S., Kalindjian, S. B., & Philpott, K. L. (2011). Principles of early drug discovery. *British Journal of Pharmacology*, *162*(6), 1239–1249.

Huiting, L. N., Laroche, F., & Feng, H. (2015). The Zebrafish as a Tool to Cancer Drug Discovery. *Austin Journal of Pharmacology and Therapeutics*, *3*(2), 1069. Retrieved from http://www.pubmedcentral.nih.gov/articlerender.fcgi?artid=4731041&tool=pmcentrez&rendertype=abstract

Hussain, H. A., Roberts, A. P., & Mullany, P. (2005). Generation of an erythromycin-sensitive derivative of Clostridium difficile strain 630 (630Δerm) and demonstration that the conjugative transposon Tn916ΔE enters the genome of this strain at multiple sites. *Journal of Medical Microbiology*, *54*(2), 137–141.

Hutton, M. L., Mackin, K. E., Chakravorty, A., & Lyras, D. (2014). Small animal models for the study of Clostridium difficile disease pathogenesis. *FEMS Microbiology Letters*, *352*(2), 140–149.

Inagaki, T., Moschetta, A., Lee, Y.-K., Peng, L., Zhao, G., Downes, M., … Kliewer, S. A. (2006). Regulation of antibacterial defense in the small intestine by the nuclear bile acid receptor. *Proceedings of the National Academy of Sciences*, *103*(10), 3920–3925.

Inui, M., Ishida, Y., Kimura, A., Kuninaka, Y., Mukaida, N., & Kondo, T. (2011). Protective roles of CX3CR1-mediated signals in toxin A-induced enteritis through the induction of heme oxygenase-1 expression. *Journal of Immunology (Baltimore, Md. : 1950)*, *186*(1), 423–31.

Jafari, N. V., Kuehne, S. A., Bryant, C. E., Elawad, M., Wren, B. W., Minton, N. P., … Bajaj-Elliott, M. (2013). Clostridium difficile Modulates Host Innate Immunity via Toxin-Independent and Dependent Mechanism(s). *PLoS ONE*, *8*(7), 1–10.

Jagannathan-Bogdan, M., & Zon, L. I. (2013). Hematopoiesis. *Development*, *140*(12), 2463–2467.

Jank, T., & Aktories, K. (2008). Structure and mode of action of clostridial glucosylating toxins: the ABCD model. *Trends in Microbiology*, *16*(5), 222–229.

Jank, T., Giesemann, T., & Aktories, K. (2007). Rho-glucosylating Clostridium difficile toxins A and B : new insights into structure and function, *17*(4), 15–22.

Jarchum, I., Liu, M., Shi, C., Equinda, M., & Pamer, E. G. (2012). Critical role for myd88-Mediated Neutrophil recruitment during Clostridium difficile colitis. *Infection and Immunity*, *80*(9), 2989–2996.

Jin, H., Sood, R., Xu, J., Zhen, F., English, M. a, Liu, P. P., & Wen, Z. (2009). Definitive

hematopoietic stem/progenitor cells manifest distinct differentiation output in the zebrafish VDA and PBI. *Development (Cambridge, England)*, *136*(4), 647–654.

Jin, S., Sarkar, K. S., Jin, Y. N., Liu, Y., Kokel, D., Van Ham, T. J., … Peterson, R. T. (2013). An in vivo zebrafish screen identifies organophosphate antidotes with diverse mechanisms of action. *Journal of Biomolecular Screening*, *18*(1), 108–15.

Johal, S. S., Lambert, C. P., Hammond, J., James, P. D., Borriello, S. P., & Mahida, Y. R. (2004). Colonic IgA producing cells and macrophages are reduced in recurrent and non-recurrent Clostridiumdifficile associated diarrhoea. *Journal of Clinical Pathology*, *57*(9), 973–979.

Johansson, M. E. V, Gustafsson, J. K., Sjöberg, K. E., Petersson, J., Holm, L., Sjövall, H., & Hansson, G. C. (2010). Bacteria penetrate the inner mucus layer before inflammation in the dextran sulfate colitis model. *PLoS ONE*, *5*(8).

Jose, S., & Madan, R. (2016). Neutrophil-mediated inflammation in the pathogenesis of Clostridium difficile infections. *Anaerobe*, *41*, 85–90.

Juven-Gershon, T., Cheng, S., & Kadonaga, J. T. (2006). Rational design of a super core promoter that enhances gene expression. *Nature Methods*, *3*(11), 917–922.

Keel, M., Ungethüm, U., Steckholzer, U., Niederer, E., Hartung, T., Trentz, O., & Ertel, W. (1997). Interleukin-10 counterregulates proinflammatory cytokine-induced inhibition of neutrophil apoptosis during severe sepsis. *Blood*, *90*(9), 3356–3363.

Kelly, C. P., Becker, S., Linevsky, J. K., Joshi, M. A., O'Keane, J. C., Dickey, B. F., … Pothoulakis, C. (1994). Neutrophil recruitment in Clostridium difficile toxin A enteritis in the rabbit. *Journal of Clinical Investigation*, *93*(3), 1257–1265.

Kelly, C. P., & Kyne, L. (2011). The host immune response to Clostridium difficile. *Journal of Medical Microbiology*, *60*(8), 1070–1079.

Killgore, G., Thompson, A., Johnson, S., Brazier, J., Kuijper, E., Pepin, J., … McDonald, L. C. (2008). Comparison of seven techniques for typing international epidemic strains of Clostridium difficile: Restriction endonuclease analysis, pulsed-field gel electrophoresis, PCR-ribotyping, multilocus sequence typing, multilocus variable-number tandem-repeat an. *Journal of Clinical Microbiology*, *46*(2), 431–437.

Kim, B., & Little, J. W. (1992). Dimerization of a specific DNA-binding protein on the DNA. *Science (New York, N.Y.)*, *255*(5041), 203–206.

Kim, J. H., Lee, S. R., Li, L. H., Park, H. J., Park, J. H., Lee, K. Y., … Choi, S. Y. (2011). High cleavage efficiency of a 2A peptide derived from porcine teschovirus-1 in human cell lines,

zebrafish and mice. *PLoS ONE*, *6*(4), 1–8.

Kimmel, C. B., Ballard, W. W., Kimmel, S. R., Ullmann, B., & Schilling, T. F. (1995). Stages of embryonic development of the zebrafish. *Developmental Dynamics*, *203*(3), 253–310.

Kociolek, L. K., & Gerding, D. N. (2016). Breakthroughs in the treatment and prevention of Clostridium difficile infection. *Nature Reviews. Gastroenterology & Hepatology*, *13*(3), 150–60.

Kokel, D., Bryan, J., Laggner, C., White, R., Cheung, C. Y. J., Mateus, R., … Peterson, R. T. (2010). Rapid behavior-based identification of neuroactive small molecules in the zebrafish. *Nature Chemical Biology*, *6*(3), 231–237.

Koon, H. W., Shih, D. Q., Hing, T. C., Yoo, J. H., Ho, S., Chen, X., … Pothoulakis, C. (2013). Human monoclonal antibodies against Clostridium difficile toxins A and B inhibit inflammatory and histologic responses to the toxins in human colon and peripheral blood monocytes. *Antimicrobial Agents and Chemotherapy*, *57*(7), 3214–3223.

Korsmeyer, S. J., Wei, M. C., Saito, M., Weiler, S., Oh, K. J., & Schlesinger, P. H. (2000). Pro-apoptotic cascade activates BID, which oligomerizes BAK or BAX into pores that result in the release of cytochrome c. *Cell Death and Differentiation*, *7*(12), 1166–1173.

Kyne, L., Warny, M., Qamar, a, & Kelly, C. P. (2000). Asymptomatic carriage of Clostridium difficile and serum levels of IgG antibody against toxin A. *The New England Journal of Medicine*, *342*(6), 390–397.

LaFrance, M. E., Farrow, M. a., Chandrasekaran, R., Sheng, J., Rubin, D. H., & Lacy, D. B. (2015). Identification of an epithelial cell receptor responsible for *Clostridium difficile* TcdB-induced cytotoxicity. *Proceedings of the National Academy of Sciences*, *112*(22), 7073–7078.

Lagier, J.-C. (2016). Gut microbiota and Clostridium difficile infections. *Human Microbiome Journal*, *2*(November), 10–14.

Lahoz-Beneytez, J., Elemans, M., Zhang, Y., Ahmed, R., Salam, A., Block, M., … Macallan, D. (2016). Human neutrophil kinetics: Modeling of stable isotope labeling data supports short blood neutrophil half-lives. *Blood*, *127*(26), 3431–3438.

Lai, S.-L., & Lee, T. (2006). Genetic mosaic with dual binary transcriptional systems in Drosophila. *Nature Neuroscience*, *9*(5), 703–9.

Laing, K. J., Purcell, M. K., Winton, J. R., & Hansen, J. D. (2008). A genomic view of the NOD-like receptor family in teleost fish: identification of a novel NLR subfamily in zebrafish.

BMC Evolutionary Biology, *8*(1), 42.

Lawley, T. D., Clare, S., Walker, A. W., Goulding, D., Stabler, R. A., Croucher, N., … Dougan, G. (2009). Antibiotic treatment of Clostridium difficile carrier mice triggers a supershedder state, spore-mediated transmission, and severe disease in immunocompromised hosts. *Infection and Immunity*, *77*(9), 3661–3669.

Lawley, T. D., Croucher, N. J., Yu, L., Clare, S., Sebaihia, M., Goulding, D., … Dougan, G. (2009). Proteomic and genomic characterization of highly infectious Clostridium difficile 630 spores. *Journal of Bacteriology*, *191*(17), 5377–5386.

Leber, A., Viladomiu, M., Hontecillas, R., Abedi, V., Philipson, C., Hoops, S., … Bassaganya-Riera, J. (2015). Systems modeling of interactions between mucosal immunity and the gut microbiome during Clostridium difficile infection. *PLoS ONE*, *10*(7), 1–19.

Lee, a, Whyte, M. K., & Haslett, C. (1993). Inhibition of apoptosis and prolongation of neutrophil functional longevity by inflammatory mediators. *Journal of Leukocyte Biology*, *54*(4), 283–288.

Lee, S. M., Donaldson, G. P., Mikulski, Z., Boyajian, S., Ley, K., & Mazmanian, S. K. (2013). Bacterial colonization factors control specificity and stability of the gut microbiota. *Nature*, *501*(7467), 426–429.

Leitch, a E., Duffin, R., Haslett, C., & Rossi, a G. (2008). Relevance of granulocyte apoptosis to resolution of inflammation at the respiratory mucosa. *Mucosal Immunology*, *1*(5), 350–363.

Leong, C., & Zelenitsky, S. (2013). Treatment Strategies for Recurrent Clostridium difficile Infection. *The Canadian Journal of Hospital Pharmacy*, *66*(6), 361–8.

Lessa, F. C., Gould, C. V., & Clifford McDonald, L. (2012). Current status of clostridium difficile infection epidemiology. *Clinical Infectious Diseases*, *55*(SUPPL.2), 65–70.

Liao, F., Xu, H., Torrey, N., Road, P., & Jolla, L. (2015). HHS Public Access, *2*(74), 1–10.

Lieschke, G. J., & Currie, P. D. (2007). Animal models of human disease: zebrafish swim into view. *Nat Rev Genet*, *8*(5), 353–367. Retrieved from http://dx.doi.org/10.1038/nrg2091

Linevsky, J. K., Pothoulakis, C., Keates, S., Warny, M., Keates, A. C., Lamont, J. T., & Kelly, C. P. (1997). IL-8 release and neutrophil activation by Clostridium difficile toxin-exposed human monocytes. *The American Journal of Physiology*, *273*(6 Pt 1), G1333-40. Retrieved from http://www.ncbi.nlm.nih.gov/pubmed/9435559

Little, J. W. (1991). Mechanism of specific LexA cleavage: Autodigestion and the role of RecA

coprotease. *Biochimie*, *73*(4), 411–421.

Little, J. W., & Mount, D. W. (1982). The SOS regulatory system of Escherichia coli. *Cell*, *29*(1), 11–22.

Littlewood, T. D., Hancock, D. C., Danielianl, P. S., Parker, M. G., & Evan, G. (1995). A modified oestrogen receptor ligand-binding domain as an improved switch for the regulation of heterologous proteins, *23*(27), 1686–1690.

Longo, D. L., Leffler, D. A., & Lamont, J. T. (2015). *Clostridium difficile* Infection. *New England Journal of Medicine*, *372*(16), 1539–1548.

Lowy Israel, S. A., Kramer, M. R., & Narayan, K. M. V. (2010). Treatment with Monoclonal Antibodies against Clostridium difficile Toxins. *New England Journal of Medicine*, *370*(5), 403–411.

Lucas, C. D., Dorward, D. A., Tait, M. A., Fox, S., Marwick, J. A., Allen, K. C., … Rossi, A. G. (2014). Downregulation of Mcl-1 has anti-inflammatory pro-resolution effects and enhances bacterial clearance from the lung. *Mucosal Immunology*, *7*(4), 857–868.

Macarron, R., Banks, M. N., Bojanic, D., Burns, D. J., Cirovic, D. A., Garyantes, T., … Schopfer, U. (2011). Impact of high-throughput screening. *Nature*, *10*(March 2011), 188–195.

MacDonald, B. T., Tamai, K., & He, X. (2009). Wnt/β-Catenin Signaling: Components, Mechanisms, and Diseases. *Developmental Cell*, *17*(1), 9–26.

MacRae, C. A., & Peterson, R. T. (2015). Zebrafish as tools for drug discovery. *Nature Reviews Drug Discovery*, *14*(10), 721–731.

Madan, R., & Petri, W. A. (2012). Immune responses to Clostridium difficile infection. *Trends in Molecular Medicine*, *18*(11), 658–666.

Magnarin, M., Spessotto, P., Soranzo, M. R., Pontillo, A., & Zabucchi, G. (2000). Human neutrophils specifically interact with human monocyte-derived macrophage monolayers. *Inflammation*, *24*(1), 89–98.

Mahamed, D., Boulle, M., Ganga, Y., Mc Arthur, C., Skroch, S., Oom, L., … Sigal, A. (2017). Intracellular growth of Mycobacterium tuberculosis after macrophage cell death leads to serial killing of host cells. *ELife*, *6*, 1–26.

Mahida, Y. R., Galvin, a, Makh, S., Hyde, S., Sanfilippo, L., Borriello, P., & Sewell, H. F. (1998). Effect of Clostridium difficile Toxin A on Human Colonic Lamina Propria Cells : Early Loss of Macrophages Followed by T-Cell Apoptosis Effect of Clostridium difficile Toxin A on Human Colonic Lamina Propria Cells : Early Loss of Macrophages Followed by T-. *Infection*

and Immunity, *66*(11), 5462.

Maianski, N. A., Maianski, A. N., Kuijpers, T. W., & Roos, D. (2004). Apoptosis of neutrophils. *Acta Haematologica*, *111*(1–2), 56–66.

Maiden, M. C. J. (2006). Multilocus sequence typing of bacteria. *Annu Rev Microbiol*, *60*, 561–88.

Mani, N., & Dupuy, B. (2001). Regulation of toxin synthesis in Clostridium difficile by an alternative RNA polymerase sigma factor. *Proceedings of the National Academy of Sciences of the United States of America*, *98*(10), 5844–5849.

Marjoram, L., & Bagnat, M. (2015). Infection, Inflammation and Healing in Zebrafish: Intestinal Inflammation. *Current Pathobiology Reports*, *3*(2), 147–153.

Masumoto, J., Zhou, W., Chen, F. F., Su, F., Kuwada, J. Y., Hidaka, E., … Inohara, N. (2003). Caspy, a zebrafish caspase, activated by ASC oligomerization is required for pharyngeal arch development. *Journal of Biological Chemistry*, *278*(6), 4268–4276.

Matarrese, P., Falzano, L., Fabbri, A., Gambardella, L., Frank, C., Geny, B., … Fiorentini, C. (2007). Clostridium difficile toxin B causes apoptosis in epithelial cells by thrilling mitochondria: Involvement of ATP-sensitive mitochondrial potassium channels. *Journal of Biological Chemistry*, *282*(12), 9029–9041.

Mathias, J. R., Saxena, M. T., & Mumm, J. S. (2012). Advances in zebrafish chemical screening technologies. *Future Medicinal Chemistry*, *4*(14), 1811–1822.

Mazaheri, F., Breus, O., Durdu, S., Haas, P., Wittbrodt, J., Gilmour, D., & Peri, F. (2014). Distinct roles for BAI1 and TIM-4 in the engulfment of dying neurons by microglia. *Nature Communications*, *5*(May), 4046.

McCoy-Simandle, K., Hanna, S. J., & Cox, D. (2016). Exosomes and nanotubes: Control of immune cell communication. *The International Journal of Biochemistry & Cell Biology*, *71*, 44–54.

McCracken, J. M., & Allen, L.-A. H. (2014). Regulation of Human Neutrophil Apoptosis in Health and Disease. *Journal of Cell Death*, *7*, 15–23.

McDermott, A. J., Falkowski, N. R., McDonald, R. A., Pandit, C. R., Young, V. B., & Huffnagle, G. B. (2016). Interleukin-23 (IL-23), independent of IL-17 and IL-22, drives neutrophil recruitment and innate inflammation during Clostridium difficile colitis in mice. *Immunology*, *147*(1), 114–124.

McFarland, L. V. (2009). Evidence-based review of probiotics for antibiotic-associated diarrhea

and Clostridium difficile infections. *Anaerobe*, *15*(6), 274–280.

Merrigan, M., Sambol, S., Johnson, S., & Gerding, D. (2003). Prevention of Fatal Clostridium difficile–Associated Disease during Continuous Administration of Clindamycin in Hamsters. *Journal of Infectious Diseases*, *188*, 1922–1927.

Metcalf, D., Avery, B. P., Janecko, N., Matic, N., Reid-Smith, R., & Weese, J. S. (2011). Clostridium difficile in seafood and fish. *Anaerobe*, *17*(2), 85–86.

Milligan-Myhre, K., Charette, J. R., Phennicie, R. T., Stephens, Z. W., Rawls, J. F., Guillemin, K., & Kim, C. H. (2011). *Study of host-microbiome interactions in zebrafish*. *Methods in Cell Biology* (Vol. 105).

Milot, E., & Filep, J. G. (2011). Regulation of Neutrophil Survival/Apoptosis by Mcl-1. *The Scientific World JOURNAL*, *11*, 1948–1962.

Mohana-Borges, R., Pacheco, A. B. F., Sousa, F. J. R., Foguel, D., Almeida, D. F., & Silva, J. L. (2000). LexA repressor forms stable dimers in solution. The role of specific DNA in tightening protein-protein interactions. *Journal of Biological Chemistry*, *275*(7), 4708–4712.

Morton, S. K., Chaston, D. J., Baillie, B. K., Hill, C. E., & Matthaei, K. I. (2014). Regulation of endothelial-specific transgene expression by the LacI repressor protein in vivo. *PLoS ONE*, *9*(4).

Mowat, A. M., & Bain, C. C. (2011). Mucosal Macrophages in Intestinal Homeostasis and Inflammation. *Journal of Innate Immunity*, *3*(6), 550–564.

Müller, J., Oehler, S., & Müller-Hill, B. (1996). Repression of lac Promoter as a Function of Distance, Phase and Quality of an Auxiliary lac Operator. *Journal of Molecular Biology*, *257*(1), 21–29.

Muller, W. A. (2003). Leukocyte–endothelial-cell interactions in leukocyte transmigration and the inflammatory response. *Trends in Immunology*, *24*(6), 326–333.

Munoz, L. E., Lauber, K., Schiller, M., Manfredi, A. A., & Herrmann, M. (2010). The role of defective clearance of apoptotic cells in systemic autoimmunity. *Nat Rev Rheumatol*, *6*(5), 280–289. Retrieved from http://dx.doi.org/10.1038/nrrheum.2010.46

Murayama, E., Kissa, K., Zapata, A., Mordelet, E., Briolat, V., Lin, H. F., … Herbomel, P. (2006). Tracing Hematopoietic Precursor Migration to Successive Hematopoietic Organs during Zebrafish Development. *Immunity*, *25*(6), 963–975.

Murphy, B. M., O'Neill, A. J., Adrain, C., Watson, R. W. G., & Martin, S. J. (2003). The

apoptosome pathway to caspase activation in primary human neutrophils exhibits dramatically reduced requirements for cytochrome C. *The Journal of Experimental Medicine*, *197*(5), 625–632.

Murray, P. J., & Wynn, T. a. (2011). Protective and pathogenic functions of macrophage subsets. *Nature Reviews Immunology*, *11*(11), 723–737.

Na, X., Kim, H., Moyer, M. P., Pothoulakis, C., & LaMont, J. T. (2008). gp96 is a human colonocyte plasma membrane binding protein for Clostridium difficile toxin A. *Infection and Immunity*, *76*(7), 2862–2871.

Nathan, C. (2002). Points of control in inflammation. *Nature*, *420*(6917), 846–852.

Nathan, C. (2006). Neutrophils and immunity: challenges and opportunities. *Nature Reviews Immunology*, *6*(3), 173–182.

Nathan, C., & Ding, A. (2010). Nonresolving Inflammation. *Cell*, *140*(6), 871–882.

Ng, J., Hirota, S. A., Gross, O., Li, Y., Ulke-Lemee, A., Potentier, M. S., … Beck, P. L. (2010). Clostridium difficile toxin-induced inflammation and intestinal injury are mediated by the inflammasome. *Gastroenterology*, *139*(2), 542–552.e3.

Nguyen, H. X., & Tidball, J. G. (2003). Interactions between neutrophils and macrophages promote macrophage killing of rat muscle cells in vitro. *Journal of Physiology*, *547*(1), 125–132.

Nikaido, M., Law, E. W. P., & Kelsh, R. N. (2013). A Systematic Survey of Expression and Function of Zebrafish frizzled Genes. *PLoS ONE*, *8*(1).

Nitzan, O., Elias, M., Chazan, B., Raz, R., & Saliba, W. (2013). Clostridium difficile and inflammatory bowel disease: Role in pathogenesis and implications in treatment. *World Journal of Gastroenterology*, *19*(43), 7577–7585.

North, T. E., Goessling, W., Walkley, C. R., Lengerke, C., Kopani, K. R., Lord, A. M., … Zon, L. I. (2007). Prostaglandin E2 regulates vertebrate haematopoietic stem cell homeostasis. *Nature*, *447*(7147), 1007–11.

Nottrott, S., Schoentaube, J., Genth, H., Just, I., & Gerhard, R. (2007). Clostridium difficile toxin A-induced apoptosis is p53-independent but depends on glucosylation of Rho GTPases. *Apoptosis*, *12*(8), 1443–1453.

Nourshargh, S., & Alon, R. (2014). Leukocyte Migration into Inflamed Tissues. *Immunity*, *41*(5), 694–707.

O ’shea, J. M., & Perkins, N. D. (2008). Regulation of the RelA (p65) transactivation domain.

Biochemical Society Transactions, *36*, 603–608.

Olson, A., Diebel, L. N., & Liberati, D. M. (2013). Effect of host defenses on Clostridium difficile toxin-induced intestinal barrier injury. *The Journal of Trauma and Acute Care Surgery*, *74*(4), 983-89; discussion 989-90.

Onai, N., & Ohteki, T. (2014). Bipotent or Oligopotent? A Macrophage and DC Progenitor Revisited. *Immunity*, *41*(1), 5–7.

Önfelt, B., Nedvetzki, S., Benninger, R. K. P., Purbhoo, M. A., Sowinski, S., Hume, A. N., … Davis, D. M. (2006). Structurally Distinct Membrane Nanotubes between Human Macrophages Support Long-Distance Vesicular Traffic or Surfing of Bacteria. *The Journal of Immunology*.

Onfelt, B., Nedvetzki, S., Yanagi, K., & Davis, D. M. (2004). Cutting Edge: Membrane Nanotubes Connect Immune Cells. *The Journal of Immunology*, *173*(3), 1511–1513.

Orellana, J., & Thomas, J. (1992). Human Colonic Aspirates Containing Immunoglobulin A Antibody to Clostridium dificile Toxin A Inhibit Toxin A-Receptor Binding. *GASTROENTEROLOGY*, 35–40.

Orrell, K. E., Zhang, Z., Sugiman-Marangos, S. N., & Melnyk, R. A. (2017). Clostridium difficile toxins A and B: Receptors, pores, and translocation into cells. *Critical Reviews in Biochemistry and Molecular Biology*, *52*(4), 461–473.

Orry, A. J. W., Abagyan, R. A., & Cavasotto, C. N. (2006). Structure-based development of target-specific compound libraries. *Drug Discovery Today*, *11*(5–6), 261–266.

Orth, P., Xiao, L., Hernandez, L. D., Reichert, P., Sheth, P. R., Beaumont, M., … Therien, A. G. (2014). Mechanism of action and epitopes of Clostridium difficile toxin B-neutralizing antibody bezlotoxumab revealed by X-ray crystallography. *Journal of Biological Chemistry*, *289*(26), 18008–18021.

Page, D. M., Wittamer, V., Bertrand, J. Y., Lewis, K. L., Pratt, D. N., Schale, S. E., … Yang, H. (2014). An evolutionarily conserved program of B-cell development and activation in zebrafish An evolutionarily conserved program of B-cell development and activation in zebra fi sh. *Blood*, *122*(8), 1–12.

Paredes-Sabja, D., Cofre-Araneda, G., Brito-Silva, C., Pizarro-Guajardo, M., & Sarker, M. R. (2012). Clostridium difficile spore-macrophage interactions: Spore survival. *PLoS ONE*, *7*(8).

Paredes-Sabja, D., Shen, A., & Sorg, J. A. (2014). Clostridium difficile spore biology: Sporulation, germination, and spore structural proteins. *Trends in Microbiology*, *22*(7), 406–416.

Park, Y. H., Roth, T. L., & Mcgavern, D. B. (2014). Pyrin Inflammasome Activation and RhoA Signaling in the Autoinflammatory Diseases FMF and HIDS Yong, *17*(2), 367–402.

Pawlowski, S. W., Calabrese, G., Kolling, G. L., Platts-Mills, J., Freire, R., AlcantaraWarren, C., … Guerrant, R. L. (2010). Murine model of Clostridium difficile infection with aged gnotobiotic C57BL/6 mice and a BI/NAP1 strain. *The Journal of Infectious Diseases*, *202*(11), 1708–12.

Pépin, J., Epin, J., Valiquette, L., Gagnon, S., Routhier, S., & Brazeau, I. (2007). Outcomes of Clostridium difficile-associated disease treated with metronidazole or vancomycin before and after the emergence of NAP1/027. *American Journal of Gastroenterology*, *102*(12), 2781–2788.

Pépin, J., Saheb, N., Coulombe, M.-A., Alary, M.-E., Corriveau, M.-P., Authier, S., … Lanthier, L. (2005). Emergence of fluoroquinolones as the predominant risk factor for Clostridium difficile-associated diarrhea: a cohort study during an epidemic in Quebec. *Clinical Infectious Diseases : An Official Publication of the Infectious Diseases Society of America*, *41*(9), 1254–60.

Perez-Lopez, A., Behnsen, J., Nuccio, S.-P., & Raffatellu, M. (2016). Mucosal immunity to pathogenic intestinal bacteria. *Nature Reviews Immunology*, *16*(3), 135–148.

Peterson, R. T., Link, B. A., Dowling, J. E., & Schreiber, S. L. (2000). Small molecule developmental screens reveal the logic and timing of vertebrate development. *Proceedings of the National Academy of Sciences of the United States of America*, *97*(24), 12965–9.

Peterson, R. T., Shaw, S. Y., Peterson, T. A., Milan, D. J., Zhong, T. P., Schreiber, S. L., … Fishman, M. C. (2004). Chemical suppression of a genetic mutation in a zebrafish model of aortic coarctation. *Nature Biotechnology*, *22*(5), 595–599.

Petrie, T. A., Strand, N. S., Tsung-Yang, C., Rabinowitz, J. S., Moon, R. T., Yang, C.-T., … Moon, R. T. (2014). Macrophages modulate adult zebrafish tail fin regeneration. *Development (Cambridge, England)*, *141*(13), 406–406.

Pfeiffer, B. D., Ngo, T. T. B., Hibbard, K. L., Murphy, C., Jenett, A., Truman, J. W., & Rubin, G. M. (2010). Refinement of tools for targeted gene expression in Drosophila. *Genetics*, *186*(2), 735–755.

Phelps, C. B., Sengchanthalangsy, L. L., Malek, S., & Ghosh, G. (2000). Mechanism of ??B DNA binding by Rel/NF-??b dimers. *Journal of Biological Chemistry*, *275*(32), 24392–24399.

Pieters, J. (2008). Mycobacterium tuberculosis and the Macrophage: Maintaining a Balance. *Cell Host and Microbe*, *3*(6), 399–407.

Pisharath, H., Rhee, J. M., Swanson, M. A., Leach, S. D., & Parsons, M. J. (2007). Targeted ablation of beta cells in the embryonic zebrafish pancreas using E. coli nitroreductase. *Mechanisms of Development*, *124*(3), 218–229.

Pothoulakis, C. (2000). Effects of Clostridium difficile toxins on epithelial cell barrier. *Ann N Y Acad Sci*, *915*, 347–356.

Pothoulakis, C., Gilbert, R. J., Cladaras, C., Castagliuolo, I., Semenza, G., Hitti, Y., … Lamont, J. T. (1996). Rabbit sucrase-isomaltase contains a functional intestinal receptor for Clostridium difficile toxin A. *Journal of Clinical Investigation*, *98*(3), 641–649.

Potter, C. J., & Luo, L. (2011). Using the Q system in Drosophila melanogaster. *Nature Protocols*, *6*(8), 1105–1120.

Priest, D. G., Kumar, S., Yan, Y., Dunlap, D. D., Dodd, I. B., & Shearwin, K. E. (2014). Quantitation of interactions between two DNA loops demonstrates loop domain insulation in *E. coli* cells. *Proceedings of the National Academy of Sciences*, *111*(42), E4449–E4457.

Pruitt, R. N., & Lacy, D. B. (2012). Toward a structural understanding of Clostridium difficile toxins A and B. *Frontiers in Cellular and Infection Microbiology*, *2*(March), 1–14.

Pyati, U. J., Gjini, E., Carbonneau, S., Lee, J. S., Guo, F., Jette, C. A., … Look, A. T. (2011). P63 mediates an apoptotic response to pharmacological and disease-related er stress in the developing epidermis. *Developmental Cell*, *21*(3), 492–505.

Qa'Dan, M., Ramsey, M., Daniel, J., Spyres, L. M., Safiejko-Mroczka, B., Ortiz-Leduc, W., & Ballard, J. D. (2002). Clostridium difficile toxin B activates dual caspase-dependent and caspase-independent apoptosis in intoxicated cells. *Cellular Microbiology*, *4*(7), 425–434.

Ransom, E. M., Ellermeier, C. D., & Weiss, D. S. (2015). Use of mCherry red fluorescent protein for studies of protein localization and gene expression in Clostridium difficile. *Applied and Environmental Microbiology*, *81*(5), 1652–1660.

Razaq, N., Sambol, S., Nagaro, K., Zukowski, W., Cheknis, A., Johnson, S., & Gerding, D. N. (2007). Infection of Hamsters with Historical and Epidemic BI Types of Clostridium difficile. *The Journal of Infectious Diseases*, *196*(12), 1813–1819. Retrieved from http://dx.doi.org/10.1086/523106

Reinert, D. J., Jank, T., Aktories, K., & Schulz, G. E. (2005). Structural basis for the function of Clostridium difficile toxin B. *Journal of Molecular Biology*, *351*(5), 973–981.

Rennekamp, A. J., & Peterson, R. T. (2015). 15 Years of Zebrafish Chemical Screening. *Current Opinion in Chemical Biology*, *24*, 58–70.

Renshaw, S. A., Parmar, J. S., Singleton, V., Rowe, S. J., Dockrell, D. H., Dower, S. K., … Whyte, M. K. B. (2003). Acceleration of human neutrophil apoptosis by TRAIL. *Journal of Immunology (Baltimore, Md. : 1950)*, *170*(2), 1027–1033.

Reznikoff, W. S., Winter, R. B., & Hurley, C. K. (1974). The location of the repressor binding sites in the lac operon. *Proceedings of the National Academy of Sciences of the United States of America*, *71*(6), 2314–2318.

Ridges, S., Heaton, W. L., Joshi, D., Choi, H., Eiring, A., Batchelor, L., … Trede, N. S. (2012). Plenary paper Zebrafish screen identifies novel compound with selective toxicity against leukemia, *119*(24), 5621–5631.

Ridlon, J. M. (2005). Bile salt biotransformations by human intestinal bacteria. *The Journal of Lipid Research*, *47*(2), 241–259.

Rivera, A., Siracusa, M. C., Yap, G. S., & Gause, W. C. (2016). Innate cell communication kick-starts pathogen-specific immunity. *Nature Immunology*, *17*(4), 356–363.

Rohlke, F., & Stollman, N. (2012). Fecal microbiota transplantation in relapsing Clostridium difficile infection. *Therapeutic Advances in Gastroenterology*, *5*(6), 403–420.

Rosano, G. L., & Ceccarelli, E. A. (2014). Recombinant protein expression in Escherichia coli: Advances and challenges. *Frontiers in Microbiology*, *5*(APR), 1–17.

Rupnik, M., Wilcox, M. H., & Gerding, D. N. (2009). Clostridium difficile infection: new developments in epidemiology and pathogenesis. *Nature Reviews Microbiology*, *7*(7), 526–536.

Sadighi Akha, A. A., Theriot, C. M., Erb-Downward, J. R., Mcdermott, A. J., Falkowski, N. R., Tyra, H. M., … Huffnagle, G. B. (2013). Acute infection of mice with Clostridium difficile leads to eIF2α phosphorylation and pro-survival signalling as part of the mucosal inflammatory response. *Immunology*, *140*(1), 111–122.

Sagoo, P., Garcia, Z., Breart, B., Lemaître, F., Michonneau, D., Albert, M. L., … Bousso, P. (2015). In vivo imaging of inflammasome activation reveals a subcapsular macrophage burst response that mobilizes innate and adaptive immunity. *Nature Medicine*, *22*(1), 64–71.

Sambol, S. P., Merrigan, M. M., Tang, J. K., Johnson, S., & Gerding, D. N. (2002). Colonization for the Prevention of *Clostridium difficile* Disease in Hamsters. *The Journal of Infectious Diseases*, *186*(12), 1781–1789.

Sambol, S. P., Tang, J. K., Merrigan, M. M., Johnson, S., & Gerding, D. N. (2001). Infection of hamsters with epidemiologically important strains of Clostridium difficile. *The Journal of Infectious Diseases*, *183*(12), 1760–6.

Sams-Dodd, F. (2005). Target-based drug discovery: Is something wrong? *Drug Discovery Today*, *10*(2), 139–147.

Sandoval, I. T., Manos, E. J., Van Wagoner, R. M., Delacruz, R. G. C., Edes, K., Winge, D. R., … Jones, D. A. (2013). Juxtaposition of chemical and mutation-induced developmental defects in zebrafish reveal a copper-chelating activity for kalihinol F. *Chemistry and Biology*, *20*(6), 753–763.

Sartor, R. B., & Mazmanian, S. K. (2012). Intestinal Microbes in Inflammatory Bowel Diseases. *The American Journal of Gastroenterology Supplements*, *1*(1), 15–21.

Savill, J. S., Wyllie, A. H., Henson, J. E., Walport, M. J., Henson, P. M., & Haslett, C. (1989). Macrophage phagocytosis of aging neutrophils in inflammation. Programmed cell death in the neutrophil leads to its recognition by macrophages. *Journal of Clinical Investigation*, *83*(3), 865–875.

Saydmohammed, M., Vollmer, L. L., Onuoha, E. O., Vogt, A., & Tsang, M. (2011). A high-content screening assay in transgenic zebrafish identifies two novel activators of fgf signaling. *Birth Defects Research Part C - Embryo Today: Reviews*, *93*(3), 281–287.

Scapini, P., Lapinet-Vera, J. A., Gasperini, S., Calzetti, F., Bazzoni, F., & Cassatella, M. A. (2000). The neutrophil as a cellular source of chemokines. *Immunological Reviews*, *177*(1), 195–203.

Schall, K. A., Holoyda, K. A., Grant, C. N., Levin, D. E., Torres, E. R., Maxwell, A., … Grikscheit, T. C. (2015). Adult zebrafish intestine resection: a novel model of short bowel syndrome, adaptation, and intestinal stem cell regeneration. *American Journal of Physiology - Gastrointestinal and Liver Physiology*, *309*(3), G135–G145.

Schmitz, M. L., & Baeuerle, P. A. (1991). The p65 subunit is responsible for the strong transcription activating potential of NF-kappa B. *The EMBO Journal*, *10*(12), 3805–3817. Retrieved from http://www.pubmedcentral.nih.gov/articlerender.fcgi?artid=453117&tool=pmcentrez&rendertype=abstract

Schwan, C., Stecher, B., Tzivelekidis, T., Van Ham, M., Rohde, M., Hardt, W. D., … Aktories, K. (2009). Clostridium difficile toxin CDT induces formation of microtubule-based

protrusions and increases adherence of bacteria. *PLoS Pathogens*, *5*(10).

Sebaihia, M., Wren, B. W., Mullany, P., Fairweather, N. F., Minton, N., Stabler, R., … Parkhill, J. (2006). The multidrug-resistant human pathogen Clostridium difficile has a highly mobile, mosaic genome. *Nature Genetics*, *38*(7), 779–786.

Sekirov, I., Russell, S. L., Antunes, L. C. M., & Finlay, B. B. (2010). Gut Microbiota in Health and Disease. *Physiological Reviews*, *90*(3), 859 LP-904. Retrieved from http://physrev.physiology.org/content/90/3/859.abstract

Semenyuk, E. G., Poroyko, V. A., Johnston, P. F., Jones, S. E., Knight, K. L., Gerding, D. N., & Driks, A. (2015). Analysis of Bacterial Communities during Clostridium difficile Infection in the Mouse, *83*(11), 4383–4391.

Serhan, C. N., Brain, S. D., Buckley, C. D., Gilroy, D. W., Haslett, C., O'Neill, L. A. J., … Wallace, J. L. (2007). Resolution of inflammation: state of the art, definitions and terms. *The FASEB Journal*, *21*(2), 325–332.

Setola, V., Sprague, J., Jin, S., Jin, Y. N., Bruni, G., Woolf, C., … Peterson, R. T. (2013). Photochemical activation of TRPA1 channels in neurons and animals, *9*(4), 257–263.

Sheedy, F. J., Grebe, A., Rayner, K. J., Kalantari, P., Ramkhelawon, B., Carpenter, S. B., … Moore, K. J. (2013). CD36 coordinates NLRP3 inflammasome activation by facilitating intracellular nucleation of soluble ligands into particulate ligands in sterile inflammation. *Nature Immunology*, *14*(8), 812–820.

Shen, A. (2012). Clostridium difficile toxins: Mediators of inflammation. *Journal of Innate Immunity*, *4*(2), 149–158.

Shiau, C. E., Kaufman, Z., Meireles, A. M., & Talbot, W. S. (2015). Differential requirement for irf8 in formation of embryonic and adult macrophages in zebrafish. *PLoS ONE*, *10*(1), 1–15.

Shim, J. K., Johnson, S., Samore, M. H., Bliss, D. Z., & Gerding, D. N. (1998). Primary symptomless colonisation by Clostridium difficile and decreased risk of subsequent diarrhoea. *Lancet*, *351*(9103), 633–636.

Shiomi, A., & Usui, T. (2015). Pivotal roles of GM-CSF in autoimmunity and inflammation. *Mediators of Inflammation*, *2015*.

Sickles, E. A., Orsi, C. D., Berns, E. A., Ph, D., Cutter, G., Ph, D., … Elmore, J. G. (2017). New England Journal, 1399–1409.

Silva, M. T. (2010). When two is better than one: macrophages and neutrophils work in concert

in innate immunity as complementary and cooperative partners of a myeloid phagocyte system. *Journal of Leukocyte Biology*, *87*(1), 93–106.

Silva, M. T., & Correia-Neves, M. (2012). Neutrophils and macrophages: The main partners of phagocyte cell systems. *Frontiers in Immunology*, *3*(JUL), 2008–2013.

Simor, A. E., Bradley, S. F., Strausbaugh, L. J., Crossley, K., & Nicolle, L. E. (2002). Clostridium difficile in Long-Term–Care Facilities for the Elderly. *Infection Control & Hospital Epidemiology*, *23*(11), 696–703.

Sisson, B. E., & Topczewski, J. (2009). Expression of five frizzleds during zebrafish craniofacial development. *Gene Expression Patterns*, *9*(7), 520–527.

Solomon, K. (2013). The host immune response to Clostridium difficile infection. *Therapeutic Advances in Infectious Disease*, *1*(1), 19–35.

Solomon, K., Webb, J., Ali, N., Robins, R. A., & Mahida, Y. R. (2005). Monocytes are highly sensitive to Clostridium difficile toxin A-induced apoptotic and nonapoptotic cell death. *Infection and Immunity*, *73*(3), 1625–1634.

Sommer, F., & Backhed, F. (2013). The gut microbiota [mdash] masters of host development and physiology. *Nat Rev Micro*, *11*(4), 227–238. Retrieved from http://dx.doi.org/10.1038/nrmicro2974

Sonenberg, N., & Hinnebusch, A. G. (2009). Regulation of Translation Initiation in Eukaryotes: Mechanisms and Biological Targets. *Cell*, *136*(4), 731–745.

Song, C., Wang, C., & Huang, L. (2011). Human neonatal neutrophils are resistant to apoptosis with lower caspase-3 activity. *The Tohoku Journal of Experimental Medicine*, *225*(1), 59–63.

Sorg, J. A., & Sonenshein, A. L. (2008). Bile salts and glycine as cogerminants for Clostridium difficile spores. *Journal of Bacteriology*, *190*(7), 2505–2512.

Sorg, J. A., & Sonenshein, A. L. (2010). Inhibiting the initiation of Clostridium difficile spore germination using analogs of chenodeoxycholic acid, a bile acid. *Journal of Bacteriology*, *192*(19), 4983–4990.

Stabler, R. A., Valiente, E., Dawson, L. F., He, M., Parkhill, J., Wren, B. W., & Brendan, E. (2010). and Inversions. *DNA Sequence*, (August), 269–276.

Stinchcombe, J. C., Bossi, G., Booth, S., & Griffiths, G. M. (2001). The immunological synapse of CTL contains a secretory domain and membrane bridges. *Immunity*, *15*(5), 751–761.

Strowig, T., Henao-Mejia, J., Elinav, E., & Flavell, R. (2012). Inflammasomes in health and

disease. *Nature*, *481*(7381), 278–286.

Subedi, A., Macurak, M., Gee, S. T., Monge, E., Goll, M. G., Potter, C. J., … Halpern, M. E. (2014). Adoption of the Q transcriptional regulatory system for zebrafish transgenesis. *Methods*, *66*(3), 433–440.

Summers, C., Rankin, S. M., Condliffe, A. M., Singh, N., Peters, A. M., & Chilvers, E. R. (2010). Neutrophil kinetics in health and disease. *Trends in Immunology*, *31*(8), 318–324.

Sun, X., & Hirota, S. A. (2015). The roles of host and pathogen factors and the innate immune response in the pathogenesis of Clostridium difficile infection. *Molecular Immunology*, *63*(2), 193–202.

Sun, X., Xianyun, H., & Tzipori, S. (2012). Essential role of the glucosyltransferase activity in Clostridium difficile toxin-induced secretion of TNF-α by macrophages, *76*(October 2009), 211–220.

Swinney, D. C., & Anthony, J. (2011). How were new medicines discovered? *Nature Reviews Drug Discovery*, *10*(7), 507–519.

Szüts, D., & Bienz, M. (2000). LexA chimeras reveal the function of Drosophila Fos as a context-dependent transcriptional activator. *Proceedings of the National Academy of Sciences of the United States of America*, *97*(10), 5351–6.

Tan, B. H., Meinken, C., Bastian, M., Bruns, H., Legaspi, A., Ochoa, M. T., … Stenger, S. (2006). Macrophages Acquire Neutrophil Granules for Antimicrobial Activity against Intracellular Pathogens. *The Journal of Immunology*, *177*(3), 1864–1871.

Tao, L., Zhang, J., Meraner, P., Tovaglieri, A., Wu, X., Gerhard, R., … Dong, M. (2016). Frizzled proteins are colonic epithelial receptors for C. difficile toxin B. *Nature*, *538*(7625), 350–355.

Tauzin, S., Starnes, T. W., Becker, F. B., Lam, P. ying, & Huttenlocher, A. (2014). Redox and Src family kinase signaling control leukocyte wound attraction and neutrophil reverse migration. *Journal of Cell Biology*, *207*(5), 589–598.

Taylor, K. L., Grant, N. J., Temperley, N. D., & Patton, E. E. (2010). Small molecule screening in zebrafish: an in vivo approach to identifying new chemical tools and drug leads. *Cell Communication and Signaling*, *8*(1), 11.

Teichert, M., Tatge, H., Schoentaube, J., Just, I., & Gerhard, R. (2006). Application of Mutated Clostridium difficile Toxin A for Determination of Glucosyltransferase-Dependent Effects, *74*(10), 6006–6010.

Theriot, C. M., Bowman, A. a, & Young, V. B. (2015). Antibiotic-Induced Alterations of the Gut Microbiota Alter Secondary Bile Acid Production and Allow for Clostridium difficile Spore Germination and Outgrowth in the Large Intestine. *MSphere*, *1*(1), e00045-15.

Theriot, C. M., Koenigsknecht, M. J., Carlson, P. E., Hatton, G. E., Nelson, A. M., Li, B., … Young, V. B. (2014). Antibiotic-induced shifts in the mouse gut microbiome and metabolome increase susceptibility to Clostridium difficile infection. *Nature Communications*, *5*.

Thliveris, A. T., Little, J. W., & Mount, D. W. (1991). Repression of the E coli recA gene requires at least two LexA protein monomers. *Biochimie*, *73*(4), 449–456.

Thursby, E., & Juge, N. (2017). Introduction to the human gut microbiota. *Biochemical Journal*, *474*(11), 1823–1836.

Tobin, D. M., Vary, J. C., Ray, J. P., Walsh, G. S., Dunstan, S. J., Bang, N. D., … Ramakrishnan, L. (2010). The lta4h Locus Modulates Susceptibility to Mycobacterial Infection in Zebrafish and Humans. *Cell*, *140*(5), 717–730.

Traven, A., Jelicic, B., & Sopta, M. (2006). Yeast Gal4: a transcriptional paradigm revisited. *EMBO Reports*, *7*(5), 496–9.

Tucker, K. D., & Wilkins, T. D. (1991). Toxin A of *Clostridium difficile* binds to the human carbohydrate antigens I, X, and Y. *Infection and Immunity*, *59*(1), 73–78.

Turner, J. R. (2009). Intestinal mucosal barrier function in health and disease. *Nature Reviews Immunology*, *9*(11), 799–809.

Tzeng, T. C., Schattgen, S., Monks, B., Wang, D., Cerny, A., Latz, E., … Golenbock, D. T. (2016). A Fluorescent Reporter Mouse for Inflammasome Assembly Demonstrates an Important Role for Cell-Bound and Free ASC Specks during In Vivo Infection. *Cell Reports*, *16*(2), 571–582.

Ueda, H., Morphew, M. K., McIntosh, J. R., & Davis, M. M. (2011). CD4+ T-cell synapses involve multiple distinct stages. *Proceedings of the National Academy of Sciences*, *108*(41), 17099–17104.

Valiquette, L., Cossette, B., Garant, M.-P., Diab, H., & Pépin, J. (2007). Impact of a reduction in the use of high-risk antibiotics on the course of an epidemic of Clostridium difficile-associated disease caused by the hypervirulent NAP1/027 strain. *Clinical Infectious Diseases : An Official Publication of the Infectious Diseases Society of America*, *45 Suppl 2*(Suppl 2), S112–S121.

van der Flier, L. G., & Clevers, H. (2009). Stem Cells, Self-Renewal, and Differentiation in the

Intestinal Epithelium. *Annual Review of Physiology*, *71*(1), 241–260.

Van Der Sar, A. M., Appelmelk, B. J., Vandenbroucke-Grauls, C. M. J. E., & Bitter, W. (2004). A star with stripes: Zebrafish as an infection model. *Trends in Microbiology*, *12*(10), 451–457.

van Eijk, E., Anvar, S. Y., Browne, H. P., Leung, W. Y., Frank, J., Schmitz, A. M., … Smits, W. K. (2015). Complete genome sequence of the Clostridium difficile laboratory strain 630Δerm reveals differences from strain 630, including translocation of the mobile element CTn5. *BMC Genomics*, *16*(1), 31.

van Gisbergen, K. P. J. M., Sanchez-Hernandez, M., Geijtenbeek, T. B. H., & van Kooyk, Y. (2005). Neutrophils mediate immune modulation of dendritic cells through glycosylation-dependent interactions between Mac-1 and DC-SIGN. *The Journal of Experimental Medicine*, *201*(8), 1281–1292.

van Ham, T. J., Mapes, J., Kokel, D., & Peterson, R. T. (2010). Live imaging of apoptotic cells in zebrafish. *The FASEB Journal*, *24*(11), 4336–4342.

van Nood, E., Vrieze, A., Nieuwdorp, M., Fuentes, S., Zoetendal, E. G., de Vos, W. M., … Keller, J. J. (2013). Duodenal infusion of donor feces for recurrent Clostridium difficile. *N Engl J Med*, *368*(5), 407–415.

van Soest, J. J., Stockhammer, O. W., Ordas, A., Bloemberg, G. V, Spaink, H. P., & Meijer, A. H. (2011). Comparison of static immersion and intravenous injection systems for exposure of zebrafish embryos to the natural pathogen Edwardsiella tarda. *BMC Immunology*, *12*(1), 58.

Varol, C., Mildner, A., & Jung, S. (2015). *Macrophages: development and tissue specialization*. *Annu Rev Immunol* (Vol. 33).

Vincent, W. J. B., Harvie, E. A., Sauer, J. D., & Huttenlocher, A. (2017). Neutrophil derived LTB4 induces macrophage aggregation in response to encapsulated Streptococcus iniae infection. *PLoS ONE*, *12*(6), 1–16.

Vollaard, E. J., & Clasener, H. A. (1994). Colonization resistance. *Antimicrobial Agents and Chemotherapy*, *38*(3), 409–414. Retrieved from http://www.ncbi.nlm.nih.gov/pmc/articles/PMC284472/

Voth, D. E., & Ballard, J. D. (2005). Clostridium difficile Toxins: Mechanism of Action and Role in Disease. *Clin. Microbiol. Rev.*, *18*(2), 247–263.

W Patrick Walters, & Mark Namchuk. (2003). Designing screens: How to make your hits a hit.

Nature Reviews Drug Discovery, *4*(2), 259–266.

Walker, S. L., Ariga, J., Mathias, J. R., Coothankandaswamy, V., Xie, X., Distel, M., … Mumm, J. S. (2012). Automated reporter quantification in vivo: High-throughput screening method for reporter-based assays in zebrafish. *PLoS ONE*, *7*(1).

Wang, G., Rajpurohit, S. K., Delaspre, F., Walker, S. L., White, D. T., Ceasrine, A., … Mumm, J. S. (2015). First quantitative high-throughput screen in zebrafish identifies novel pathways for increasing pancreatic β-cell mass. *ELife*, *4*(JULY2015), 3.

Warny, M., Keates, A. C., Keates, S., Castagliuolo, I., Zacks, J. K., Aboudola, S., … Kelly, C. P. (2000). p38 MAP kinase activation by Clostridium difficile toxin A mediates monocyte necrosis, IL-8 production, and enteritis. *Journal of Clinical Investigation*, *105*(8), 1147–1156.

Weber, T., Namikawa, K., Winter, B., Müller-Brown, K., Kühn, R., Wurst, W., & Köster, R. W. (2016). Caspase-mediated apoptosis induction in zebrafish cerebellar Purkinje neurons. *Development*, *143*(22), 4279–4287.

Wei, S., Liu, J. H., Epling-Burnette, P. K., Gamero, A. M., Ussery, D., Pearson, E. W., … Djeu, J. Y. (1996). Critical role of Lyn kinase in inhibition of neutrophil apoptosis by granulocyte-macrophage colony-stimulating factor. *The Journal of Immunology*, *157*(11), 5155 LP-5162. Retrieved from http://www.jimmunol.org/content/157/11/5155.abstract

Wei Zheng, Natasha Thorne, and J. C. M. (2015). Phenotypic screens as a renewed approach for drug discovery. *Child Welfare*, *94*(4), 19–51.

Weingarden, A. R., Chen, C., Bobr, A., Yao, D., Lu, Y., Nelson, V. M., … Khoruts, A. (2014). Microbiota transplantation restores normal fecal bile acid composition in recurrent Clostridium difficile infection. *American Journal of Physiology. Gastrointestinal and Liver Physiology*, *306*(4), G310-9.

Weiss, K., Lentnek, A., Golan, Y., Gorbach, S., Sears, P., Ph, D., & Shue, Y. (2014). Fidaxomicin versus Vancomycin for.

Whitaker, W. R., Shepherd, E. S., & Sonnenburg, J. L. (2017). Tunable Expression Tools Enable Single-Cell Strain Distinction in the Gut Microbiome. *Cell*, *169*(3), 538–546.e12.

Whited, J. L., Lehoczky, J. a., & Tabin, C. J. (2012). Inducible genetic system for the axolotl. *Proceedings of the National Academy of Sciences*, *109*(34), 13662–13667.

Wilcox, M. H., Gerding, D. N., Poxton, I. R., Kelly, C., Nathan, R., Birch, T., … Dorr, M.-B. (2017). Bezlotoxumab for Prevention of Recurrent *Clostridium difficile* Infection. *New England*

Journal of Medicine, *376*(4), 305–317.

William, H., Johnson, P. F., & Mcknight, S. L. (1988). Proteins Kg.

Williams, C. H., & Hong, C. C. (2016). Zebrafish small molecule screens: Taking the phenotypic plunge. *Computational and Structural Biotechnology Journal*, *14*, 350–356.

Wilson, K. H. (1983). Efficiency of various bile salt preparations for stimulation of Clostridium difficile spore germination. *Journal of Clinical Microbiology*, *18*(4), 1017–1019. Retrieved from http://www.ncbi.nlm.nih.gov/pmc/articles/PMC270959/

Wilson, K. H., Kennedy, M. J., & Fekety, F. R. (1982). Use of sodium taurocholate to enhance spore recovery on a medium selective for Clostridium difficile. *Journal of Clinical Microbiology*, *15*(3), 443–446.

Winston, J. A., & Theriot, C. M. (2016). Impact of microbial derived secondary bile acids on colonization resistance against Clostridium difficile in the gastrointestinal tract. *Anaerobe*, *41*, 44–50.

Wulfing, C., Purtic, B., Klem, J., & Schatzle, J. D. (2003). Stepwise cytoskeletal polarization as a series of checkpoints in innate but not adaptive cytolytic killing. *Proceedings of the National Academy of Sciences*, *100*(13), 7767–7772.

Xu, H., Yang, J., Gao, W., Li, L., Li, P., Zhang, L., … Shao, F. (2014). Innate immune sensing of bacterial modifications of Rho GTPases by the Pyrin inflammasome. *Nature*, *513*(7517), 237–241.

Yagi, R., Mayer, F., & Basler, K. (2010). Refined LexA transactivators and their use in combination with the Drosophila Gal4 system. *Proceedings of the National Academy of Sciences*, *107*(37), 16166–16171.

Yang, Y. (2014). Could a Swimming Creature Inform Us on Intestinal Diseases? Lessons from Zebrafish. *Inflamm Bowel Dis.*, *20*(5), 956–966.

Yang, Z., Ramsey, J., Hamza, T., Zhang, Y., Li, S., Yfantis, H. G., … Feng, H. (2015). Mechanisms of protection against Clostridium difficile infection by the monoclonal antitoxin antibodies actoxumab and bezlotoxumab. *Infection and Immunity*, *83*(2), 822–831.

Yilmaz, L. S., & Noguera, D. R. (2004). Mechanistic Approach to the Problem of Hybridization Efficiency in Fluorescent In Situ Hybridization. *Society*, *70*(12), 7126–7139.

Yousefi, S., Green, D. R., Blaser, K., & Simon, H. U. (1994). Protein-tyrosine phosphorylation regulates apoptosis in human eosinophils and neutrophils. *Proceedings of the National Academy of Sciences of the United States of America*, *91*(23), 10868–72. Retrieved from

http://www.pubmedcentral.nih.gov/articlerender.fcgi?artid=45127&tool=pmcentrez&rendertype=abstract

Yuan, P., Zhang, H., Cai, C., Zhu, S., Zhou, Y., Yang, X., … Wei, W. (2015). Chondroitin sulfate proteoglycan 4 functions as the cellular receptor for Clostridium difficile toxin B. *Cell Research*, *25*(2), 157–68.

Yutin, N., & Galperin, M. Y. (2013). A genomic update on clostridial phylogeny: Gram-negative spore formers and other misplaced clostridia. *Environmental Microbiology*, *15*(10), 2631–2641.

Zhang, A. P. P., Pigli, Y. Z., & Rice, P. a. (2010). Structure of the LexA-DNA complex and implications for SOS box measurement. *Nature*, *466*(7308), 883–6.

Zhang, G. H., Gurtu, V., Kain, S. R., & Yan, G. C. (1997). Early detection of apoptosis using a fluorescent conjugate of annexin V. *Biotechniques.*, *23*(3), 525–526.

Zhang, J., Wang, X., Cui, W., Wang, W., Zhang, H., Liu, L., … Li, B. (2013). Visualization of caspase-3-like activity in cells using a genetically encoded fluorescent biosensor activated by protein cleavage. *Nature Communications*, *4*, 2157.

Zhao, H., & Dean, A. (2005). Organizing the genome: enhancers and insulators. *Biochemistry and Cell Biology*, *83*(4), 516–524.

Zon, L. I., & Peterson, R. T. (2005). In vivo drug discovery in the zebrafish. *Nature Reviews Drug Discovery*, *4*(1), 35–44.

Zuo, J., Niu, Q. W., & Chua, N. H. (2000). An estrogen receptor-based transactivator XVE mediates highly inducible gene expression in transgenic plants. *Plant Journal*, *24*(2), 265–273.